Titre: Title:	Biomécanique de l'articulation du genou humain durant la marche - un modèle musculosquelettique hybride
Auteur: Author:	Hafedh Marouane
Date:	2017
Type:	Mémoire ou thèse / Dissertation or Thesis
Référence: Citation:	Marouane, H. (2017). Biomécanique de l'articulation du genou humain durant la marche - un modèle musculosquelettique hybride [Thèse de doctorat, École Polytechnique de Montréal]. PolyPublie. https://publications.polymtl.ca/2500/

URL de PolyPublie: PolyPublie URL:	https://publications.polymtl.ca/2500/
Directeurs de recherche: Advisors:	Aboulfazl Shirazi
Programme: Program:	Génie mécanique

UNIVERSITÉ DE MONTRÉAL

BIOMÉCANIQUE DE L'ARTICULATION DU GENOU HUMAIN DURANT LA MARCHE - UN MODÈLE MUSCULOSQUELETTIQUE HYBRIDE

HAFEDH MAROUANE

DÉPARTEMENT DE GÉNIE MÉCANIQUE

ÉCOLE POLYTECHNIQUE DE MONTRÉAL

THÈSE PRÉSENTÉE EN VUE DE L'OBTENTION

DU DIPLÔME DE PHILOSOPHIAE DOCTOR

(GÉNIE MÉCANIQUE)

MARS 2017

UNIVERSITÉ DE MONTRÉAL

ÉCOLE POLYTECHNIQUE DE MONTRÉAL

Cette thèse intitulée :

BIOMÉCANIQUE DE L'ARTICULATION DU GENOU HUMAIN DURANT LA MARCHE – UN MODÈLE MUSCULOSQUELETTIQUE HYBRIDE

présentée par : MAROUANE Hafedh

en vue de l'obtention du diplôme de : Philosophiae Doctor

a été dûment acceptée par le jury d'examen constitué de :

M. LAKIS Aouni A., Ph. D., président

M. SHIRAZI-ADL Aboulfazl, Ph. D., membre et directeur de recherche

M. BUSCHMANN Michael, Ph. D., membre

M. MOGLO Kodjo, Ph. D., membre externe

DÉDICACE

À ma chère mère: Tu représentes pour moi le symbole de la bonté, la source de tendresse et l'exemple du dévouement qui n'a pas cessé de m'encourager et de prier pour moi. Ta prière et ta bénédiction m'ont été d'un grand secours pour mener à bien mes études et ma vie. Aucune dédicace ne saurait exprimer ce que tu mérites pour tous les sacrifices que tu n'as cessé de me donner depuis ma naissance, durant mon enfance et même à l'âge adulte. Tu as fait plus qu'une mère puisse faire pour que ses enfants suivent le bon chemin dans leur vie et leurs études. Je te dédie ce travail en témoignage de mon profond amour. Puisse Dieu, le tout puissant, te préserver et t'accorder santé, bonheur et longue vie.

À mon père: Aucune dédicace ne saurait exprimer l'amour, l'estime, le dévouement et le respect que j'ai toujours eu pour vous. Rien au monde ne vaut les efforts fournis jour et nuit pour notre éducation et notre bien-être. Vous resterez toujours une référence à mes yeux. Ce travail est le fruit de tes sacrifices que tu as consentis pour mon éducation et ma formation. Je vous souhaite une longue vie avec tout le bonheur du monde.

À ma chère femme: Quand je t'ai connu, j'ai trouvé la femme de ma vie, mon âme sœur et la lumière de mon chemin. Ma vie à tes cotés est remplie de belles surprises. Tu es et tu resteras la plus belle chose qui me soit jamais arrivé. Que dieu réunisse nos chemins pour un long commun serein et que ce travail soit témoignage de ma reconnaissance et de mon amour sincère et fidèle, pour toi et pour nos futurs enfants.

À mes frères et sœurs: Les mots ne suffisent pas pour exprimer l'attachement, l'amour et l'affection que je porte pour vous. Je vous dédie ce travail avec tous mes vœux de bonheur, de santé et de réussite.

À mes professeurs: Un remerciement particulier et sincère pour tous vos efforts fournis. Que ce travail soit un témoignage de ma gratitude et mon profond respect.

REMERCIEMENTS

Je tiens tout d'abord à remercier le Professeur Aboulfazl Shirazi-Adl, mon directeur de recherche, pour m'avoir donné la possibilité d'accomplir ce travail, pour sa grande rigueur scientifique et pour son encadrement très efficace. Je tiens particulièrement à le remercier pour la grande liberté qu'il m'a accordée et pour son soutien et ses conseils qui m'ont été d'une grande utilité dans la réalisation de ce travail.

Je tiens également à adresser mes remerciements les plus profonds aux membres du jury; à Messieurs Aouni Lakis et Michael Buschmann, professeurs à l'école Polytechnique de Montréal. Merci pour cet honneur. À l'examinateur externe Monsieur Kodjo Moglo, professeur agrégé, Royal Military College of Canada. Merci pour cet honneur.

Mes remerciements vont également au personnel et à mes collègues du département de génie mécanique, section Mécanique Appliquée de l'École Polytechnique de Montréal. Je vous remercie de ces belles années passées en votre compagnie; chacun de vous a contribué, d'une manière ou d'une autre, à faire de cet espace de recherche un environnement exceptionnel.

Je remercie également la mission universitaire de Tunisie en Amérique du Nord (MUTAN) et le conseil de recherches en sciences naturelles et en génie (CRSNG) pour leurs apports financiers à la réalisation de la présente étude.

Je remercie tout particulièrement M.Z. Bendjaballah, K.E. Moglo, W. Mesfar, R. Shirazi et M. Adouni pour leurs efforts antérieurs dans le développement du modèle.

Enfin, je tiens à remercier tous ceux qui se sont intéressés à mon travail, qui m'ont soutenu et encouragé au cours de cette belle aventure. À ma famille, mes parents, ma femme, mes sœurs, mes frères, mes amis, tous ceux que j'aime et tout particulièrement Haïfa Oueslati, Mohamed Ben Salem, Youssef, Lina et Yahia …

RÉSUMÉ

L’articulation du genou est l’une des articulations les plus complexes du corps humain. Elle est exposée à des charges et des mouvements de grandeurs importantes pendant les activités professionnelles, récréatives et même quotidiennes. Cet environnement mécanique exigeant l’expose à diverses contraintes et déformations excessives, des blessures impliquant à la fois les articulations patello-fémorales (PF) et tibio-fémorales (TF). L'arthrose (OA) est l'un des troubles musculo-squelettiques les plus répandus touchant environ 27 millions d'adultes aux États-Unis seulement. La rupture du ligament croisé antérieur (LCA) est également une lésion articulaire commune avec une prévalence beaucoup plus élevée chez les sujets féminins que chez les sujets masculins. Une bonne connaissance de la biomécanique fonctionnelle de l’articulation du genou et des facteurs qui l'affectent, dans des conditions saines et pathologiques, est une condition préalable pour élaborer des stratégies efficaces pour la prévention et le traitement de ces blessures.

Les modèles musculo-squelettiques (MS) de l'extrémité inférieure promettent d'améliorer notre compréhension de la fonction articulaire du genou, de ses blessures et aussi des programmes de prévention et des traitements associés. Plusieurs modèles analytiques et d'éléments finis (EF) avec différents degrés de précision et de raffinement ont été développés. Ils se sont présentés comme une alternative fiable aux méthodes expérimentales qui ont des limitations majeures, principalement liées à leurs coûts élevés, aux difficultés liées aux précisions des mesures et à la reproduction parfois impossible de certaines situations physiologiques. Cependant, de nombreuses hypothèses sont souvent formulées dans certains modèles MS (lors de l'estimation des forces musculaires et des forces de contacts articulaires). Le genou est généralement idéalisé comme une articulation 2D avec son mouvement contraint dans le plan sagittal, négligeant ainsi les déplacements et les équations d'équilibre dans les plans restants. Avec les forces musculaires estimées, l'équilibre statique dans le plan frontal est donc considéré pour estimer les forces du plateau tibial négligeant la résistance passive du genou, la géométrie articulaire, et en supposant des centres de contact médial/latéral fixes.

Pour évaluer les effets de telles hypothèses, un modèle MS hybride de l'extrémité inférieure incluant un modèle élément finis (EF) du genou 3D a été utilisé pour simuler la phase d’appui de la marche. Ce modèle EF est constitué de trois structures osseuses (tibia, fémur et

patella) et leurs couches de cartilage articulaires, les deux ménisques, les principaux ligaments TF (LCA; ligament croisé antérieur, LCP; ligament croisé postérieur, LCL; ligament collatéral latéral, LCM; ligament collatéral médial) et PF (LPFM; ligament PF médial, LPFL; ligament PF latéral), le tendon rotulien (TP), et les différents composants des muscles du quadriceps, du hamstring et de gastrocnemius. Les cartilages articulaires et les ménisques ont été représentés comme des matériaux composites non linéaires formés d'une matrice hyperélastique renforcée par des réseaux des fibres de collagène non-homogène. Les structures osseuses ont été représentées comme des corps rigides et les ligaments ont été modélisés par des ressorts non linéaires avec des déformations initiales.

(1) L'effet de la variation de la pente postière du tibia (PTP) par ± 5° (± 10°) sur la biomécanique de l'articulation du genou en général et sur la force/déformation du LCA en particulier a été étudié (1) sous l'action d'une force de compression (1400N) avec le modèle du genou passif en plusieurs angles de flexion et (2) durant la phase d'appui de la marche dans le modèle MS. Pour étudier l'effet de la PTP en compression, quatre angles de flexion ont été étudiés (0, 15, 30 et 45°) et la force a été appliquée au niveau du point d'équilibre mécanique (MBP);le point où l'application de la force de compression ne génère aucune rotation.

(2) Afin d'étudier l'effet de certaines hypothèses généralement considérées dans les modèles MS (modèle 2D au lieu 3D), en négligeant les rotations et les équations d'équilibre dans les plans hors-sagittal, le modèle a été considéré comme un modèle 2D et les résultats ont été comparés aux résultats du modèle de référence 3D.

(3) L'effet de la variation du moment varus/valgus versus l'effet de la variation de la rotation varus/valgus sur le chargement du plateau médial a été également étudié en variant ces deux mesures par l'écart-type enregistré durant la marche des sujets sains tel que rapporté dans la littérature.

(4) Enfin, nos prédictions ainsi que celles de nos travaux antérieurs, durant la phase d'appui de la marche, ont été utilisées pour localiser exactement les centres de contact et les comparer à ceux localisés par d'autres méthodes.

Pour simuler la marche humaine avec notre modèle MS, la cinétique (les moments de la hanche/genou/cheville et la force de réaction au sol) et la cinématique (rotations de la hanche, du

genou et de la cheville) ont été collectées à partir des mesures in-vivo des sujets asymptomatiques/OA durant la marche. Les forces de réaction au sol étaient également basées sur des mesures in-vivo. La cohérence de ces deux ensembles (moment et GRF) a été assurée en appliquant la force de réaction à l'endroit qui génère les moments articulaires du genou rapportés dans les études antérieures. Les analyses ont été effectuées dans six périodes de la phase d'appui; 0, 5, 25, 50 et 100%. À chaque période, les forces musculaires ont été évaluées itérativement, en utilisant la technique d'optimisation statique, et appliquées comme des forces externes supplémentaires avec les forces de réaction au sol, le poids de jambe/pied et les rotations/moments des joints. Le modèle MS et du genou sont basés sur un sujet féminin avec 61.9 Kg poids du corps (BW).

Durant la phase d'appui de la marche, les variations de la PTP ont modérément affecté les forces musculaires et les forces de contact. La translation tibiale antérieure et la force du LCA augmentent avec une PTP plus grande et diminuent avec une PTP plus petite. À 50% de la phase d'appui, la force du LCA passe d'une valeur référence de 181N à une valeur de 317N (460N) avec une augmentation de la PTP par 5° (10°), et de sa valeur référence à 102N (0N) avec une diminution de la PTP par -5° (-10°). En outre, la variation de la PTP par ± 5° ou ± 10° a eu des effets négligeables sur les forces de contact totales. En diminuant la PTP par 10°, la position du le centre du contact (CC) se déplace antérieurement dans tous les cas, atteignant un pic de 5,2 mm sur le plateau médial et 5,6 mm sur le plateau latéral. De même, dans le modèle passif, avec une PTP plus grande, la force du LCA augmente considérablement à tous les angles de flexion. La portion de la force transportée par le faisceau LCA-am augmente avec l'angle de flexion, passant de 1% en pleine extension (0°) à 43% à un angle de flexion de 45°. En revanche, une diminution de la PTP par 5° décharge complètement la force du LCA même en pleine extension, mais augmente plutôt les forces du LCL et du LCP (en particulier lorsque la flexion augmente). Conformément à des études d'imagerie antérieures, nos résultats montrent qu'une PTP plus grande est un facteur de risque pour le chargement du LCA et de sa vulnérabilité aux blessures. Les programmes de réadaptation et de prévention des lésions du LCA pourraient bénéficier de ces résultats.

Durant la phase d'appui de la marche, les forces de contact sont plus grandes sur le plateau latéral au début de la phase (0 et 5%) et sur le plateau médial pour le reste (de 25 à 100%). On calcule des grandes excursions de la position du CC (> 17 mm), en particulier sur le

plateau médial dans la direction médio-latérale (ML). Les différentes méthodes utilisées pour localiser le CC, révèlent des CC très différents avec des variations beaucoup plus grandes (~ 15 mm) dans la direction ML sur les deux plateaux. Nos prédictions montrent qu'il faut tenir compte des grands mouvements dans la localisation de CC lorsque l'on essaie d'estimer les forces de contact durant la marche.

En négligeant les rotations et les équations d'équilibre dans les plans hors-sagittals, des moments assez grands non équilibrés, allant jusqu'à 30Nm moment varus et 12Nm moment interne, ont été trouvés avec le modèle 2D à 25% de la phase. La considération du genou comme un joint 2D diminue considérablement les forces musculaires, la force du LCA et les forces de contact comparativement au modèle de référence 3D. À 25% de la phase d'appui, la force de contact totale de 4.2BW calculée dans le modèle 3D diminue à 3.0 BW dans le modèle 2D. La position du CC sur chaque plateau change de façon considérable également (jusqu'à 5 mm). Les forces de contact changent également en utilisant le modèle 1D (la position des centres de contact sur chaque plateau est fixe). En comparant les 3 modèles, nos prédictions mettent en évidence l'importance de la simulation précise des mouvements 3D et des équations d'équilibre ainsi que les propriétés passives des joints et des centres de contact.

Au fur et à mesure que la rotation varus augmente (avec un moment varus constant), la force des hamstrings latéraux diminue et celle des hamstrings médiaux augmente. À 25/75% de la phase d'appui, la diminution de la rotation varus (de + SD à -SD avec moment constant) a réduit considérablement la force de contact médiale par 44/30% et le rapport entre la force médiale et latérale ainsi que celle de la surface de contact par 92/79% et 64/51%, respectivement. En revanche, la diminution équivalente du moment varus (avec rotation constante) a eu peu d'effets (<7%). Ces résultats indiquent clairement une mauvaise corrélation entre la variation du moment varus/valgus et la répartition de charge sur le plateau TF, suggérant que la rotation VV devrait être la mesure principale de la répartition des charges articulaires et des interventions de prévention et de traitement associés.

Les prédictions sur la cinématique articulaire, les forces ligamentaires, et les forces et pressions de contact concordent avec les résultats rapportés dans la littérature. Les prévisions actuelles ont des implications importantes dans l'évaluation et le traitement appropriés des

troubles de l'articulation du genou afin d'éviter non seulement d'autres blessures mais aussi de retrouver un fonctionnement proche de la normale pour l'ensemble du joint.

ABSTRACT

Human knee joints experience loads and movements of substantial magnitudes during occupational, recreational and even regular daily living activities. This demanding mechanical environment exposes them to a host of painful and debilitating deformities, injuries and degenerations involving both patellofemoral (PF) and tibiofemoral (TF) articulations. Osteoarthritis (OA) is one of the most prevalent musculoskeletal (MS) disorders affecting approximately 27 million adults in the US alone. ACL rupture is, also, a common joint injury with much higher prevalence reported in female athletes compared to their male counterparts. Effective preventive measures and treatment managements of such disorders require a sound knowledge of the joint behavior in both healthy and pathologic conditions.

MS modeling of the lower extremity is promising to improve the current understanding of the knee joint function and injuries and consequently associated prevention and treatment programs. Several analytical and finite element (FE) models with different degrees of precision and refinement have been developed. They are considered as a reliable alternative to experimental methods that have major limitations, mainly related to their high costs, difficulties related to measurement accuracy and reproduction of some physiological situations. However, numerous assumptions are often made in some MS models (when estimating muscle forces and joint contact loads). The knee is commonly idealized as a planar (2D) joint with its motion constrained to remain in the sagittal plane, neglecting thus both displacements and equilibrium equations in remaining planes. With muscle forces predicted, the static equilibrium in the frontal plane is consequently considered to estimate tibial compartmental loads neglecting the knee joint passive resistance, the knee geometry, and assuming medial/lateral contact centers.

To evaluate the effects of such assumptions, a hybrid MS model of the lower extremity incorporating a detailed validated 3D knee FE model was used to simulate the stance phase of gait. This model of the knee joint is made of bony structures (tibia, femur and patella) and their compliant cartilage layers as well as menisci, major TF (anterior cruciate ligament, ACL; posterior cruciate ligament, PCL; lateral collateral ligament, LCL; medial collateral ligament, MCL) and PF (medial PF ligament, MPFL; lateral PF ligament, LPFL) ligaments, patellar tendon (PT), and lower extremity muscles (e.g., quadriceps, hamstrings and gastrocnemius). Articular cartilage layers and menisci are simulated as non-homogeneous depth-dependent composites of

nonlinear collagen fibril networks and hyperelastic matrices while the bony structures are represented as rigid bodies. Ligaments are each simulated by a number of nonlinear axial elements with initial pre-strains and non-linear material properties.

(1) The effect of $\pm5^{o}$ (and $\pm10^{o}$) changes in posterior tibial slope (PTS) on knee joint biomechanics in general and ACL force/strain in particular was investigated under 1400N compression force in the passive model alone and during the entire stance phase of gait in the MS model. To study the effect of PTS under compression we used the isolated unconstrained passive tibiofemoral (TF) joint of the whole model at four different knee flexion angles (0^{o}-45^{o}). The compression force was applied at the joint mechanical balance point (MBP) causing no varus/valgus and internal/external rotations.

(2) The model was also used to comprehensively investigate the effects of 2D representation of the joint on predicted results. While simulating gait and using a hybrid lower extremity model that incorporates a detailed validated 3D finite element model of the knee joint, analyses were repeated with out-of-sagittal plane rotations and moment equilibrium equations neglected (2D model) and tibial compartmental forces estimated using equilibrium in the frontal plane while disregarding passive resistance and assuming fixed contact centers (1D model).

(3) This study also examined the validity of certain reported strategies used in vivo to decrease the medial tibial contact force during the stance phase of gait by reducing knee adduction moment (KAM) that is considered as a surrogate measure of medial compartmental loading. Results of altered KAM (by reported ±SD) during gait were compared with those of altered knee adduction angle (KAR, by reported ±SD).

(4) Finally, the predicted results of our model studies on biomechanics of the knee joint during the stance phase of gait in normal and OA subjects, varus-valgus altered subjects (at mid-stance period) and subjects with different posterior tibial slope were used to estimate total contact forces (CF) and location of contact centers (CC) on the medial and lateral plateaus. Using foregoing contact results, six methods commonly used in the literature were also applied to estimate and compare locations of CC at different periods.

To drive the MS model, kinetics (hip/knee/ankle joint moments and GRF) as well as kinematics (hip/knee/ankle joint rotations) data were taken from the mean of asymptomatic and severe knee OA subjects collected in gait. Ground reaction forces were based on reported measurements. The consistency of these two datasets at various periods of gait were assured by applying the latter forces on the foot at locations that generate the knee joint moments reported in the gait studies. Analyses were performed at six periods of the stance phase; 0% (heel strike), 5%, 25%, 50% (mid-stance), 75% and 100% (toe off). At each period, muscle forces were evaluated iteratively, using static optimization, and applied as additional external forces along with the ground reaction forces and in vivo joint rotations/moments. In our analyses, a body weight of 61.9 kg was considered for our female hybrid lower extremity model.

Changes in PTS moderately affected muscle forces and joint contact forces at stance phase of gait. Both active (at stance period) and passive (at all flexion angles) models showed a substantial increase in the anterior tibial translation and ACL force as PTS increased with reverse trends as PTS decreased. In the active model of gait at mid-stance, ACL force increased from 181 N to 317 N and 460 N as PTS increased by 5^o and 10^o, respectively, while dropped to 102 N and 0 N as PTS changed by -5^o and -10^o, respectively. These effects are caused primarily by change in PTS at the tibial plateau that carries a larger portion of joint contact force. Variations in the posterior tibial slope by ±5° or ±10° had negligible effects on total CFs. The location of CC shifted anteriorly in all cases, reaching peaks of 5.2 mm on the medial and 5.6 mm on the lateral plateaus for the case with 10^o flatter tibial slope. On the medial plateau with much larger CF, CC shifted medially by 1.3 mm in 10^o steeper posterior tibial slope whereas laterally by 2 mm in 10^o flatter slope. The ACL force substantially increased at all flexion angles in steeper PTS with a clear gradual shift from its posterlateral bundle (ACLpl) that carries almost the entire force (99%) at smaller flexion angles to its anteromedial bundle (ACLam) that resists 43% of the total force at 45^o flexion. In contrast, flattening of PTS by 5^o completely unloaded ACL force even at full extension but instead markedly increased forces in LCL and PCL (especially as joint flexion increased). The anterolateral bundle of PCL carried larger shares as flexion increased reaching a maximum of 80% at 45^o. In accordance with earlier imaging studies, steeper PTS is a major risk factor, especially under activities with large compression, in markedly increasing ACL force and its vulnerability to injury. Rehabilitation and ACL injury prevention programs could benefit from these findings.

TF joint contact forces were greater on the lateral plateau very early in stance and on the medial plateau thereafter during 25-100% stance periods. Large excursions in the location of CC (>17 mm), especially on the medial plateau in the mediolateral direction, were computed. Use of various reported models caused quite different CCs with much greater variations (~15 mm) in the mediolateral direction on both plateaus. Compared to our accurately computed CCs taken as the gold standard, the centroid of contact area algorithm yielded least differences (except in the mediolateral direction on the medial plateau at ~5 mm) whereas the contact point and weighted center of proximity algorithms resulted overall in greatest differences. Large movements in the location of CC should be considered when attempting to estimate TF compartmental contact forces in gait.

Large unbalanced out-of-sagittal plane moments reaching peaks of 30 Nm abduction moment and 12 Nm internal moment at 25% stance period were computed that were overlooked in the 2D model. Consideration of the knee as a planar 2D joint substantially diminished muscle forces, anterior cruciate ligament force and tibiofemoral contact forces/stresses when compared to the 3D reference model. Total tibiofemoral contact force peaked at 25% stance at 4.2 BW in the 3D model that dropped to 3.0 BW in the 2D model. The location of contact centers on each plateau also noticeably altered (by as much as 5 mm). Tibiofemoral contact forces further changed when the location of contact centers on each plateau was fixed. Results highlight the importance of accurate simulation of 3D motions and equilibrium equations as well as passive joint properties and contact centers.

As KAR increased (at constant KAM), so did the passive moment resistance of the knee joint which as a result substantially reduced forces in lateral hamstrings while increasing those in medial hamstrings. At 25/75% stance as two highly loaded periods of gait, the drop in KAR (from +SD to –SD while at constant KAM) drastically reduced the medial contact force by 44/30% and the medial over lateral contact load and area ratios by 92/79% and 64/51%, respectively. In contrast, the equivalent decrease in KAM (at constant KAR) had little effects (<7%) showing no sensitivity to changes in KAM alone. These findings clearly indicate a poor correlation between KAM and TF load distribution suggesting instead that KAR should be the focus as the primary surrogate measure of knee joint load partitioning and associated prevention and treatment interventions.

The predicted results on joint kinematics, ligament forces and contact forces/pressures were found in general agreement with reported results in the literature. The current predictions have important implications in proper evaluation and treatment of knee joint disorders in order to not only prevent further injuries and degenerations but to regain a near-normal function of the entire joint.

TABLE DES MATIÈRES

LISTE DES TABLEAUX

LISTE DES FIGURES

LISTE DES SIGLES ET ABRÉVIATIONS

ACL	anterior cruciate ligament
AP	antéro-postérieur
ATT	anterior tibial translation
BFLH	biceps femoris long head
BFSH	biceps femoris short head
CC	contact center
FC	force de contact
GM	gastrocnemius médial
GL	gastrocnemius latéral
GRF	ground reaction force
LCA	ligament croisé antérieur
LCL	ligament collateral lateral
LCP	ligament croisé postérieur
LPFL	ligament patellofemoral lateral
MBP	mechanical balance point
MCL	medial collateral ligament
ML	medio-latéral
MPFL	medial patellofemoral ligament
MS	musculosqueletique
OA	osteoarthritis
PCL	posterior cruciate ligament
PF	patellofemoral
PTS	posterior tibial slope

PT	patellar tendon
PTP	pente tibiale postérieure
RF	rectus femoris
SM	semimembranous
TF	tibiofemoral
TFL	tensor facia lata
VMO	vastus medilalis oblique
VI	vastus intermidus
VM	vastus medialis
VL	vastus laterlalis

LISTE DES ANNEXES

CHAPITRE 1 INTRODUCTION

L’articulation du genou est l'une des articulations biologiques les plus complexes du corps humain, à la fois solide, flexible et résistante. Elle présente, en effet, le paradoxe de devoir assurer des fonctions antagonistes comme celle de transmettre des charges très importantes et celle d’assurer la mobilité et la stabilité de la jambe (Hafedh Marouane, 2012). En raison de son emplacement distal dans le corps, de ses grands mouvements relatifs et en raison des charges importantes qu'elle supporte (poids du corps et les charges externes), cette structure est très susceptible aux blessures qui touchent à la fois les articulations tibio et patelo-fémorales (TF et PF).

La lésion du ligament croisé antérieur (LCA) est l’une des blessures les plus fréquentes au genou, avec une prévalence beaucoup plus élevée chez les femmes que chez les hommes (Agel, Arendt, & Bershadsky, 2005; Hutchinson & Ireland, 1995; Jones & Rocha, 2012; E. G. Meyer, Baumer, Slade, Smith, & Haut, 2008); Hutchinson and Ireland 1995; Jones and Rocha 2012; Meyer et al. 2008). Cette lésion est la blessure sportive la plus courante avec ~ 100000 nouvelles blessures par an aux États-Unis à un taux de reconstruction de ~ 50% (Jones & Rocha, 2012). Elle est, généralement, accompagnée par une perte au niveau de la stabilité sagittale et rotatoire de l'articulation du genou (A. A. Amis, 2012; K. L. Markolf, Gorek, Kabo, & Shapiro, 1990) et entraîne, également, des effets débilitant à long terme. En effet, les maladies dégénératives comme l'arthrose (OA) sont évidentes dans le genou affecté, peu de temps après la chirurgie reconstructive (Daniel et al., 1994; Lohmander, Östenberg, Englund, & Roos, 2004). Cette dernière affecte le genou plus que tout autre articulation porteur de poids dans le corps humain et est présente dans ~ 13% de la population générale et > 70% dans la population de plus de 65 ans aux États-Unis (Guilak, 2011). La prothèse du genou est rapportée comme une procédure chirurgicale efficace et fiable, permettent le soulagement des douleurs, l’amélioration fonctionnelle et la satisfaction du patient atteint d'arthrite du genou en phase terminale (Bourne, Chesworth, Davis, Mahomed, & Charron, 2010; Bourne, McCalden, MacDonald, Mokete, & Guerin, 2007). Sur la base de ce succès et d'un nombre croissant de candidats chirurgicaux atteints d'arthrite avancée du genou, la demande d'arthroplasties totales du genou devrait augmenter de 673% à 3,48 millions de procédures aux États-Unis d’ici 2030 (Kurtz, Ong, Lau,

Mowat, & Halpern, 2007). Ainsi, une bonne compréhension de la biomécanique de l'articulation du genou est nécessaire pour améliorer à la fois la prévention et le traitement de ces blessures.

Dans ce contexte, l'un des buts les plus importants de la recherche en biomécanique du genou est de bien comprendre les risques derrière les blessures et les dégénérescences qui touchent l'articulation, telle que la rupture du LCA. Toutefois, ces risques sont probablement multifactoriels (Hashemi et al., 2010; Renstrom et al., 2008). Ils peuvent être la combinaison des variables anatomiques, neuromusculaires, génétiques et environnementales (Arnason, Gudmundsson, Dahl, & Johannsson, 1996). Celles liées à l'anatomie (la hauteur, le poids, l'alignement anatomique, la largeur de l'échancrure fémorale, la taille du LCA, l'angle Q et la laxité antéropostérieure) ont été bien étudiées et il est prouvé que chacune peut jouer un rôle important qui prédispose l'individu à un risque de lésion du LCA (Hashemi et al., 2010). Mais de nos jours la morphologie articulaire, comme autre facteur de risque, est celle qui suscite le plus d'intérêt (Matsuda et al., 1999; Stijak, Herzog, & Schai, 2008). Cependant, du fait de la complexité du problème et de la diversité des méthodologies utilisées, une controverse existe entre les différents travaux qui ont étudié l'effet de la pente tibiale postérieure (PTP) sur la réponse du joint. En effet, bien que les études basées sur l'analyse des images radiographiques supportent l'hypothèse que la géométrie du plateau tibial est associée aux lésions du ligament croisé antérieur (Boden, Breit, & Sheehan, 2009a; Brandon et al., 2006; Hashemi et al., 2008; Hashemi et al., 2009; McLean, Lucey, Rohrer, & Brandon, 2010; Sonnery-Cottet et al., 2011), les études in-vitro (Fening et al., 2008; Giffin, Vogrin, Zantop, Woo, & Harner, 2004; Nelitz et al., 2013) l'ont rejeté. Toutefois, ces derniers restent douteux vu que l'ostéotomie antérieure, qui est généralement utilisée dans les études cadavériques pour étudier l'effet des changements de la PTP, ne conserve pas les insertions ligamentaires (et donc les orientations et les déformations primaires des ligaments). La modélisation numérique a l'avantage de contourner ces lacunes en modifiant l'une des composantes tout en gardant inchangeable le reste de la structure. À noter également que les facteurs de risques liés aux chargements externes ont été étudiés dans des études in-vitro où la rupture du LCA a été produite dans des genoux cadavériques fléchis à plusieurs angles de flexion sous l'action d'une grande force de compression appliquée seule (E. G. Meyer et al., 2008; E. G. Meyer & Haut, 2005) ou combinée avec un chargement du quadriceps (Wall, Rose, Sutter, Belkoff, & Boden, 2012).

Dans le but de faire face à ces problèmes affectant le joint du genou, plusieurs modèles analytiques et d'éléments finis (EF) avec différents degrés de précision et de raffinement ont été élaborés (M Adouni & Shirazi-Adl, 2014a; Haut Donahue & Hull, 2002; Moglo & Shirazi-Adl, 2005; Pena, Calvo, Martinez, & Doblare, 2006; K.B. Shelburne, Torry, & Pandy, 2006; Wang et al., 2014). Ils se sont présentés comme une alternative fiable aux méthodes expérimentales qui ont des limitations majeures, principalement liées à leurs coûts élevés, les difficultés liées aux précisions des mesures (contraintes et forces de contact) et à la reproduction parfois impossible de certaines conditions (comme par exemple la variation de la PTP). En outre, les modèles EF se sont révélés être en mesure de fournir un éclaircissement précieux sur la biomécanique articulaire, les effets des différents paramètres impliqués et les propriétés mécaniques des tissus biologiques, tout en réduisant le coût et le temps (R. Shirazi, Shirazi-Adl, & Hurtig, 2008). Toutefois, les modèles analytiques sont sujets à des simplifications/hypothèses pouvant affecter les conclusions tirées de ces études. À date, la modélisation numérique détaillée de l'effet de la morphologie articulaire sur la réponse passive/active de l'articulation, l'effet de certaines simplifications (genou 2D, 1D), l'effet de la cinématique/cinétique dans le plan frontal et la position du centre de contact du genou durant la marche ou sous l'action d'une force physiologique comme la force de compression sont des études à effectuer.

CHAPITRE 2 REVUE DE LA LITTÉRATURE

2.1 Anatomie des membres inférieurs

Les membres inférieurs chez les êtres humains sont les membres de la locomotion, permettant aux humains de se maintenir debout et de se déplacer dans l'espace. Ils sont formés de quatre segments (le bassin, la cuisse, la jambe et le pied) liés entre eux par trois articulations: à savoir l'articulation de la hanche, l'articulation du genou et l'articulation du pied.

L'articulation de la hanche est l'articulation la plus proximale du membre inférieur. C'est une articulation sphéroïde qui relie le fémur à l'os coxal. Elle est constituée de deux surfaces articulaires; à savoir la cavité cotyloïde et la tête fémorale. L'articulation du pied, ou plus précisément l'articulation du cou-de-pied, est l'articulation qui permet de joindre la jambe au pied. Se trouvant dans la partie distale du corps, cette articulation permet les mouvements dans les plans sagittal et frontal. L'articulation du genou (Figure2.1), quant à elle, est l'articulation qui permet de joindre la jambe à la cuisse. D'un point de vue anatomique, cette structure est constituée de deux jointures soit: la jointure tibio-fémorale et la jointure patello-fémorale. L'articulation tibio-fémorale est formée de plusieurs surfaces non congruentes; les condyles fémoraux ainsi que le plateau tibial. Ce dernier est formé de deux cavités glénoïdes: la cavité glénoïde médiale et la cavité glénoïde latérale (Mellal, 2010). Chacune des surfaces de l'articulation TF est couverte par des couches de cartilage d'épaisseurs variables, entre lesquelles s'interposent les deux ménisques médial et latéral. Les ligaments assurent la cohésion et la stabilité de cette articulation.

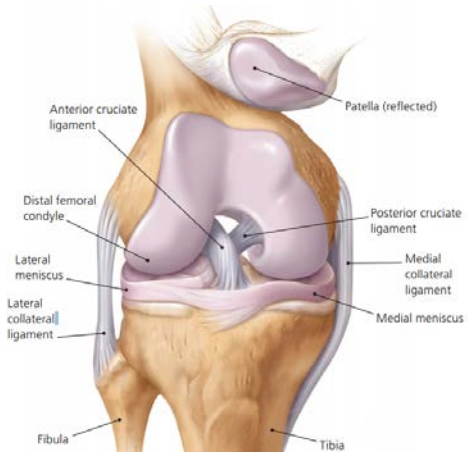

Figure 2.1: L'articulation du genou, adaptée de (Calmbach & Hutchens, 2003).

2.1.1 Bilan articulaire des membres inférieurs

La figure ci-dessous (Figure 2.2) résume les rotations qui peuvent se produire aux niveaux des articulations des membres inférieures. Nous revenons en détail dans une autre section sur la manière dont ces mouvements ont été définis (voir section 2.2.4).

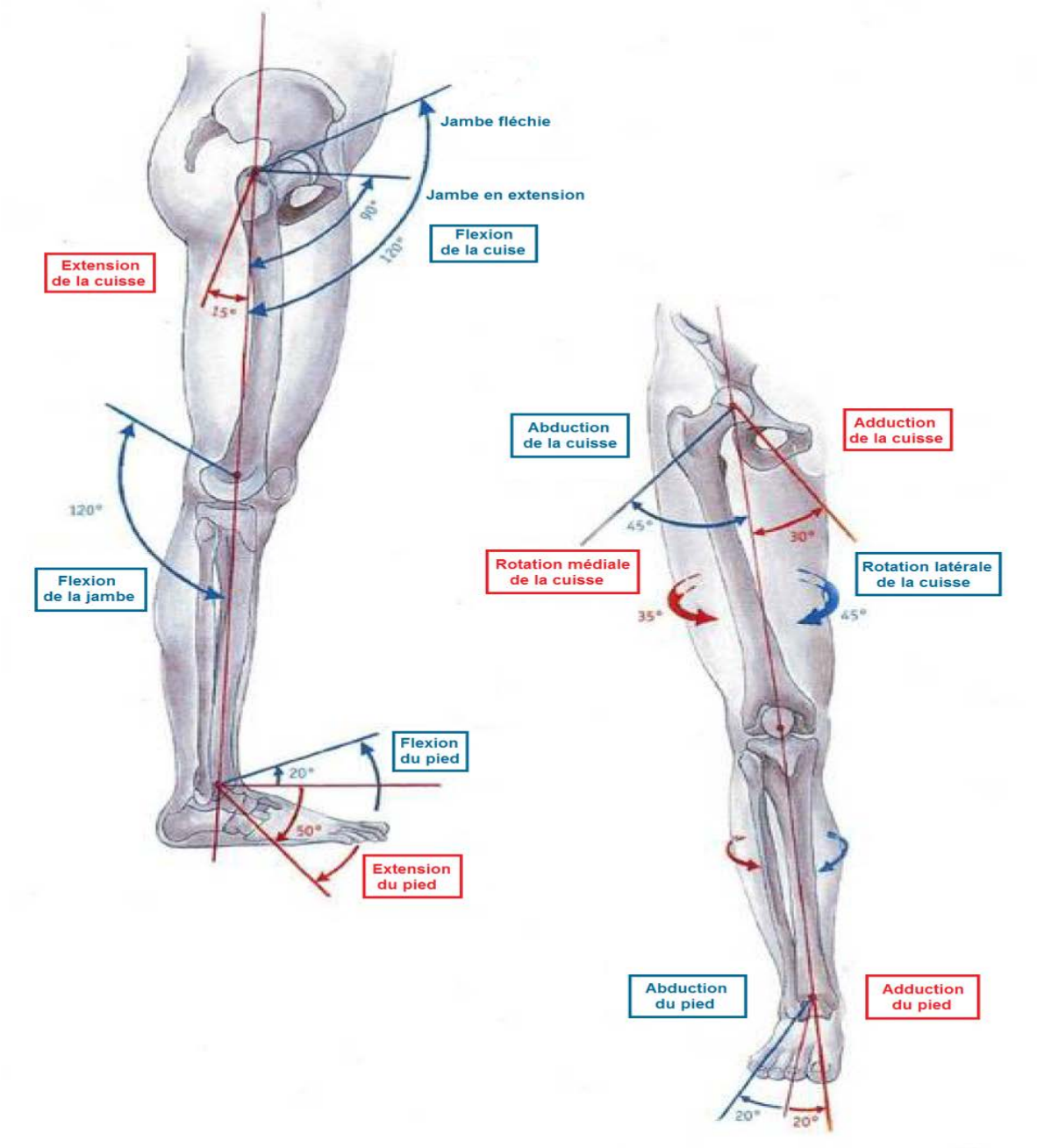

Figure 2.2: Bilan articulaire des membres inférieurs, adaptée du livre ‘’Atlas d’Anatomie’’

2.1.2 Les muscles des membres inférieurs

Comme les segments des membres inférieurs, le système musculaire (Figure 2.3) peut être également divisé en quatre groupes: les muscles de la hanche, de la cuisse, de la jambe et du pied. Chaque muscle a son propre rôle dans le maintien de la stabilité et du contrôle du mouvement durant l'exécution des différentes activités quotidiennes (la phase debout, la marche, le sport…). Nous faisons une description détaillée de ces muscles entourant les joints dans les sous-sections suivantes (Fraysse, 2009; Hughes, Hsu, & Matava, 2002; Viel, 2000).

a. Muscles de la Hanche

Les muscles de la hanche peuvent être classés en quatre catégories:

- Les fléchisseurs: le psoas et l'iliaque sont deux chefs distincts possédant la même insertion distale sur le petit trochanter. Un autre fléchisseur puissant est le droit antérieur (rectus femoris). Le sartorius et le tenseur du fasia lata ont également une action significative (environ le tiers de la puissance du RF durant la flexion de la hanche).
- Les extenseurs: se divisent en deux groupes selon leurs points d'insertions; mono-articulaire et donc s'insèrent sur le fémur ou bien bi-articulaires et s'insèrent sous le genou. Le grand fessier est le seul extenseur mono-articulaire; c'est le muscle le plus volumineux et le plus puissant du corps. Le long-biceps, le demi-tendineux et le demi-membraneux sont les trois extenseurs bi-articulaires. Selon Kapandji (1994) l'efficacité de ces trois muscles pris ensembles est environ deux tiers de celle du grand fessier.
- Les abducteurs: le muscle principal de l'abduction est le moyen fessier. Le petit fessier est essentiellement abducteur et son efficacité est d'environ un tiers de celle du moyen fessier. Toutefois, ces deux muscles sont également fléchisseurs par leurs faisceaux antérieurs et extenseurs par leurs faisceaux postérieurs. Le tensor fascia lata (TFL) est aussi un abducteur puissant lorsque la hanche est en position neutre de flexion-extension.
- Les adducteurs: le principal adducteur est le grand adducteur. Le droit interne possède également une action d'adduction importante. Et avec une action d'adduction bien plus faible, on trouve le moyen et le petit adducteur. Enfin, les trois muscles ischio-jambiers bi-articulaires, à savoir le long biceps, le semi-membraneux et le semi-tendineux, ont aussi une importante action d'adduction de la hanche, bien qu'ils soient principalement extenseurs de la hanche et fléchisseurs du genou.

b. Muscles du genou

Le mécanisme musculaire qui entoure l'articulation du genou est constitué de deux sous mécanismes; à savoir le mécanisme extenseur (quadriceps) et le mécanisme fléchisseur (hamstrings et gastrocnemius). Le premier contient les muscles rectus-femoris (RF), vastus lateralis (VL), vastus intermedius (VIM) et vastus medialis (VM) et le deuxième contient les muscles gastrocnemius latéral (LG), gastrocnemius médiale (MG), biceps femoris (BF short et long heads), semimembranosus (SM) et une combinaison du sartorius (SR), garcilis (GR) et semitendinosus (ST). Ce dernier groupe est appelé le TRIPOD (Figure 2.3).

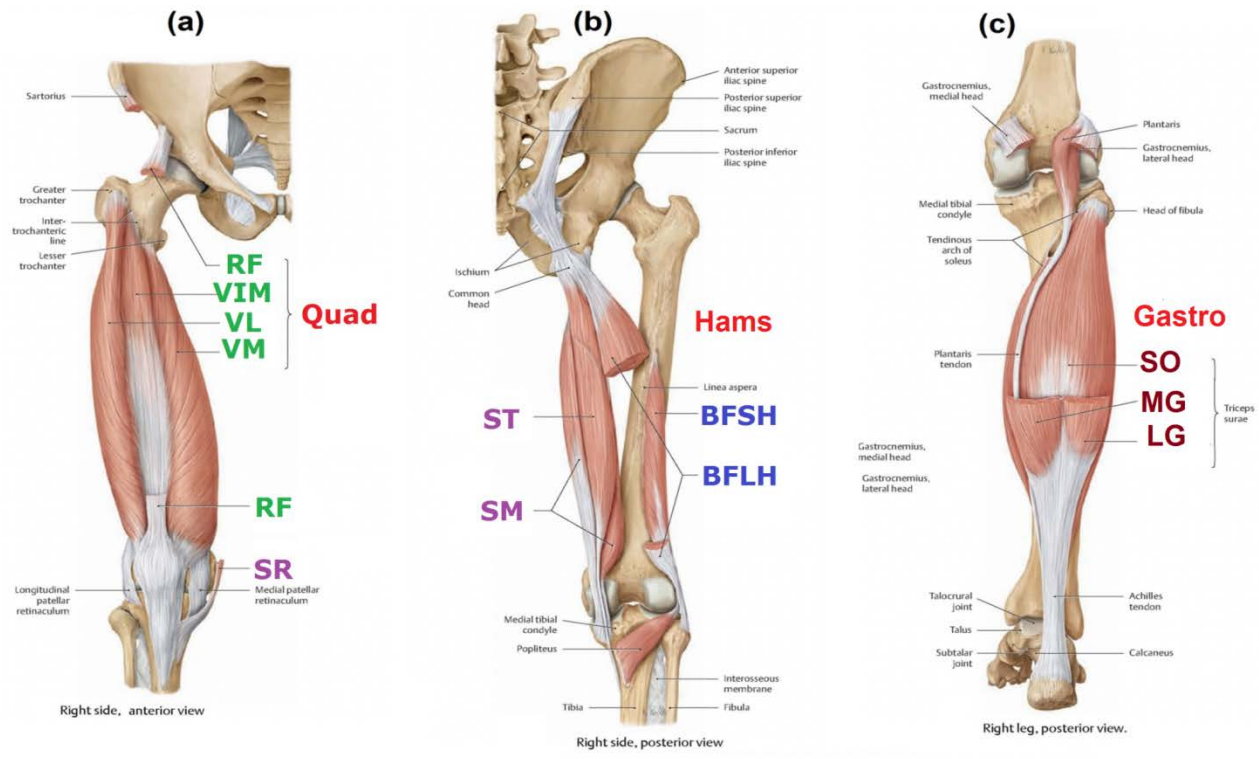

Figure 2.3: Les muscles entourant l'articulation du genou (a) vue antérieure, (b) et (c) vue postérieure (www.thieme.com/taa)

c. Muscles de la cheville

Tous les muscles de la cheville ont à la fois une action de flexion ou d'extension et d'abduction ou d'adduction. Ainsi, ils peuvent être classés en quatre groupes:

- Les fléchisseurs et adducteurs: le jambier antérieur et l'extenseur du gros orteil. Ce dernier est légèrement moins adducteur que l'autre.

- Les fléchisseurs et abducteur: l'extenseur commun des orteils et le péronier antérieur. Le péronier antérieur est beaucoup plus abducteur que l'extenseur commun des orteils.
- Les extenseurs et adducteurs: le jambier postérieur, le fléchisseur commun des orteils et le fléchisseur propre du gros orteil.
- Les extenseurs et abducteur: le long et le court péronier latéral.

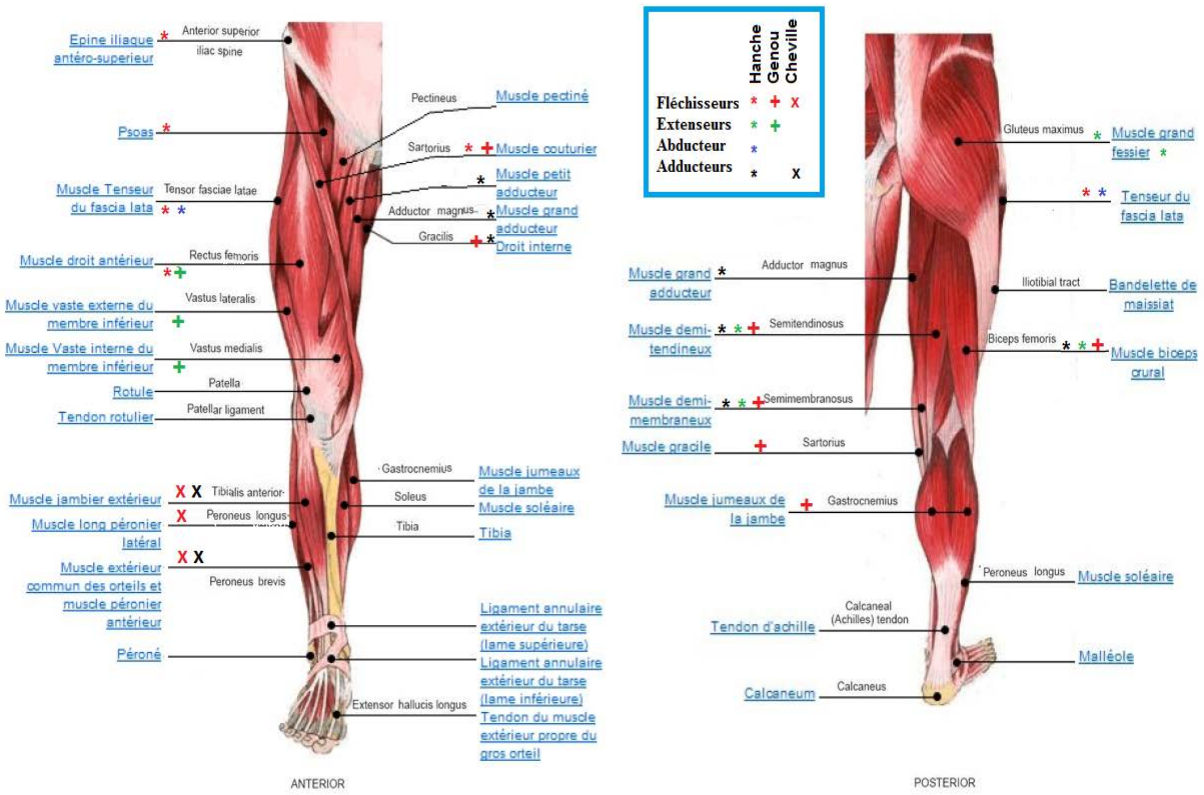

Figure 2.4: Muscles des membres inférieurs (vue antérieure et postérieure)

(http://decathlondom.franceolympique.com/decathlondom/fichiers/pages/fiches_techniques/sante/muscles/muscles-jambes.htm)

2.1.3 Cartilage

En tant que composite non homogène saturé en liquide, le cartilage articulaire assure une articulation lisse entre les surfaces articulaires, absorbe les chocs et répartit les charges appliquées à l'os. La composition et la structure du cartilage articulaire changent avec son épaisseur (Clarke, 1974; Kääb, Ap Gwynn, & Nötzli, 1998; Koay & Athanasiou, 2009; Van C Mow & Guo, 2002; V.C. Mow, Holmes, & Michael Lai, 1984; Ratcliffe, Fryer, & Hardingham, 1984; Shepherd & Seedhom, 1999; Wilson, Huyghe, & Van Donkelaar, 2007). Au niveau de la zone superficielle, les fibres de collagène sont orientées horizontalement parallèlement à la

surface articulaire, alors qu'elles deviennent plutôt aléatoires dans la zone transitionnelle et deviennent finalement perpendiculaires à l'interface os-cartilage dans la zone profonde (Broom & Marra, 1986; Kääb et al., 1998; Minns & Steven, 1977). La teneur en collagène est plus élevée dans les zones superficielle et profonde du cartilage articulaire, et plus faible dans la zone transitionnelle (Van C Mow & Guo, 2002).

2.1.4 Ménisque

Le ménisque est un tissu fibro-cartilagineux semi-lunaire dont les extrémités sont insérées dans l'éminence intercondylienne au niveau du plateau tibial. Il est composé principalement des fibres de collagène de type I, d'eau et de protéoglycanes. Le ménisque médial, en forme de C, accroît la concavité glénoïdienne médiale. Le ménisque latéral, en forme de O, transforme la convexité de la cavité glénoïde latérale en une cavité épousant mieux le condyle externe. Ces ménisques participent à la stabilité et à la lubrification du genou (Levy, Torzilli, Gould, & Warren, 1989; Radin, de Lamotte, & Maquet, 1984), à la protection du cartilage (Fithian, Kelly, & Mow, 1990; Kawamura, Lotito, & Rodeo, 2003; Seedhom, 1979), à la transmission et à l'amortissement des charges (Levy, Torzilli, & Warren, 1982) et à la limitation des mouvements extrêmes de flexion et d'extension (Kawamura et al., 2003; Seedhom, 1979).

2.1.5 Ligaments

Comme les autres tissus mous, les ligaments du genou sont faits d'une substance riche en eau renforcée par des fibres de collagène de type I (Duthon et al., 2006). Quatre ligaments principaux (LCA, ligament croisé antérieur, LCP, ligament croisé postérieur, LCL, ligament collatéral latéral, LCM, ligament collatéral médial), parmi d’autres, contrôlent les mouvements relatifs de l'articulation tibio-fémorale. Selon les conditions de chargement, un ou plusieurs de ces ligaments agissent comme des contraintes primaires pour assurer la stabilité de l'articulation. Les ligaments collatéraux résistent principalement à la rigidité globale de l'articulation sous des moments varus/valgus (K. Markolf, Mensch, & Amstutz, 1976; Nielsen, Rasmussen, Ovesen, & Andersen, 1984), alors que les ligaments croisés résistent au mouvements antérieur/postérieur et aux rotations interne/externe de l’articulation (K. L. Markolf et al., 1995; Sakane et al., 1997). Les ligaments croisés peuvent être chacun séparés en deux faisceaux: antéro-médial (am) et postéro-latéral (pl) pour le LCA, et anéro-lateral (al) et postero-médial (pm) pour le LCP. Des

études cadavériques ont confirmé le rôle principal du LCA-am en flexion et LCA-pl à des angles proches de l'extension au cours de la flexion passive du genou (A. Amis & Dawkins, 1991).

2.2 La marche humaine

2.2.1 Définition

La marche humaine est définie comme un mouvement acquis, permettant le déplacement du corps dans une direction déterminée. Selon Viel (2000), la marche est une activité qui nécessite un apprentissage difficile, et avec le temps sa réalisation devient quasi automatique. Deux conditions sont nécessaires pour se propulser vers l'avant: soit le maintien de l'équilibre du corps lors des différents types d'appuis et la coordination des conditions de la propulsion en s'adaptant à chaque instant aux contraintes de l'environnement extérieur. La vitesse de la marche varie entre 1.3 m/s et 1.64 m/s pour les sujets normaux (Dahlstedt, 1978; Spyropoulos, Pisciotta, Pavlou, Cairns, & Simon, 1991).

2.2.2 Historique de l'analyse de la marche

Datée de 1836, les frères Weber ont fourni la première description claire du cycle de marche en faisant des estimations précises de la cadence de marche et de l'oscillation pendulaire de la jambe d'un cadavre (T. P. Andriacchi & Alexander, 2000; Cappozzo, Marchetti, & Tosi, 1992; Weber & Weber, 1836). Tout de suite après, en 1862, Borelli a estimé le centre de masse du corps humain et a décrit la façon dont l'équilibre est maintenu au cours de la marche par un déplacement constant vers l'avant de l'appui au sol. Et c'est vers la fin du 19^{éme} siècle, que les principales connaissances biomécaniques de la marche humaine ont été acquises grâce aux techniques photographiques introduites par Muybridge (1883) et Marey (1884). Toutefois, ces études restent qualitatives mais introduisent déjà la notion de segments corporels rigides à la base des études actuelles (Figure 2.5).

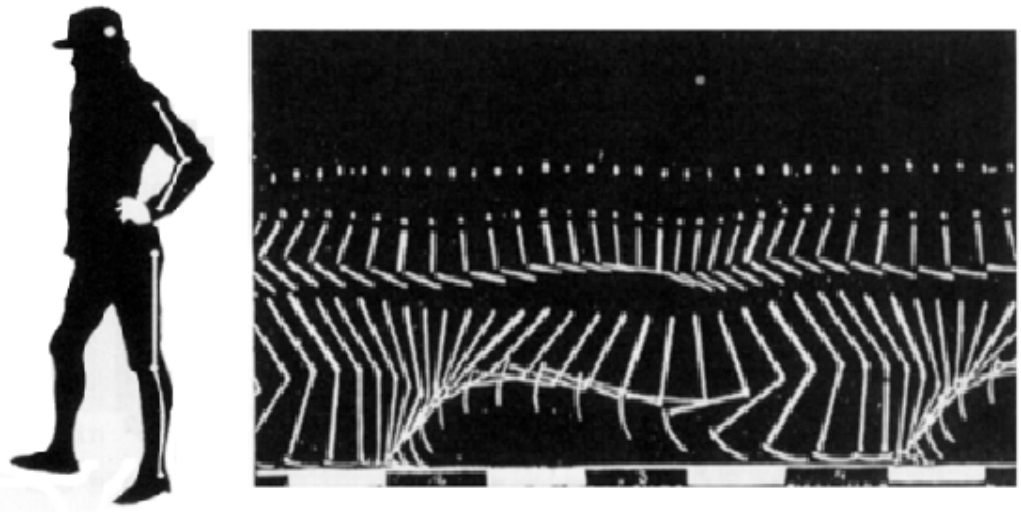

Figure 2.5: Matérialisation des segments corporels par des lignes blanches sur habit noir d'après Marey (1884)

Des analyses approfondies se concentrant sur l'activité musculaire au cours du cycle de marche ont été réalisées par l'équipe de Inman (Inman et al., 1981) avec le but d'évaluer les forces de réaction au sol, l'effet de la gravité sur les segments corporels et les forces d'inertie. Au cours des années 1970 et 1980, le développement des systèmes de capture du mouvement, basés sur l'électronique plutôt que sur la photographie, reliés à des plateformes de force ainsi qu'à des systèmes d'électromyographie a permis de disposer de données tridimensionnelles du mouvement nettement plus précises. Actuellement, les systèmes de mesure les plus performants pour ce type d'étude sont les systèmes d'analyse du mouvement optoélectroniques, utilisant des marqueurs actifs ou passifs pour suivre les trajectoires de segments corporels dans l'espace.

2.2.3 Matériel utilisé

De nos jours, des systèmes d'analyse quantifiée du mouvement sont à la disposition des chercheurs et des cliniciens. Ils associent (Figure 2.6): systèmes optoélectroniques (pour mesurer la cinématique des segments), plates-formes de force (pour l'enregistrement des forces de réaction au sol), matériel vidéo (pour filmer le patient dans plusieurs incidences), système électromyographique (pour enregistrer l'activité des muscles) et parfois des dispositifs de mesure de la consommation d'oxygène ou de la pression plantaire des pieds sur le sol.

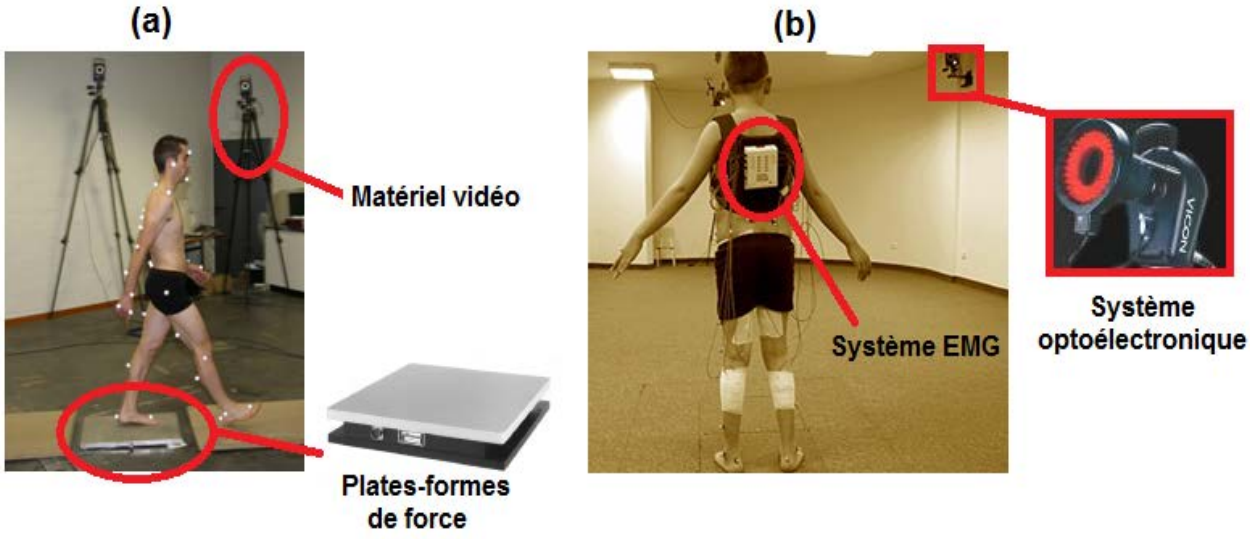

Figure 2.6: Matériel standard d'un laboratoire d'analyse du mouvement. (a) Systèmes utilisant des marqueurs passifs (http://spiral.univ-lyon1.fr), (b) Systèmes utilisant des marqueurs actifs (http://www.jeromelecoq.org)

Schématiquement, les systèmes d'analyse du mouvement peuvent être classés en trois grandes catégories:

- Les systèmes adaptés à des analyses de mouvement globales: ils sont constitués de deux caméras vidéographiques (analogiques ou numériques) qui enregistrent le sujet en mouvement sous deux incidences (généralement face et profil).
- Les systèmes utilisant des marqueurs actifs (Figure 2.6.b): les marqueurs peuvent être soit des diodes émettant des signaux infrarouges, soit des émetteurs de signaux ultrasons. Ces systèmes permettent l'identification automatique des marqueurs ainsi qu'une excellente précision des trajectoires spatiales. Cependant, une des limites est que les marqueurs disposés sur le sujet sont reliés par des fils d'alimentation, ce qui limite les mouvements possibles à analyser tant sur la distance parcourue que sur la complexité du geste.
- Les systèmes utilisant des marqueurs passifs (Figure 2.6.a): les marqueurs sont des sphères de plastique recouvertes de matériau rétroréfléchissant. Ces systèmes travaillent soit en lumière infrarouge soit en lumière rouge et contrairement aux systèmes précédents, le sujet peut ici se déplacer librement dans le champ de vision des caméras.

2.2.4 Terminologie utilisée

a. plans anatomiques et mouvements articulaires

Pour décrire les mouvements des segments corporels on définit trois plans de l'espace tridimensionnel (Figure 2.7):

- Plan sagittal: qui divise le corps humain en portion de droite à gauche.
- Plan frontal (plan coronal): qui divise le corps en portions antérieures et postérieures.
- Plan transversal: qui divise le corps en portions supérieures et inférieures.

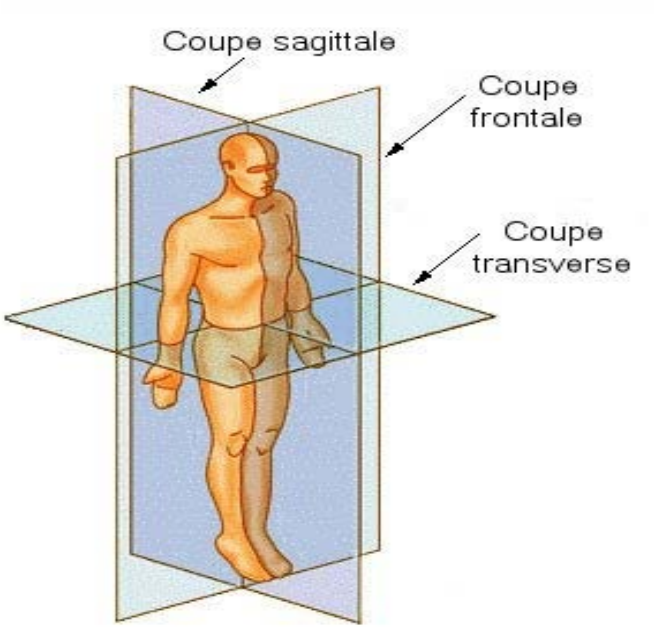

Figure 2.7: Les trois plans de l'espace (https:// upload.wikimedia.org/ wikipedia/ commons/1/17/ Coupe_anatomie.jpg)

Les déplacements articulaires au cours de la marche peuvent être décrits en utilisant les définitions du mouvement dans les trois plans de référence (Figure 2.8). Pour la hanche, et le genou, les rotations dans le plan sagittal sont définies comme la flexion et l'extension. En ce qui concerne la cheville, les rotations dans le plan sagittal sont définies comme la flexion dorsale (dorsiflexion) et la flexion plantaire (plantarflexion). Les mouvements dans le plan frontal sont l'abduction et l'adduction. Les mouvements susceptibles d'apparaitre dans le plan transverse sont les rotations internes et externes.

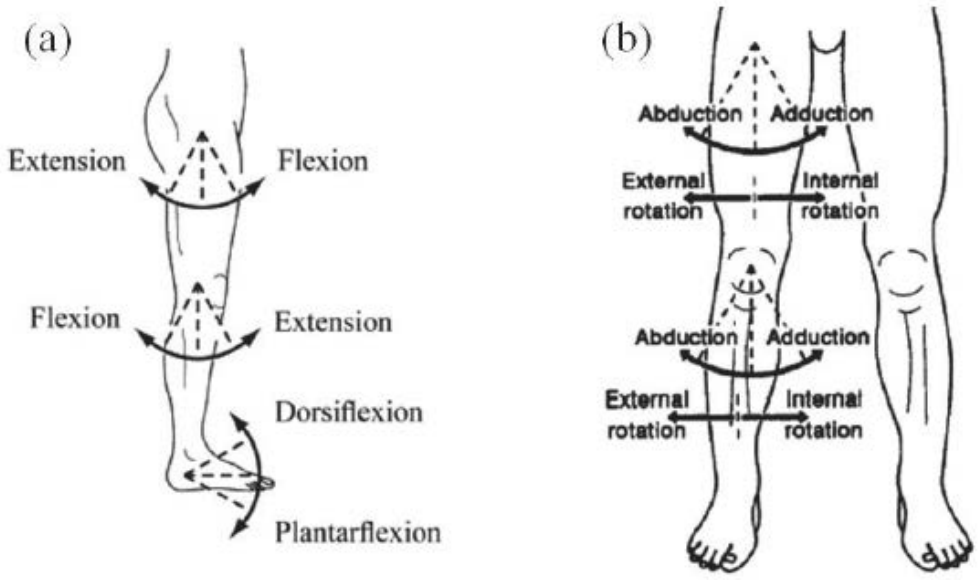

Figure 2.8: Les mouvements des membres inférieurs dans (a) le plan sagittal et (b) le plan frontal

b. Axes du corps humain

Les études expérimentales de la cinétique de l'articulation en trois dimensions nécessitent la description et la mesure des six composantes de mouvement (3 translations et 3 rotations). Quelques aspects importants de toutes les méthodologies de mesure sont la précision, la facilité et l'interprétation clinique lorsque les données sont communiquées aux lecteurs. Dans ce contexte, et afin de décrire la cinématique et la cinétique des membres inférieurs (hanche, genou, cheville), Grood et Santy (1983) ont défini un système d'axe non orthogonal (Figure 2.9) facilitant la communication entre les différentes disciplines. Selon les auteurs, la construction d'un tel système d'axe pour l'articulation du genou ou n'importe quelle autre articulation, nécessite:

- La définition du système de coordonnée cartésienne fixe sur chaque composante.

- La définition des axes fixes et des axes de référence du système de coordonnée du joint.

- Et afin de décrire les translations du joint, définir les positions de deux points de référence situés sur chaque composante.

Le système d'axe de l'articulation du genou est défini par deux axes fixes (sur le tibia et sur le fémur) et un axe flottant. L'axe z du tibia, qui passe distalement à travers le centre de la cheville et proximalement à mi-chemin entre les deux éminences inter-condyliennes, a été choisi comme étant l'axe fixe du tibia. Toutefois, la rotation autour de cet axe est un mouvement

d'intérêt clinique. Pour le segment fémoral, l'axe fixe est l'axe des X (l'axe médial/latéral) qui passe à travers les centres des deux condyles fémorales. Le troisième axe est la perpendiculaire commune à ces deux axes fixes. La rotation flexion-extension prend place autour de l'axe médio-latéral du fémur. La rotation interne-externe se produit autour de l'axe z du tibia et la rotation varus-valgus autour de l'axe flottant. Toutefois, les translations du joint sont décrites par la position relative des deux points de référence situés sur chacune des composantes de l'articulation.

Pour être en mesure de décrire mathématiquement le mouvement de l'articulation, la position du segment distal doit prendre en compte la position du segment proximal (Edward S Grood & Wilfredo J Suntay, 1983). En plus de la détermination des axes du système de coordonnée de l'articulation, l'ordre dans lequel les rotations cliniques sont appliquées est d'une grande importance. Toute orientation souhaitée peut être réalisée en effectuant des rotations dans l'ordre autour des trois axes (Brinckmann, Frobin, & Leivseth, 2002). Grood et Suntay (1983) ont proposé un ordre temporel strict dans lequel les rotations se produisent: en commençant par la rotation dans le plan sagittal, ensuite l'abduction/adduction et pour finir la rotation interne/externe.

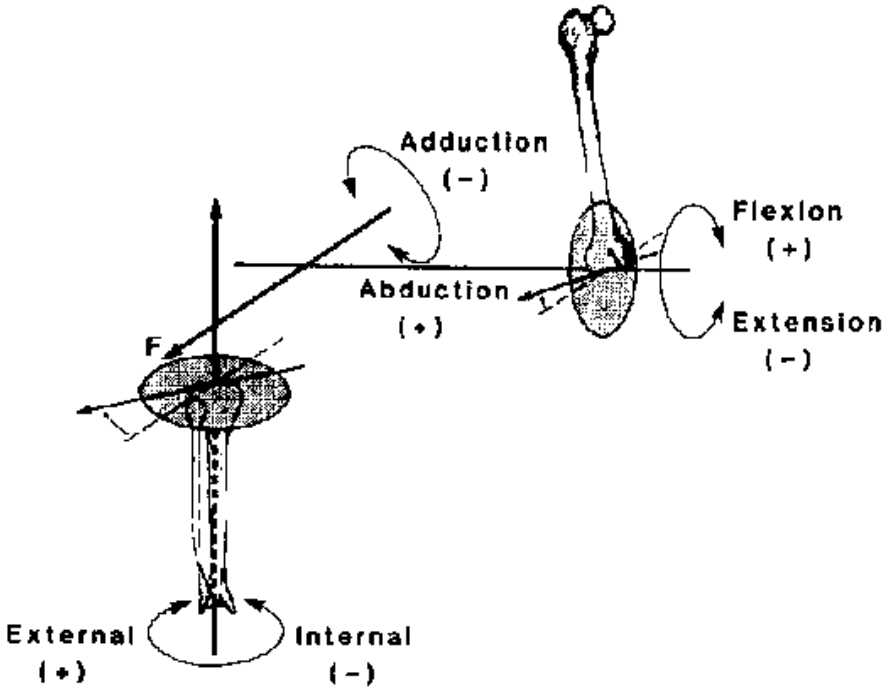

Figure 2.9: Référentiel non orthogonal défini par Grood et Santy (1983), employé pour décrire la cinétique et la cinématique des articulations des membres inférieurs

c. Les paramètres spatio-temporels

Les paramètres spatio-temporels sont couramment étudiés car ils illustrent les caractéristiques de la marche (Titianova, Mateev, & Tarkka, 2004; Viel, 2000; Zatsiorky, Werner, & Kaimin, 1994). Les paramètres principalement retenus sont la vitesse de marche, la longueur du pas, la durée du pas, la durée du déroulement du pas et le temps de propulsion. Concernant la vitesse de marche, différentes études relèvent des vitesses de marche très diverses : Variant de 1,3 m/s à 1,64 m/s pour les sujets normaux (Dahlstedt, 1978; Dujardin, Roussignol, Mejjad, Weber, & Thomine, 1997; Spyropoulos et al., 1991). L'étendue de variable 'vitesse' est importante et montre sa grande variabilité, en fonction des groupes de sujets testés.

d. Cycle de marche

La marche est le déplacement du centre de masse dans la direction de progression du mouvement (dans un plan parallèle au plan sagittal). Le cycle de marche est le temps écoulé entre deux contacts successifs d'un seul pied. Ainsi, un cycle de marche commence lorsque le talon rentre en contact avec le sol et se termine lorsqu'il répond le même contact (Kaufman & Sutherland, 2006). La durée du cycle est d'environ 1 seconde (Bouisset, 2002; Perry & Davids, 1992) et il peut être décomposé en deux phases (Figure 2.10): une phase d'appui (stance phase) qui occupe environ 60% du cycle de marche, et une phase d'oscillation (swing phase) de 40%. Ces phases sont elles-mêmes divisées en petites sous-phases (Shumway-Cook & Woollacott, 2007).

En ce qui concerne la phase d'appui: elle est composée de trois périodes:

- **La réception:** débute lors du contact du talon sur le sol et dure environ 25% de la durée de la phase d'appui (15% du cycle de marche). Au moment du contact, la jambe est inclinée de 25° par rapport à la verticale, la hanche est en flexion, le genou en extension presque complète et le cheville en légère extension. Cette période se termine au moment où le genou est en flexion maximale.
- **La période intermédiaire:** dure environ 42% de la phase d'appui (25 % du cycle de marche). Durant cette période l'appui est unilatéral. Dans le plan sagittal, la hanche qui était fléchie, réalise une extension. Le genou se fléchit d'abord et s'étend ensuite. La cheville est à 0° de flexion dorso plantaire au moment où la jambe oscillante passe à la verticale du pied. Dans le plan transverse (horizontal), les lignes du bassin et des épaules sont perpendiculaires à l'axe

d’avancement. Dans le plan frontal, le bassin est incliné du coté portant alors que l’épaule s’incline coté oscillant.

- **La période de poussée:** qui débute quand le centre de gravité du corps passe à la verticale de la jambe d’appui. Cette période dure 33% de la phase d'appui. Durant cette phase, les actions musculaires du membre inférieur projettent l’ensemble du corps vers l’avant. Dans le plan sagittal, la hanche et le genou tendent vers l’extension, la cheville réalise une flexion dorsale. Dans le plan transverse la hanche et les épaules du côté de l’oscillation passent devant la hanche en appui. Dans le plan frontal, il y a une inclinaison latérale du bassin du côté de la jambe oscillante.

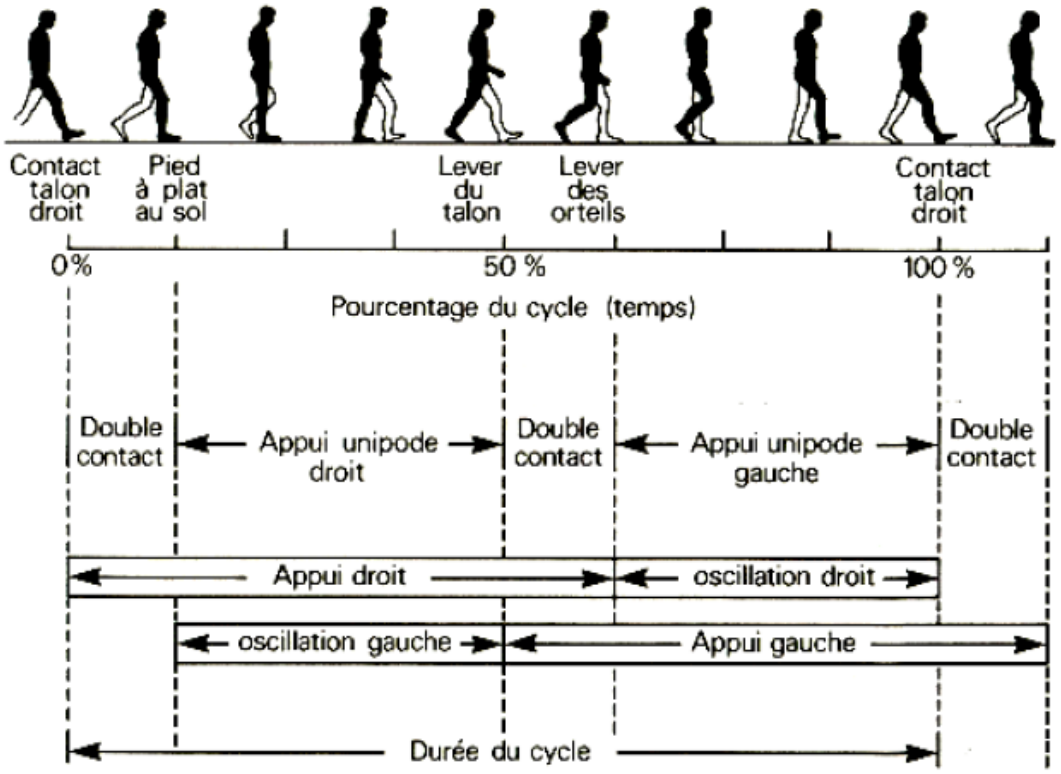

Figure 2.10: Représentation d’un cycle de marche (Viel 2000)

Pour la phase d'oscillation; elle représente 40 % de cycle de marche. Cette phase et comme son nom l'indique, débute lorsque la jambe quitte le sol et devient oscillante (plus précisément lorsque les orteils quittent le sol). Le genou qui est légèrement fléchi quand la jambe quitte le sol, accentue sa flexion jusqu’à ce que la cuisse passe par la verticale. L’extension s’installe alors et elle sera presque complète à l’instant ou la cuisse sera inclinée de 20 à 25° par rapport à la verticale. La cheville passe d’abord en flexion dorsale puis tend vers la flexion

plantaire. Au début de cette phase, la hanche s'élève puis redescend tout en avançant dans la direction du déplacement. Cette phase d'oscillation se termine lorsque le talon reprend contact avec le sol. Sa durée représente 40% de la durée du cycle de marche.

2.2.5 Données cinématiques de la marche

Plusieurs études expérimentales ont été réalisées pour décrire la cinématique des membres inférieurs durant la marche dite ‘‘normale’’, (Anderson & Pandy, 2001; Eng & Winter, 1995; A. E. Hunt, M Smith, Torode, & Keenan, 2001; M. A. Hunt, Birmingham, Giffin, & Jenkyn, 2006; Hurwitz, Sumner, Andriacchi, & Sugar, 1998; Neptune, Zajac, & Kautz, 2004; Perron, Malouin, Moffet, & McFadyen, 2000; C. R. Winby, Lloyd, Besier, & Kirk, 2009; Zajac, Neptune, & Kautz, 2002, 2003). Le but premier était de donner les rotations tridimensionnelles des trois articulations des membres inférieurs; soit la hanche, le genou et la cheville. Selon Plas et al., (1989) l'angle de flexion/extension de l'articulation du genou prend trois phases: la première lors de la phase d'appui (de 15 à 45% du cycle de marche) qui induit une flexion du genou d'environ 20°, la seconde est une phase d'extension jusqu'à 60% du cycle de marche et la troisième est une phase de flexion d'environ 60° afin de faciliter le passage du pied sous le bassin, lors de la phase d'oscillation.

La littérature contient également des travaux qui ont étudié la cinématique de l'articulation tibio-fémorale (Chen et al., 2011; Kozanek et al., 2009; Lafortune, Cavanagh, Sommer Iii, & Kalenak, 1992; Guoan Li, Kozanek, Hosseini, & Liu, 2009). Kozanek et al., (2009) ont utilisé la technique d'imagerie fluoroscopique pour étudier les six degrés de liberté de l'articulation du genou lors de la phase d'appui de la marche sur un tapis roulant. Dans la figure 2.11, on présente les translations relatives du fémur par rapport au tibia, rapportées dans cette étude. À noter que les translations du joint dépendent de la position des points de référence (Edward S Grood & Wilfredo J Suntay, 1983).

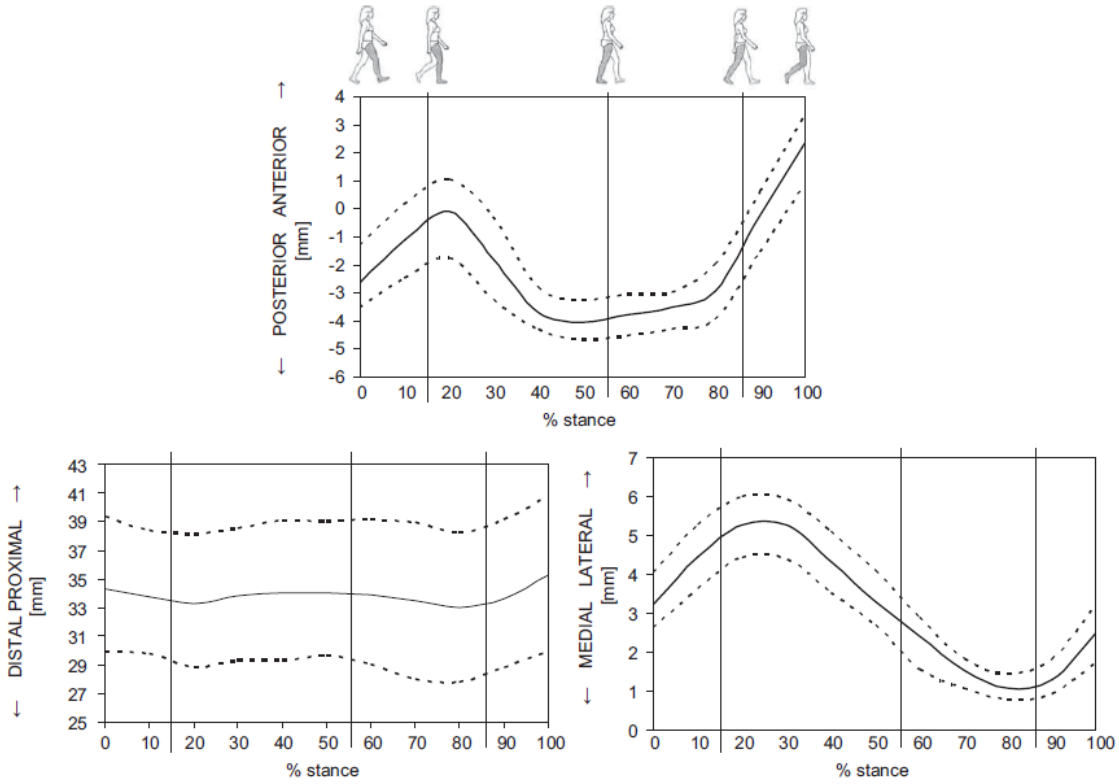

Figure 2.11: Les trois translations de l'articulation du genou rapportés dans l'étude de Kozanek et al., (2009)

Alors que la cinématique dans le plan sagittal est comparable entre les différents travaux, la cinématique dans les plans frontal et coronal (transversal) existe avec une certaine controverse. En effet, l'interprétation des mouvements de l'articulation du genou lors de la marche dans ces plans reste difficile. Les données disponibles sur les mouvements angulaires et linéaires dans le plan transversal et coronal varient en termes de quantité et de direction ce qui laisse des ambiguïtés pour notre compréhension des mouvements physiologiques (Dyrby & Andriacchi, 2004; Kozanek et al., 2009; Lafortune et al., 1992; Landry, McKean, Hubley-Kozey, Stanish, & Deluzio, 2007; Ramakrishnan & Kadaba, 1991). La méthodologie utilisée est sans doute la cause première derrière ce problème. En effet les méthodes utilisées comprennent des erreurs importantes dues à la peau et aux mouvements des tissus mous (Akbarshahi et al., 2010; T. Andriacchi, Alexander, Toney, Dyrby, & Sum, 1998; Dyrby & Andriacchi, 2004; Pandy & Andriacchi, 2010).

Une controverse existe entre les travaux qui ont étudié les mouvements de l'articulation tibio-fémorale. Certaines études ont rapporté une rotation fémorale externe durant la phase

d'appui de la marche (T. Andriacchi et al., 1998; Dyrby & Andriacchi, 2004; Lafortune et al., 1992) et d'autres ont trouvé que le centre de rotation du genou dans le plan transversal est situé essentiellement sur le côté latéral de l'articulation (Koo & Andriacchi, 2008). Ces résultats, qui suggèrent que le condyle interne du fémur devrait faire plus d'excursions que son latéral du fait qu'il est plus éloigné du centre de rotation, ont été supportés par l'étude de Kozanec et al., (2009). Toutefois, cela est contradictoire avec d'autres travaux (Cappozzo et al., 1992; Dennis, Mahfouz, Komistek, & Hoff, 2005; Guoan Li, DeFrate, Park, Gill, & Rubash, 2005; Guoan Li, Moses, et al., 2006; Logan et al., 2004; K.B. Shelburne et al., 2006) qui affirment que le condyle fémoral interne est moins mobile que le condyle latéral. Dans le but comprendre et de visualiser la différence entre les différents travaux présentés dans la littérature, nous avons mené une étude comparative (J.L Astephen, 2007; Gao & Zheng, 2010; Kadaba, Ramakrishnan, & Wootten, 1990; Kozanek et al., 2009; Perron et al., 2000; Sutherland, 2001; Whittle, 1996; Zhang, Shiavi, Limbird, & Minorik, 2003) dans la figure 2.12.

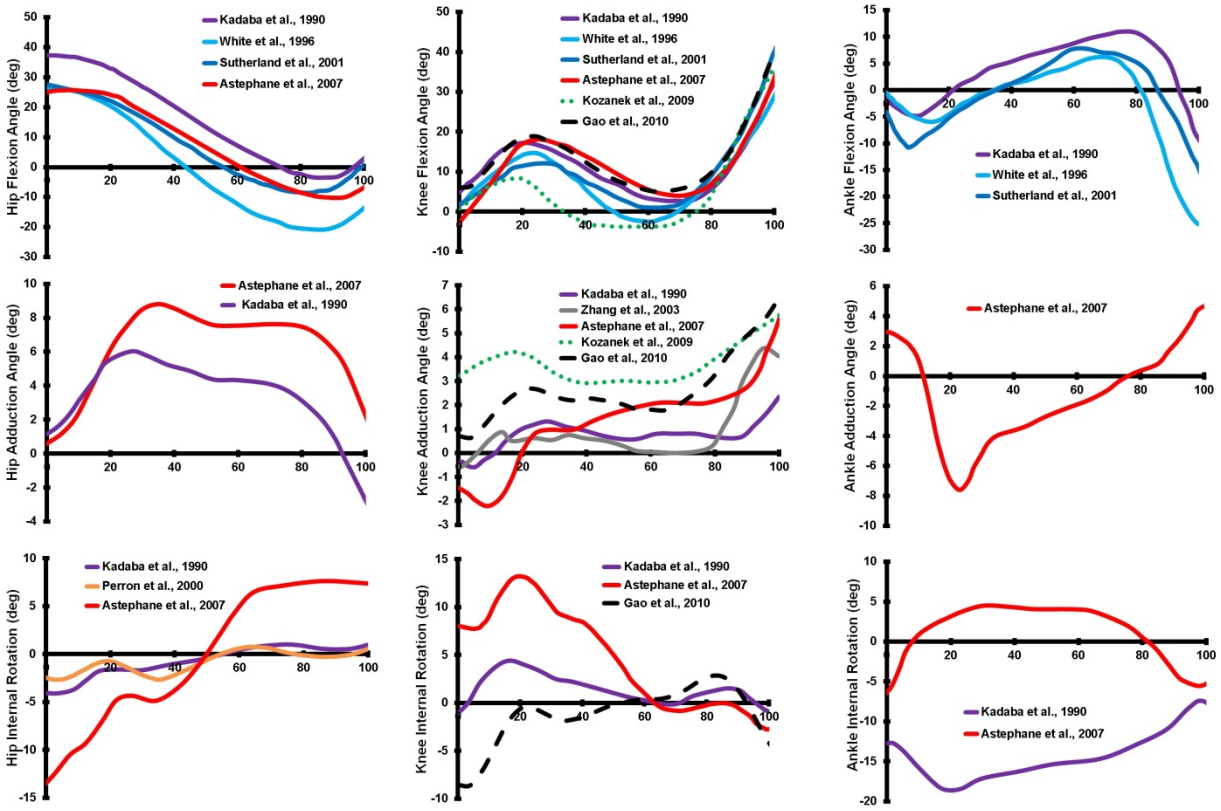

Figure 2.12: Comparaison entre les résultats cinématiques des différentes articulations des membres inférieurs dans les trois plans durant la phase d'appui. Le sens positif est pour la flexion, l'adduction et la rotation interne

2.2.6 Données cinétiques de la marche

a. La force de réaction du sol

Lors de la marche, l'être humain produit une certaine quantité de force à chaque fois qu'il met le pied sur le sol. Le sol donc, applique la même quantité de force au pied et c'est ce qu'on appelle la force de réaction du sol (GRF). Cette force était le sujet de plusieurs études dans la littérature (Chao, Laughman, Schneider, & Stauffer, 1983; A. E. Hunt, M Smith, et al., 2001; Neptune et al., 2004; Riley, Paolini, Della Croce, Paylo, & Kerrigan, 2007). Hunt et al., (2001), en étudiant la réponse de l'articulation du pied dans les trois plans (sagittal, frontal et transversal) ainsi que la force de réaction du sol, ont donné l'allure du GRF toute au long de la phase d'appui (Figure 2.13). Une comparaison des trois composantes du GRF avec les autres travaux (A. E. Hunt, M Smith, et al., 2001; Neptune et al., 2004; Riley et al., 2007; Zajac et al., 2003) est aussi présentée dans la figure 2.13.

Pour la composante verticale de la force de réaction du sol, toutes les études s'accordent et la tendance est presque la même; trois pics de force (P1, P2 et P3 sur la figure 2.13) dont deux sont caractéristiques des phases de réception et de propulsion (qui possèdent des valeurs supérieures à la masse corporelle). Le troisième pic se situe au moment du passage du pied plat (à 50% de la phase d'appui). Sur l'axe médio-latéral deux phases peuvent être distinguées: une phase de réception où la force s'exerce suivant l'axe latéral, suivie d'une phase plus longue où la force est orientée selon l'axe médial. Enfin pour l'axe antéro-postérieur, deux phases sont identifiées. Il s'agit d'une phase de réception où le sujet freine, la force est alors exercée vers l'arrière et d'une phase de propulsion où le sujet propulse son corps vers l'avant, la force de réaction est orientée vers l'avant. Toutefois, les amplitudes des forces sont plus importantes selon l'axe vertical, puis viennent les forces selon l'axe antéro-postérieur et enfin celles selon l'axe transverse.

Dans les études cliniques, les forces de réaction du sol dans les trois plans sont très étudiées car elles renseignent sur l'état du patient par rapport à un trouble dont l'origine peut être neurologique (White, Agouris, Selbie, & Kirkpatrick, 1999) ou orthopédique (T. P. Andriacchi & Hurwitz, 1997). La modélisation des forces de réaction du sol en fonction de la vitesse de déplacement (marche et course) pour les hommes et les femmes a été abordée par Keller et al., (1996) qui ont déterminé des équations liant ces paramètres.

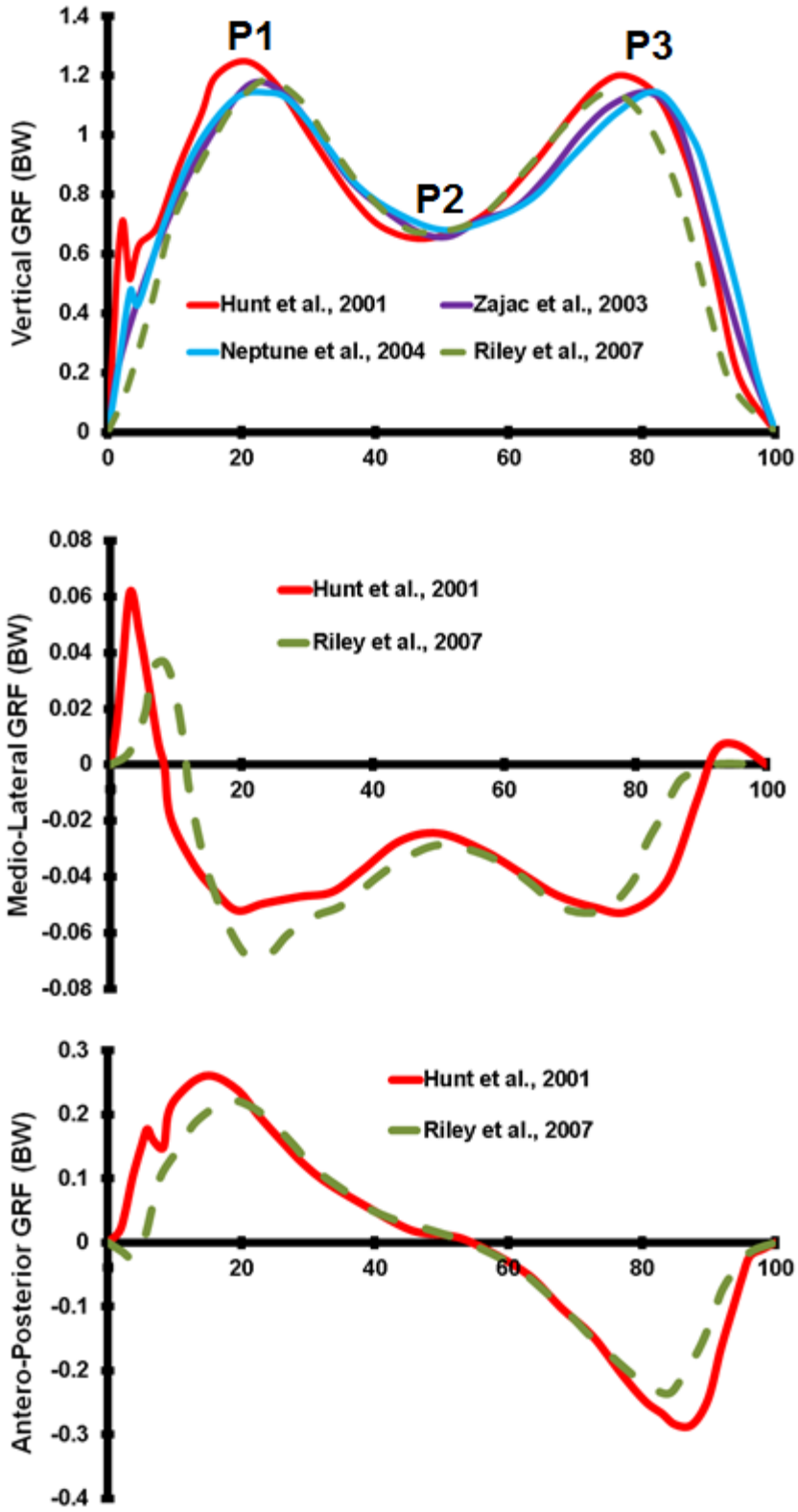

Figure 2.13: Force de réaction du sol (GRF) au cours de la phase d'appui. Les valeurs positives représentent les forces latérales et postérieures agissant sur le pied

b. Les moments sur les joints et les forces musculaires

En plus des données cinématiques et de la force de réaction du sol, la masse et le moment d'inertie de chaque segment, et l'emplacement (accélérations linéaire-angulaire) de son centre de gravité sont des facteurs utiles pour l'analyse de la marche. Une telle information n'est pas directement disponible, mais elle peut être estimée à partir du poids du corps et un certain nombre de mesures linéaires. Les tentatives précédentes pour déterminer les forces musculaires dans le mouvement humain ont massivement appliqué la dynamique inverse (Pandy & Andriacchi, 2010). La dynamique inverse est utilisée pour calculer les moments et les forces du joint. Une comparaison des moments tridimensionnels agissant sur les articulations des membres inférieurs est présentée à la figure 2.14 (J.L Astephen, 2007; Eng & Winter, 1995; Geoffrey, Franz, Dicharry, Croce, & Kerrigan, 2011; C. Winby, Gerus, Kirk, & Lloyd, 2013).

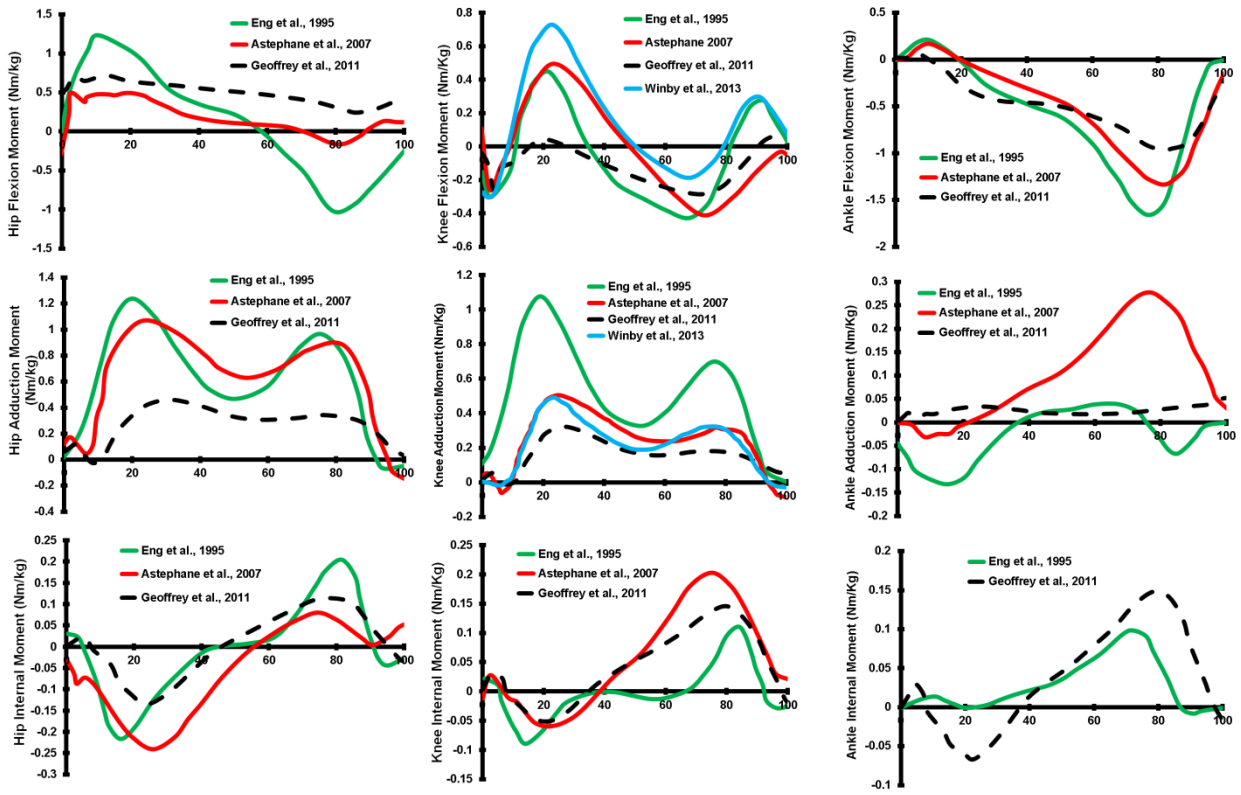

Figure 2.14: Comparaison: Moments articulaires (normalisés par le poids de sujet) dans les trois plans de l'espace. Moments positifs: Flexion, Adduction et Interne

Ainsi la modélisation mathématique et numérique permettent, en combinant les données cinématiques et la force de réaction du sol, d'estimer les forces musculaires et ligamentaires

(Anderson & Pandy, 2001; Delp et al., 2007; K.B. Shelburne et al., 2006). Pour la marche normale: ce sont les muscles qui contribuent le plus dans le soutien et la transmission de la progression du corps (Anderson & Pandy, 2003). La plupart des muscles sont actifs au début et à la fin de la phase d'oscillation, ce qui suggère que la principale fonction des muscles lors de la marche est d'accélérer et de décélérer la jambe (Boakes & Rab, 2006). Dans la figure 2.15, Boakes et Rab (2006) ont donné une description de l'activité musculaire lors d'un cycle de marche.

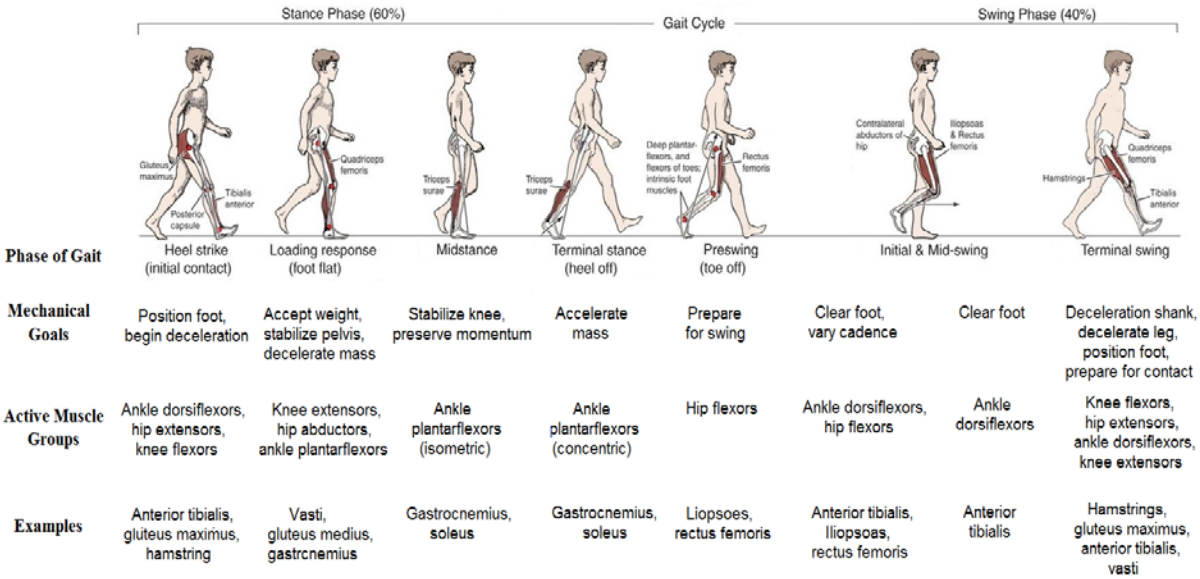

Figure 2.15: Activité musculaire durant le cycle de marche (Boakes & Rab, 2006) et (plexuspandr.co.uk)

2.3 Pente tibiale postérieure

2.3.1 Méthodes de mesure

La littérature contient plusieurs méthodes pour mesurer la pente tibiale postérieure de l'articulation du genou (Dejour & Bonnin, 1994). Généralement, en analysant une image radiographique 2D, la pente tibiale postérieure est définie comme étant l'angle entre la ligne qui représente l'inclinaison du plateau tibial et la perpendiculaire à un axe de référence. Soit:

- **Méthode 1:** La diaphyse (**T**ibial **P**roximal **A**natomical **A**xis).

La pente tibiale est définie comme étant l'angle entre la perpendiculaire à la partie médiane de la diaphyse du tibia et la ligne qui représente l'inclinaison postérieure du plateau

tibial (Chaudhari, Zelman, Flanigan, Kaeding, & Nagaraja, 2009; Dejour & Bonnin, 1994; Genin, Weill, & Julliard, 1993; Giffin et al., 2004). Dans ce cas, la diaphyse est la ligne qui relie deux points équidistants entre les bords antérieurs et postérieurs du tibia (Figure 2.16), l'une est juste en dessous de la tubérosité tibiale, et l'autre à 10 cm en dessous de la première (Dejour & Bonnin, 1994).

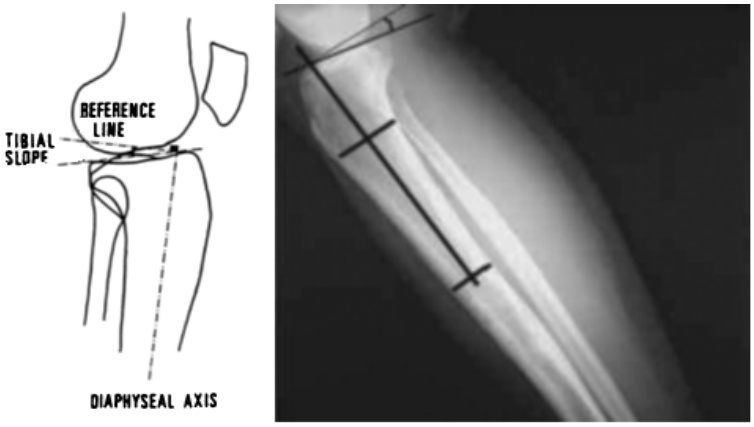

Figure 2.16: Méthode TPAA pour la mesure de la pente tibiale (Dejour & Bonnin, 1994)

- **Méthode 2:** La corticale tibiale postérieure (**P**osterior **T**ibial **C**ortex).

Cette méthode a été utilisée dans plusieurs travaux (Brazier et al., 1996; Hernigou & Goutallier, 1990; Hohmann, Bryant, Reaburn, & Tetsworth, 2010). La pente tibiale a été définie comme étant l'angle entre le plateau tibial et la perpendiculaire à la partie postérieure du cortex tibial (Figure 2.17-a).

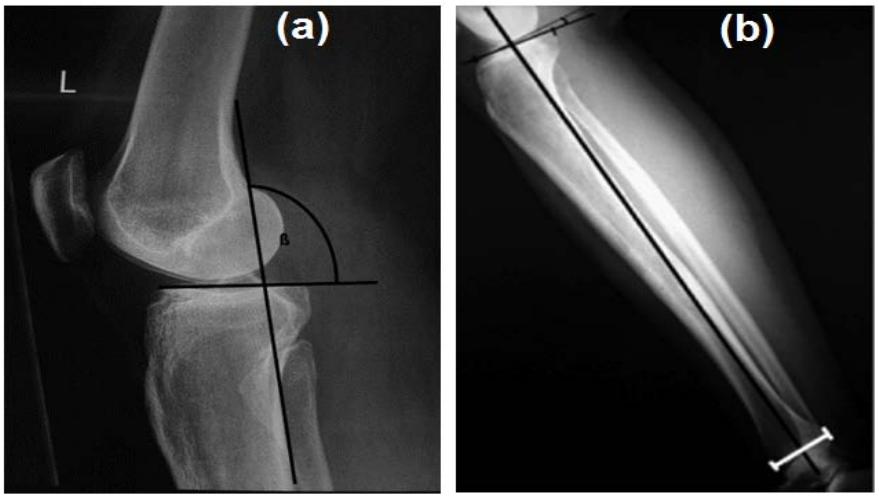

Figure 2.17: Méthode (a) PTC (Hohmann et al., 2010) et (b) TSAA (Sonnery-cottet et al., (2011) pour la mesure de la pente tibiale.

- **Méthode 3:** Cortex tibial antérieur (**A**nterior **T**bial **C**ortex).

Cette méthode a été utilisée également dans les travaux de Brazier et al. (1996) et dans ceux de Moore et Harvey (1974). La pente tibiale a été définie comme étant l'angle entre le plateau tibial et la perpendiculaire à la partie antérieure du cortex tibial.

- **Méthode 4:** Axe mécanique du tibia (**T**ibial **S**haft **A**natomical **A**xis).

La pente tibiale fonctionnelle (Figure 2.17-b) a été définie comme étant l'angle formé par la tangente au plateau tibial médial et la perpendiculaire à l'axe mécanique latéral de la jambe (Brazier et al., 1996; Julliard, Genin, Weil, & Palmkrantz, 1993; Sonnery-Cottet et al., 2011). Sonnery-Cottet et al. (2011) ont mentionné que cette méthode est la plus appropriée du fait qu'elle tient compte de toute la longueur du tibia.

- **Méthode 5:** Axe anatomique fibulair proximal court du (**F**ibular **P**roximal **A**natomical **A**xis) (Brazier et al., 1996).
- **Méthode 6:** Axe diaphysaire fibulair ou axe fibulair long (**F**ibular **S**haft **A**xis) (Brazier et al., 1996).

Une comparaison entre ces 6 méthodes a été faite dans l'étude de Brazier et al. (1996). Dans cette étude, 83 radiographies des genoux intacts ont été analysées et la pente tibiale a été définie comme étant l'angle entre la tangente au plateau tibial interne et la ligne perpendiculaire à l'un des six axes anatomiques: TPAA, TSAA, PTC, FPAA, FSA et ATC (Figure 2.18). Les valeurs trouvées dans cette étude dépendent fortement de la méthode de mesure utilisée, et se situent entre un maximum de 11,44° ± 3.61° trouvé par la méthode ATC et un minimum de 6.96° ± 3.28° trouvé par la méthode PTC. En outre, cette étude révèle que la méthode PTC est la méthode la plus fiable. D'une part, les valeurs trouvées par cette méthode n'ont pas été influencées par les variables morpho-métriques (taille, sexe, âge…). Et d'autre part, le pourcentage d'erreur de cette méthode entre la mesure manuelle et la mesure numérisée est plus faible, encomparaison aux autres méthodes. Dans le tableau 2.1 on présente une comparaison entre les PTPs rapportées dans la littérature.

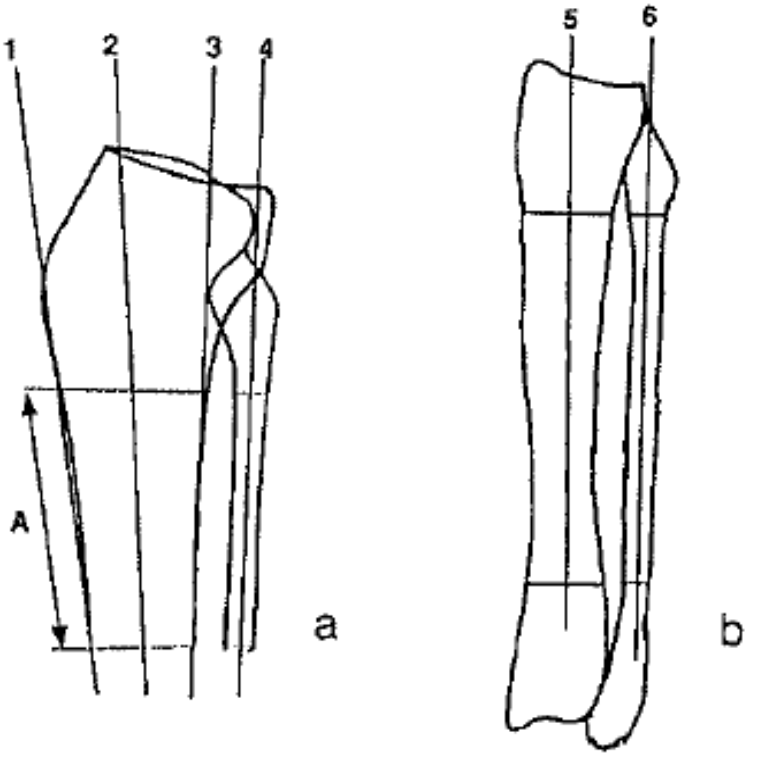

Figure 2.18: Différents axes de référence utilisés dans l'étude de Brazier et al. (1996) pour la mesure de la pente tibiale. 1: ATC, 2: TPAA, 3: PTC, 4: FPAA, 5: TSAA, 6: FSA. A=10 cm

Dans le but d'analyser l'effet de l'emplacement de mesure (plan de coupe sagittal), Boer et al. (2009) ont mesuré la pente tibiale de 105 os tibial dans trois plans sagittaux (latéralement, médialement et au milieu du plateau tibial médial avec une séparation de 5mm), et ont trouvé des valeurs situées entre un minimum de -3° et un maximum de 16° avec un moyen de 8.4° ± 3.7°. L'emplacement du mesure dans cette étude n'a pratiquement aucune influence sur les valeurs trouvées, soit 8.7° ± 3.7; 8.4° ± 3.6° et 8.2° ± 3.9°, respectivement pour le plan sagittal latéral, médial et celui du milieu.

Toutefois, dans toutes ces études la mesure principale consiste à identifier la pente postérieure sur des radiographies latérales, sur lesquelles les plateaux interne et externe se superposent. L'inclinaison du plateau tibial interne est en pratique la seule analysée, compte-tenu des difficultés de reconnaissance des limites du plateau tibial externe (Brazier et al., 1996). Hashemi et al. (2008) ont proposé une nouvelle technique de mesure qui garantit une description plus fiable du plateau tibial. En effet, la géométrie en question a été définie par 3 pentes tibiales:

une pente médiale (MTS), une pente latérale (LTS) et une pente coronale (CTS), et par la profondeur de la concavité du plateau médial tibial médial (MTD) (Figure 2.19).

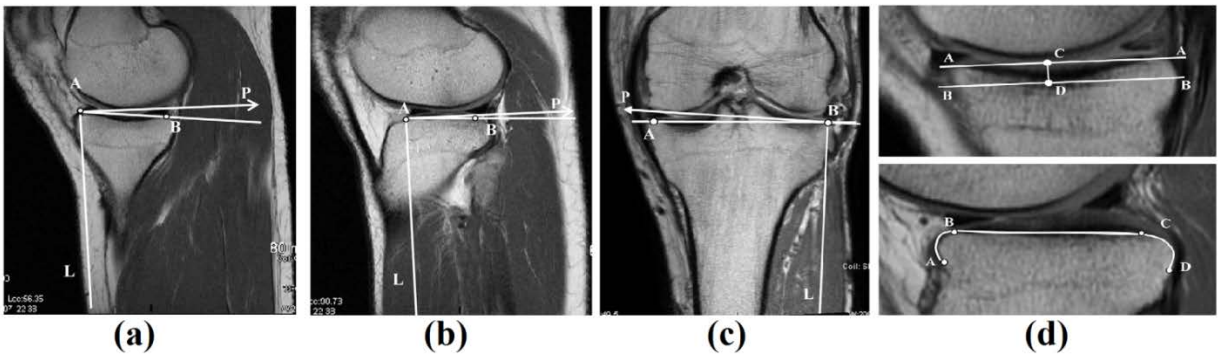

Figure 2.19: IRM illustrant les pentes tibiales (a) médiale, (b) latérale et (c) coronale. (d) méthode utilisée pour déterminer la profondeur de la concavité médiale (en haut) et latérale (en bas). L: partie médiane de la diaphyse, P: la perpendiculaire à L (Hashemi et al., 2008)

En utilisant la radiographie, quatre étapes ont été suivies pour définir le CTS:

- Identifier un plan transversal passant par l'articulation TF.
- Identifier un plan frontal qui passe le plus proche possible du centre de gravité du plateau tibial.
- Déterminer l'orientation de l'axe longitudinal du tibia dans le plan frontal. Cet axe passe au milieu de deux lignes (4 à 5 cm en dessous du plateau tibial) qui relient les bords antérieur et postérieur du tibia.
- Ensuite, le CTS est défini comme étant l'angle entre la ligne reliant les deux points de crêtes sur les faces médiale et latérale du plateau (point A et B dans la Figure 2.19-c) et la ligne perpendiculaire à l'axe longitudinal.

Une approche similaire a été suivie pour déterminer les pentes des plateaux latéral et médial (LTS et MTS). Ils ont commencé par identifier les deux plans sagittaux (sur le plateau latéral et médial). Ensuite, ils ont déterminé de la même manière l'axe longitudinal. Cet axe qui est l'axe de référence pour la mesure de LTS et MTS. En effet, le LTS et le MTS sont respectivement les angles entre la ligne perpendiculaire à cet axe et la ligne tangente au plateau latéral/médial. La profondeur de la concavité de la face médiale du plateau tibial a été mesurée en traçant une ligne reliant les crêtes supérieures et inférieures du plateau tibial dans le même plan, dans lequel la pente tibiale a été mesurée (ligne AA de la figure 2.19-d). Une ligne parallèle à

cette ligne a été ensuite tirée tangent au point le plus bas de la concavité, ce qui représente la plus faible limite de l'os sous-chondral (ligne BB de la figure 2.19-d). La distance perpendiculaire entre les deux lignes (ligne CD dans la figure 2.19-d) a ensuite été mesurée et est utilisée pour représenter la profondeur de la concavité du plateau tibial médial. Une approche similaire a été suivie pour le plateau latéral.

Les résultats de cette étude, comme présentés au tableau 2.1, montrent que la pente tibiale du plateau latéral est plus grande que celle du plateau médial, surtout chez les sujets féminins. Soit une pente tibiale médiale de 5.9°±3° [0° à 10°] chez les femmes contre 3.7°±3.1° [-3° à 10°] chez les hommes, et une pente tibiale latérale de 7°±3.1° [1° à 14°] et de 5.4°±2.8° [0° à 9°] respectivement chez les sujets féminins et les sujets masculins. Cette étude révèle également que pour les sujets masculins la pente tibiale coronaire est de 3.5°±1.9° [0° à 6°], et de 2.5°±1.9° [-1° à 6°] chez les femmes. La profondeur de la concavité du compartiment médiale du tibia est de 2.7±0.76mm [1.4 à 4.2 mm] chez les femmes et de 3.1±0.99mm [1.2 à 5.2 mm] pour les sujets de sexe masculin. Cependant le plateau latéral est convexe (figure 2.19-d).

Tableau 2.1: Pente tibiale postérieure rapportée dans les études antérieures

	Nb	Technique utilisée	Axe de référence	Pente tibiale [min-max]	
				Médial	Latéral
(Hashemi et al., 2008)	33F/ 22M	IRM	TPAA	(Femme/Homme)	(Femme/Homme)
				(5.9°±3°/3.7°±3.1°)	(7°±3.1°/5.4°±2.8°)
Chiu et al. (2000) **	50	Radiographie	ATC	14.8°±4.2° [5°-25°]	11.8°±3.8° [4°-23°]
Jiang et al. (1994)	50	Radiographie	TPAA	10° ± 4°	
Moller et al. (1985) **	30	Étude cadavérique	TPAA	10° ± 2.5° [5°-15°]	8° [4°-15°]
Matsuda et al. (1999)	30	IRM	TSAA	10.7° ± 1.3°	
Kuwanu et al. (2005)	50	CT-imaging	TSAA	9° ± 5°	
Boer et al. (2009) **	102	goniométrie manual	TSAA	8.4° ± 3.7° [-3°-16°]	

Tableau 2.1 (suite): Pente tibiale postérieure rapportée dans les études antérieures

Hofmann et al. (1991)	33	Radiographie	TSAA	7° ± 3°
Brazier et al. (1996)	83	Radiographie	ATC	11.44° ± 3.61° [3.47°-20.29°]
			TSAA	10.39° ± 3.72° [2.82°-19.29°]
			FPAA	9.54° ± 3.62° [0°-17.34°]
			TPAA	9.16° ± 3.37° [2.54°-17.91°]
			FSA	8.23° ± 3.51° [1.59°-16.59°]
			PTC	6.96° ± 3.28° [0°-15.44°]

** cadavérique

2.3.2 Effet de la pente tibiale sur la biomécanique de l'articulation

La géométrie du plateau tibial a été associée dans plusieurs études au risque des blessures observées dans le LCA (Brandon et al., 2006; Meister et al., 1998). Giffin et al. (2004) ont montré que l'augmentation de la pente tibiale pourrait jouer un rôle bénéfique pour réduire l'instabilité dans les genoux avec déficience du LCP, et une diminution de celle-ci pourrait avoir un rôle protecteur dans un genou avec déficience du LCA. Il a été montré également que les personnes souffrant déjà d'une lésion du LCA (Brandon et al., 2006), et en particulier les femmes (Todd, Lalliss, Garcia, DeBerardino, & Cameron, 2010), possèdent une plus grande pente tibiale postérieure que les autres sujets. En accordance, plusieurs études ont montré que les athlètes féminines sont plus susceptibles aux lésions du LCA que les athlètes masculins (Agel et al., 2005; E. Arendt & Dick, 1995; E. A. Arendt, Agel, & Dick, 1999). La littérature indique que de nombreux facteurs de risque sont influencés par le sexe d'un individu (E. A. Arendt et al., 1999; Lephart, Ferris, & Fu, 2002; Renstrom et al., 2008). Brandon et al., (2006) ont rapporté que les femmes, à cause d'une pente tibial postérieure plus grande, sont plus à risque à la blessure du LCA que les hommes. Meyer et al., (2008) ont rapporté que sous l'action d'une force de compression, le déplacement antérieur du tibia peut être attribué à l'inclinaison inhérente du plateau tibial (Figure 2.20).

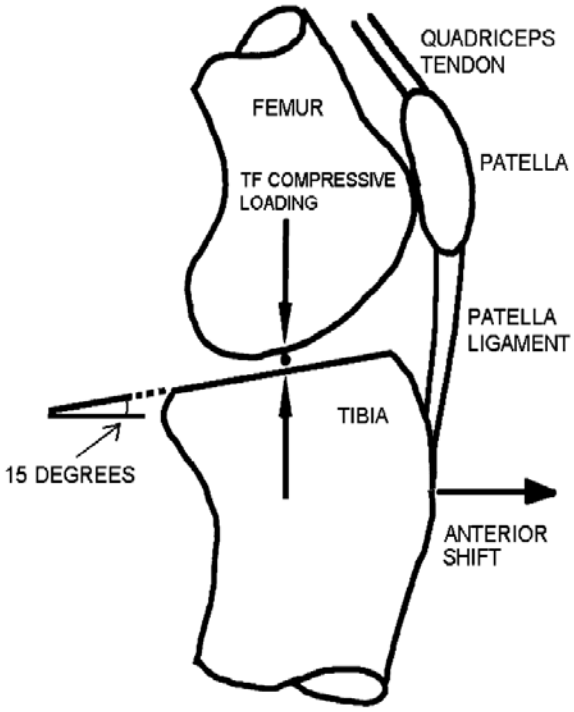

Figure 2.20: La translation antérieure peut être la cause de la PTP (Meyer et al., 2008)

En utilisant la radiographie, Brandom et al. (2006) ont rapporté une pente tibiale postérieure plus grande pour les participants avec lésion du LCA par rapport à ceux (groupe du control) avec douleur patello-fémorale. De même, Stijak et al. (2008) ont mesuré par IRM la pente tibiale postérieure des mêmes groupes (groupe 1: participants avec lésion du LCA; groupe 2: groupe de contrôle (participants avec LCA intact et des douleurs au niveau de l'articulation patello-fémorale)). Les résultats indiquent que dans le groupe 1, le plateau tibial externe était significativement plus élevé (pente dirigée postérieurement) que dans le groupe de contrôle. Cependant, la pente du plateau tibial interne était plus faible pour le groupe 1. La valeur moyenne de la pente tibiale est de 6.08 ± 3.30° pour le groupe 1, contre 5.50 ± 2.23° pour le groupe de contrôle.

Outre le travail de Simon et al. (2010), la majorité des études ont étudié séparément l'effet de la pente tibiale postérieure / de l'indice de largeur de l'encoche (largeur de l'échancrure divisée par largeur de la partie distale du fémur) sur le chargement du LCA. Il a été trouvé qu'une pente tibiale postérieure plus grande ou un indice de largeur d'encoche plus étroite peuvent être considérés comme un facteur de risque dans la rupture du LCA. Cependant, il existe une certaine contradiction dans leurs significations. Sonnery-Cottet et al., (2011) ont mentionné que, pour les

études qui visent à étudier les facteurs de risques dans la lésion du LCA, il faut tenir compte à la fois de la pente tibiale postérieure et de la largeur d'encoche.

Récemment, Wahl et al., (2012) ont identifié d'une façon quantitative et qualitative les différences dans la géométrie de la surface articulaire fémoro-tibiale latérale (le rayon de courbure du plateau tibial, le rayon de courbure de la partie distale du fémur et la longueur maximale antéro-postérieure du fémur et du tibia) qui peuvent aider à expliquer le risque de lésion du LCA. Les résultats suggèrent qu'il existe un phénotype géométrique à risque de la surface articulaire fémoro-tibiale latérale, caractérisé par un plateau tibial court et plus convexe relativement au fémur et par une surface plus petite et plus convexe du fémur distal, ce qui peut rendre le genou plus sensible à la lésion du LCA. Dans ce contexte également, Hashemi et al. (2010) ont trouvé qu'une PTP (médial et latéral à la fois) plus grande, ainsi qu'une profondeur tibiale médiale plus petite peuvent être associées à un risque de blessure du LCA.

Cependant, une controverse existe entre les différents travaux: des études qui se mettent d'accord que la géométrie du plateau tibial est associée aux lésions du LCA (Brandon et al., 2006; Stijak et al., 2008), surtout chez les sujets féminins (Brandon et al., 2006; Hashemi et al., 2008; Hashemi et al., 2010),et des études qui ne rapportent aucune relation entre la pente du tibia et la lésion du LCA (Meister et al., 1998). Dans le tableau ci-dessous, on compare les résultats trouvés par plusieurs études en ce qui concerne la pente tibiale et sa relation avec la déficience du ligament croisé antérieur.

Tableau 2.2: Pente tibiale postérieure selon le sujet d'étude

				Pente tibiale	
	Nombre (I/D)	Méthode	Technique utilisée	Sujets intacts	Sujet avec déficience du LCA
(Sonnery-Cottet et al., 2011)	50/50	TSAA	IRM	7.52° ± 2.13° (Note : LE = 0.27 ± 0.02 mm)	10.1° ± 3.3° (Note : LE = 0.22 ± 0.02 mm)
(Hashemi et al., 2010)	55/49	TPAA	IRM	5.91° ± 2.96°	6.85° ± 3.61°

Tableau 2.2 (suite): Pente tibiale postérieure selon le sujet d'étude

Hohmann et al. (2010)	24/44	PTC	Radiographie	7.20°±4.49° (**@R**) [2.5°-12.4°]	6.10°±3.57° [2.5°-11.7°]
Stijak et al. (2008)	33/33	TPAA	Rayon X	4.36 ± 2.26°/ 6.58 ± 3.21°	L/M 7.52 ± 3.39°/ 5.24 ± 3.60°

(I/D) : Sujet Intact ou avec déficience du LCA
LE : Longueur d'encoche
(R): ACL reconstruit

2.4 Genou en compression

La force de compression sur le joint du genou est omniprésente dans les activités quotidiennes et elle varie suivant plusieurs facteurs, externes et internes. Dans le but de comprendre l'effet d'une telle force sur la réponse de l'articulation (intacte ou avec déficience de l'une de ses structures), plusieurs études expérimentales et d'élément finis ont été menées (Ahmed & Burke, 1983; Alhalki, Howell, & Hull, 1999; Allaire, Muriuki, Gilbertson, & Harner, 2008; Brown & Shaw, 1984; Fukubayashi & Kurosawa, 1980; Huang, Hull, & Howell, 2003; Krause, Pope, Johnson, & Wilder, 1976; Kurosawa, Fukubayashi, & Nakajima, 1980; Lee et al., 2006; K. L. Markolf, Jackson, Foster, & McAllister, 2013; H Marouane, Shirazi-Adl, & Adouni, 2013; E. G. Meyer et al., 2008; E. G. Meyer & Haut, 2005; Paci et al., 2009; Poh et al., 2011; Sekaran, Hull, & Howell, 2002; P. Walker & Hajek, 1972; P. S. Walker & Erkman, 1975). Une tendance générale révélée par ces études est que la zone de contact augmente avec la force de compression, et diminue avec l'angle de flexion. En outre, plusieurs études s'accordent à dire que les ménisques intacts peuvent transmettre plus de 50% de la charge totale en compression pour une articulation en position d'extension complète (Ahmed & Burke, 1983; Fairbank, 1948; P. S. Walker & Erkman, 1975).

Pour la majorité de ces travaux, l'analyse de l'articulation du genou sous des forces de compression est une tâche difficile à étudier. Elle nécessite un bon choix des conditions aux limites ainsi qu'un bon ajustement de la direction et la position d'application de la force; il est évident que la réponse dépend directement de la position (ML et AP) du point où on applique la charge de compression. La plupart de ces études ont maintenu le fémur fixe et ont appliqué la force de compression sur le tibia, avec un intérêt commun; qui consiste à conserver la stabilité et

la mobilité de l'articulation. En effet, à cause de l'instabilité du joint face à une telle charge, plusieurs études ont choisi de fixer les rotations dans le plan frontal et sagittal (Brown & Shaw, 1984; Lee et al., 2006). Seuls quelques travaux ont laissé le tibia complètement libre lors de l'application de la force de compression (Ahmed & Burke, 1983; Paci et al., 2009). Cette tâche a été précédée par un ajustement adéquat afin d'assurer que la force soit appliquée perpendiculairement aux surfaces de contact de l'articulation et de manière à ne pas générer des rotations flexion-extension. Cependant, la plupart des études n'ont pas tenu compte de l'ajustement de la force dans le plan frontal. Dans nos études antérieures (Hafedh Marouane, 2012; H Marouane, Shirazi-Adl, & Adouni, 2015a), on applique la force de compression à un point d'équilibre mécanique (MBP) afin de ne pas générer des rotations, ni dans le plan transversal, ni dans le plan frontal (Figure 2.21).

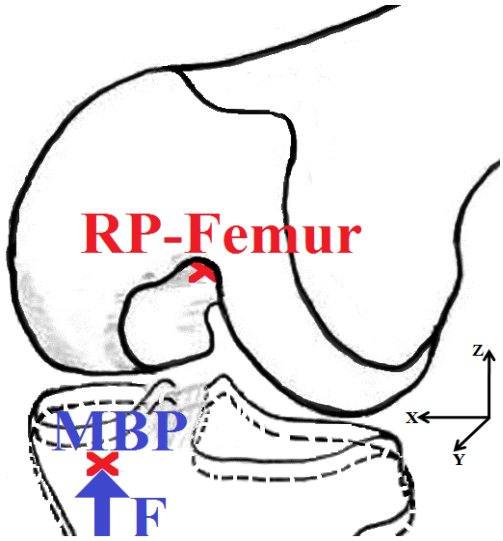

Figure 2.21: Méthode utilisée dans notre étude antérieure (Marouane et al., 2015a) pour appliquer la force de compression au point d'équilibre mécanique (MBP)

Dans des études cadavériques, Meyer et al. (2008; 2005) ont montré qu'une force de compression appliquée sur l'articulation du genou fléchi à une position fixe, provoque la rupture du LCA. Toutefois une telle étude néglige l'effet des forces stabilisatrices des muscles et la réponse du joint est globalement contrôlée par la structure passive (et dont l'effet de la morphologie articulaire joue son rôle). Sous l'action d'une force de compression de 1600N appliquée à 0, 15 et 30° de flexion, Liu-Barbara et al., **(2007)** ont comparé les mesures cinématiques des deux groupes; un groupe avec LCA intact et un autre avec LCA déficient. Avec

les genoux intacts, ces auteurs ont rapporté à 0° (à 30°) de flexion des pics des mouvements couplés de 3.8° (-4.9°), 1.4° (-1.9°), 1.4mm (2.3mm) et 5.3mm (10.2mm), respectivement pour la rotation interne, la rotation varus, la translation médiale et la translation antérieure. En outre, ces auteurs n'ont pas rapporté de différences entre les deux groupes testés. Markolf et al. (2013) ont étudié l'effet de la force de compression appliquée sur des genoux intacts au cours d'un cycle de flexion-extension entre 0 et 50°, et ont montré que la direction du mouvement de flexion-extension est une variable importante lors de l'étude de l'effet de la compression sur la force/déformation du LCA en particulier et sur la cinématique de l'articulation en général.

2.5 Les modèles musculo-squelettiques

Plusieurs modèles d'éléments finis (EF) avec différents degrés de précision et de raffinement ont été développés (Mohamed Z Bendjaballah, Shirazi-Adl, & Zukor, 1995; Halonen et al., 2016; Kazemi & Li, 2014; W. Mesfar & Shirazi-Adl, 2006b; Pena et al., 2006; Shim, Besier, Lloyd, Mithraratne, & Fernandez, 2016; N. Yang, Canavan, Nayeb-Hashemi, Najafi, & Vaziri, 2010a) pour mieux comprendre la biomécanique de l’articulation du genou. Également, plusieurs modèles musculo-squelettiques (MS) de l'extrémité inférieure (soit hybride avec un modèle détaillé en EF de genou ou non hybride avec un modèle simplifié de genou) ont été développés dans le but d’estimer les activités musculaires et de mieux comprendre la biomécanique fonctionnelle de l'articulation du genou dans des conditions normales et pathologiques et dans des conditions de charge et de mouvement physiologiques (M. Adouni, Shirazi-Adl, & Shirazi, 2012; M Adouni & Shirazi-Adl, 2014a; Delp et al., 1990; Lerner, Haight, DeMers, Board, & Browning, 2014; Lloyd & Besier, 2003; Manal & Buchanan, 2013; H Marouane, Shirazi-Adl, & Adouni, 2016a, 2016b; H Marouane, Shirazi-Adl, & Hashemi, 2015b; N. H. Yang, Nayeb-Hashemi, Canavan, & Vaziri, 2010b). Alors que les modèles d’EF fournissent des informations détaillées précieuses (c'est-à-dire les contraintes et les déformations des tissues) dans les matériaux constitutifs des joints, les modèles MS (non hybride) offrent des résultats cruciaux sur les modes d'activation musculaires et le mécanisme de chargement durant des activités physiologiques complexes comme la marche (Kim et al., 2009; Taylor, Heller, Bergmann, & Duda, 2004; C. R. Winby et al., 2009). En raison de la complexité, de nombreuses hypothèses sont souvent nécessaires pour tenter d'estimer les forces musculaires et les forces de contact dans les modèles MS.

Dans de nombreux modèles MS existants, le moment de flexion-extension est souvent le seul moment considéré au niveau de l'articulation du genou, ce qui entraîne une seule équation d'équilibre lors de l'estimation des forces musculaires (Delp et al., 1990; DeMers, Pal, & Delp, 2014; KB Shelburne & Pandy, 1998; Kevin B Shelburne, Pandy, Anderson, & Torry, 2004; K.B. Shelburne et al., 2006; Thelen, Anderson, & Delp, 2003). L'articulation de la hanche, d'autre part, est généralement modélisée comme une articulation sphérique avec trois rotations dans les plans anatomiques (Arnold, Ward, Lieber, & Delp, 2010; Delp et al., 2007; Delp et al., 1990; Horsman, Koopman, Veeger, & van der Helm, 2007) ou encore une seule rotation dans le plan sagittal (KB Shelburne & Pandy, 1998; Kevin B Shelburne & Pandy, 1997, 2002). Ces modèles négligent également le rôle important des structures passives articulaires du genou dans le soutien des charges externes et donc la réduction de l'activité des muscles tout en améliorant la marge de stabilité articulaire. Des études antérieures ont également démontré que la rigidité passive de l'articulation du genou augmente encore sous des forces de compression plus importantes qui existent dans la plupart des activités physiologiques comme la marche et la descente/monter d'escalier (H Marouane et al., 2015a).

Une autre distinction entre ces modèles MS est l'approche utilisée pour prédire les forces de contact TF. De nombreuses études utilisent l'algorithme de point de contact qui suppose que les forces de contact médiale et latérale agissent à un point unique prédéterminé dans une articulation intacte ou implantée. Ce point de contact était supposé être au milieu de chaque condyle (Gerus et al., 2013; C. R. Winby et al., 2009), 25% de la largeur tibiale (Manal & Buchanan, 2013), 25% de la largeur inter-condylienne (Kumar, Rudolph, & Manal, 2012), les points les plus proches entre les composantes fémorale et tibiale (Sandholm et al., 2011) ou encore basé sur d’autres hypothèses (Blagojevic, Jinks, Jeffery, & Jordan, 2010; Lerner, Board, & Browning, 2015b; Lerner, DeMers, Delp, & Browning, 2015; Guoan Li et al., 2005; Miller, Esterson, & Shim, 2015). Brièvement, les forces de contact sont déterminées en utilisant l'équilibre statique autour des points de contact médial et latéral dans le plan frontal tibial (Figure 2.22), où le moment varus / valgus externe (par dynamique inverse) déterminé à un point de contact sélectionné est équilibré par les moments musculaires relatifs à ce point de contact (c'est-à-dire le produit des forces musculaires et les bras de leviers par rapport à ce point de contact). Lerner et al (2015) indiquent que chaque déplacement de un millimètre dans la translation

médiale/latérale des points de contact du compartiment modifie le premier pic de la force de contact du compartiment médial par 41N.

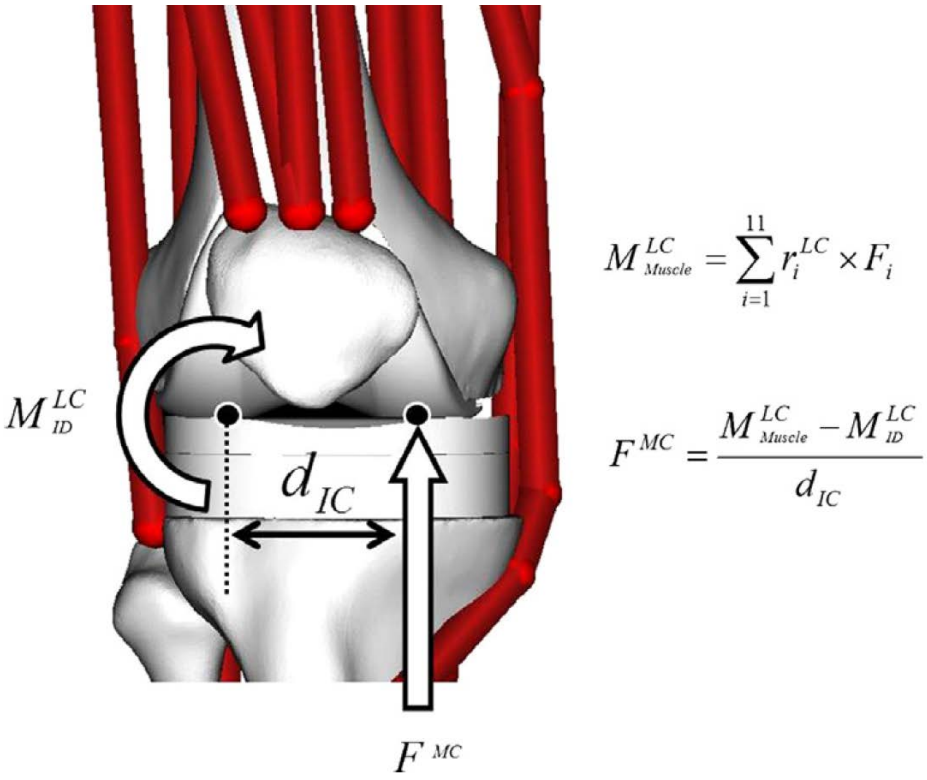

Figure 2.22: Méthode utilisé par les modèles MS pour estimer les forces de contact (Gerus et al., 2013)

Avec l'avancement des outils d'imagerie pour la reconstruction géométrique du joint et avec la disponibilité des propriétés mécaniques des tissus mous (ligaments, cartilages, ménisques) plusieurs modèles d'EF ont été développés et améliorés. Passant par les modèles qui négligent la présence des ménisques (Atkinson, Atkinson, Huang, & Doane, 2000; Blankevoort & Huiskes, 1991c; Blankevoort, Kuiper, Huiskes, & Grootenboer, 1991a; Crowninshield, Pope, & Johnson, 1976; Grood & Hefzy, 1982), les modèles qui négligent l'anisotropie et l'inhomogénéité des cartilages (Mohamed Z Bendjaballah et al., 1995; G Li, Gil, Kanamori, & Woo, 1999; G. Li, Suggs, & Gill, 2002; Moglo & Shirazi-Adl, 2005; Pena et al., 2006), aux modèles qui touchent la réalité en tenant compte de la structure anisotrope et inhomogène des couches des cartilages et des ménisques et qui tient compte de tous les ligaments et les muscles qui entourent l'articulation du genou (M Adouni & Shirazi-Adl, 2014a; R. Shirazi et al., 2008) (voir Annexe 1).

Pour valider les résultats d'une telle étude biomécanique, les forces musculaires sont généralement validées qualitativement en comparant le niveau d'activation des muscles avec les données EMG enregistrées durant la même activité (M Adouni & Shirazi-Adl, 2013; M Adouni & Shirazi-Adl, 2014a; Kim et al., 2009) ou encore en comparant les forces de contact avec celles enregistrés chez un patient avec implant du genou (DeMers et al., 2014; Kim et al., 2009; Steele, DeMers, Schwartz, & Delp, 2012). Les prédictions ont été jugées sensibles à de nombreux facteurs, tels que les modèles d'activation musculaire, la pondération musculaire et les propriétés musculotendoniques (DeMers et al., 2014; Lerner et al., 2015; Steele et al., 2012). Les forces de contact provenant d'un sujet avec implant du genou ont été utilisées également pour calibrer les modèles MS (Gerus et al., 2013; Steele et al., 2012), en minimisant l'erreur entre les prédictions du modèle et les forces expérimentales. Du fait que les forces musculaires contribuent significativement aux forces du contact (K.B. Shelburne et al., 2006), des prédictions précises des charges de contact impliqueraient que les estimations des forces musculaires correspondantes sont également raisonnables. En simulant la marche avec différente vitesse (de 0.8m/s à 1.52m/s), Kim et al., (2009) ont rapporté un accord entre les prédictions du modèle en ce qui concerne les forces de contact et les résultats provenant d'un sujet avec implant. Le pic de la force de contact est d'environ deux fois le poids du corps et est généralement supporté par le plateau médial. Kutzner et al. (2010) ont mesuré les forces de contact et les moments agissant sur l'articulation de genou chez cinq sujets avec implant durant l'exercice de différentes activités quotidiennes. La force du contact sur le plateau tibial enregistré durant la marche est d'environ 261% BW (Body Weight).

CHAPITRE 3 DESCRIPTION DE LA DÉMARCHE SCIENTIFIQUE

La revue de la littérature nous a permis d'avoir une vue d'ensemble sur les travaux qui se sont intéressés à l'étude de l'articulation du genou et qui touchent directement ou indirectement notre travail. Ce travail envisage de faire suite aux études antérieures de Bendjaballah et al., (1997; 1995; 1998), de Moglo et Shirazi-Adl (2003; 2003; 2005), de Mesfar et al., (2005, 2006a, 2006b, 2008a, 2008b), de Shirazi et al., (2005, 2009; 2008) et de Adouni et al., (2009; 2013, 2014b; 2015; 2012; 2014a) en utilisant un modèle MS jugé le plus complet dans la littérature. Ce modèle tient compte de la géométrie 3D de l'articulation du genou, de la structure passive et active et a été utilisé et validé durant la marche dans les travaux de Adouni (2009; 2013, 2014b; 2015; 2012; 2014a). Entre autre, on formule ici nos objectifs et nos hypothèses de travail.

3.1 Objectifs et hypothèses

Objectif général:

L'objectif principal de ce projet de thèse est d'étudier l'effet de la pente tibiale, la rotation varus/valgus, le moment varus/valgus, et de certaines simplifications couramment utilisés dans les modèles musculosqueletiques, sur la réponse de l'articulation du genou durant les activités physiologiques.

Objectifs spécifiques:

Afin de parvenir à atteindre cet objectif général, six objectifs spécifiques ont dû être déterminés et formulés:

- Analyser l'effet de la variation de la pente tibiale postérieure sur la réponse passive de l'articulation tibio-fémorale en compression et à différents angles de flexion.
- Analyser l'effet de la variation de la pente tibiale postérieure sur la réponse de l'articulation du genou durant la phase d'appui de la marche.
- Sous l'action de la force de compression et durant nos analyses de la marche, déterminer les variations de la position du centre de contact sur le plateau tibial.
- Prédire, par différentes méthodes, la position du centre de contact et quantifier les forces de contact durant la phase d'appui de la marche avec des conditions intactes et altérées.

- Étudier l'effet des simplifications, couramment utilisées dans les modèles MS, en simulant l'articulation du genou comme une articulation plane (dans le plan sagittal) sur la réponse biomécanique du genou.
- Étudier la sensitivité du joint du genou, en comparant l'effet de la variation de l'angle varus/vagus contre la variation du moment varus/valgus durant la phase d'appui de la marche.

Hypothèses:

- La morphologie articulaire a un effet prépondérant sur le mécanisme du chargement du LCA. Une PTP plus grande augmente les risques des blessures du LCA. En outre, une PTP du plateau latéral supérieure à celle du plateau médial augmente également les risques des blessures du LCA.
- La position du centre de contact varie durant la marche et aussi avec la méthodologie utilisée.
- Si on simplifie la géométrie 3D complexe de l'articulation du genou à un simple joint 2D dans le plan sagittal, on perd qualitativement et quantitativement l'exactitude de nos prédictions.
- Les forces de contact sur les plateaux médial et latéral dépendent plutôt de la rotation varus/valgus que du moment varus/valgus.

3.2 Plan de la thèse

La présentation de ce travail est divisée en neuf chapitres:

Le premier chapitre présente l'introduction dans laquelle nous spécifions, de façon générale, le cadre de notre étude.

Dans le deuxième chapitre, une étude bibliographique est effectuée. Cette revue est composée de cinq parties principales. L'anatomie de la hanche, du genou et de la cheville est dans un premier temps détaillée. La deuxième partie traite l'analyse de la marche humaine en passant par la cinématique et la cinétique des membres inférieurs et les différentes approches utilisées actuellement pour simuler cette activité complexe. La troisième partie présente, quant à elle, les différentes techniques utilisées pour définir la morphologie articulaire en général et la pente tibiale postérieure en particulier. Dans la quatrième partie, l'ensemble des travaux de

recherche réalisés pour étudier la réponse de l'articulation en compression est présenté. Finalement, la dernière partie présente l'ensemble des modèles MS et d'élément finis présents dans la littérature.

Le troisième chapitre expose, quant à lui, la démarche scientifique qui a été adoptée dans ce travail de thèse afin d'atteindre nos objectifs du départ.

Les chapitres quatre à huit présentent nos cinq articles:

Article 1: Marouane, H., Shirazi-Adl, A., Adouni, M., & Hashemi, J. (2014). Steeper posterior tibial slope markedly increases ACL force in both active gait and passive knee joint under compression. Journal of biomechanics, 47(6), 1353-1359.

Article 2: Marouane, H., Shirazi-Adl, A., & Hashemi, J. (2015). Quantification of the role of tibial posterior slope in knee joint mechanics and ACL force in simulated gait. Journal of biomechanics, 48(10), 1899-1905.

Article 3 : Marouane, H., Shirazi-Adl, A., & Adouni, M. (2016). Alterations in knee contact forces and centers in stance phase of gait: A detailed lower extremity musculoskeletal model. Journal of biomechanics, 49(2), 185-192.

Article 4 : Marouane, H., Shirazi-Adl, A., & Adouni, M. (2016). 3D active-passive response of human knee joint in gait is markedly altered when simulated as a planar 2D joint. Biomechanics and Modeling in Mechanobiology, in press, 1-11.

Article 5 : Marouane, H., & Shirazi-Adl, A. (December 2016). Medial-lateral load distribution in the knee joint is influenced by changes in the adduction rotation and not in the adduction moment. Submitted in Biomechanics and Modeling in Mechanobiology, submitted.

Finalement, une discussion générale est présentée dans le neuvième chapitre suivie par une conclusion qui viendra mentionner brièvement les points importants de ce travail de recherche afin d'en rappeler la contribution scientifique et nous permettra de poser des jalons de perspectives pour continuer à améliorer les connaissances scientifiques.

CHAPITRE 4 ARTICLE 1: STEEPER POSTERIOR TIBIAL SLOPE MARKEDLY INCREASES ACL FORCE IN BOTH ACTIVE GAIT AND PASSIVE KNEE JOINT UNDER COMPRESSION

H. Marouane, A. Shirazi-Adl, M. Adouni and J. Hashemi

Article published in

Journal of Biomechanics 2014

4.1 Abstract

The role of the posterior tibial slope (PTS) in anterior cruciate ligament (ACL) risk of injury has been supported by many imaging studies but refuted by some in vitro works. The current investigation was carried out to compute the effect of ±5° change in PTS on knee joint biomechanics in general and ACL force/strain in particular. Two validated finite element (FE) models of the knee joint were employed; one active lower extremity musculoskeletal model including a complex FE model of the knee joint driven by in vivo kinematics/kinetics collected in gait of asymptomatic subjects, and the other its isolated unconstrained passive tibiofemoral (TF) joint considered under 1400 N compression at four different knee flexion angles (0°–45°). In the TF model, the compression force was applied at the joint mechanical balance point causing no rotations in sagittal and frontal planes.

Changes in PTS moderately affected muscle forces and joint contact forces at mid-stance period. Both active (at mid-stance) and passive (at all flexion angles) models showed a substantial increase in the anterior tibial translation and ACL force as PTS increased with reverse trends as PTS decreased. In the active model of gait at mid-stance, ACL force increased by 75% (from 181 N to 317 N) in steeper PTS but decreased by 44% (to 102 N) in flatter PTS. The posterolateral bundle of ACL carried the load at smaller flexion angles with a shift to its anteromedial bundle as flexion increased. In accordance with earlier imaging studies, greater PTS is a major risk factor for ACL rupture especially in activities involving large compression forces.

Keywords: Knee Joint; Finite element; Posterior tibial slope; Compression; Gait; Anterior cruciate ligament

4.2 Introduction

It is recognized that the anterior cruciate ligament (ACL) plays an important biomechanical role in the knee joint response under loads in particular in the anterior–posterior (A–P) and internal–external (I–E) movements (Amis, 2012 and Markolf et al., 1990). Due to large loads and motions during various activities, the knee joint in general and ACL in particular are susceptible to injuries. The ACL rupture is one of the most common joint injuries with much higher prevalence reported in female athletes compared to their male counterparts (Hutchinson and Ireland, 1995, Loud and Micheli, 2001 and Myer et al., 2008). With the expectation to regain the joint near-normal function and to prevent further damages to remaining tissues, approximately 200,000 ACL reconstructions are performed annually in the United States alone (NIH, http://clinicaltrials.gov/ct2/show/NCT00463099). A sound knowledge of joint functional biomechanics is a prerequisite for the delineation of the existing sex-based disparity in ACL injuries and the development of effective strategies for the prevention and treatment of ACL injuries regardless of sex.

ACL ruptures have been produced in vitro in cadaver studies at different flexion angles under very large axial compression forces applied alone (Meyer et al., 2008, Meyer and Haut, 2005 and Meyer and Haut, 2008) or along with a simulated quadriceps force (Wall et al., 2012). Similar ACL ruptures have also been reported in porcine knee under large compression forces (Yeow et al., 2008). The normal posterior tibial slope of about 10° (Dejour and Bonnin, 1994) has been blamed for the ACL rupture as the main cause of excessive tibial anterior (or equivalently femoral posterior) translations under large compression forces (Meyer and Haut, 2005). Knee morphologic aspects have extensively been investigated in search for factors that could play a role in the risk of ACL rupture in both sexes as well as in higher prevalence of non-contact ACL ruptures in female athletes. Many image-based studies of patients with non-contact ACL rupture versus the control subjects have identified the higher posterior tibial slope (PTS) as a risk factor (Boden et al., 2009a, Brandon et al., 2006, Hashemi et al., 2009, McLean et al., 2010 and Sonnery-Cottet et al., 2011). With PTS being greater in female subjects than male subjects, it has been argued to play a role in the higher prevalence of ACL rupture in the former group (Hashemi et al., 2008, Hashemi et al., 2009, Hashemi et al., 2010, Hohmann et al., 2011 and Todd et al., 2010). Every 10° increase in PTS has been found in radiographic studies of normal and ACL deficient subjects to increase ATT by 6 mm in stance test and 3.5 mm in

Lachman test (Dejour and Bonnin, 1994). Musculoskeletal model studies of the lower extremity in gait, despite limitations such as absence of cartilage layers and menisci, have corroborated above clinical findings on the substantial increase in ATT (Liu and Maitland, 2003) and in ACL force (Shao et al., 2011 and Shelburne et al., 2011) in the knee joints with steeper PTS. It is to be noted that the high tibial osteotomy performed with the intention to prevent or decelerate medial osteoarthritis also increases PTS that could in turn increase ATT (Agneskirchner et al., 2004) and the risk of ACL injury (Am Jung et al., 2009).

The PTS on a knee joint image is determined based on the angle between the tibial plateau and a line perpendicular to the joint reference axis. This latter axis has however been defined in different manners along tibial proximal anatomical axis, posterior or anterior tibial cortex, tibial shaft anatomical axis, fibular proximal anatomical axis or fibular shaft axis. Using radiographs, Brazier et al. (1996) reported that PTS could vary, depending on the definition of this axis, from a maximum of 11.44±3.61° found on the basis of the anterior tibial cortex to a minimum of 6.96±3.28° based on the posterior tibial cortex. Measurements on lateral radiographs have reported PTS values of about 10±3° (Dejour and Bonnin, 1994) with minimum of −3° (i.e., 3° anterior tibial slope) (de Boer et al., 2009) to a maximum 25° (Chiu et al., 2000).

To investigate the likely effects of changes in PTS on ATT and ACL force/strain, in vitro cadaver investigations have attempted to simulate steeper PTS via anterior wedge osteotomy (Agneskirchner et al., 2004, Fening et al., 2008, Giffin et al., 2004 and Nelitz et al., 2013). Under small compression forces (peak of 200 N or 418 N), much smaller than those expected in gait or jump landing, with and without additional loads in other directions steeper PTS has been reported to either decrease strain recorded at the ACL anteromedial bundle (ACLam) (Fening et al., 2008 and Nelitz et al., 2013) or to have no effect at all on ACL force (Giffin et al., 2004) thus apparently refuting foregoing image-based findings. Increased PTS however significantly increases ATT under compression alone (Giffin et al., 2004) and quadriceps force (Agneskirchner et al., 2004). It is to be noted that anterior wedge opening osteotomies nevertheless alter the entire joint articular configuration, contact areas and ligaments orientations/initial lengths when pivoting the tibial epiphysis about a posterior location to produce 5–10 mm anterior opening. In addition to very small load magnitudes considered, these undesired alterations cast doubt on the validity of such cadaver models to adequately study the effect of changes in PTS on joint biomechanics and ACL strain/force. Computational modeling

on the other hand offers the potential to circumvent such shortcomings in altering PTS without undue changes in remaining joint structures.

In the current study we compute the effects of changes in both medial and lateral PTSs by ±5° on the knee joint biomechanics in general and ACL force in particular. Two models are used: (1) an active lower extremity musculoskeletal model including a validated complex finite element, FE, model of the entire knee joint (Adouni and Shirazi-Adl, 2013 and Adouni et al., 2012) driven by in vivo kinematics/kinetics collected in gait of asymptomatic subjects (Astephen et al., 2008) and (2) the isolated unconstrained passive tibiofemoral joint of this model (Marouane et al., 2013 and Shirazi et al., 2008) considered under a compression force of 1400 N at four different knee flexion angles (0°, 15°, 30° and 45°). Changes in tibial medial and lateral PTSs in both models are made with no alterations in tibial ligaments and muscles foot prints, lengths and orientations while tibial articular geometries are rigidly rotated about local axes to cause minimal alterations in articular configuration. Following earlier imaging studies, it is hypothesized that changes in PTS influence the joint biomechanics and that a steeper PTS increases ACL forces at all simulated tasks and joint flexion angles.

4.3 Methods

An existing validated FE model of the knee joint that consists of bony structures (tibia, femur and patella) and their compliant cartilage layers as well as menisci and major ligaments is employed (Adouni et al., 2012). Bony structures are simulated as rigid bodies due to their much higher stiffness (Donahue and Hull, 2002) while the articular cartilage layers and menisci are simulated as non-homogeneous nonlinear depth dependent composites of collagen fibrils and hyperelastic matrices. Cartilage layers are reinforced by distinct fibril networks running parallel to the articular surface in the superficial zone, randomly oriented in the middle zone and vertical in the deep zone. Each ligament is simulated by a number of uniaxial connector elements with initial pre-strains, non-linear (tension-only) material properties and initial cross-sectional areas of 42, 60, 18, 25, 42.7 and 28.5 mm^2 for cruciates (ACL and PCL), collaterals (LCL and MCL) and patellofemorals (MPFL and LPFL), respectively (Mesfar and Shirazi-Adl, 2005). Two FE models are used here (Figure 4.1): one with this detailed 3D knee model within a 3D musculoskeletal model of the lower extremity including also hip and ankle joints to simulate mid-stance phase under in vivo kinematics/kinetics reported for asymptomatic subjects in gait (Adouni et al., 2012)

while the second model is its passive tibiofemoral (TF) portion alone investigated here at different flexion angles (0–45°) under 1400 N compression.

In our model, the initial PTS value is defined separately for each plateau as the angle between a line perpendicular to the gravity (z) axis and another line connecting both extreme ends of the cartilage insertion into the tibial bone on its compartmental mid-plane (parallel to the sagittal plane). In both models and in order to evaluate the effect of changes in PTS, the initial medial (~9.8°) and lateral (~5°) PTSs are altered both either by +5° or −5° by rigidly rotating tibial cartilage layers (including insertion points into the underlying tibial bone) around lateral–medial (L–M) axes placed at the center of their respective tibial articulations (see Figure 4.2). In this manner, minimal changes are made in tibial articular geometries (see Figure 4.1C). In the meantime, ligaments footprints are not altered; their lengths and orientations remain unchanged. These changes in PTS hence affect only the tibial slope with minimal effects on the geometry of the articular cartilage layers and overlying menisci.

Following PTS changes, the nonlinear knee joint responses in the passive model are computed at 4 flexion angles (0°, 15°, 30° and 45°) under a compression force of 1400 N and results are compared to those in the reference case with no changes in PTS as reported elsewhere (Marouane et al., 2013). At the first step, the undeformed joint resting configuration is established by considering the joint response under the prestrains in ligaments (Mesfar and Shirazi-Adl, 2006). The femur is then flexed about its epicondylar axis to the desired joint flexion angle (0°, 15°, 30° and 45°) and fixed thereafter in all directions whereas the tibia is left fully unconstrained throughout. To avoid the artifact moments expected in compression, the external compression force is applied at the joint mechanical balance point (Marouane et al., 2013) defined as the location where the applied compression does not generate any rotations in the sagittal (flexion–extension) and frontal (varus–valgus) planes in an unconstrained joint. This point is identified in the FE model by an iterative algorithm and alters with changes in the applied compression force, PTS and joint flexion angle.

For the gait analyses in the active model, muscle forces are evaluated iteratively and applied along with the ground reaction forces and in vivo kinematics/kinetics to investigate the knee joint biomechanics at mid-stance period. The joints motions/moments and the ground-reaction forces for normal gait are taken from in vivo measurement studies on asymptomatic

subjects (Astephen et al., 2008). Details of the lower limb model and non-linear formulation have been presented elsewhere (Adouni and Shirazi-Adl, 2013 and Adouni et al., 2012). In this case and similar to that in the passive model, PTS is varied by ±5° and results of the joint response and ACL force at mid stance phase of gait are compared with those at the reference joint configuration presented elsewhere (Adouni and Shirazi-Adl, 2013 and Adouni et al., 2012). The nonlinear elastostatic analyses are performed using ABAQUS (version 6.11, Simulia Inc., Providence, RI) finite element package program and Matlab (Optimization Tool Box, genetic algorithm).

4.4 Results

In the tibiofemoral (TF) model alone under 1400 N compression, the position of mechanical balance point (where compression is applied on the unconstrained tibia resulting in no coupled F–E and V–V rotations) substantially shifts medially as PTS alters; at all angles when PTS decreases and at 30° and 45° when PTS increases (Figure 4.2). It also moves anteriorly as PTS increases and posteriorly as PTS decreases. Due to the location of MBP, total contact force is transmitted via primary the lateral plateau at smaller flexion angles that gradually shifts to the medial plateau as joint flexion angle increases and as PTS alters (Figure 4.3). At all flexion angles, the contact force on the medial plateau is transmitted primarily at the uncovered cartilage–cartilage zone rather than at covered area (via the medial meniscus) (Figure 4.3). Steeper PTS increases ATT (or equivalently decreases posterior translation) and internal rotation (or decreases external rotation) at all flexion angles while reverse trends are computed in the case with reduced PTS (Figure 4.4). Tibial displacements are markedly larger at 45°.

The ACL force substantially increases at all flexion angles in steeper PTS (Figure 4.5) with a clear gradual shift from its posterolateral bundle (ACLpl) that carries almost the entire force (99%) at smaller flexion angles to its anteromedial bundle (ACLam) that resists 43% of the total force at 45° flexion (Figure 4.5). In contrast, flattening of PTS by 5° completely unloads ACL force even at full extension and markedly increases forces in LCL and PCL (especially as joint flexion increases). The anterolateral bundle of PCL carries larger shares as flexion increases reaching a maximum of 80% at 45°. Forces in MCL remain overall small not exceeding 30 N at different conditions. In accordance with the compartmental loads and coupled motions, contact

pressures are overall larger on the lateral plateau and shift posteriorly as joint flexes, especially on the lateral plateau and at steeper PTS (Figure.4.6).

In the musculoskeletal model at mid-stance period of gait, changes in PTS have moderate effects on estimated muscle forces (Figure 4.7b). Forces in lateral hamstrings (BFLH and BFSH), lateral gastrocnemius (GL) and quadriceps drop with increases in PTS from −5° to the reference case and to +5°. The tibiofemoral contact force on the medial plateau slightly increases in steeper PTS (Figure 4.7c). The total ACL force, in accordance with substantial changes in ATT, markedly increases by 75% in steeper PTS but decreases by 44% in flatter PTS (Fig. 7a). Negligible forces are computed in remaining ligaments while the total force in patellar ligament decreases from 132 N in flatter tibial surface to 105 N in the reference condition and to 100 N in steeper surface in accordance with changes in quadriceps activations. Due to the adduction rotation of the joint, the medial plateau supports most of the joint compression that is transmitted via primarily the uncovered cartilage–cartilage areas (Figure 4.7c). Accordingly, much larger contact pressures are computed on the medial plateau (Figure 4.8).

4.5 Discussion

Following our earlier studies on biomechanics of the passive TF joint under compression force alone (Marouane et al., 2013) and of the lower extremity including the entire knee joint during the stance phase of gait (Adouni and Shirazi-Adl, 2013 and Adouni et al., 2012), the purpose of this study was set to determine how changes in PTS affect joint response and ACL forces. To reach this objective, we used two models (Figure 4.1): (1) an active lower extremity musculoskeletal model including a detailed complex knee joint FE model driven by in vivo kinematics/kinetics collected in gait of asymptomatic subjects at mid stance phase and (2) its isolated unconstrained passive TF joint under a compression force of 1400 N at different flexion angles (0°, 15°, 30° and 45°). Computed results confirm our hypothesis that, regardless of the task and flexion angle considered, alterations in PTS affect joint biomechanics and that steeper PTS substantially increases ATT and ACL force while reverse trends are found with flatter PTS.

Our results of the passive TF model indicate that ACL force at near full extension is primarily supported by the posterolateral bundle and that the anteromedial bundle share slowly grows with joint flexion when PTS increases (Figure 4.5). The shift from ACLpl to ACLam as joint flexes had also been reported earlier in both model studies (Moglo and Shirazi-Adl, 2005)

and in vitro measurements (Amis, 2012;Woo et al., 1998). This suggests that the measurement of a drop in ACL strain at the anteromedial bundle in steeper PTS following a wedge osteotomy reported at the small flexion angle of 15° (Fening et al., 2008) cannot represent a true picture of the entire ACL strain and hence the force. Moreover substantial changes in ACL and collateral ligaments orientation/resting length and articular geometry (contact areas) caused during anterior wedge opening (5–10 mm) osteotomy while attempting to alter PTS likely influence the joint response and hence cast doubt on conclusions of earlier cadaver studies on the effect of steeper PTS on ACL force (Fening et al., 2008 and Giffin et al., 2004). The finding of no change or a drop in ACL strain after wedge osteotomy performed to increase PTS in these studies could also have been influenced by the application of very small compression forces far below those expected in gait. In our current FE model studies, the medial and lateral plateaus are rotated by ±5° about medial–lateral axes that pass through centroids of these surfaces thus minimizing overall changes in tibial articular geometry (Figures 4.1c and 4.2). In this way, identical medial/lateral cartilage layers and overlying menisci are actually placed on the proximal tibia with three different posterior slopes; reference case without or with ±5° while the remaining structures are left unchanged. The tibial footprints of all ligaments including ACL are left completely unaltered thus keeping ACL length and orientation unchanged. Alterations in predictions when compared to the reference model are hence due to the changes in PTS alone.

Generated by external loads, upper body weight, inertia and muscle forces, axial compression force is omnipresent in almost all daily activities. Due to artifact moments and joint instability, experimental and model studies often find it difficult to apply compression loads of physiological magnitudes. To avoid the response dependency on the position of the compression force, constraints on joint rotations in sagittal and frontal planes are usually imposed (Brown and Shaw, 1984, Kurosawa et al., 1980, Lee et al., 2006, Maquet et al., 1975 and Meyer and Haut, 2005). In the current study with the femur fixed but the tibia free, a novel approach (Marouane et al., 2013) is used to circumvent these concerns. The MBP of the joint is iteratively searched in a manner not to cause coupled tibial rotations in flexion–extension and varus–valgus angulations. The location of MBP varies with the compression preload, joint flexion and PTS. Ahmed and Burke (1983) reported that up to a 1 cm posterior shift in the position of applied compression force was necessary for equilibrium at a desired joint flexion angle when the joint rotated from 0° to 90° flexion.

The current observation of the increases in ATT and in the tibial internal rotation with steeper PTS in both active and passive FE models is in line with earlier in vitro studies of the knee joint under compression (Agneskirchner et al., 2004; Markolf et al., 2014; Meyer et al., 2008; Meyer and Haut, 2005, 2008) and is primarily due to the posterior slope of the tibial plateau (Li et al., 1998; Meyer and Haut, 2005). Radiographic investigations of normal and ACL deficient subjects (Dejour and Bonnin, 1994) reported substantial increases in ATT with steeper PTS. In our models, when PTS is increased by 10°, ATT increases by 2.3 mm at mid-stance of gait in the active model and by 4.4 mm at 1400 N compression force in the passive model. In association with computed changes in kinematics, both models estimate much greater ACL forces at all flexion angles in steeper PTS while smaller forces in flatter PTS; for example ACL force alters from 181 N in the reference case at the mid-stance phase to 102 N and 317 N when PTS changes by −5° and +5°, respectively (Figure 4.7a). These findings corroborate previous in vivo observations indicating larger PTS as a major risk factor for ACL injuries (Sonnery-Cottet et al., 2011 and Todd et al., 2010). Large ACL forces in steeper PTS under 1400 N compression also point to ACL vulnerability to rupture under greater compression forces in corroboration of in vitro studies (Meyer et al., 2008, Meyer and Haut, 2005, Meyer and Haut, 2008, Wall et al., 2012 and Yeow et al., 2008).

As PTS increases (by −5° to the reference case and further by +5° to the steeper model), forces in quadriceps, hamstrings and GM muscles crossing the knee joint in the active model at mid-stance continue to drop (Figure 4.7b). The total contact force on the tibial plateaus follows the same trend and decreases from 1211 N to 1118 N in the reference case but on the contrary, the trend reverses reaching 1217 N in the model with steepest PTS. These changes in contact forces are due to the substantial increase in ACL force from 102 N in flatter PTS to 317 N in the steeper one (Figure 4.7a).

Previous model studies of the lower extremity in gait, despite negligence of cartilage layers and menisci in addition to the consideration of equilibrium only in the sagittal plane (Shelburne et al., 2011) or 2D sagittal representation of the joint (Liu and Maitland, 2003 and Shao et al., 2011), agree with our predictions on the substantial increase in ATT (Liu and Maitland, 2003) and in ACL force (Shao et al., 2011 and Shelburne et al., 2011) in the knee joints with steeper PTS. In the study of Shelburne et al. (2011), alteration in PTS of +5° and −5° in walking resulted respectively in +80 N and −75 N changes in ACL force as well as +2.4 and

−2.3 mm in ATT relative to the reference values which are in line with changes of +136 N and −79 N in ACL force and +1.2 and −1.2 mm in ATT computed in our active model at the mid-stance phase.

In summary, PTS was altered at both lateral and medial plateaus with minimal changes in articular configuration and none in ligament foot-prints, muscle insertions and material properties. Alterations in PTS were found to influence active and passive biomechanics of the knee joint. At mid-stance, despite lower forces in all muscles crossing the knee joint with increase in the tibial slope, the total tibial contact force increased due to much larger ACL force. In both active and passive models and under all compression forces and flexion angles considered in this work, steeper PTS significantly increased ATT and ACL forces. Steeper PTS is hence a major risk factor in markedly increasing ACL force and its vulnerability to injury. Future studies should extend this work to cover the entire stance phase while simulating changes in PTS individually at each tibial plateau.

4.6 Acknowledgements

The current work has been supported by a grant from the Natural Sciences and Engineering Research Council of Canada (NSERC). The partial scholarship of MUTAN-Tunisia to the first author is also gratefully acknowledged.

4.7 References

Adouni, M., Shirazi-Adl, A., 2013. Consideration of equilibrium equations at the hip joint alongside those at the knee and ankle joints has mixed effects on knee joint response during gait. Journal of Biomechanics 46, 619-624.

Adouni, M., Shirazi-Adl, A., Shirazi, R., 2012. Computational biodynamics of human knee joint in gait: from muscle forces to cartilage stresses. Journal of Biomechanics 45, 2149-2156.

Agneskirchner, J., Hurschler, C., Stukenborg-Colsman, C., Imhoff, A., Lobenhoffer, P., 2004. Effect of high tibial flexion osteotomy on cartilage pressure and joint kinematics: a biomechanical study in human cadaveric knees. Archives of Orthopaedic and Trauma Surgery 124, 575-584.

Ahmed, A., Burke, D., 1983. In vitro measurement of static pressure distribution in synovial joints. I: Tibial surface of the knee. Journal of Biomechanical Engineering 105, 216-225.

Am Jung, K., Lee, S.C., Hwang, S.H., Song, M.B., 2009. ACL injury while jumping rope in a patient with an unintended increase in the tibial slope after an opening wedge high tibial osteotomy. Archives of Orthopaedic and Trauma Surgery 129, 1077-1080.

Astephen, J.L., Deluzio, K.J., Caldwell, G.E., Dunbar, M.J., 2008. Biomechanical changes at the hip, knee, and ankle joints during gait are associated with knee osteoarthritis severity. Journal of Orthopaedic Research 26, 332-341.

Boden, B.P., Breit, I., Sheehan, F.T., 2009a. Tibiofemoral alignment: contributing factors to noncontact anterior cruciate ligament injury. The Journal of Bone & Joint Surgery 91, 2381-2389.

Brandon, M.L., Haynes, P.T., Bonamo, J.R., Flynn, M.I., Barrett, G.R., Sherman, M.F., 2006. The association between posterior-inferior tibial slope and anterior cruciate ligament insufficiency. Arthroscopy: The Journal of Arthroscopic & Related Surgery 22, 894-899.

Brazier, J., Migaud, H., Gougeon, F., Cotten, A., Fontaine, C., Duquennoy, A., 1996. Evaluation of methods for radiographic measurement of the tibial slope. A study of 83 healthy knees. Revue de chirurgie orthopédique et réparatrice de l'appareil moteur 82, 195.

Brown, T.D., Shaw, D.T., 1984. In vitro contact stress distribution on the femoral condyles. Journal of Orthopaedic Research 2, 190-199.

Chiu, K., Zhang, S., Zhang, G., 2000. Posterior slope of tibial plateau in Chinese. The Journal of Arthroplasty 15, 224-227.

de Boer, J.J., Blankevoort, L., Kingma, I., Vorster, W., 2009. In vitro study of inter-individual variation in posterior slope in the knee joint. Clinical Biomechanics 24, 488-492.

Dejour, H., Bonnin, M., 1994. Tibial translation after anterior cruciate ligament rupture. Two radiological tests compared. Journal of Bone & Joint Surgery, British Volume 76, 745-749.

Donahue, T.L.H., Hull, M., 2002. A finite element model of the human knee joint for the study of tibio-femoral contact. Journal of Biomechanical Engineering 124, 273.

Farshad-Amacker, N.A., Potter, H.G., 2013. MRI of knee ligament injury and reconstruction. Journal of Magnetic Resonance Imaging 38, 757-773.

Fening, S.D., Kovacic, J., Kambic, H., McLean, S., Scott, J., Miniaci, A., 2008. The effects of modified posterior tibial slope on acl strain and knee kinematics: a human cadaveric study. The Journal of Knee Surgery 21, 205.

Giffin, J.R., Vogrin, T.M., Zantop, T., Woo, S.L., Harner, C.D., 2004. Effects of increasing tibial slope on the biomechanics of the knee. The American Journal of Sports Medicine 32, 376-382.

Hashemi, J., Breighner, R., Jang, T.-H., Chandrashekar, N., Ekwaro-Osire, S., Slauterbeck, J.R., 2010. Increasing pre-activation of the quadriceps muscle protects the anterior cruciate ligament during the landing phase of a jump: An in vitro simulation. The Knee 17, 235-241.

Hashemi, J., Chandrashekar, N., Gill, B., Beynnon, B.D., Slauterbeck, J.R., SchuttJr, R.C., Mansouri, H., Dabezies, E., 2008. The geometry of the tibial plateau and its influence on the biomechanics of the tibiofemoral joint. The Journal of Bone & Joint Surgery 90, 2724-2734.

Hashemi, J., Chandrashekar, N., Mansouri, H., Gill, B., Slauterbeck, J.R., Schutt, R.C., Dabezies, E., Beynnon, B.D., 2009. Shallow Medial Tibial Plateau and Steep Medial and Lateral Tibial Slopes New Risk Factors for Anterior Cruciate Ligament Injuries. The American Journal of Sports Medicine 38, 54-62.

Hohmann, E., Bryant, A., Reaburn, P., Tetsworth, K., 2011. Is there a correlation between posterior tibial slope and non-contact anterior cruciate ligament injuries? Knee Surgery, Sports Traumatology, Arthroscopy 19, 109-114.

Hutchinson, M.R., Ireland, M.L., 1995. Knee injuries in female athletes. Sports medicine 19, 288-302.

Kurosawa, h., Fukubayashi, t., Nakajima, h., 1980. Load-bearing mode of the knee joint: physical behavior of the knee joint with or without menisci. Clinical orthopaedics and related research 149, 283-290.

Lee, S.J., Aadalen, K.J., Malaviya, P., Lorenz, E.P., Hayden, J.K., Farr, J., Kang, R.W., Cole, B.J., 2006. Tibiofemoral contact mechanics after serial medial meniscectomies in the human cadaveric knee. The American Journal of Sports Medicine 34, 1334-1344.

Li, G., Rudy, T.W., Allen, C., Sakane, M., Woo, S.L.Y., 1998. Effect of combined axial compressive and anterior tibial loads on in situ forces in the anterior cruciate ligament: a porcine study. Journal of Orthopaedic Research 16, 122-127.

Liu, W., Maitland, M.E., 2003. Influence of anthropometric and mechanical variations on functional instability in the ACL-deficient knee. Annals of Biomedical Engineering 31, 1153-1161.

Loud, K.J., Micheli, L.J., 2001. Common athletic injuries in adolescent girls. Current Opinion in Pediatrics 13, 317-322.

Maquet, P.G., Van de Berg, A., Simonet, J., 1975. Femorotibial weight-bearing areas. J Bone Joint Surg A 57, 766-772.

Markolf, K.L., Jackson, S.R., Foster, B., McAllister, D.R., 2013. ACL forces and knee kinematics produced by axial tibial compression during a passive flexion–extension cycle. Journal of Orthopaedic Research.

Marouane, H., Shirazi-Adl, A., Adouni, M., 2013. Knee joint passive stiffness and moment in sagittal and frontal planes markedly increase with compression. Computer Methods in Biomechanics and Biomedical Engineering, 1-12.

McLean, S.G., Lucey, S.M., Rohrer, S., Brandon, C., 2010. Knee joint anatomy predicts high-risk in vivo dynamic landing knee biomechanics. Clinical Biomechanics 25, 781-788.

Mesfar, W., Shirazi-Adl, A., 2005. Biomechanics of the knee joint in flexion under various quadriceps forces. The Knee 12, 424-434.

Mesfar, W., Shirazi-Adl, A., 2006. Biomechanics of changes in ACL and PCL material properties or prestrains in flexion under muscle force-implications in ligament reconstruction. Computer Methods in Biomechanics and Biomedical Engineering 9, 201-209.

Meyer, E.G., Baumer, T.G., Slade, J.M., Smith, W.E., Haut, R.C., 2008. Tibiofemoral contact pressures and osteochondral microtrauma during anterior cruciate ligament rupture due to excessive compressive loading and internal torque of the human knee. The American Journal of Sports Medicine 36, 1966-1977.

Meyer, E.G., Haut, R.C., 2005. Excessive compression of the human tibio-femoral joint causes ACL rupture. Journal of Biomechanics 38, 2311-2316.

Meyer, E.G., Haut, R.C., 2008. Anterior cruciate ligament injury induced by internal tibial torsion or tibiofemoral compression. Journal of Biomechanics 41, 3377-3383.

Moglo, K., Shirazi-Adl, A., 2005. Cruciate coupling and screw-home mechanism in passive knee joint during extension–flexion. Journal of Biomechanics 38, 1075-1083.

Myer, G.D., Ford, K.R., Paterno, M.V., Nick, T.G., Hewett, T.E., 2008. The effects of generalized joint laxity on risk of anterior cruciate ligament injury in young female athletes. The American Journal of Sports Medicine 36, 1073-1080.

Nelitz, M., Seitz, A.M., Bauer, J., Reichel, H., Ignatius, A., Dürselen, L., 2013. Increasing posterior tibial slope does not raise anterior cruciate ligament strain but decreases tibial rotation ability. Clinical Biomechanics 28, 285-290.

Shao, Q., MacLeod, T.D., Manal, K., Buchanan, T.S., 2011. Estimation of ligament loading and anterior tibial translation in healthy and ACL-deficient knees during gait and the influence of increasing tibial slope using EMG-driven approach. Annals of Biomedical Engineering 39, 110-121.

Shelburne, K.B., Kim, H.J., Sterett, W.I., Pandy, M.G., 2011. Effect of posterior tibial slope on knee biomechanics during functional activity. Journal of Orthopaedic Research 29, 223-231.

Shirazi, R., Shirazi-Adl, A., Hurtig, M., 2008. Role of cartilage collagen fibrils networks in knee joint biomechanics under compression. Journal of Biomechanics 41, 3340-3348.

Sonnery-Cottet, B., Archbold, P., Cucurulo, T., Fayard, J.-M., Bortolletto, J., Thaunat, M., Prost, T., Chambat, P., 2011. The influence of the tibial slope and the size of the intercondylar notch on rupture of the anterior cruciate ligament. Journal of Bone & Joint Surgery, British Volume 93, 1475-1478.

Todd, M.S., Lalliss, S., Garcia, E.S., DeBerardino, T.M., Cameron, K.L., 2010. The relationship between posterior tibial slope and anterior cruciate ligament injuries. The American Journal of Sports Medicine 38, 63-67.

Wall, S.J., Rose, D.M., Sutter, E.G., Belkoff, S.M., Boden, B.P., 2012. The Role of Axial Compressive and Quadriceps Forces in Noncontact Anterior Cruciate Ligament Injury A Cadaveric Study. The American Journal of Sports Medicine 40, 568-573.

Woo, S.L., Fox, R.J., Sakane, M., Livesay, G.A., Rudy, T.W., Fu, F.H., 1998. Biomechanics of the ACL: measurements of in situ force in the ACL and knee kinematics. The knee 5, 267-288.

Yeow, C.H., Cheong, C.H., Ng, K.S., Lee, P.V.S., Goh, J.C.H., 2008. Anterior Cruciate Ligament Failure and Cartilage Damage During Knee Joint Compression A Preliminary Study Based on the Porcine Model. The American Journal of Sports Medicine 36, 934-942.

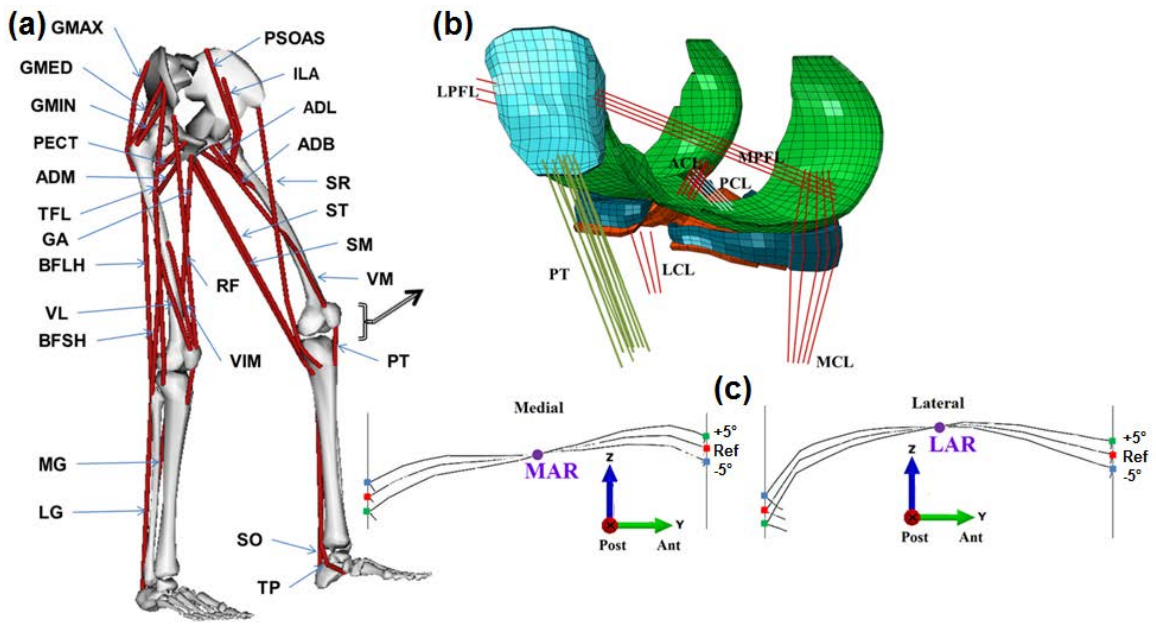

Figure 4.1: **(a)** Schematic diagram showing the 34 muscles incorporated into the lower extremity model (Open Sim, Delp et al., 2007). Quadriceps components are vastus medialis obliqus (VMO), rectus femoris (RF), vastus intermidus medialis (VIM) and vastus lateralis (VL). Hamstrings components include biceps femoris long head (BFLH), biceps femoris short head (BFSH), semi membranous (SM) and TRIPOD made of sartorius (SR), gracilis (GA) and semitendinosus (ST). Gastrocnemius components are gastrocnemius medial (GM) and gastrocnemius lateral (GL). Tibialis posterior (TP) and soleus (SO) muscles are uni-articular ankle muscles. Hip joint muscles (not all shown) include adductor, long (ADL), mag (3 components ADM) and brev (ADB); gluteus max (3 components GMAX), med (3 components GMED) and min (3 components GMIN), iliacus (ILA), iliopsoas (PSOAS), quadriceps femoris; pectineus (PECT), tensor facia lata (TFL), periformis. **(b)** Knee FE model; tibiofemoral (TF) and patellofemoral (PF) cartilage layers, menisci, patellar Tendon (PT). Joint ligaments include lateral patellofemoral (LPFL), medial patellofemoral (MPFL), anterior cruciate (ACL), posterior cruciate (PCL), lateral collateral (LCL) and medial collateral (MCL). **(c)** Posterior tibial slope in the model is changed by rotating by ±5° the medial and lateral plateaus about their local axes (M and L) passing through centroids of these surfaces.

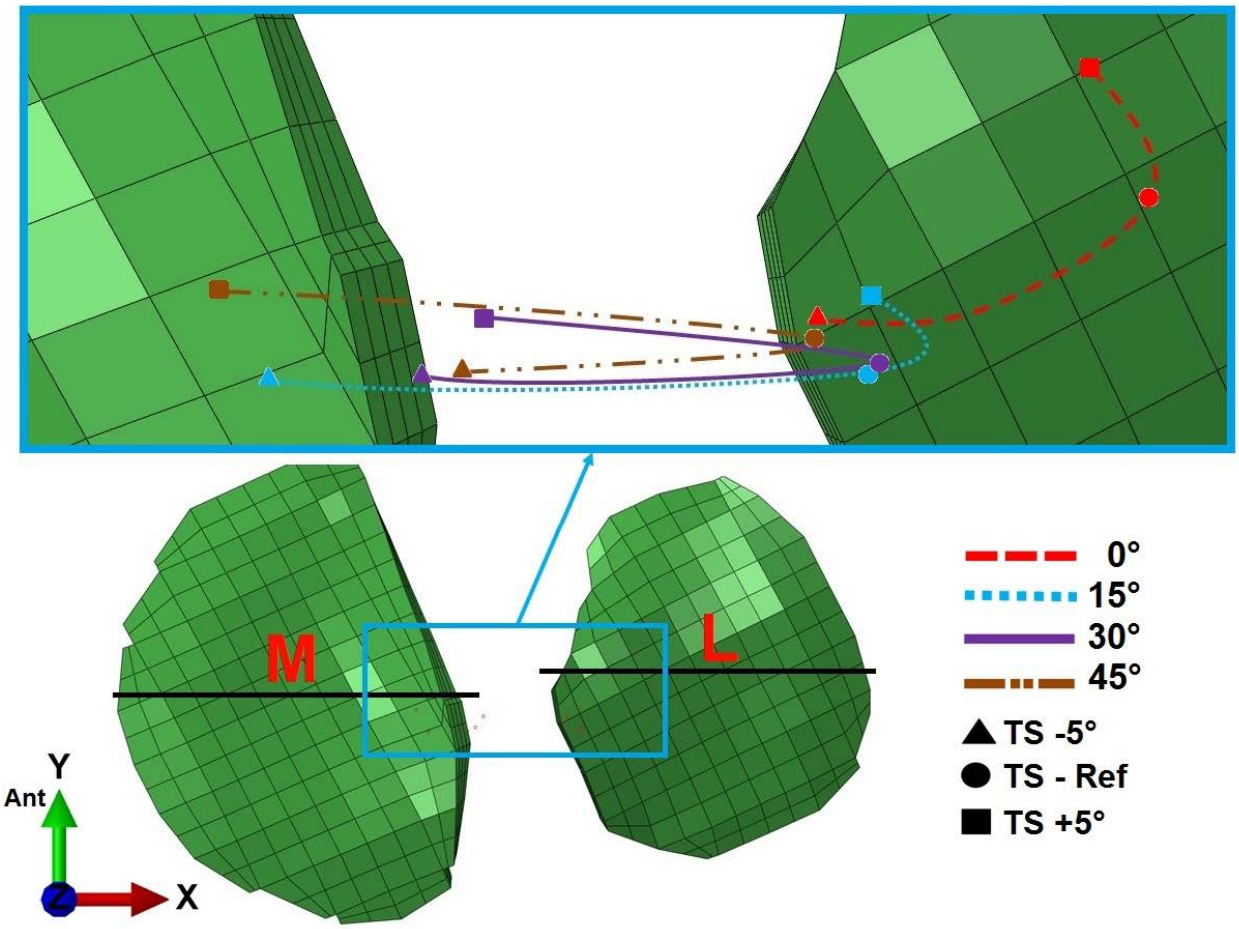

Figure 4.2: Shift in MBP location on the tibial plateaus as a function of joint flexion angle and changes in PTS. When applied at these locations, the 1400 N compression does not cause any sagittal and frontal rotations in the unconstrained tibia. Local axes of medial (M) and lateral (L) plateaus used for changes in PTS are also shown.

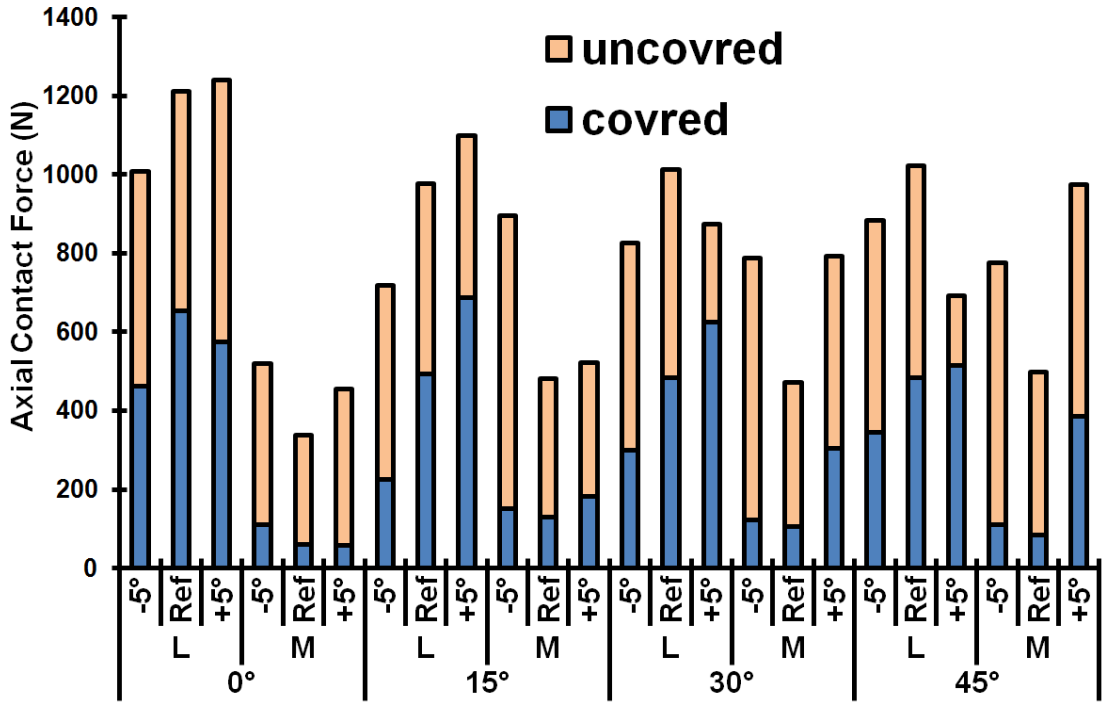

Figure 4.3: Predicted total axial contact forces under 1400 N compression on TF medial (M) and lateral (L) plateaus at covered (via menisci) and uncovered (via cartilage-cartilage) areas for different flexion angles and PTS values.

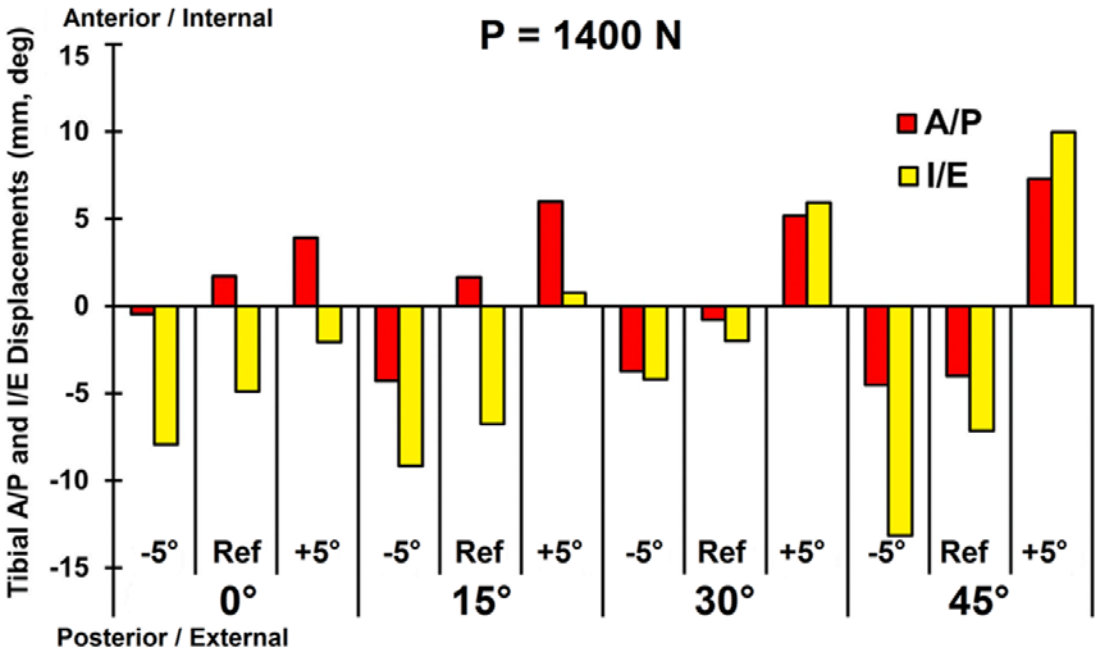

Figure 4.4: Anterior/posterior and internal/external tibial displacements under the applied compression force of 1400 N for different knee flexion angles and PTS.

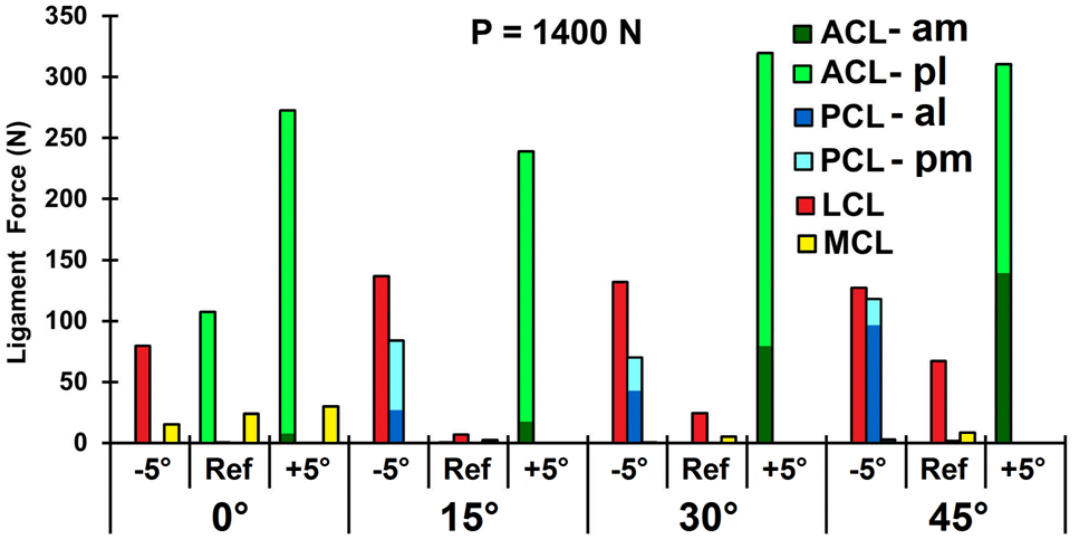

Figure 4.5: Predicted variation of total forces in ligaments (and their bundles) under compression force of 1400 N at different flexion angles and PTS.

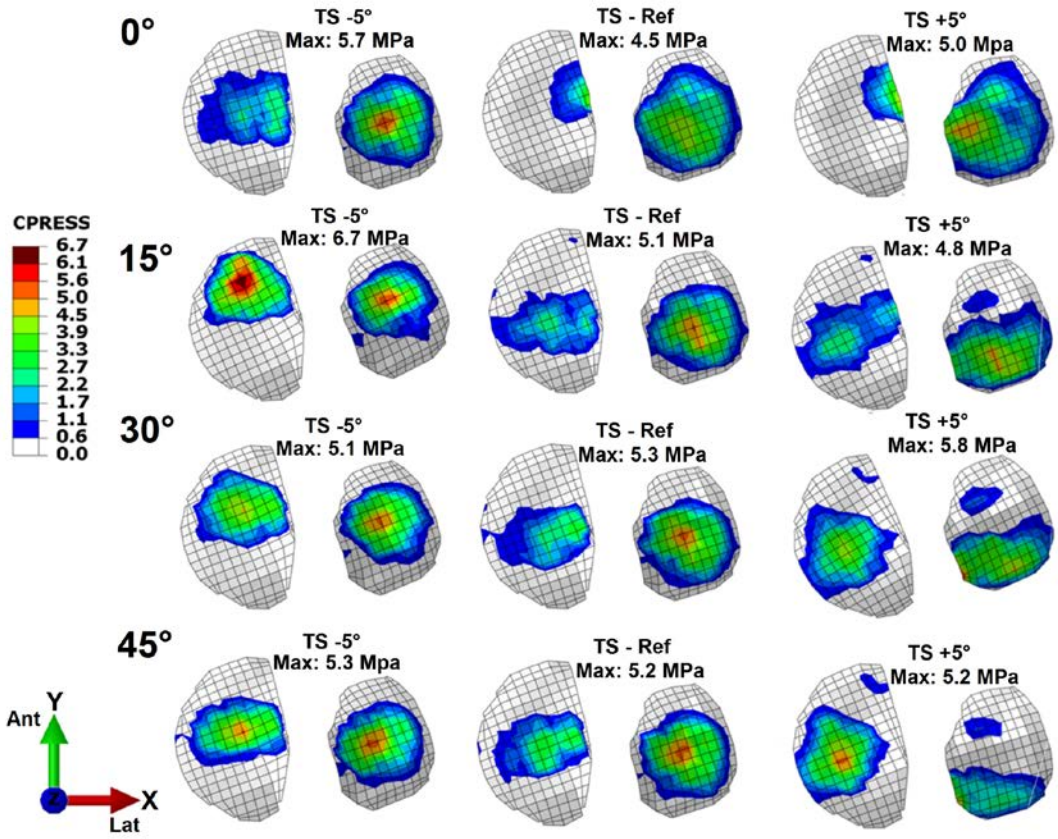

Figure 4.6: Predicted contact pressures at articular surface of lateral and medial tibial plateaus under 1400 N at different knee flexion angles and PTS. Note that a common legend is used for ease in comparisons.

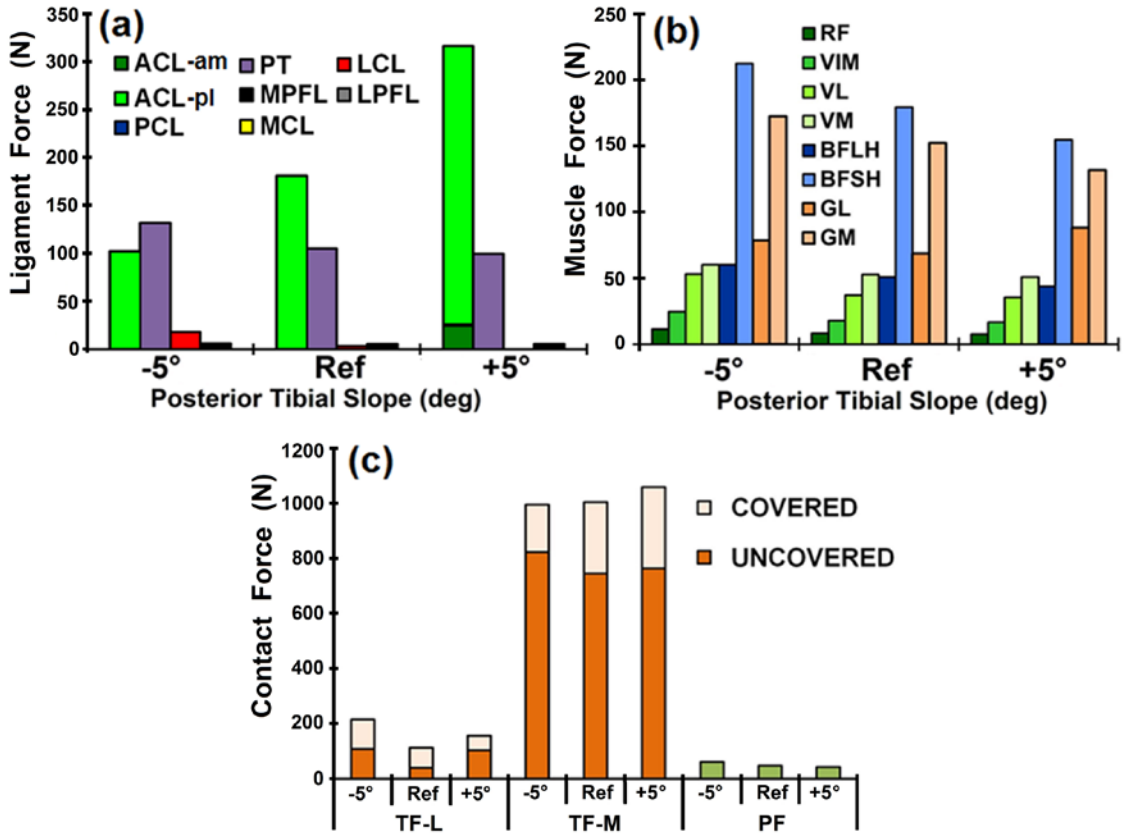

Figure 4.7: Predicted ACL, muscle and tibial contact forces at mid-stance phase of gait for different PTS.

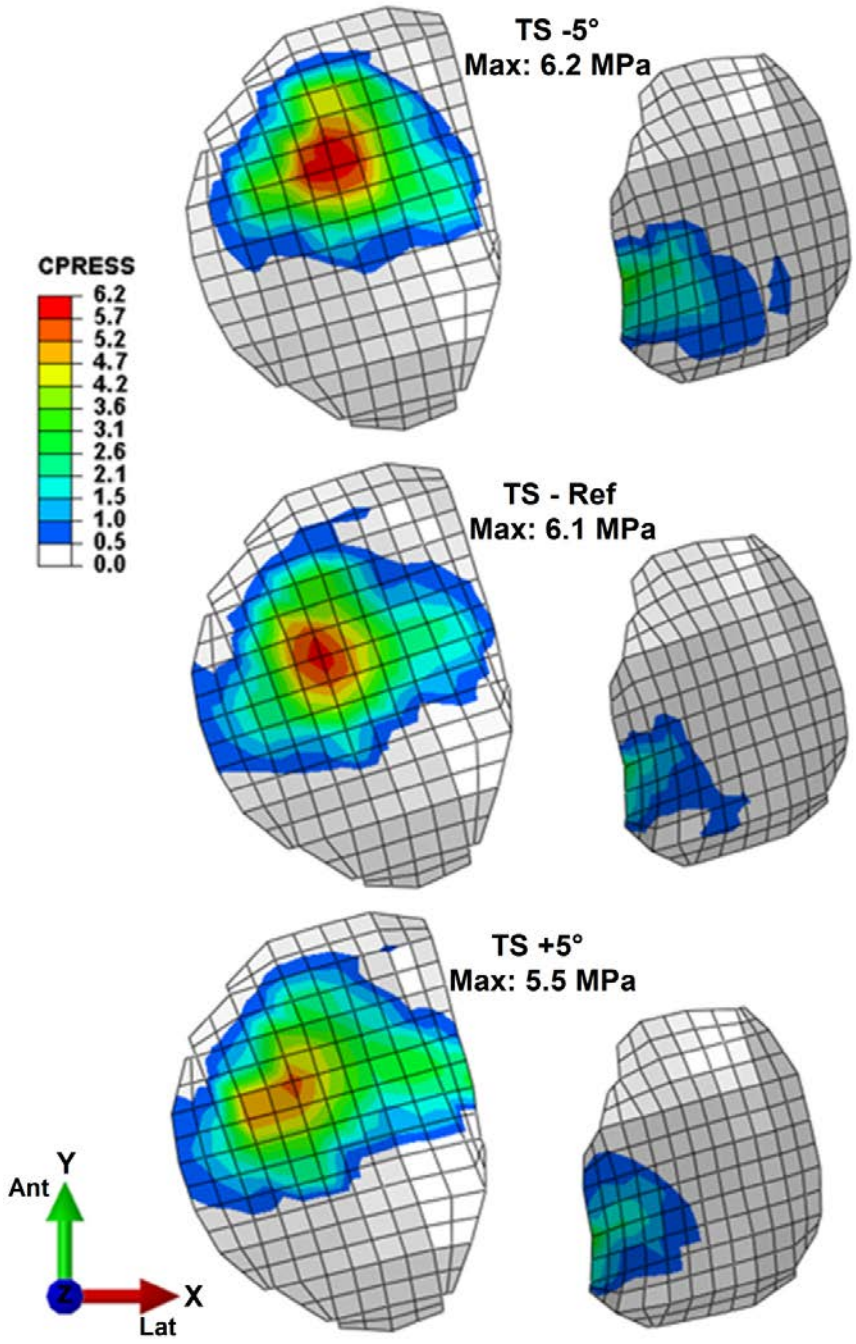

Figure 4.8: Predicted contact pressures at articular surface of lateral and medial tibial plateaus at mid-stance of gait at different PTS. Note that a common legend is used for ease in comparisons.

CHAPITRE 5 ARTICLE 2: QUANTIFICATION OF THE ROLE OF TIBIAL POSTERIOR SLOPE IN KNEE JOINT MECHANICS AND ACL FORCE IN SIMULATED GAIT

H. Marouane, A. Shirazi-Adl, and J. Hashemi

Article published in

Journal of Biomechanics 2015

5.1 Abstract

The anterior cruciate ligament (ACL) rupture is a common knee joint injury with higher prevalence in female athletes. In search of contributing mechanisms, clinical imaging studies of ACL-injured individuals versus controls have found greater medial–lateral posterior tibial slope (PTS) in injured population irrespective of the sex and in females compared to males, with stronger evidence on the lateral plateau slope. To quantify these effects, we use a lower extremity musculoskeletal model including a detailed finite element (FE) model of the knee joint to compute the role of changes in medial and/or lateral PTS by ±5° and ±10° on knee joint biomechanics, in general, and ACL force, in particular, throughout the stance phase of gait. The model is driven by reported kinematics/kinetics of gait in asymptomatic subjects. Our predictions showed, at all stance periods, a substantial increase in the anterior tibial translation (ATT) and ACL force as PTS increased with reverse trends as PTS decreased. At mid-stance, for example, ACL force increased from 181 N to 317 N and 460 N as PTS increased by 5° and 10°, respectively, while dropped to 102 N and 0 N as PTS changed by –5° and –10°, respectively. These effects are caused primarily by change in PTS at the tibial plateau that carries a larger portion of joint contact force. Steeper PTS is a major risk factor, especially under activities with large compression, in markedly increasing ACL force and its vulnerability to injury. Rehabilitation and ACL injury prevention programs could benefit from these findings.

Keywords: Anterior cruciate ligament; Knee joint; Finite element; Tibial posterior slope; Biomechanics

5.2 Introduction

During activities of daily living the knee joint is exposed to large loads (due to body weight, inertia, muscles) and movements that could initiate and/or accelerate joint degeneration and injuries. The anterior cruciate ligament (ACL) rupture is a common joint injury with much higher prevalence in female athletes compared to their male counterparts (Arendt and Dick, 1995, Hewett et al., 2006 and Myer et al., 2008). Approximately 200,000 ACL ruptures and 175,000 reconstructions are reported each year in US alone (MacDonald et al., 2014). Being a major load-bearing component and a restraint in compression-induced tibial anterior translation (ATT) and rotations (Fleming et al., 2001, Meyer et al., 2008a and Sakane et al., 1997), an ACL injury could confound joint biomechanics and predispose the knee to instability and risk of osteoarthritis (OA) (Gabriel et al., 2004, Keays et al., 2010 and Lohmander et al., 2004). Improved knowledge of knee joint functional biomechanics, in general, and ACL forces, in particular, is crucial to delineate the existing sex-based disparity in ACL injuries and to improve surgical and rehabilitation management of ACL-deficient/reconstructed patients regardless of sex.

In search of mechanisms responsible for the sex disparity due to disproportionately higher number of injuries in females, both intrinsic (e.g., anatomical) and extrinsic (e.g., footwear-surface) variables have been indicated (Arendt and Dick, 1995, Hewett et al., 2006, Hootman et al., 2007 and Lipps et al., 2012). Excessive joint compression has been identified as a risk factor for ACL rupture (Beynnon et al., 2002, DeMorat et al., 2004, Fleming et al., 2001, Li et al., 1998, Markolf et al., 2013, Meyer et al., 2008a, Meyer and Haut, 2005, Wall et al., 2012 and Yeow et al., 2008). In this regard, the posterior slope of the tibial plateau (PTS) has been blamed as a primary cause of tibial internal rotation and large ATT (Dejour and Bonnin, 1994 and Meyer and Haut, 2005). Imaging of patients with non-contact ACL injury versus controls has led to a general consensus on higher PTS, especially on the lateral plateau, recognized as a risk factor (Beynnon et al., 2014, Boden et al., 2009a, Brandon et al., 2006, Hashemi et al., 2009, Khan et al., 2011, Li et al., 2014, McLean et al., 2010, Sonnery-Cottet et al., 2011, Terauchi et al., 2011, Todd et al., 2010, van Diek et al., 2014, Webb et al., 2013 and Zeng et al., 2014). With medial and lateral PTS being greater in females than in males, it could hence play an intrinsic role in this disparity (Hashemi et al., 2010, Hashemi et al., 2008, Hashemi et al., 2009, Hohmann et al., 2011 and Todd et al., 2010). In a radiographic study

of normal and ACL deficient subjects, Dejour and Bonnin (1994) reported that every 10° increase in PTS increases ATT by 6 mm instance and 3.5 mm in Lachman test. Musculoskeletal model studies of the lower extremity in gait, despite limitations such as the absence of cartilage layers and menisci, have corroborated these clinical findings on the substantial increases in ATT (Liu and Maitland, 2003) and ACL force (Shao et al., 2011 and Shelburne et al., 2011) in joints with steeper PTS. Similarly, using a 2D model, Liu and Maitland (2003) demonstrated an increase in ATT from 7.5 to 17.8 mm in ACL-deficient knees during walking as PTS increased from 4° to 12°. High tibial osteotomy performed with the intention to prevent or decelerate medial OA could also increase PTS that then in turn increases ATT (Agneskirchner et al., 2004) and the risk of ACL injury (Am Jung et al., 2009).

In contrast to foregoing findings, steeper PTS in cadaver investigations has either decreased strains recorded at ACL anteromedial bundle (ACLam) (Fening et al., 2008 and Nelitz et al., 2013) or left no effect on ACL force (Giffin et al., 2004). In vitro cadaver investigations simulating steeper PTS via anterior wedge osteotomy (Agneskirchner et al., 2004, Fening et al., 2008, Giffin et al., 2004 and Nelitz et al., 2013) however alter the entire joint articular configuration. Contact areas and ligaments orientations/initial lengths also change when pivoting the tibial epiphysis about a posterior location to produce 5–10 mm anterior opening. These undesired alterations cast doubt on the validity of such cadaver models to adequately investigate the effect of changes in PTS on joint biomechanics and ACL strains/forces. Computational modeling on the other hand offers the potential to circumvent such shortcomings in altering PTS without undue changes in remaining joint structures. In an earlier finite element (FE) study of both a passive knee joint model in compression at 0–45° flexion angles and a musculoskeletal lower extremity model at mid-stance period, ATT and ACL forces substantially increased in steeper PTS but decreased in flatter PTS (Marouane et al., 2014).

In continuation of our previous study (Marouane et al., 2014), we aim to quantify the effects of ±5° and ±10° changes at medial and lateral PTS, alone or together, on the knee joint biomechanics and ACL force. To reach this objective, an active lower extremity musculoskeletal model including a complex finite element (FE) model of the knee joint (Adouni and Shirazi-Adl, 2013) driven by in vivo kinematics/kinetics collected in gait of asymptomatic subjects (Astephen et al., 2008) is used. To avoid confounding effects, changes in medial and lateral PTSs are made with no alterations in tibial ligaments and muscles footprints, lengths and orientations. We

hypothesize that alterations in PTS influence ACL forces with the extent of changes dependent on the variations in PTS.

5.3 Methods

5.3.1 Finite element model

A validated FE model of the entire knee joint (Figure 5.1) consisting of bony structures (tibia, femur and patella) and their compliant cartilage layers as well as menisci, major tibiofemoral (TF: ACL, PCL, CL, MCL) and patellofemoral (PF: MPFL, LPFL) ligaments, patellar tendon (PT), quadriceps (four components), hamstrings (six components) and gastrocnemius (two components) is employed (Adouni and Shirazi-Adl, 2013). Bony structures are simulated as rigid bodies (Haut Donahue and Hull, 2002) while the articular cartilage layers and menisci are represented as non-homogeneous nonlinear depth-dependent composites of collagen fibril networks and hyperelastic matrices. Ligaments are simulated by a number of nonlinear axial elements with initial pre-strains, non-linear (tension-only) material properties, and initial cross-sectional areas of 42, 60, 18, 25, 99, 42.7, and 28.5 mm2 respectively for ACL, PCL, LCL, MCL, PT, MPFL, and LPFL (Mesfar and Shirazi-Adl, 2005 and Shirazi-Adl and Moglo, 2005). Details of the model are provided elsewhere (Adouni and Shirazi-Adl, 2013, Marouane et al., 2015 and Marouane et al., 2014).

5.3.2 Changes in PTS

Notwithstanding different methods to estimate PTS from images (Brazier et al., 1996, Chaudhari et al., 2009, Giffin et al., 2004, Hohmann et al., 2011 and Sonnery-Cottet et al., 2011) and the complex spatial shapes of tibial plateaus that hardly resemble a plane with a single slope (Hashemi et al., 2008), measurements based on lateral images report tibial slopes ranging from 3° anterior (de Boer et al., 2009) to 25° posterior (Chiu et al., 2000). In our model, the initial PTS is defined as the angle between a line perpendicular to the gravity axis (z) and another line connecting both ends (in the sagittal plane, see Figure 5.1) of the cartilage insertion into the tibial bone. In order to evaluate the effect of changes in PTS, the initial medial (~9.8°) and/or lateral (~5°) PTSs in the undeformed model are altered both by ±5° by rigidly rotating tibial cartilage layers around local lateral–medial (L–M) axes placed at the center of tibial articulations in a manner to yield minimal changes in tibial articular cartilage geometry (Figure 5.1). At the

same time, ligaments footprints and hence their lengths and orientations remain unchanged. These changes in PTS alter hence only the tibial slope with minimal effects on the geometry of the articular cartilage layers. At 5% and 50% stance periods additional simulations are performed in which medial and lateral PTSs are altered, alone or combined, by ±5° as well as ±10° (Figure 5.1).

5.3.3 Muscle force estimation

The detailed knee model is introduced in a musculoskeletal model of the lower extremity (Delp et al., 2007) including hip (3D spherical) and ankle (1D spherical) joints as well as uni- and bi-articular muscles to simulate the stance phase of gait under in vivo kinematics/kinetics reported for normal subjects (Astephen et al., 2008). Muscle forces are evaluated iteratively and applied as additional external forces along with the ground reaction forces (Hunt et al., 2001) and in vivo joint rotations/moments (Astephen et al., 2008). Static optimization along with a cost function of the sum of cubed stresses of all muscles (Eq. 1), subject to moment equilibrium equations (Eq. 2) and inequality equations on muscle forces (Eq. 3), are used to iteratively estimate muscle forces at each instance.

$$\text{(Eq. 1)} \qquad \sum_{i=1}^{n}\left(\frac{F_i}{PCSA_i}\right)^3$$

$$\text{(Eq. 2)} \qquad \sum_{i=1}^{n} r_{ij} \times F_{ij} = M_j$$

$$\text{(Eq. 3)} \qquad F_{pi} \le F_i \le (F_{pi} + \sigma_{imax} \, X \, PCSA_i)$$

where Fi, Fpi, rij, σimax, and PCSAi are the force, passive force component, lever arms in different planes j, maximum stress, and physiological cross-sectional area of muscle i, respectively. Mj are moments to be resisted by muscles taken as reported in gait (Astephen, 2007) for the hip and ankle whereas as calculated by the FE model under prescribed rotations (Astephen et al., 2008) at the knee joint thus accounting for the knee joint passive contributions. Due to expected small changes in muscle length, the passive force component in all muscles is neglected.

Following application of initial prestrains in knee joint ligaments with/without variations in PTS, the hip/knee/ankle rotations/moments and ground reaction forces (GRF) reported at each period of stance phase (0%, 5%, 25%, 50%, 75% and 100%) (Astephen, 2007 and Hunt et al., 2001) are applied and iterative nonlinear analyses carried out till convergence (i.e., unbalanced moments under final muscle forces <0.1 Nm). The location of GRF at each period is determined so as to generate reported knee joint moments (Astephen et al., 2008) accounting for the leg/foot weights (29.78/7.98 N). Since our model is constructed based on a female knee, a body weight of 60.6 kg is considered (De Leva, 1996). The nonlinear elastostatic analyses are performed using ABAQUS (version 6.11, Simulia Inc., Providence, RI) finite element package program and Matlab (Optimization Tool Box, genetic algorithm).

5.4 Results

Results of the reference case with no changes in PTS (Adouni and Shirazi-Adl, 2013) are also presented here for comparison. Throughout the stance phase, changes in PTS had relatively small effects on muscle forces (<50 N) (Figure 5.2). On the other hand, steeper PTS markedly increased ATT at all periods with reverse trends under flatter PTS (Figure 5.3). As a result and throughout stance, ACL force significantly increased with steeper PTS but dropped as PTS reduced so that it even completely disappeared at mid-stance with −10° change in PTS of either medial plateau or both medial–lateral plateaus (Figure 5.4). The effect was much more pronounced at mid-stance (50%) where ACL force, respectively, increased by 135 N and 279 N as PTS increased by 5° and 10° but decreased by 79 N and 181 N (to nil) at 5° and 10° flatter PTS. In all cases, the posterolateral bundle carried nearly all ACL forces with the anteromedial bundle contributing only at steeper PTS (Figure 5.4). At 5% and 50% periods, changes in PTS at the lateral and medial plateaus, respectively, played the primary role in foregoing alterations (Figure 5.4). Variations in PTS had negligible to small effects on forces in remaining ligaments (Figure 5.5).

In accordance with muscle forces, changes in PTS had small effects on estimated TF (Figure 5.6) and PF contact forces and contact pressure centers. Throughout the stance phase, TF contact force was transmitted primarily at the uncovered cartilage–cartilage zone rather than the covered zone via the medial meniscus (Figure 5.6). The TF and PF contact areas/pressures

followed the same trends as their respective contact forces and did not change much as PTS altered (Figure 5.7).

5.5 Discussion

Using an active lower extremity musculoskeletal model including a detailed complex knee joint FE model driven by in vivo joint rotations/moments and ground reaction forces collected in gait of normal subjects, we aimed here to quantify the effect of variations in PTS on the joint response and ACL forces. Computed results, in corroboration of the existing consensus (e.g., Beynnon et al., 2014; Sonnery-Cottet et al., 2011; Webb et al., 2013), confirmed our hypothesis in that, throughout the stance phase of gait, ATT and ACL forces markedly increased with steeper PTS but decreased with flatter PTS. The extent of changes also markedly increased as PTS variations doubled from ±5° to ±10°. For example at mid-stance, the total ACL force of 181 N increased to 317 N and further to 460 N as PTS increased by 5° and 10°, respectively (Fig. 4). On the contrary, ACL force dropped to 102 N and 0 N (i.e., unloaded) as PTS altered by −5° and −10°, respectively. While it is expected that various intrinsic and extrinsic factors influence ACL force, current results clearly highlight a much greater risk of ACL injury in knee joints having greater PTS. In agreement, increased PTS has been blamed as a primary cause of tibial internal rotation and large ATT (Dejour and Bonnin, 1994 and Meyer and Haut, 2005). Larger compression on the joint under higher muscle activation and external loads expected during sport activities and drop landing, for example, likely further increase this effect. Cadaveric studies (Meyer et al., 2008a, Meyer and Haut, 2005, Wall et al., 2012 and Yeow et al., 2008) have reported ACL rupture in the joint under large compression.

With regard to the disproportionately higher number of non-contact ACL injuries in females than in males, various intrinsic (e.g., anthropometric, alignment, ACL cross sectional area) and extrinsic (e.g., footwear-surface, external loads/motions) variables are indicated (Arendt and Dick, 1995, Feucht et al., 2013, Hewett et al., 2006 and Lipps et al., 2012). With PTS being greater in females than in males, it could also play, as an intrinsic parameter, a crucial role in this disparity (Hashemi et al., 2010, Hashemi et al., 2008, Hashemi et al., 2009, Hohmann et al., 2011 and Todd et al., 2010). Such parameter can hence be used as a marker to identify individuals at greater risk and in more effective prevention and management of ACL injuries.

Foregoing findings on the marked effect of changes in PTS on ATT and ACL force are however in contradiction with the results of some cadaveric studies that simulated alterations in PTS by anterior tibial osteotomy (Fening et al., 2008, Giffin et al., 2004 and Nelitz et al., 2013). Under compressive load (up to 418 N) and/or anterior–posterior load (up to 209 N), Fening et al. (2008) found that an anterior opening wedge of 5 mm or 10 mm had nearly no effect on ATT and even reduced ACL-am strain. In similar studies under up to 200 N compression, ACL-am strain and ACL force was found either unaffected or decreased with steeper PTS (Giffin et al., 2004 and Nelitz et al., 2013). Measurement of strain at ACL-am bundle may however not depict a true picture of ACL force as our results show much greater forces in ACL-pl bundle throughout stance (Figure 5.4). Application of rather small compression forces in these studies may also be a reason not to detect the effect of changes in PTS on response. Finally anterior wedge opening osteotomies alter the entire joint articular configuration, contact areas and ligaments orientations/initial lengths when pivoting the tibial epiphysis about a posterior location to produce 5–10 mm anterior opening. A recent study on the effect of anterior wedge opening in the sagittal plane recorded significant alterations in contact pressure/area distribution on the tibial plateau leading to decompression of the posterior half of the plateau (Agneskirchner et al., 2004).

Our earlier study simulating the effect of changes in PTS in a passive tibiofemoral joint (Marouane et al., 2014) found substantial increases in ATT, tibial internal rotation, and ACL force at steeper PTS under moderate compression forces at joint flexion angles of 0° to 45°. In the current lower extremity musculoskeletal model study in gait, however, the knee joint internal–external rotation along with flexion–extension and varus–valgus rotations were all prescribed throughout stance phase in accordance with the data from in vivo measurements (Astephen et al., 2008). Changes in ATT and ACL forces as PTS varied (Figure 5.3 and Figure 5.4) were hence computed under identical internal–external rotations. Since ACL is known as a major restrain in axial rotation (Fleming et al., 2001, Markolf et al., 2013 and Markolf et al., 2009), greater changes in ACL force could have been estimated had we varied tibial internal rotations in accordance with our earlier studies (Marouane et al., 2014). Proper resolution of this issue, however, requires collection of gait data as a function of PTS magnitude.

An interesting aspect of this work was the novel simulation of variation of PTS in each medial and lateral plateau separately in order to identify the relative role of each plateau. Alterations in PTS separately in each plateau at a time demonstrated that ATT and ACL forces

were influenced primarily by changes in the plateau supporting a larger proportion of the joint compression force. In this manner, ATT and ACL forces were influenced by changes in PTS at the lateral plateau at 5% stance period whereas at the medial plateau at 50% mid-stance (Figure 5.3 and Figure 5.4). This is because, the contact forces were much larger in the lateral plateau only in early stance after the heel-strike and shifted side to the medial plateau from 25% to the toe-off at the end (i.e., 100%) (Figure 5.6). These results further emphasize the importance of joint compression force on the extent of changes in ATT and ACL force following alterations in PTS. Once again as discussed earlier, results could have been affected in these cases had we not prescribed reported knee joint internal–external rotations in our musculoskeletal model.

The current model study has some limitations that could affect predicted results though relative effects and conclusions as PTS varied are however expected to hold. We used a single knee geometry reconstructed from a female cadaveric specimen. Though the input structural and material properties in the knee joint are taken from the literature and could vary with age, sex and between subjects, we have extensively validated this model with available in vitro and in vivo data. The lower extremity musculature as well as joint kinematics/kinetics were taken from the data in the literature. Antagonistic co-activity was not considered. The incompressible elastic response of soft tissues considered here is appropriate for short-term loading present during gait. Finally in our simulations, we only altered PTS of medial and/or lateral plateaus with remaining anthropometric features left unchanged; variations in depth (i.e., curvature or shallowness) of plateaus were not simulated due to the likely confounding effects on TF contact mechanics.

In summary, results of the present study suggest that at all periods of gait, from heel strike to toe off, an increase in PTS, either at both plateaus together or at the one carrying larger contact force, significantly increases ATT and ACL force (resisted mainly by its posterolateral bundle). Reverse trends are found when PTS decreases. Steeper PTS is hence a major risk factor, especially in females and under activities with large compression forces, in markedly increasing ACL force and its vulnerability to injury. Future training and ACL injury prevention programs could benefit from these findings.

5.6 Acknowledgements

The current work is supported by a grant from the Natural Sciences and Engineering Research Council of Canada (NSERC). The partial scholarship of MUTAN-Tunisia to the first author is also gratefully acknowledged.

5.7 References

Adouni, M., Shirazi-Adl, A., 2013. Consideration of equilibrium equations at the hip joint alongside those at the knee and ankle joints has mixed effects on knee joint response during gait. Journal of Biomechanics 46, 619-624.

Agneskirchner, J., Hurschler, C., Stukenborg-Colsman, C., Imhoff, A., Lobenhoffer, P., 2004. Effect of high tibial flexion osteotomy on cartilage pressure and joint kinematics: a biomechanical study in human cadaveric knees. Archives of orthopaedic and trauma surgery 124, 575-584.

Am Jung, K., Lee, S.C., Hwang, S.H., Song, M.B., 2009. ACL injury while jumping rope in a patient with an unintended increase in the tibial slope after an opening wedge high tibial osteotomy. Archives of orthopaedic and trauma surgery 129, 1077-1080.

Arendt, E., Dick, R., 1995. Knee injury patterns among men and women in collegiate basketball and soccer NCAA data and review of literature. The American journal of sports medicine 23, 694-701.

Astephen, J.L., 2007. Biomechanical Factors in the Progression of Knee Osteoarthritis. School of Biomedical Engineering, Dalhousie University, Halifax.

Astephen, J.L., Deluzio, K.J., Caldwell, G.E., Dunbar, M.J., 2008. Biomechanical changes at the hip, knee, and ankle joints during gait are associated with knee osteoarthritis severity. Journal of Orthopaedic Research 26, 332-341.

Beynnon, B.D., Fleming, B.C., Labovitch, R., Parsons, B., 2002. Chronic anterior cruciate ligament deficiency is associated with increased anterior translation of the tibia during the transition from non-weightbearing to weightbearing. Journal of Orthopaedic Research 20, 332-337.

Beynnon, B.D., Vacek, P.M., Sturnick, D.R., Holterman, L.A., Gardner-Morse, M., Tourville, T.W., Smith, H.C., Slauterbeck, J.R., Johnson, R.J., Shultz, S.J., 2014. Geometric

profile of the tibial plateau cartilage surface is associated with the risk of non-contact anterior cruciate ligament injury. Journal of Orthopaedic Research 32, 61-68.

Boden, B.P., Breit, I., Sheehan, F.T., 2009a. Tibiofemoral alignment: contributing factors to noncontact anterior cruciate ligament injury. The Journal of Bone & Joint Surgery 91, 2381-2389.

Brandon, M.L., Haynes, P.T., Bonamo, J.R., Flynn, M.I., Barrett, G.R., Sherman, M.F., 2006. The association between posterior-inferior tibial slope and anterior cruciate ligament insufficiency. Arthroscopy: The Journal of Arthroscopic & Related Surgery 22, 894-899.

Brazier, J., Migaud, H., Gougeon, F., Cotten, A., Fontaine, C., Duquennoy, A., 1996. Evaluation of methods for radiographic measurement of the tibial slope. A study of 83 healthy knees. Revue de chirurgie orthopédique et réparatrice de l'appareil moteur 82, 195.

Chaudhari, A.M., Zelman, E.A., Flanigan, D.C., Kaeding, C.C., Nagaraja, H.N., 2009. Anterior Cruciate Ligament–Injured Subjects Have Smaller Anterior Cruciate Ligaments Than Matched Controls A Magnetic Resonance Imaging Study. The American journal of sports medicine 37, 1282-1287.

Chiu, K., Zhang, S., Zhang, G., 2000. Posterior slope of tibial plateau in Chinese. The Journal of arthroplasty 15, 224-227.

de Boer, J.J., Blankevoort, L., Kingma, I., Vorster, W., 2009. In vitro study of inter-individual variation in posterior slope in the knee joint. Clinical Biomechanics 24, 488-492.

De Leva, P., 1996. Adjustments to Zatsiorsky-Seluyanov's segment inertia parameters. Journal of Biomechanics 29, 1223-1230.

Dejour, H., Bonnin, M., 1994. Tibial translation after anterior cruciate ligament rupture. Two radiological tests compared. Journal of Bone & Joint Surgery, British Volume 76, 745-749.

Delp, S.L., Anderson, F.C., Arnold, A.S., Loan, P., Habib, A., John, C.T., Guendelman, E., Thelen, D.G., 2007. OpenSim: open-source software to create and analyze dynamic simulations of movement. Biomedical Engineering, IEEE Transactions on 54, 1940-1950.

DeMorat, G., Weinhold, P., Blackburn, T., Chudik, S., Garrett, W., 2004. Aggressive quadriceps loading can induce noncontact anterior cruciate ligament injury. The American journal of sports medicine 32, 477-483.

Fening, S.D., Kovacic, J., Kambic, H., McLean, S., Scott, J., Miniaci, A., 2008. The effects of modified posterior tibial slope on acl strain and knee kinematics: a human cadaveric study. The journal of knee surgery 21, 205.

Feucht, M.J., Mauro, C.S., Brucker, P.U., Imhoff, A.B., Hinterwimmer, S., 2013. The role of the tibial slope in sustaining and treating anterior cruciate ligament injuries. Knee Surgery, Sports Traumatology, Arthroscopy 21, 134-145.

Fleming, B.C., Renstrom, P.A., Beynnon, B.D., Engstrom, B., Peura, G.D., Badger, G.J., Johnson, R.J., 2001. The effect of weightbearing and external loading on anterior cruciate ligament strain. Journal of Biomechanics 34, 163-170.

Gabriel, M.T., Wong, E.K., Woo, S.L.Y., Yagi, M., Debski, R.E., 2004. Distribution of in situ forces in the anterior cruciate ligament in response to rotatory loads. Journal of Orthopaedic Research 22, 85-89.

Giffin, J.R., Vogrin, T.M., Zantop, T., Woo, S.L., Harner, C.D., 2004. Effects of increasing tibial slope on the biomechanics of the knee. The American journal of sports medicine 32, 376-382.

Hashemi, J., Breighner, R., Jang, T.-H., Chandrashekar, N., Ekwaro-Osire, S., Slauterbeck, J.R., 2010. Increasing pre-activation of the quadriceps muscle protects the anterior cruciate ligament during the landing phase of a jump: An< i> in vitro</i> simulation. The knee 17, 235-241.

Hashemi, J., Chandrashekar, N., Gill, B., Beynnon, B.D., Slauterbeck, J.R., SchuttJr, R.C., Mansouri, H., Dabezies, E., 2008. The geometry of the tibial plateau and its influence on the biomechanics of the tibiofemoral joint. The Journal of Bone & Joint Surgery 90, 2724-2734.

Hashemi, J., Chandrashekar, N., Mansouri, H., Gill, B., Slauterbeck, J.R., Schutt, R.C., Dabezies, E., Beynnon, B.D., 2009. Shallow Medial Tibial Plateau and Steep Medial and Lateral Tibial Slopes New Risk Factors for Anterior Cruciate Ligament Injuries. The American journal of sports medicine 38, 54-62.

Haut Donahue, T.L., Hull, M., 2002. A finite element model of the human knee joint for the study of tibio-femoral contact. Journal of biomechanical engineering 124, 273.

Hewett, T.E., Myer, G.D., Ford, K.R., 2006. Anterior cruciate ligament injuries in female athletes part 1, mechanisms and risk factors. The American journal of sports medicine 34, 299-311.

Hohmann, E., Bryant, A., Reaburn, P., Tetsworth, K., 2011. Is there a correlation between posterior tibial slope and non-contact anterior cruciate ligament injuries? Knee Surgery, Sports Traumatology, Arthroscopy 19, 109-114.

Hootman, J.M., Dick, R., Agel, J., 2007. Epidemiology of collegiate injuries for 15 sports: summary and recommendations for injury prevention initiatives. Journal of athletic training 42, 311.

Hunt, A.E., M Smith, R., Torode, M., Keenan, A.-M., 2001. Inter-segment foot motion and ground reaction forces over the stance phase of walking. Clinical Biomechanics 16, 592-600.

Keays, S.L., Newcombe, P.A., Bullock-Saxton, J.E., Bullock, M.I., Keays, A.C., 2010. Factors involved in the development of osteoarthritis after anterior cruciate ligament surgery. The American journal of sports medicine 38, 455-463.

Khan, M.S., Seon, J.K., Song, E.K., 2011. Risk factors for anterior cruciate ligament injury: assessment of tibial plateau anatomic variables on conventional MRI using a new combined method. International orthopaedics 35, 1251-1256.

Li, G., Rudy, T.W., Allen, C., Sakane, M., Woo, S.L.Y., 1998. Effect of combined axial compressive and anterior tibial loads on in situ forces in the anterior cruciate ligament: a porcine study. Journal of Orthopaedic Research 16, 122-127.

Li, Y., Hong, L., Feng, H., Wang, Q., Zhang, J., Song, G., Chen, X., Zhuo, H., 2014. Posterior Tibial Slope Influences Static Anterior Tibial Translation in Anterior Cruciate Ligament Reconstruction A Minimum 2-Year Follow-up Study. The American journal of sports medicine 42, 927-933.

Lipps, D.B., Oh, Y.K., Ashton-Miller, J.A., Wojtys, E.M., 2012. Morphologic characteristics help explain the gender difference in peak anterior cruciate ligament strain during a simulated pivot landing. The American journal of sports medicine 40, 32-40.

Liu, W., Maitland, M.E., 2003. Influence of anthropometric and mechanical variations on functional instability in the ACL-deficient knee. Annals of Biomedical Engineering 31, 1153-1161.

Lohmander, L., Östenberg, A., Englund, M., Roos, H., 2004. High prevalence of knee osteoarthritis, pain, and functional limitations in female soccer players twelve years after anterior cruciate ligament injury. Arthritis & Rheumatism 50, 3145-3152.

MacDonald, P.B., Rhodes, D.A., Mascarenhas, R., Stuart, M.J., 2014. Approach to the Multiply Revised ACL-Deficient Knee. Revision ACL Reconstruction. Springer,pp.247-254

Markolf, K.L., Jackson, S.R., Foster, B., McAllister, D.R., 2013. ACL forces and knee kinematics produced by axial tibial compression during a passive flexion–extension cycle. Journal of Orthopaedic Research.

Markolf, K.L., Park, S., Jackson, S.R., McAllister, D.R., 2009. Anterior-posterior and rotatory stability of single and double-bundle anterior cruciate ligament reconstructions. The Journal of Bone & Joint Surgery 91, 107-118.

Marouane, H., Shirazi-Adl, A., Adouni, M., 2015. Knee joint passive stiffness and moment in sagittal and frontal planes markedly increase with compression. Computer methods in biomechanics and biomedical engineering 18:339-350.

Marouane, H., Shirazi-Adl, A., Adouni, M., Hashemi, J., 2014. Steeper posterior tibial slope markedly increases ACL force in both active gait and passive knee joint under compression. Journal of Biomechanics 47, 1353-1359.

McLean, S.G., Lucey, S.M., Rohrer, S., Brandon, C., 2010. Knee joint anatomy predicts high-risk in vivo dynamic landing knee biomechanics. Clinical Biomechanics 25, 781-788.

Mesfar, W., Shirazi-Adl, A., 2005. Biomechanics of the knee joint in flexion under various quadriceps forces. The knee 12, 424-434.

Meyer, E.G., Baumer, T.G., Slade, J.M., Smith, W.E., Haut, R.C., 2008a. Tibiofemoral contact pressures and osteochondral microtrauma during anterior cruciate ligament rupture due to excessive compressive loading and internal torque of the human knee. The American journal of sports medicine 36, 1966-1977.

Meyer, E.G., Haut, R.C., 2005. Excessive compression of the human tibio-femoral joint causes ACL rupture. Journal of Biomechanics 38, 2311-2316.

Myer, G.D., Ford, K.R., Paterno, M.V., Nick, T.G., Hewett, T.E., 2008. The effects of generalized joint laxity on risk of anterior cruciate ligament injury in young female athletes. The American journal of sports medicine 36, 1073-1080.

Nelitz, M., Seitz, A.M., Bauer, J., Reichel, H., Ignatius, A., Dürselen, L., 2013. Increasing posterior tibial slope does not raise anterior cruciate ligament strain but decreases tibial rotation ability. Clinical Biomechanics.

Sakane, M., Fox, R.J., Glen, S.L.Y.W., Livesay, A., Li, G., Fu, F.H., 1997. In situ forces in the anterior cruciate ligament and its bundles in response to anterior tibial loads. Journal of Orthopaedic Research 15, 285-293.

Shao, Q., MacLeod, T.D., Manal, K., Buchanan, T.S., 2011. Estimation of ligament loading and anterior tibial translation in healthy and ACL-deficient knees during gait and the influence of increasing tibial slope using EMG-driven approach. Annals of Biomedical Engineering 39, 110-121.

Shelburne, K.B., Kim, H.J., Sterett, W.I., Pandy, M.G., 2011. Effect of posterior tibial slope on knee biomechanics during functional activity. Journal of Orthopaedic Research 29, 223-231.

Shirazi-Adl, A., Moglo, K., 2005. Effect of changes in cruciate ligaments pretensions on knee joint laxity and ligament forces. Computer methods in biomechanics and biomedical engineering 8, 17-24.

Sonnery-Cottet, B., Archbold, P., Cucurulo, T., Fayard, J.-M., Bortolletto, J., Thaunat, M., Prost, T., Chambat, P., 2011. The influence of the tibial slope and the size of the intercondylar notch on rupture of the anterior cruciate ligament. Journal of Bone & Joint Surgery, British Volume 93, 1475-1478.

Terauchi, M., Hatayama, K., Yanagisawa, S., Saito, K., Takagishi, K., 2011. Sagittal alignment of the knee and its relationship to noncontact anterior cruciate ligament injuries. The American journal of sports medicine 39, 1090-1094.

Todd, M.S., Lalliss, S., Garcia, E.S., DeBerardino, T.M., Cameron, K.L., 2010. The relationship between posterior tibial slope and anterior cruciate ligament injuries. The American journal of sports medicine 38, 63-67.

van Diek, F.M., Wolf, M.R., Murawski, C.D., van Eck, C.F., Fu, F.H., 2014. Knee morphology and risk factors for developing an anterior cruciate ligament rupture: an MRI comparison between ACL-ruptured and non-injured knees. Knee Surgery, Sports Traumatology, Arthroscopy 22, 987-994.

Wall, S.J., Rose, D.M., Sutter, E.G., Belkoff, S.M., Boden, B.P., 2012. The Role of Axial Compressive and Quadriceps Forces in Noncontact Anterior Cruciate Ligament Injury A Cadaveric Study. The American journal of sports medicine 40, 568-573.

Webb, J.M., Salmon, L.J., Leclerc, E., Pinczewski, L.A., Roe, J.P., 2013. Posterior Tibial Slope and Further Anterior Cruciate Ligament Injuries in the Anterior Cruciate Ligament–Reconstructed Patient. The American journal of sports medicine 41, 2800-2804.

Yeow, C.H., Cheong, C.H., Ng, K.S., Lee, P.V.S., Goh, J.C.H., 2008. Anterior Cruciate Ligament Failure and Cartilage Damage During Knee Joint Compression A Preliminary Study Based on the Porcine Model. The American journal of sports medicine 36, 934-942.

Zeng, C., Yang, T., Wu, S., Gao, S.-g., Li, H., Deng, Z.-h., Zhang, Y., Lei, G.-h., 2014. Is posterior tibial slope associated with noncontact anterior cruciate ligament injury? Knee Surgery, Sports Traumatology, Arthroscopy, 1-8.

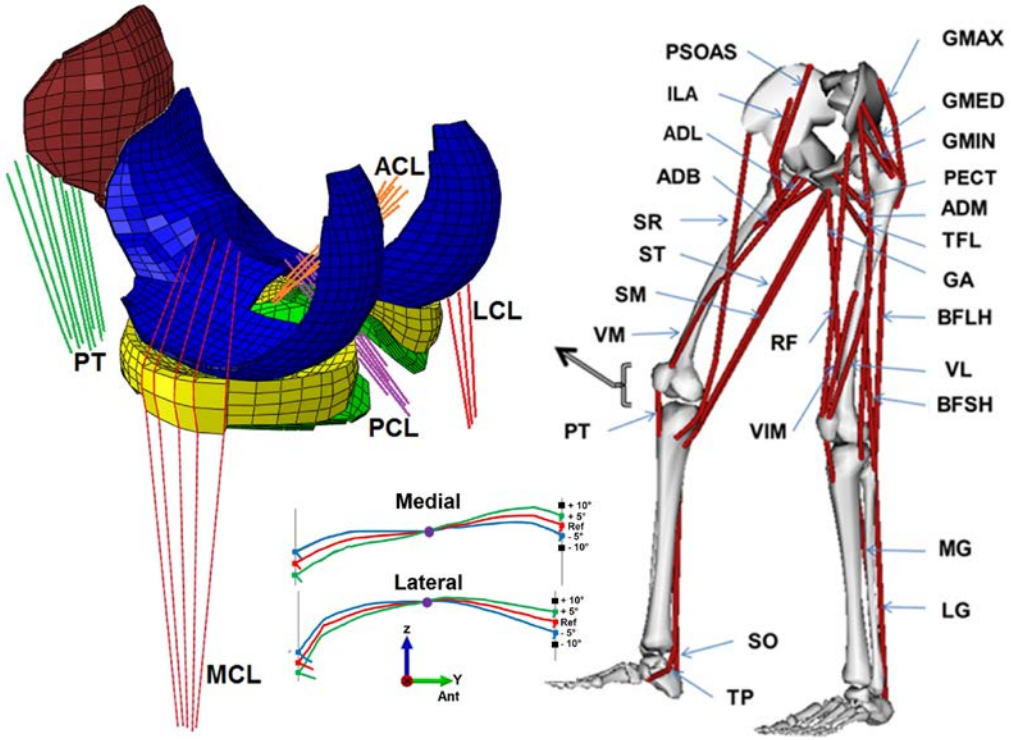

Figure 5.1: **(a)** Schematic diagram showing 34 muscles incorporated into the lower extremity model (Open Sim, Delp et al., 2007). Quadriceps components are vastus medialis obliqus (VMO), rectus femoris (RF), vastus intermidus medialis (VIM) and vastus lateralis (VL). Hamstrings components include biceps femoris long head (BFLH), biceps femoris short head (BFSH), semi membranous (SM) and TRIPOD made of sartorius (SR), gracilis (GA) and semitendinosus (ST). Gastrocnemius components are medial gastrocnemius (MG) and lateral gastrocnemius (LG). Soleus (SO) muscle is a uni-articular ankle muscle. Hip joint muscles (not all shown) include adductor, long (ADL), mag (3 components ADM) and brev (ADB); gluteus max (3 components GMAX), med (3 components GMED) and min (3 components GMIN), iliacus (ILA), iliopsoas (PSOAS), quadriceps femoris; pectineus (PECT), tensor facia lata (TFL), periformis. **(b)** Detailed knee FE model; tibiofemoral (TF) and patellofemoral (PF) cartilage layers, menisci, patellar Tendon (PT). Joint ligaments include lateral patellofemoral (LPFL), medial patellofemoral (MPFL), anterior cruciate (ACL), posterior cruciate (PCL), lateral collateral (LCL) and medial collateral (MCL). **(c)** Posterior tibial slope at medial plateau and/or lateral plateau in the model (Ref) is rotated by ±5° and ±10° about local axes in each plateau (M and L) passing through their centers. Here typical sagittal sections through both plateaus are shown.

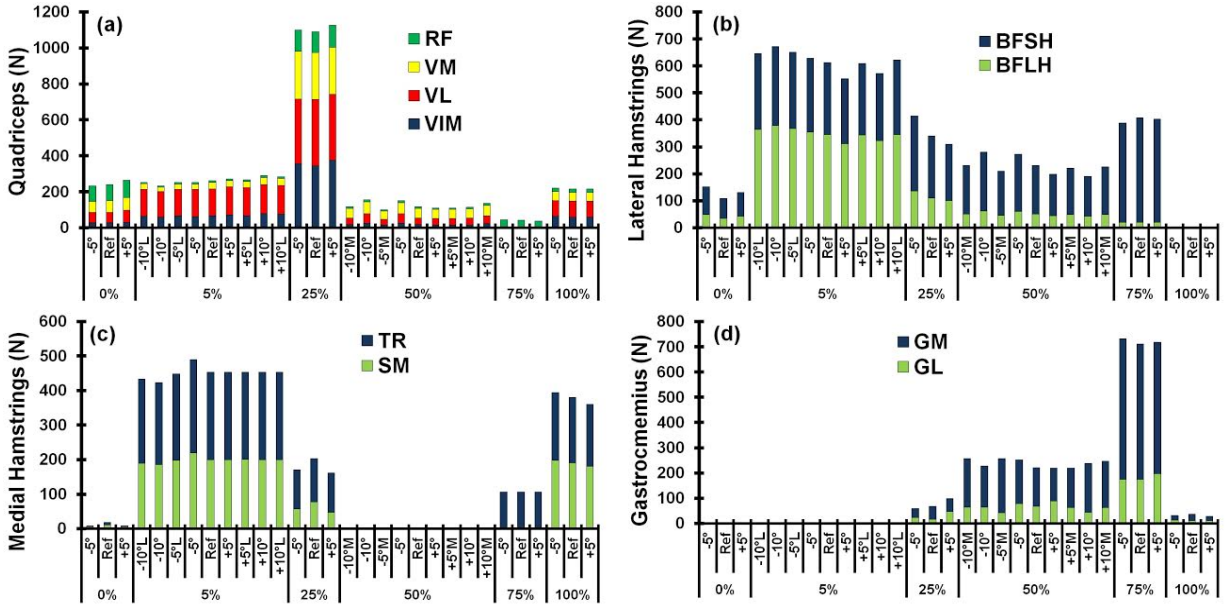

Figure 5.2: Predicted **(a)** quadriceps, **(b)** lateral hamstrings, **(c)** medial hamstrings, and **(d)** gastrocmemius muscle forces (see Fig. 1 caption for muscle abbreviations) at various periods of stance as medial and lateral PTS altered by ±5° from the reference (Ref) case. At 5% and 50% periods, both ±5° and ±10° changes in PTS were considered in either both plateaus or at one alone; indicated by M: medial alone and L: lateral alone.

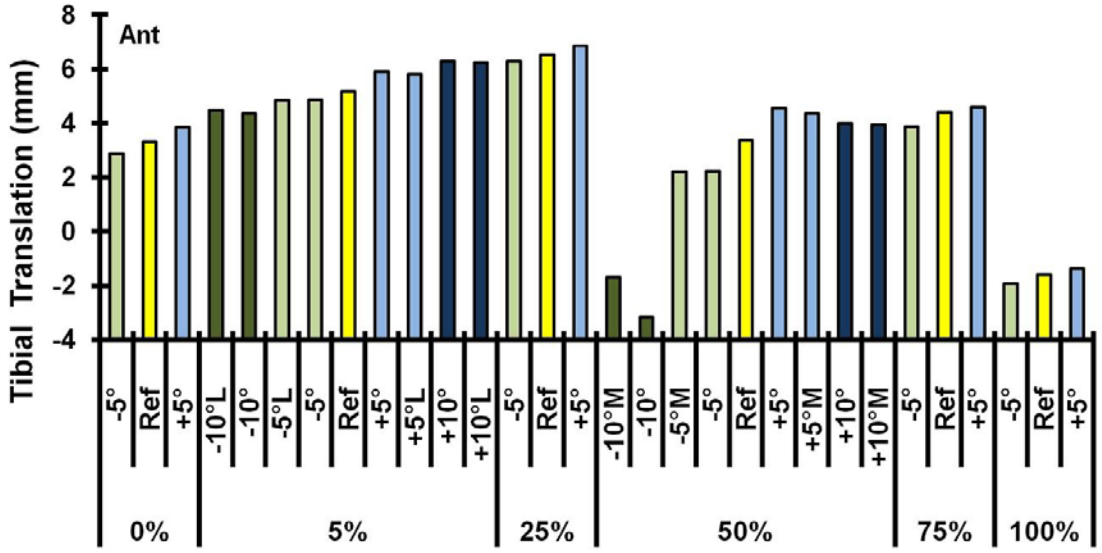

Figure 5.3: Anterior tibial translations (ATT) at various periods of stance as medial and lateral PTS altered by ±5° from the reference (Ref) case. At 5% and 50% periods, both ±5° and ±10° changes in PTS were considered in either both plateaus or at one alone; indicated by M: medial alone and L: lateral alone.

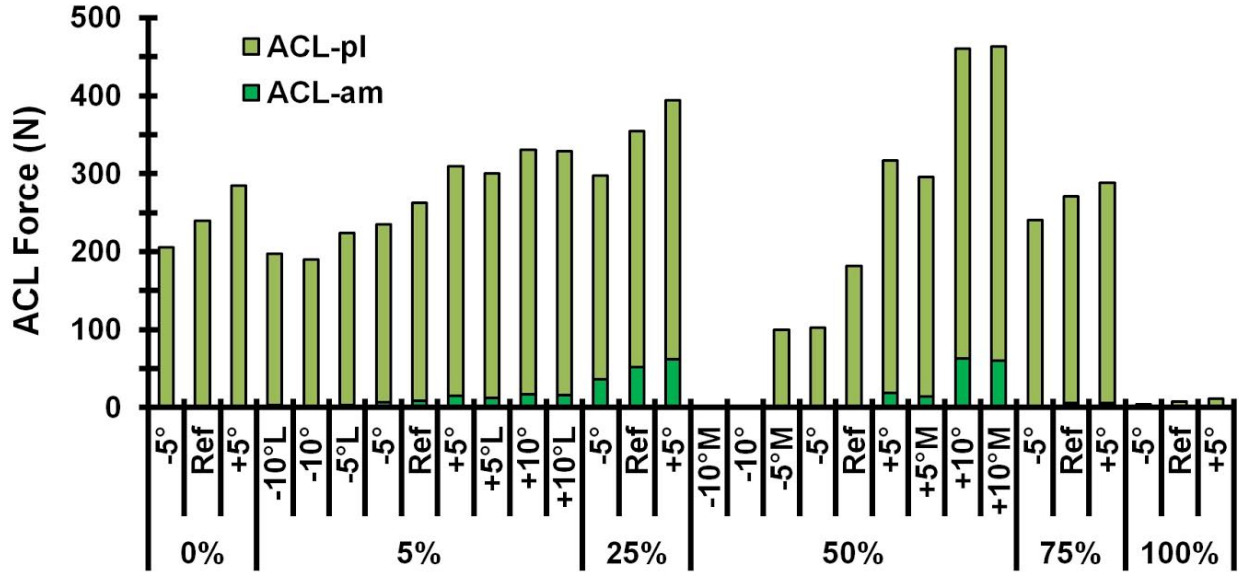

Figure 5.4: Forces in ACL bundles at various periods of stance as medial and lateral PTS altered by ±5° from the reference (Ref) case. At 5% and 50% periods, both ±5° and ±10° changes in PTS were considered in either both plateaus or at one alone; indicated by M: medial alone and L: lateral alone.

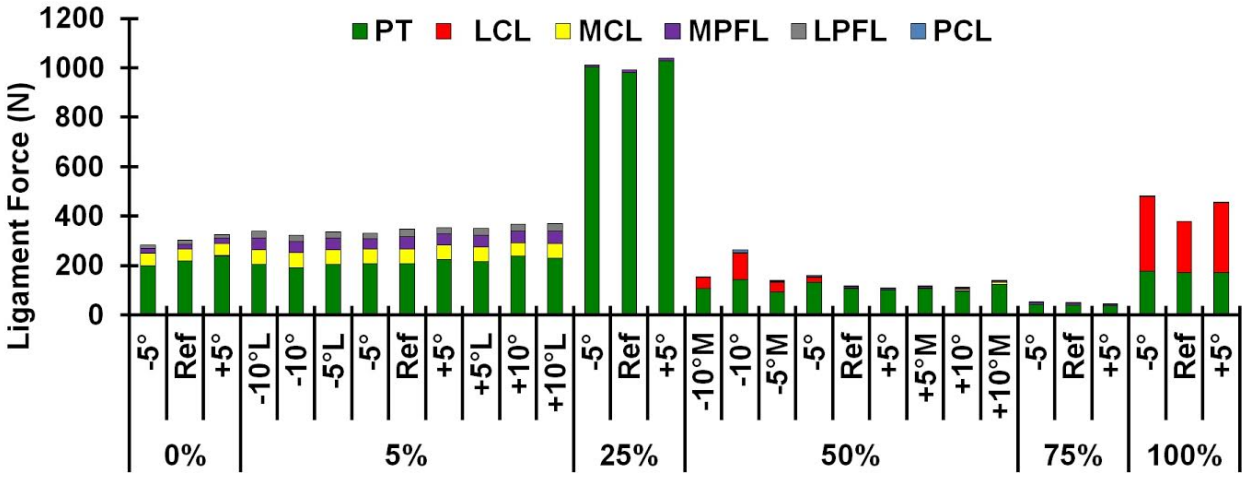

Figure 5.5: Total forces in various knee joint ligaments at various periods of stance as medial and lateral PTS altered by ±5° from the reference (Ref) case. At 5% and 50% periods, both ±5° and ±10° changes in PTS were considered in either both plateaus or at one alone; indicated by M: medial alone and L: lateral alone.

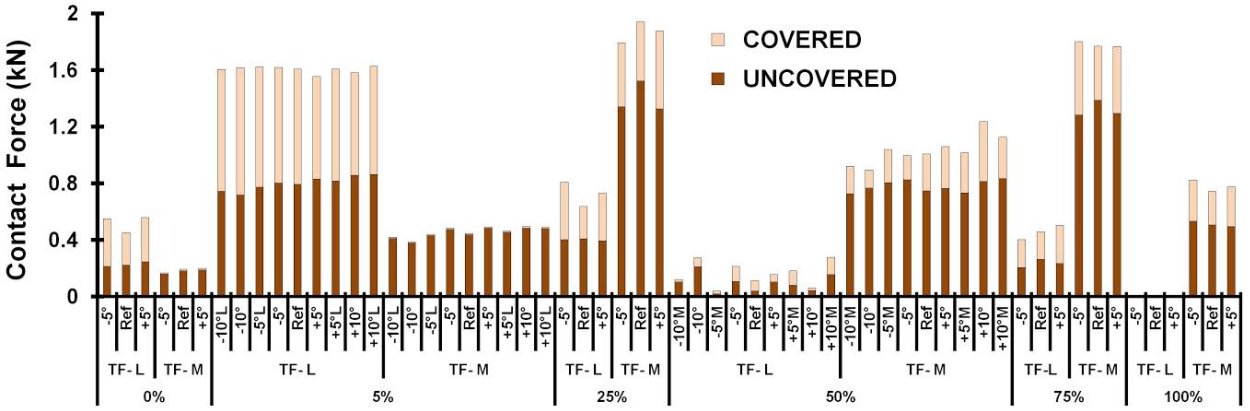

Figure 5.6: Total axial contact forces on TF medial (M) and lateral (L) plateaus at covered (via menisci) and uncovered (via cartilage-cartilage) areas at various periods of stance as medial and lateral PTS altered by ±5° from the reference (Ref) case. At 5% and 50% periods, both ±5° and ±10° changes in PTS were considered in either both plateaus or at one alone; indicated by M: medial alone and L: lateral alone.

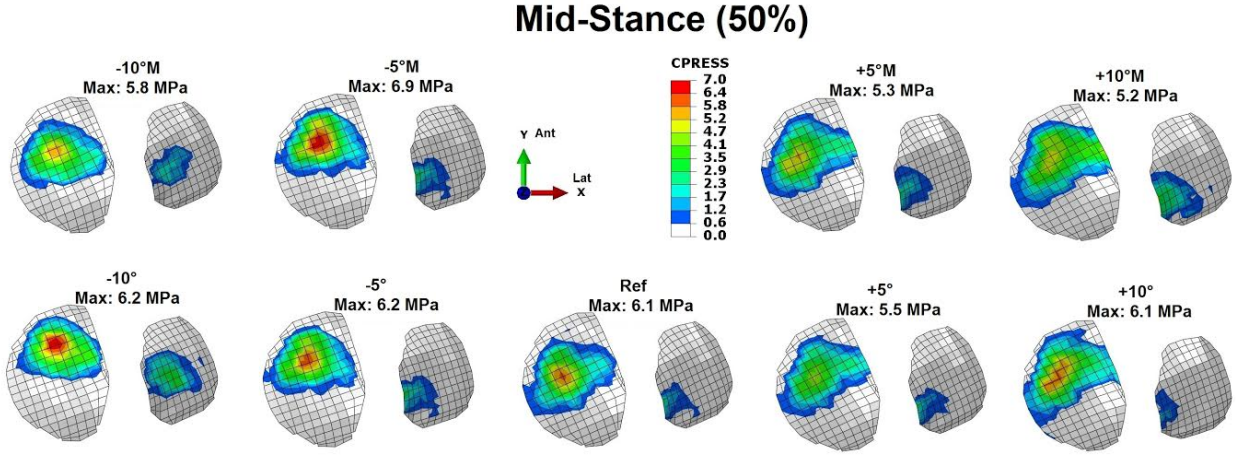

Figure 5.7: Contact pressures (MPa) at the articular surface of the tibial lateral and medial plateaus at 50% stance period. Medial and lateral PTS altered by both ±5° and ±10° from the reference case (Ref) either at both plateaus or at one alone; indicated by M: medial alone and L: lateral alone.

CHAPITRE 6 ARTICLE 3: ALTERATIONS IN KNEE CONTACT FORCES AND CENTERS IN STANCE PHASE OF GAIT: A DETAILED LOWER EXTREMITY MUSCULOSKELETAL MODEL

H. Marouane, A. Shirazi-Adl, and M. Adouni

Article published in

Journal of Biomechanics 2016

6.1 Abstract

Evaluation of contact forces-centers of the tibiofemoral joint in gait has crucial biomechanical and pathological consequences. It involves however difficulties and limitations in *in vitro* cadaver and *in vivo* imaging studies. The goal is to estimate total contact forces (CF) and location of contact centers (CC) on the medial and lateral plateaus using results computed by a validated finite element model simulating the stance phase of gait for normal as well as osteoarthritis, varus-valgus and posterior tibial slope altered subjects. Using foregoing contact results, six methods commonly used in the literature are also applied to estimate and compare locations of CC at 6 periods of stance phase (0%, 5%, 25%, 50%, 75% and 100%).

TF joint contact forces are greater on the lateral plateau very early in stance and on the medial plateau thereafter during 25–100% stance periods. Large excursions in the location of CC (>17 mm), especially on the medial plateau in the mediolateral direction, are computed. Various reported models estimate quite different CCs with much greater variations (~15 mm) in the mediolateral direction on both plateaus. Compared to our accurately computed CCs taken as the gold standard, the centroid of contact area algorithm yielded least differences (except in the mediolateral direction on the medial plateau at ~5 mm) whereas the contact point and weighted center of proximity algorithms resulted overall in greatest differences. Large movements in the location of CC should be considered when attempting to estimate TF compartmental contact forces in gait.

Keywords: Contact force; Contact center; Gait; Lower extremity model; Knee joint

6.2 Introduction

Alterations in knee joint kinetics-kinematics influence the initiation and progression of joint pathologies such as osteoarthritis (OA) that afflicts a considerable portion of adult population (Dillon et al., 2006). Effective preventive measures and treatment managements of such disorders require a sound knowledge of the joint behavior in both healthy and pathologic conditions. Changes in contact forces (CF) and contact centers (CC) on the cartilage articulating surfaces have been indicated as important markers either in the prevention/initiation/progression or alternatively in the evaluation of treatment stages of joint disorders (Andriacchi et al., 2006, Engel et al., 2014 and Harris et al., 1999). Accordingly, quantification of the joint contact mechanics in gait has been the focus of a number of investigations.

Cadaveric studies have measured contact pressure distribution across the knee joint using pressure-sensitive sensors (Gilbert et al., 2014 and Wang et al., 2014) and films (Engel et al., 2014 and Seitz et al., 2012). To identify the location of CC, the pressure weighted center of contact (pWCoC) is quantified by assigning different weights (proportional to recorded contact stresses) to each sensing element on the tibial plateau (Gilbert et al., 2014 and Wang et al., 2014). These studies remain limited to in vitro investigations and hence subject to associated short comings especially on muscle forces and kinematics when simulating gait. Alternatively using bony landmarks and cartilage layers, imaging techniques allow in vivo the recording of joint articular surface interactions in static and dynamic conditions in order to quantify various measures such as joint overlap, minimum joint space and contact area/center (Coleman et al., 2011, Koo and Andriacchi, 2008 and Wretenberg et al., 2002).

To determine dynamic joint CC location, several models have been developed based on imaged 3D geometry of contacting bones (Anderst et al., 2005, Anderst and Tashman, 2003, Asano et al., 2001, Farrokhi et al., 2014, Li et al., 2004 and Wang et al., 2014) and cartilage layers (DeFrate et al., 2004, Han et al., 2005 and Li et al., 2005a). Different techniques are employed in these studies to locate the joint CC during various activities. Shortest (minimum interface) distance gap was used to identify the location of CC at the TF joint (Asano et al., 2001 and Li et al., 2004). DeFrate et al. (2004) developed a cartilage-overlap method in which the location of CC was estimated as the geometric centroid of the cartilage at overlapping (contact) areas. Anderst and Tashman (2003) proposed the distance weighted center of proximity (WCoP) in which higher weights were assigned to points on the tibial plateau located in closer proximity to

the opposing femoral subchondral surface. During simulated walking, Wang et al. (2014) identified joint CC using either this image-based WCoP method or an alternative pressure weighted center of contact (pWCoC) accounting for measured contact pressures over contacting areas using cadaver specimens and pressure sensors. The anteroposterior (AP) location of WCoP was found to significantly correlate with that of pWCoC on both tibial plateaus but the correlation was very poor in the mediolateral (ML) direction.

In parallel, lower extremity musculoskeletal models often consider fixed paths and orientations for TF CFs independent of the external loads, kinematics and joint articular structures (Gerus et al., 2013 and Winby et al., 2009). In fact, the contact point method employed in these studies to compute CFs assumes that, in the frontal plane, the compartmental CFs remain on fixed midpoints of each condyle (Winby et al., 2009). Using the OpenSim musculoskeletal model, Lerner et al. (2015) reported substantial differences in computed medial and lateral CFs when using radiographic images to identify CC locations instead of the foregoing approximate approach. Each 1 mm deviation in the medial-lateral location of CC altered peak medial CF by 41 N.

Accurate estimation of CCs markedly influence predictions of joint passive/active response affecting thus the subsequent evaluation of preventive, treatment and rehabilitation programs. Detailed computational modeling has the advantage to circumvent many shortcomings in earlier investigations when quantifying CFs and associated CCs. Here, results of a lower extremity musculoskeletal model (Adouni et al., 2015 and Marouane et al., 2014) including a validated complex finite element model of the entire knee joint driven by mean reported values of gait kinematics/kinetics (Astephen et al., 2008 and Hunt et al., 2001) are employed to initially quantify these contact quantities and then compare computed CCs with those using existing methods. Attention is focused on the CF and CC on each tibial plateau and on the entire TF joint in the normal as well as OA, varus-valgus and posterior tibial slope altered subjects. We hypothesize that the location of CC markedly alters in gait and by the algorithm used.

6.3 Methods

This study exploits the predicted results of our earlier model studies on biomechanics of the knee joint during the stance phase of gait in normal and OA subjects (Adouni and Shirazi-Adl, 2014a), varus-valgus altered subjects (Adouni and Shirazi-Adl, 2014b) and subjects with

different posterior tibial slope (Marouane et al., 2014 and Marouane et al., 2015b). Here, a short description of the model is provided for completeness.

The FE model of the knee joint (Figure 6.1) is made of bony structures (tibia, femur and patella) and their compliant cartilage layers as well as menisci, major tibiofemoral (TF: ACL, PCL, LCL, MCL) and patellofemoral (PF: MPFL, LPFL) ligaments, patellar tendon (PT), quadriceps (four components), hamstrings (six components) and gastrocnemius (two components). Articular cartilage layers and menisci are simulated as non-homogeneous depth-dependent composites of nonlinear collagen fibril networks and hyperelastic matrices while the bony structures are represented as rigid bodies. Ligaments are each simulated by a number of nonlinear axial elements with initial pre-strains and non-linear (tension-only) material properties (Mesfar and Shirazi-Adl, 2005).

This detailed knee model is introduced into a musculoskeletal model of the lower extremity including hip and ankle joints as well as uni- and bi-articular muscles to simulate the stance phase of gait under mean values of in vivo kinematics/kinetics reported for normal and severe OA subjects (Astephen et al., 2008 and Hunt et al., 2001) while minimizing sum of cubed muscle stresses. At each period of stance, unknown muscle forces are evaluated iteratively and applied subsequently along with the ground reaction forces and kinematics/kinetics. The prescribed kinematics-kinetics data at 0%, 5%, 25%, 50%, 75% and 100% periods of stance are taken directly from in vivo gait measurements using inverse dynamics and motion capture cameras. Additional analyses in gait of normal subjects at mid-stance (50%) are performed while altering either (1) the adduction-abduction rotations or moments by ±1.5° or ±50%, respectively, or (2) both the initial medial (~9.8°) and lateral (~5°) posterior tibial slopes by ±5° or ±10° by rigidly rotating tibial cartilage layers around local lateral-medial axes placed at the center of tibial articulations in a manner to yield minimal changes in tibial articular cartilage geometry (Marouane et al., 2015b).

For our model constructed based on a female knee joint, a body weight of BW=606.6 N (61.9 kg) is considered (De Leva, 1996). The nonlinear elastostatic analyses are carried out using ABAQUS (version 6.12, Simulia, Inc., Providence, RI, USA) FE package program. Matlab (R2013a Optimization Toolbox, genetic algorithms and Fmincon) and Python (3.3.5) are used in the optimization algorithm and localization of contact centers (CC).

At each stance phase and joint condition, the calculated CF distributions on the medial and lateral plateaus are used to determine total CFs and associated CCs once on each plateau separately and once on the entire TF joint. For the sake of comparison and based on our results, various methods commonly reported in the literature are also used to calculate the location of CC for normal and OA altered gait conditions.

Contact Center (CC-Ref):

This approach used in the current study as the gold standard is based on the principle of static equilibrium in which the location of the resultant CF for the entire nodal contact loads computed by the FE model over contact areas of each plateau is evaluated in a manner such that the vector summation of moments of contact loads about this CC disappears. These vector manipulations resemble the scalar treatment in the pressure weighted center of contact (pWCoC) method that used instead the measured and not predicted contact pressure distributions (Gilbert et al., 2014 and Wang et al., 2014).

Centroid of Contact Area (CCA):

The location of the centroid of contact area (DeFrate et al., 2004) is quantified in each direction of a local coordinates system similar to CC-Ref and pWCoC approaches but assuming a constant pressure as:

$$CCA=\frac{\sum_{i=1}^{n}(A_i \times X_i)}{\sum_{i=1}^{n} A_i} \quad (1)$$

where X_i denotes the location of node-i along an axis in a local coordinate system on the tibial plateau and A_i its associated scalar contact nodal area as the weighting factor. Here to simulate the overlapped cartilage contact areas detected on MRI images, only the uncovered contact areas (cartilage-cartilage) are considered.

Modified Centroid of Contact Area (CCA-m):

This is our modified version of CCA in which both covered (meniscus-cartilage) and uncovered (cartilage-cartilage) areas of contact are considered in the above Eq. (1).

Contact Point (CP):

The contact point method used often in musculoskeletal models follows a sagittal path driven by a regression equation based on the knee flexion angle (Delp et al., 1990 and Nisell et al., 1986). In the frontal plane, lever arms of the resultant contact forces are kept constant with CC remaining on fixed midpoints of each condyle (Winby et al., 2009).

Maximum Strain (MS):

For each node on the medial and lateral tibial articular cartilage surfaces, a normal strain is calculated using the ratio of the change in the current thickness (along the local direction perpendicular to the tibial plateau) to its initial thickness. This method locates the point on the articular surface with the maximum relative penetration.

Minimum Joint Space (MJS):

This approach searches on the articular areas where the distance (perpendicular to the tibial plateau) between the femoral condyle and the opposing tibial plateau is minimum (Asano et al., 2001 and DeFrate et al., 2004). This results in a point on each plateau where the opposing subchondral surfaces are located closest to each other.

Weighted Center of Proximity (WCoP):

The location of WCoP on each plateau is calculated (Beveridge et al., 2014 and Wang et al., 2014) with higher weights assigned to points on the tibial plateau located in closer proximity to the opposing femoral subchondral bone:

$$\mathrm{WCoP}=\frac{\sum_{i=1}^{n}(w_i \times p_i)}{\sum_{i=1}^{n} w_i} \quad (2)$$

$$w_i = 4, d_i \leq 4\mathrm{mm}$$

$$w_i = 2, 4 < d_i \leq 5$$

$$w_i = 0.5, 5 < d_i \leq 6$$

where p_i denotes the location of node-i on the tibial plateau relative to the femur and w_i the weight assigned to this node according to its distance di to the opposing femoral condyle. In accordance with Beveridge et al. (2014) and acknowledging the likely effects on computed results, foregoing parameters are selected based on the range of inter-subchondral distances found in our model.

Statistical Analyses:

As a useful tool to measure differences in values (Bland and Altman, 1986 and Giavarina, 2015), Bland–Altman method is used to compare computed locations of CC in various approaches (CCA, CCA-m, CP, MS, MJS and WCoP) relative to the gold standard (CC-Ref). These are all calculated based directly on our predicted FE results on contact areas, cartilage deformations and contact pressure distributions at 6 periods of stance phase. Pearson correlation coefficient is also evaluated and reported. The regression slopes, coefficients of determination R2 and the mean/standard deviation of differences in Bland–Altman analysis are calculated using Statistics Toolbox in Matlab. It is to be noted that the Pearson correlation coefficient is not a measure of agreement but only a measure of association (Altman and Bland, 1983 and Giavarina, 2015).

6.4 Results

In both normal (N) and OA models, total CFs were much greater on the medial plateau except at early stance (0 and 5%). The total CF reached its maximum of 2467 N (~4 body weight of BW= 61.9 kg) at 25% period. In the entire TF joint (Figure 6.2), joint CC was located on the lateral plateau (close to the tibial eminence) at 0 and 5% periods but shifted to the central medial surface thereafter at 25–100% periods. In accordance with the tibial internal rotation, the location of CC was in all cases more anterior on the medial plateau. On both plateaus, larger resultant CFs (on the medial plateau at 25–100% periods whereas on the lateral plateau at 0 and 5% periods) were located more centrally on associated articular surfaces (Figure 6.3).

At the mid-stance period (50%), a 1.5° increase in the adduction rotation almost unloaded the lateral plateau (Figure 6.4). In contrast, a 1.5° decrease in the adduction rotation significantly increased CF on the lateral plateau with about 12% reduction in CF on the medial plateau (Figure 6.4). A 1.5° increase in the adduction rotation shifted CC medially on both plateaus (4.6 mm on lateral and 2 mm on medial). In contrast, CC moved laterally as the adduction rotation decreased (3.2 mm on lateral and 1.3 mm on medial). Variations in the posterior tibial slope by ±5° or ±10° had negligible effects on total CFs. The location of CC shifted anteriorly in all cases (Figure 6.5), reaching peaks of 5.2 mm on the medial and 5.6 mm on the lateral plateaus for the case with 10° flatter tibial slope. On the medial plateau with much larger CF, CC shifted medially by 1.3 mm in 10° steeper posterior tibial slope whereas laterally by 2 mm in 10° flatter slope.

Overall, large differences were found between the location of CC estimated in our (reference) case (CC-Ref) and those of other methods (Figure 6.6 and Figure 6.7). Early in stance and on the lateral plateau with larger CFs, the estimated location of CC were more lateral in CCA-m and CP approaches but more medial in the rest with CCA-m and MJS at extremes. From 25% stance to toe off and on the medial plateau with much larger CFs, MJS was located most medial (Figure 6.6 and Figure 6.7). Relatively smaller variations were found between different algorithms throughout stance in the AP direction than in the ML direction. Similar observations were made in OA cases as well (not shown here). At the TF contact area, the minimum gap distance (MJS) of 0.3 mm on the medial side (close to the intercondylar eminence) at 5% period and the maximum distance of 6.5 mm on the lateral side at 100% period were predicted. In the latter toe off period and due to a large adduction rotation, no articulation occurred on the lateral side.

Smaller mean differences (d, Table 6.1) suggest less deviations from CC-Ref (Table 6.1). Lower differences were found on both plateaus in the AP direction than in the ML direction (Table 6.1). The Bland–Altman d values are more reliable measures of comparison than are the Pearson coefficients of correlation that show overall much stronger correlations.

6.5 Discussion

Alterations in the magnitude (CF) as well as location (CC) of contact forces on tibial plateaus during gait have been indicated as markers for the risk of OA (Andriacchi et al., 2006). Accurate determination of CFs and CCs involves however difficulties and limitations in both in vitro cadaver and in vivo imaging studies. Computational modeling on the other could circumvent such shortcomings. The goal of the present study was to estimate the path and magnitude of TF medial and lateral CFs using results of a validated FE model during gait of normal as well as OA, varus-valgus and posterior tibial slope altered subjects. Using the same FE predictions, six algorithms commonly used in the literature (CCA, CCA-m, CP, MS, MJS, and WCoP) were also applied to estimate and compare CC locations (at 6 periods of stance phase). Hypothesis is confirmed in predicting large excursions in CC during gait and substantial differences when comparing our CC-Ref with other algorithms.

Maximum CFs (up to 4 BW) are found at 25% and 75% stance periods that are larger than 2.5 to 3 BW measured in vivo in patients with instrumented knee implants (Kutzner et al., 2010). Apart from early periods of stance (0 and 5%) and due mainly to abduction–adduction rotations,

the medial plateau carries a larger portion of contact forces than does the lateral plateau (Figure 6.3) which agrees with earlier estimates (Kumar et al., 2012 and Kumar et al., 2013). Others also computed small forces or none at all on the lateral compartment at the toe off phase (Guess et al., 2010 and Shelburne et al., 2006). Larger CFs on both plateaus (at 0 and 5% periods on the lateral whereas at remaining 25–100% periods on the medial) occur at more central articular regions with thicker cartilage (Li et al., 2005b). In both N and OA models at 25–100% periods with larger medial as well as medial over lateral CFs, the location of CC-Ref when compared to the early stance (0 and 5%) shifts medially (both in the entire joint and individual plateaus) and posteriorly (in plateaus only) in accordance with greater adduction and flexion rotations, respectively. The latter shift is also evident at mid-stance as the adduction rotation alters (Figure 6.4). The location of CC on the lateral plateau shifts anteriorly and laterally as the load-bearing share of the lateral plateau increases; at early stance (Figure 6.2) as well as under reduced adduction rotation (Figure 6.4) and posterior tibial slope (Figure 6.5) both at mid-stance. Moreover due to the joint internal rotation, in all cases and stance periods, CCs are more anterior on the medial plateau when compared to the lateral plateau (Figure 6.3). It should be pointed out that the CF and CC values on each tibial plateau and changes therein directly relate to the knee passive contribution in supporting joint external moments (Marouane et al., 2015a). A higher passive resistance diminishes forces in muscles crossing the joint and hence the joint contact forces.

The overall ML excursion in CC-Ref during the stance phase of normal subjects is much greater on the medial plateau (17 mm) than on the lateral plateau (<4 mm) (Figure 6.6). Similarly, the AP excursion is greater on the medial plateau (10 mm) than on the lateral plateau (8 mm). With time during stance phase and as the medial plateau carries most of the load, the location of CC moves medially towards the central areas on the medial plateau and posteriorly on both plateaus (Figure 6.6). Larger excursions on the medial plateau appear to corroborate earlier reports that the knee center of rotation is on the lateral side for most of the time during the stance phase of normal walking (Koo and Andriacchi, 2008 and Wang et al., 2014). Excursions in CC are found minimum in CCA-m followed by CCA approaches and maximum in MS and MJS models. Simulating the load bearing in supine position with increasing flexion, DeFrate et al. (2004) also reports much larger excursions in CC in both medial and lateral plateaus when using MJS algorithm versus CCA one.

Relatively large differences in the estimated location of CC, particularly in the ML direction, are found when comparing various algorithms; comparisons (Bland Altman d values) are poorer in the ML direction, especially on the lateral plateau, than in the AP direction (Table 6.1). Early in stance and on the lateral plateau that carries larger CFs, the location of CC falls more lateral in the CCA-m and CP algorithms but more medial in the MS, MJS and WCoP methods with CCA-m and MJS at extremes (Figure 6.6 and Figure 6.7). From 25% stance to toe off and on the medial plateau under much larger share of CF, MJS is positioned medial to the rest (Figure 6.6). The MS and MJS models are both defined as single point algorithms on the articular surface. The former nearly coincides with the location of the maximum contact pressure (Figure 6.7); a physical interpretation that the MJS approach lacks. The reliability of the MS model improves in conditions where the contact pressures are distributed nearly symmetrically around their peak value which is less often the case. The same limitation applies to CCA and CCA-m models where no considerations of nonhomogeneous pressure distributions in the overlapping areas are made. The accuracy improves if once again the pressure is distributed uniformly. The CCA approach, being based on the overlapped cartilage areas, also neglects the pressure transmission on covered areas and hence the crucial role of menisci in the compression load bearing. Additional consideration of the covered areas (via menisci) in the CCA-m approach is noticed, as expected, to markedly shift the CCA estimated CC medially on the medial plateau and laterally on the lateral plateau towards their respective covered cartilage-meniscus areas (Figure 6.6 and Figure 6.7). The WCoP model, on the other hand, is based on the proximity maps for bony contacting surfaces and represents a distance-weighted average location. In accordance with our preliminary tests, small differences have been reported when using different weighting functions (Beveridge et al., 2014). This algorithm similar to MJS suffers from the limitation to depend only on the relative location of contacting bony structures while not accounting for the presence and crucial contribution of menisci as well as changes in cartilage thickness over the articulating surfaces. Overall and compared to CC-Ref, the CCA algorithm yields best match except in the ML direction on the medial plateau where the MJS algorithm yields the closest results (Table 6.1). In contrast, CP and WCoP algorithms result in greatest differences.

The substantial ML excursion of CC-Ref especially on the medial plateau in stance phase raises concern on the assumption of a fixed ML location made in the CP model. The ML location of CC-Ref on the lateral plateau deviates from that in CP model by as much as 6 mm (with mean

of ~4 mm on both plateaus, Table 1) (Figure 6.6). Among different methods and on both plateaus, the CP model predictions in the ML direction are found closest in average (differences <3 mm) to those of the CCA-m model and farthest away (differences >12 mm) from those of the MJS model. Earlier studies have reported substantial (up to 63%) changes in the computed medial and lateral CFs when using more accurate image-based CCs rather than a fixed ML location as that used in the CP model (Lerner et al., 2015). The current results along with earlier ones (Lerner et al., 2015) hence question the relative accuracy of a fixed ML location of CC in the CP algorithm when calculating medial and lateral CFs (Gerus et al., 2013 and Zhao et al., 2007).

The current model study has some limitations. We used results computed for a single knee geometry reconstructed from a female cadaveric specimen. Though the input structural and material properties in the knee joint were taken from the literature and could vary with subject, age and sex, we have extensively validated this model with available in vitro and in vivo data under various passive and active load conditions for the last 20 years (e.g., Bendjaballah et al., 1997; Moglo and Shirazi-Adl, 2003; Mesfar and Shirazi-Adl, 2005 and Mesfar and Shirazi-Adl, 2006; Shirazi et al., 2008; Adouni and Shirazi-Adl, 2014a ; Marouane et al., 2015a). The musculature and input joint kinematics/kinetics were taken from the mean of gait data reported in the literature. Antagonistic cocontraction was not considered. The incompressible elastic response of soft tissues considered here is appropriate for short-term loading present during gait. Sensitivity analyses could quantify the effect of alterations in input kinematics/kinetics, material and structural properties on results. Nevertheless, it should be noted that the calculation of CCs in our model (CC-Ref) is precise and that the current conclusions on the changes in CC and CF during gait and differences in CCs estimated by various algorithms remain unaffected.

In summary, contact forces were greater on the lateral plateau very early in stance and on the medial plateau thereafter during 25-100% stance periods. Large excursions in the location of CC, especially on the medial plateau in the ML direction, were computed during stance. Various reported models estimate quite different CCs. Using our computed contact data-set in all models and compared to our CC-Ref as the gold standard, CCA (except in the mediolateral direction on the medial plateau) resulted in least differences whereas CP and WCoP yielded the greatest differences. Accurate determinations of CFs and CCs have important biomechanical and pathological consequences.

6.6 Acknowledgements

The current work is supported by a grant from the Natural Sciences and Engineering Research Council of Canada (NSERC). The partial scholarship of MUTAN-Tunisia to the first author is also gratefully acknowledged.

6.7 References

Adouni, M., Shirazi-Adl, A., 2014a. Evaluation of knee joint muscle forces and tissue stresses-strains during gait in severe OA versus normal subjects. Journal of orthopaedic research 32**,** 69-78.

Adouni, M., Shirazi-Adl, A., 2014b. Partitioning of knee joint internal forces in gait is dictated by the knee adduction angle and not by the knee adduction moment. Journal of biomechanics 47**,** 1696-1703.

Adouni, M., Shirazi-Adl, A., Marouane, H., 2015. Role of gastrocnemius activation in knee joint biomechanics: gastrocnemius acts as an ACL antagonist. Computer methods in biomechanics and biomedical engineering**,** 1-10.

Altman, D.G., Bland, J.M., 1983. Measurement in medicine: the analysis of method comparison studies. The statistician**,** 307-317.

Anderst, W., Les, C., Tashman, S., 2005. In vivo serial joint space measurements during dynamic loading in a canine model of osteoarthritis. Osteoarthritis and cartilage 13**,** 808-816.

Anderst, W.J., Tashman, S., 2003. A method to estimate in vivo dynamic articular surface interaction. Journal of biomechanics 36**,** 1291-1299.

Andriacchi, T.P., Briant, P.L., Bevill, S.L., Koo, S., 2006. Rotational changes at the knee after ACL injury cause cartilage thinning. Clinical orthopaedics and related research 442**,** 39-44.

Asano, T., Akagi, M., Tanaka, K., Tamura, J., Nakamura, T., 2001. In vivo three-dimensional knee kinematics using a biplanar image-matching technique. Clinical orthopaedics and related research 388**,** 157-166.

Astephen, J.L., Deluzio, K.J., Caldwell, G.E., Dunbar, M.J., 2008. Biomechanical changes at the hip, knee, and ankle joints during gait are associated with knee osteoarthritis severity. Journal of orthopaedic research 26**,** 332-341.

Bendjaballah, M.Z., Shirazi-Adl, A., Zukor, D.J., 1997. Finite element analysis of human knee joint in varus-valgus. Clin Biomech 12**,** 139-148.

Beveridge, J.E., Shrive, N.G., Frank, C.B., 2014. Repeatability and precision of a weighted centroid method for estimating dynamic in vivo tibiofemoral surface interactions in sheep. Computer methods in biomechanics and biomedical engineering 17**,** 1853-1863.

Bland, J.M., Altman, D., 1986. Statistical methods for assessing agreement between two methods of clinical measurement. The lancet 327**,** 307-310.

Coleman, J.L., Widmyer, M.R., Leddy, H.A., Spritzer, C.E., Moorman, C.T., Guilak, F., DeFrate, L.E., 2011. An In Vivo Tricompartmental Analysis of Diurnal Strains in Articular Cartilage of the Human Knee. *The 57th Annual Meeting of Orthopaedic Research Society.*

De Leva, P., 1996. Adjustments to Zatsiorsky-Seluyanov's segment inertia parameters. Journal of biomechanics 29**,** 1223-1230.

DeFrate, L.E., Sun, H., Gill, T.J., Rubash, H.E., Li, G., 2004. In vivo tibiofemoral contact analysis using 3D MRI-based knee models. Journal of biomechanics 37**,** 1499-1504.

Delp, S.L., Loan, J.P., Hoy, M.G., Zajac, F.E., Topp, E.L., Rosen, J.M., 1990. An interactive graphics-based model of the lower extremity to study orthopaedic surgical procedures. Biomedical Engineering, IEEE Transactions on 37**,** 757-767.

Dillon, C.F., Rasch, E.K., Gu, Q., Hirsch, R., 2006. Prevalence of knee osteoarthritis in the United States: arthritis data from the Third National Health and Nutrition Examination Survey 1991-94. The Journal of rheumatology 33**,** 2271-2279.

Engel, K., Brüggemann, G.-P., Heinrich, K., Potthast, W., Liebau, C., 2014. Do counteracting external frontal plane moments alter the intraarticular contact force distribution in the loaded human tibiofemoral joint? The Knee.

Farrokhi, S., Voycheck, C.A., Klatt, B.A., Gustafson, J.A., Tashman, S., Fitzgerald, G.K., 2014. Altered tibiofemoral joint contact mechanics and kinematics in patients with knee osteoarthritis and episodic complaints of joint instability. Clinical Biomechanics 29**,** 629-635.

Guess, T.M., Thiagarajan, G., Kia, M., Mishra, M., 2010. A subject specific multibody model of the knee with menisci. Medical Engineering & Physics 32, 505-515.

Gerus, P., Sartori, M., Besier, T.F., Fregly, B.J., Delp, S.L., Banks, S.A., Pandy, M.G., D'Lima, D.D., Lloyd, D.G., 2013. Subject-specific knee joint geometry improves predictions of medial tibiofemoral contact forces. Journal of biomechanics 46**,** 2778-2786.

Giavarina, D., 2015. Understanding Bland Altman analysis. Biochemia medica 25**,** 141-151.

Gilbert, S., Chen, T., Hutchinson, I.D., Choi, D., Voigt, C., Warren, R.F., Maher, S.A., 2014. Dynamic contact mechanics on the tibial plateau of the human knee during activities of daily living. Journal of biomechanics 47**,** 2006-2012.

Han, S.-K., Federico, S., Epstein, M., Herzog, W., 2005. An articular cartilage contact model based on real surface geometry. Journal of biomechanics 38**,** 179-184.

Harris, M., Morberg, P., Bruce, W., Walsh, W., 1999. An improved method for measuring tibiofemoral contact areas in total knee arthroplasty: a comparison of K-scan sensor and Fuji film. Journal of biomechanics 32**,** 951-958.

Hunt, A.E., Smith, R.M., Torode, M., Keenan, A.-M., 2001. Inter-segment foot motion and ground reaction forces over the stance phase of walking. Clinical Biomechanics 16**,** 592-600.

Koo, S., Andriacchi, T.P., 2008. The knee joint center of rotation is predominantly on the lateral side during normal walking. Journal of biomechanics 41**,** 1269-1273.

Kumar, D., Rudolph, K.S., Manal, K.T., 2012. EMG-driven modeling approach to muscle force and joint load estimations: Case study in knee osteoarthritis. Journal of orthopaedic research 30**,** 377-383.

Kumar, D., Manal, K.T., Rudolph, K.S., 2013. Knee joint loading during gait in healthy controls and individuals with knee osteoarthritis. Osteoarthritis and cartilage 21**,** 298-305.

Kutzner, I., Heinlein, B., Graichen, F., Rohlmann, A., Halder, A., Beier, A., Bergmann, G., 2010. Loading of the knee joint during activities of daily living measured in vivo in five subjects. Journal of Biomechanics 43, 2164-2173.

Lerner, Z.F., DeMers, M.S., Delp, S.L., Browning, R.C., 2015. How tibiofemoral alignment and contact locations affect predictions of medial and lateral tibiofemoral contact forces. Journal of biomechanics 48**,** 644-650.

Li, G., DeFrate, L.E., Park, S.E., Gill, T.J., Rubash, H.E., 2005a. In Vivo Articular Cartilage Contact Kinematics of the Knee An Investigation Using Dual-Orthogonal Fluoroscopy and Magnetic Resonance Image–Based Computer Models. The American journal of sports medicine 33**,** 102-107.

Li, G., Park, S.E., DeFrate, L.E., Schutzer, M.E., Ji, L., Gill, T.J., Rubash, H.E., 2005b. The cartilage thickness distribution in the tibiofemoral joint and its correlation with cartilage-to-cartilage contact. Clinical Biomechanics 20**,** 736-744.

Li, G., Wuerz, T.H., DeFrate, L.E., 2004. Feasibility of using orthogonal fluoroscopic images to measure in vivo joint kinematics. Journal of biomechanical engineering 126**,** 313-318.

Marouane, H., Shirazi-Adl, A., Adouni, M., Hashemi, J., 2014. Steeper posterior tibial slope markedly increases ACL force in both active gait and passive knee joint under compression. Journal of biomechanics 47**,** 1353-1359.

Marouane, H., Shirazi-Adl, A., Adouni, M., 2015a. Knee joint passive stiffness and moment in sagittal and frontal planes markedly increase with compression. Computer methods in biomechanics and biomedical engineering 18**,** 339-350.

Marouane, H., Shirazi-Adl, A., Hashemi, J., 2015b. Quantification of the role of tibial posterior slope in knee joint mechanics and ACL force in simulated gait. Journal of biomechanics.

Mesfar, W., Shirazi-Adl, A., 2005. Biomechanics of the knee joint in flexion under various quadriceps forces. The Knee 12**,** 424-434.

Mesfar, W., Shirazi-Adl, A., 2006. Knee joint mechanics under quadriceps-hamstrings muscle forces are influenced by tibial restraint. Clin Biomech 21**,** 841-848.

Moglo, K.E., Shirazi-Adl, A., 2003. Biomechanics of passive knee joint in drawer: load transmission in intact and ACL-deficient joints. Knee 10**,** 265-276.

Nisell, Ralph., Gunnar Németh., and Hans Ohlsén., 1986. Joint forces in extension of the knee: analysis of a mechanical model. Acta Orthopaedica 57(1):41-46.

Seitz, A.M., Lubomierski, A., Friemert, B., Ignatius, A., Dürselen, L., 2012. Effect of partial meniscectomy at the medial posterior horn on tibiofemoral contact mechanics and meniscal hoop strains in human knees. Journal of orthopaedic research 30**,** 934-942.

Shelburne, K.B., Torry, M.R., Pandy, M.G., 2006. Contributions of muscles, ligaments, and the ground-reaction force to tibiofemoral joint loading during normal gait. Journal of orthopaedic research 24**,** 1983-1990.

Shirazi, R., Shirazi-Adl, A., Hurtig, M., 2008. Role of cartilage collagen fibrils networks in knee joint biomechanics under compression. J Biomech 41**,** 3340-3348.

Wang, H., Chen, T., Koff, M.F., Hutchinson, I.D., Gilbert, S., Choi, D., Warren, R.F., Rodeo, S.A., Maher, S.A., 2014. Image based weighted center of proximity versus directly measured knee contact location during simulated gait. Journal of biomechanics 47**,** 2483-2489.

Winby, C.R., Lloyd, D.G., Besier, T.F., Kirk, T.B., 2009. Muscle and external load contribution to knee joint contact loads during normal gait. Journal of biomechanics 42**,** 2294-2300.

Wretenberg, P., Ramsey, D.K., Németh, G., 2002. Tibiofemoral contact points relative to flexion angle measured with MRI. Clinical Biomechanics 17**,** 477-485.

Zhao, D., Banks, S.A., D'Lima, D.D., Colwell, C.W., Fregly, B.J., 2007. In vivo medial and lateral tibial loads during dynamic and high flexion activities. Journal of orthopaedic research 25**,** 593-602.

Table 6.3: Pearson slope (S) and coefficient of determination (R^2) as well as Bland Altman mean (d) and standard deviation (SD) of differences when comparing results of 6 different contact center algorithms on medial and lateral plateaus in both mediolateral (ML) and anetroposterior (AP) directions versus our own CC-Ref estimations at 6 stance periods.

	Medial Plateau							
	ML Direction				AP Direction			
	S	R^2	d	SD	S	R^2	d	SD
MS	1.14	0.94	-1.40	2.29	0.97	0.72	1.28	2.17
CCA-m	0.32	0.76	2.56	4.90	0.75	0.87	0.29	1.38
CCA	0.60	0.98	-2.27	2.86	0.95	0.95	-0.31	0.84
MJS	1.41	0.93	0.71	4.00	0.60	0.38	0.33	3.07
WCoP	0.92	0.97	-2.13	1.24	0.68	0.95	-1.15	1.27
CP	0.00	0.00	3.97	7.01				

	Lateral Plateau							
	ML Direction				AP Direction			
	S	R^2	d	SD	S	R^2	d	SD
MS	1.35	0.75	4.10	1.47	0.49	0.93	0.37	1.74
CCA-m	-0.09	0.10	-5.76	1.93	0.49	0.97	-2.84	1.71
CCA	-0.49	0.80	0.59	2.60	0.57	0.80	-0.65	1.70
MJS	-0.33	0.56	7.75	2.34	0.31	0.42	-0.13	2.58
WCoP	-0.28	0.16	6.58	2.47	0.74	0.86	-1.50	1.31
CP	0.00	0.00	-3.88	1.72				

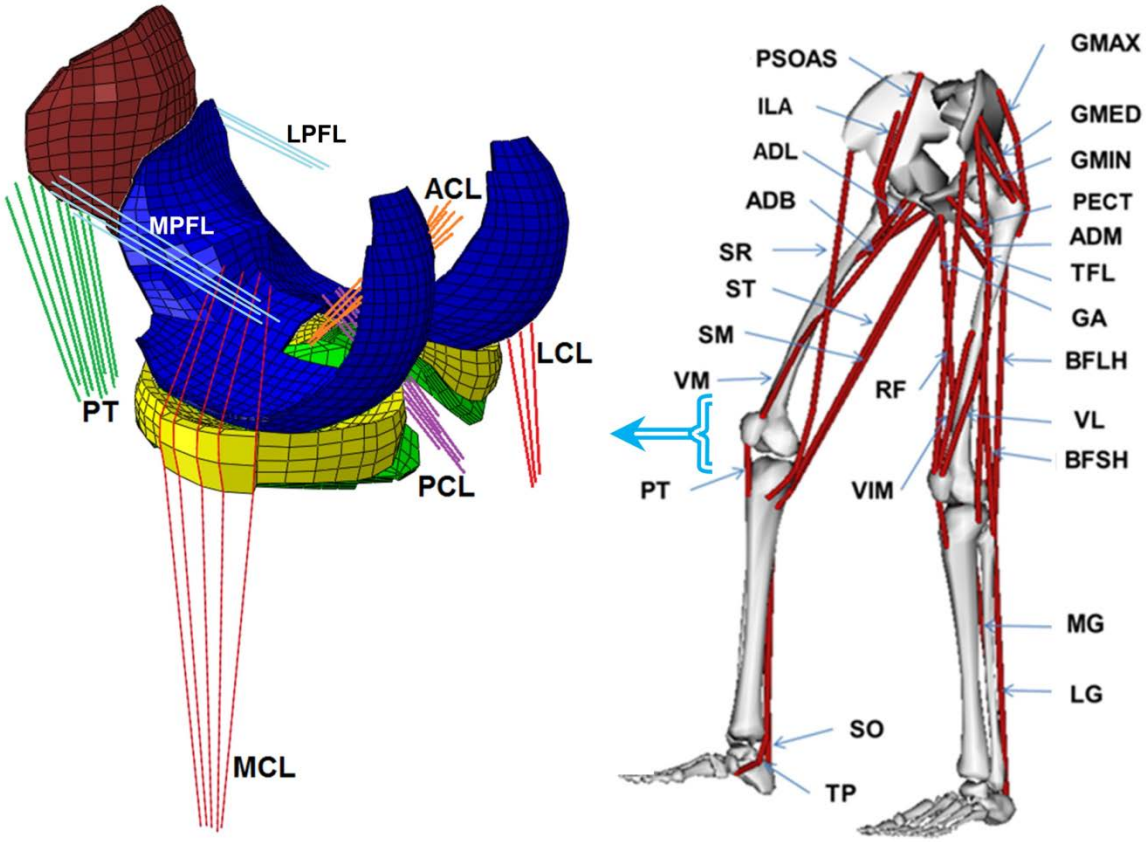

Figure 6.1: **(a)** Knee FE model; tibiofemoral (TF) and patellofemoral (PF) cartilage layers, menisci, patellar Tendon (PT). Joint ligaments include lateral patellofemoral (LPFL), medial patellofemoral (MPFL), anterior cruciate (ACL), posterior cruciate (PCL), lateral collateral (LCL) and medial collateral (MCL). **(b)** Schematic diagram showing the 34 muscles incorporated into the lower extremity model (Open Sim, Delp et al., 2007). Quadriceps components are vastus medialis obliqus (VMO), rectus femoris (RF), vastus intermidus medialis (VIM) and vastus lateralis (VL). Hamstrings components include biceps femoris long head (BFLH), biceps femoris short head (BFSH), semi membranous (SM) and TRIPOD made of sartorius (SR), gracilis (GA) and semitendinosus (ST). Gastrocnemius components are gastrocnemius medial (GM) and gastrocnemius lateral (GL). Soleus (SO) muscle is uni-articular ankle muscle. Hip joint muscles (not all shown) include adductor, long (ADL), mag (3 components ADM) and brev (ADB); gluteus max (3 components GMAX), med (3 components GMED) and min (3 components GMIN), iliacus (ILA), iliopsoas (PSOAS), quadriceps femoris; pectineus (PECT), tensor facia lata (TFL), periformis.

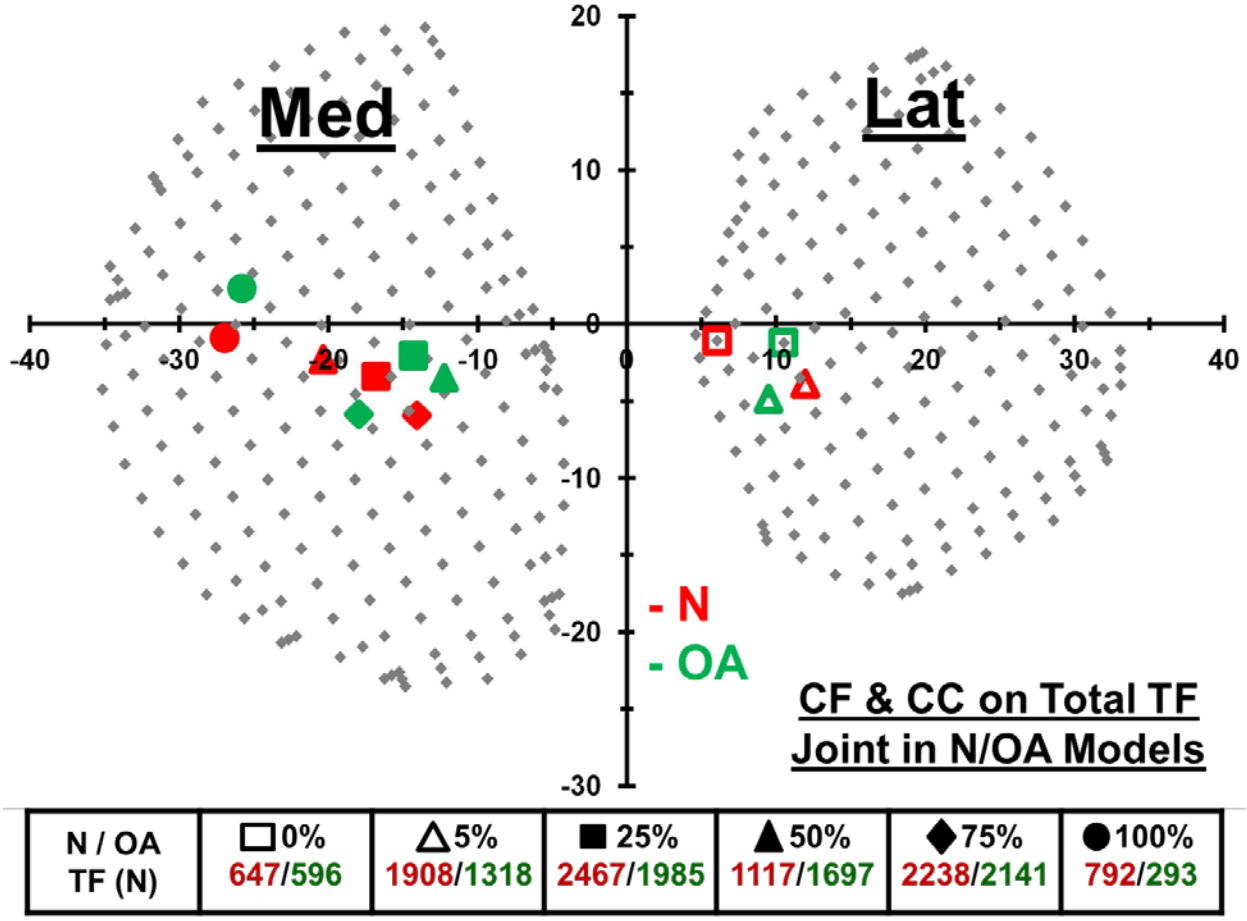

Figure 6.2: Predicted contact forces (CF) and contact centers (CC) on the entire tibiofemoral (TF) joint in normal and OA models. Med: medial plateau, Lat: lateral plateau. Lateral and anterior directions are positive here. Dimensions on axes are in mm. Mean of reported kinematics/kinetics in gait of normal and OA subjects are used to drive the model.

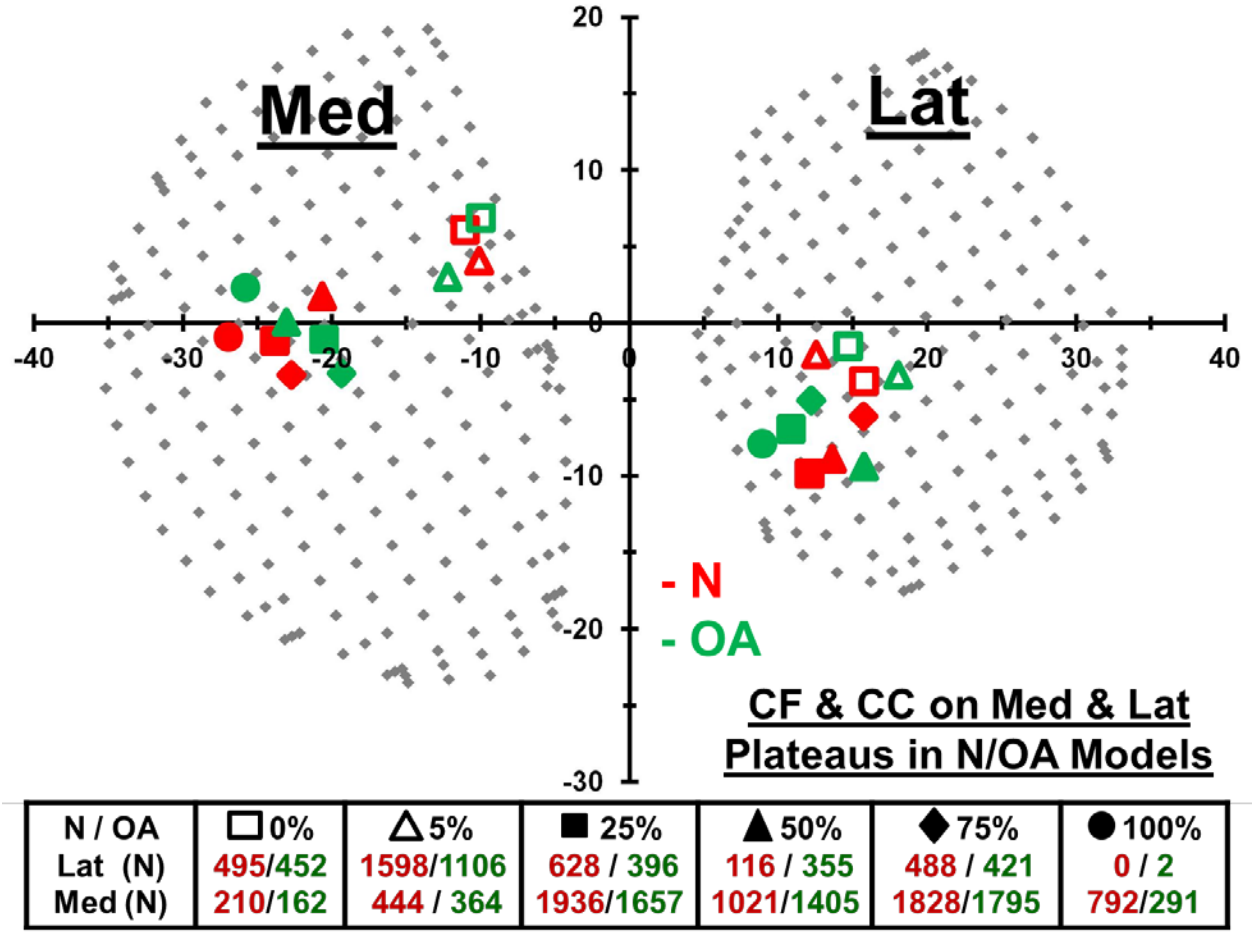

N / OA	0%	5%	25%	50%	75%	100%
Lat (N)	495/452	1598/1106	628 / 396	116 / 355	488 / 421	0 / 2
Med (N)	210/162	444 / 364	1936/1657	1021/1405	1828/1795	792/291

Figure 6.3: Predicted contact forces (CF) and contact centers (CC) on the medial (Med) and lateral (Lat) plateaus in normal and OA models. Lateral and anterior directions are positive here. Dimensions on axes are in mm. Mean of reported kinematics/kinetics in gait of normal and OA subjects are used to drive the model.

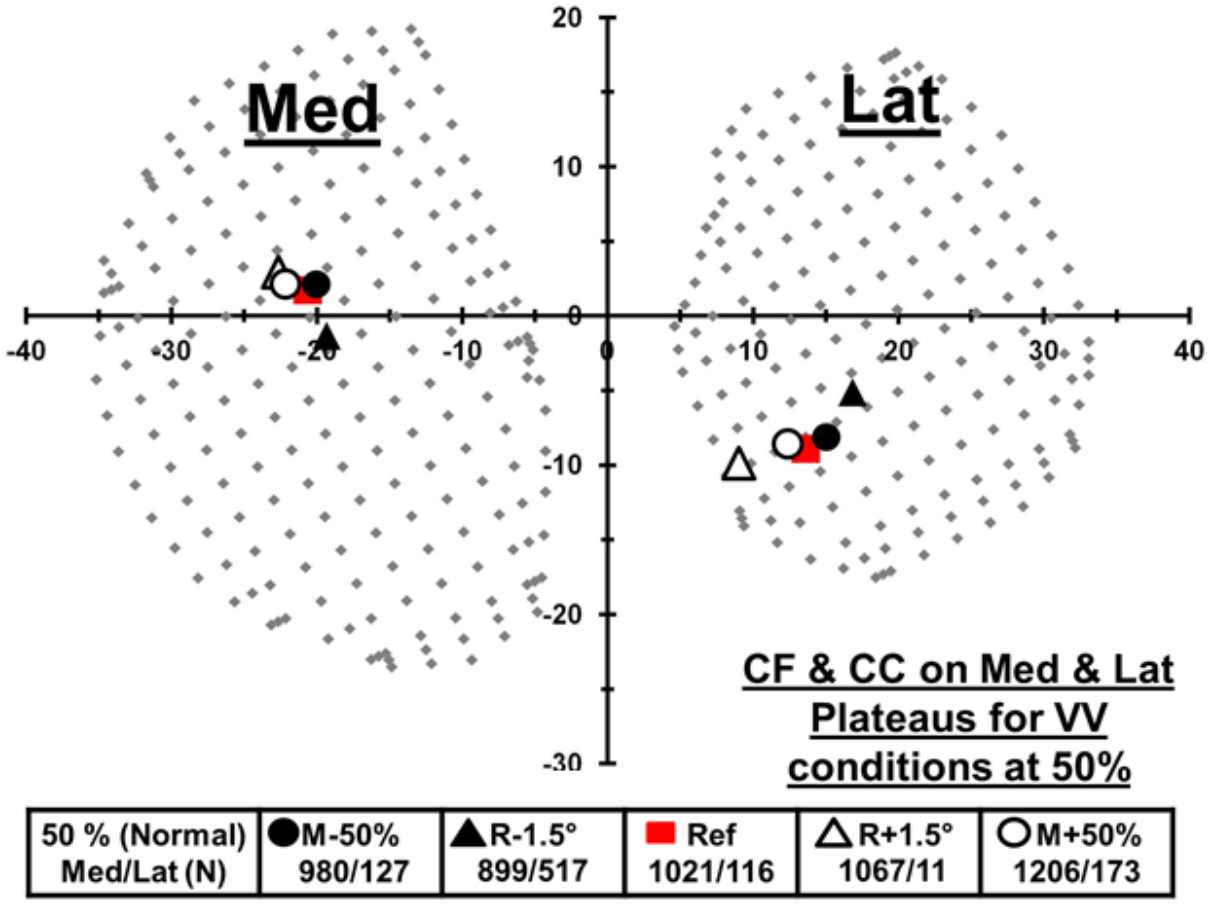

Figure 6.4: Predicted contact forces (CF) and contact centers (CC) on medial (Med) and lateral (Lat) plateaus for different varus/valgus conditions at mid-stance (50%) period. Lateral and anterior directions are positive here. Dimensions on axes are in mm. The reference case is driven by mean of reported kinematics/kinetics at mid-stance (50%) period of gait.

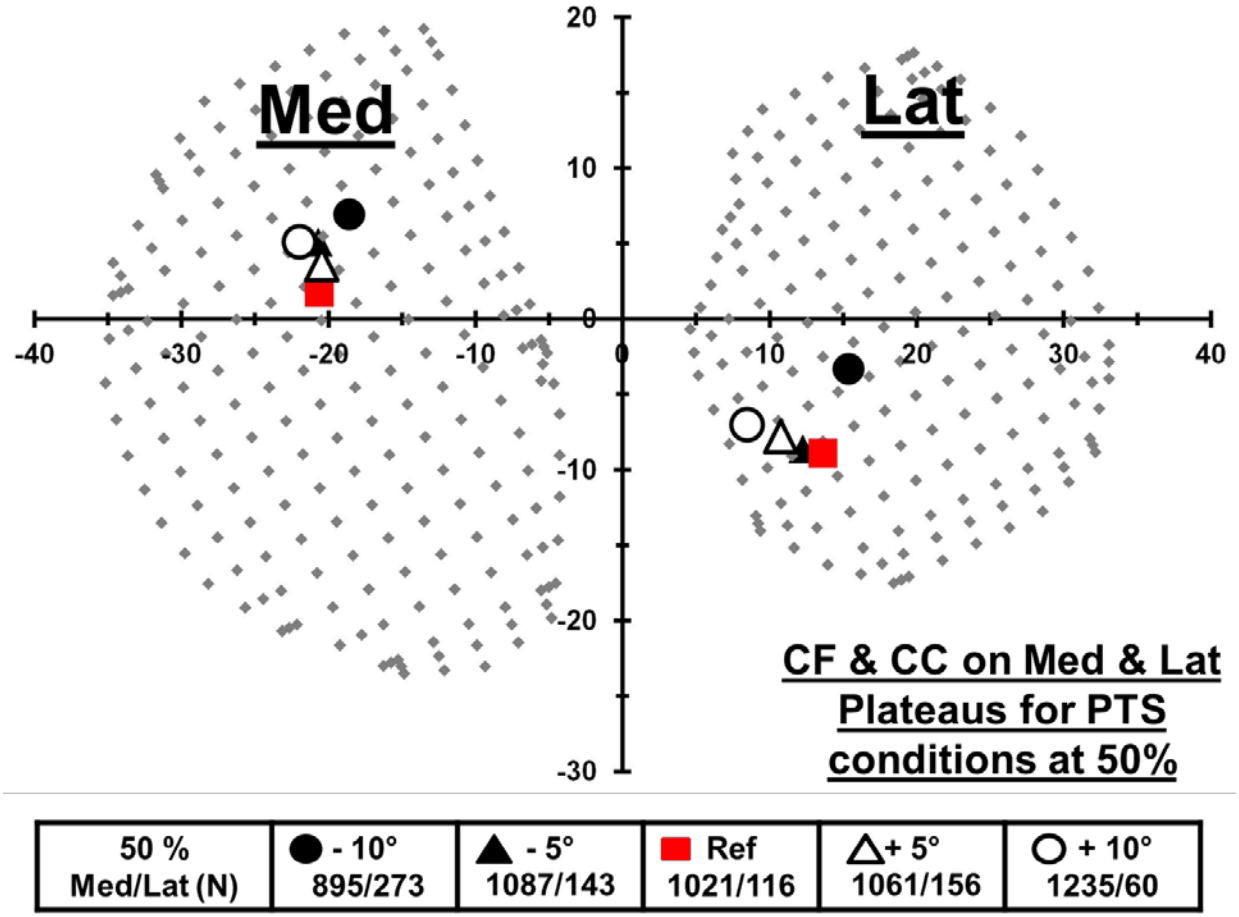

Figure 6.5: Predicted contact forces (CF) and contact centers (CC) on medial (Med) and lateral (Lat) plateaus for different posterior tibial slope (PTS) conditions at mid-stance (50%) period. Lateral and anterior directions are positive here. Dimensions on axes are in mm. All cases are driven by mean of reported kinematics/kinetics at mid-stance (50%) period of gait.

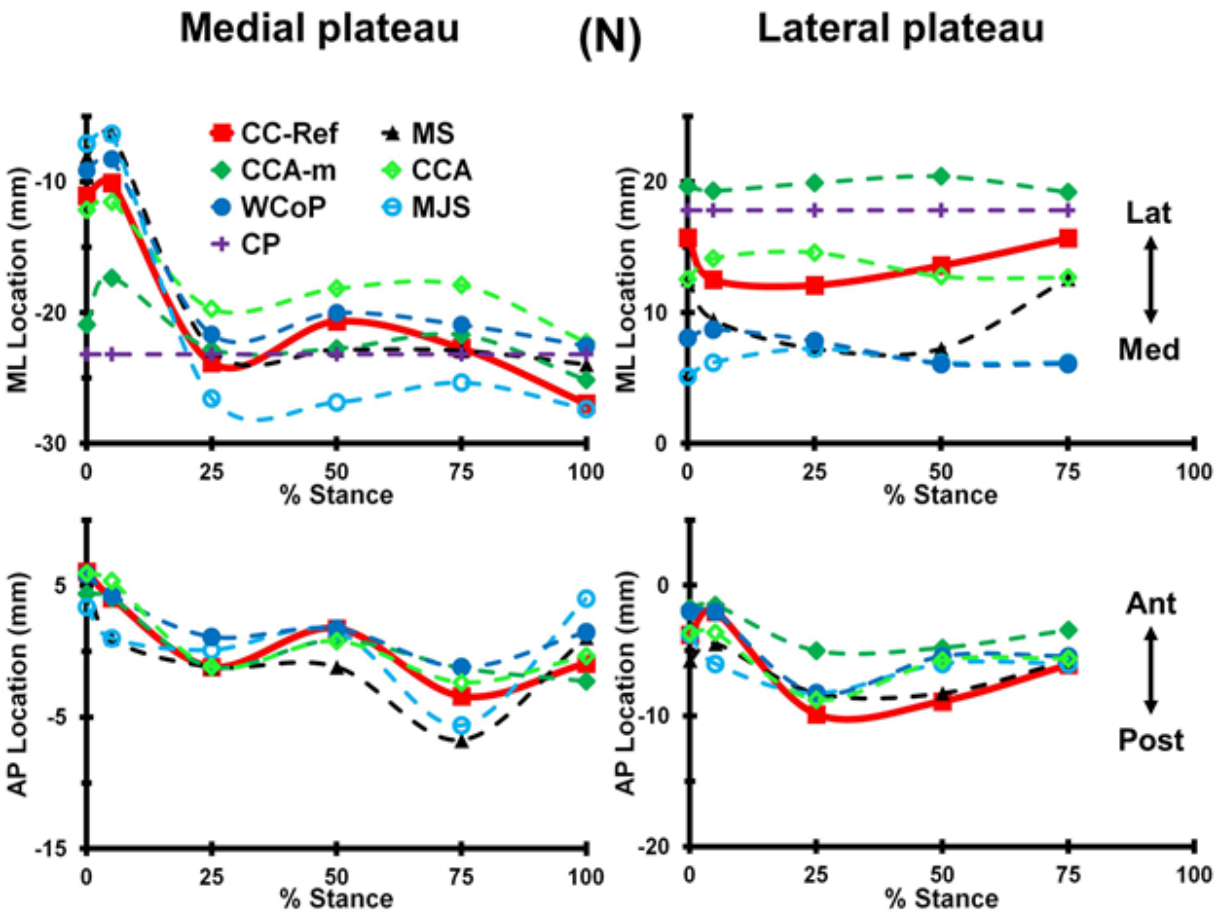

Figure 6.6: Anteroposterior (AP) and mediolateral (ML) locations of the estimated contact centers (CC) on the medial and lateral tibial plateaus at different stance periods. Our accurately estimated values (CC-Ref) taken as the gold standard are compared with those of 6 other models using identical contact data computed by our detailed lower-extremity model (MS: maximum strain, CCA: centroid of contact area, CCA-m: modified version of CCA considering both covered and uncovered contact areas on cartilage, WCoP: weighted center of proximity, MJS: minimum joint space, CP: contact point). Lateral and anterior directions are positive here.

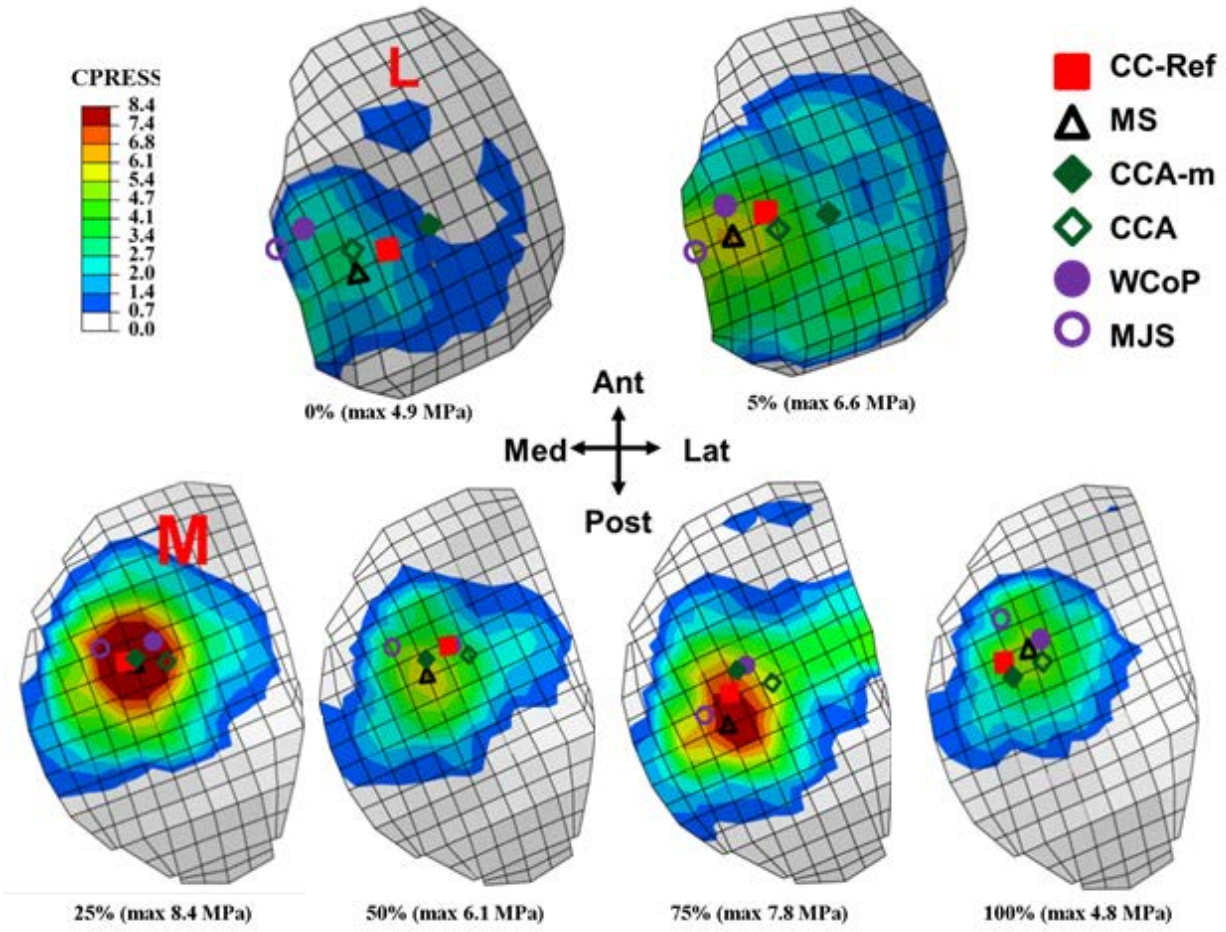

Figure 6.7: Predicted contact pressure distributions at articular surfaces of tibial plateaus at different stance periods in gait of normal subjects (on the lateral plateau at early 0 and 5% periods whereas on the medial plateau thereafter at 25, 50, 75 and 100% periods). The contact centers (CC) estimated by various methods are also shown. Note that a common legend is used for ease in comparisons.

CHAPITRE 7 ARTICLE 4: 3D ACTIVE-PASSIVE RESPONSE OF HUMAN KNEE JOINT IN GAIT IS MARKEDLY ALTERED WHEN SIMULATED AS A PLANAR 2D JOINT

H. Marouane, A. Shirazi-Adl, and M. Adouni

Article published in Biomechanics and Modeling in Mechanobiology 2016

7.1 Abstract

Musculoskeletal models of the lower extremity make a number of important assumptions when attempting to estimate muscle forces and tibiofemoral compartmental loads in activities such as gait. The knee is commonly idealized as a planar 2D joint in the sagittal plane with no consideration of motions and equilibrium in remaining planes. With muscle forces predicted, the static equilibrium in the frontal plane is then used to estimate compartmental loads neglecting also joint passive resistance and assuming condylar contact centers. We aimed here to comprehensively investigate the effects of such assumptions on predicted results. While simulating gait and using a hybrid lower extremity model that incorporates a detailed validated 3D finite element model of the knee joint, analyses are repeated with out-of-sagittal plane rotations and moment equilibrium equations neglected (2D model) and tibial compartmental forces estimated using equilibrium in the frontal plane while disregarding passive resistance and assuming fixed contact centers (1D model). Large unbalanced out-of-sagittal plane moments reaching peaks of 30 Nm abduction moment and 12 Nm internal moment at 25 % stance period are computed that are overlooked in the 2D model. Consideration of the knee as a planar 2D joint substantially diminishes muscle forces, anterior cruciate ligament force and tibiofemoral contact forces/stresses when compared to the 3D reference model. Total tibiofemoral contact force peaks at 25 % stance at 4.2 BW in the 3D model that drops to 3.0 BW in the 2D model. The location of contact centers on each plateau also noticeably alters (by as much as 5 mm). Tibiofemoral contact forces further change when the location of contact centers on each plateau is fixed. Results highlight the importance of accurate simulation of 3D motions and equilibrium equations as well as passive joint properties and contact centers.

Keywords: Musculoskeletal model; Muscles; Contact force; Contact center; Gait; Knee joint

7.2 Introduction

As a joint most commonly inflicted with osteoarthritis (OA), artificial and biologic replacements, osteotomies and sports injuries (Guilak 2011; Katz et al. 2010; Kim 2008; Losina et al. 2012), the human knee joint is in the spotlight in need for more effective prevention and treatment programs. In response, several finite element (FE) models with different degrees of precision and refinement have been developed (Bendjaballah et al. 1995; Kazemi and Li 2014; Pena et al. 2006; Yang et al. 2010a). Likewise, various active musculoskeletal (MS) models of the lower extremity have been constructed with the objective to further existing understanding of knee joint functional biomechanics in normal and disturbed conditions (Adouni and Shirazi-Adl 2014a; Delp et al. 1990; Lloyd and Besier 2003; Manal and Buchanan 2013; Marouane et al. 2015b). While former FE models provide valuable detailed information (i.e., tissue stresses and strains) in joint constituent materials, MS models offer crucial results on activation patterns in musculature and resulting global joint loads in complex physiological activities such as gait (Kim et al. 2009; Taylor et al. 2004; Winby et al. 2009). Our recent lower extremity hybrid MS model investigations, by explicit incorporation of a validated detailed FE model of the entire knee joint, offer, however, improved estimations both at the global (muscle and joint forces) and local (tissue stresses and strains, contact pressure and center) levels (Adouni and Shirazi-Adl 2014a; Marouane et al. 2014, 2015a, b, 2016) by consideration of active-passive synergy.

Existing MS models of lower extremity make a number of important assumptions when attempting to estimate muscle forces and tibiofemoral compartmental loads in activities such as gait. The knee is commonly idealized, when calculating lower extremity muscle forces, as a planar (2D) joint with its motion constrained to remain in the sagittal plane and governed by the flexion-extension rotation (Delp et al. 1990; DeMers et al. 2014; Shelburne and Pandy 1998; Shelburne et al. 2004, 2006), neglecting thus both displacements and equilibrium equations in remaining planes. With muscle forces predicted, the static equilibrium in the frontal plane is consequently considered to estimate tibial compartmental loads neglecting the knee joint passive resistance and assuming medial/lateral contact centers (Gerus 2013; Miller et al. 2015; Winby et al. 2009). It is recognized that the femoral condyles roll and slide on the tibial plateau during joint motions (Bull et al. 2008; Freeman and Pinskerova 2005). The complex relative movements

of the femur on the tibia along with the load transmission via menisci, however, markedly influence the location of the centers of contact in both medial and lateral directions on each plateau during all instances of gait (Marouane et al. 2016).

Notwithstanding suggestions to set joint model complexity according to the application (Valente et al. 2015), substantial sensitivity of MS model estimations to foregoing common simplifications on contact centers (Lerner et al. 2015a) and knee planar (2D) configuration (Sandholm et al. 2011) has been demonstrated. Sartori et al. (2012), using an EMG-driven MS model, reported the violation of moment equilibrium equations in planes other than the one used to evaluate muscle forces and recommended the simultaneous consideration of moment equations in all planes. In a recent study, Mokhtarzadeh et al. (2014) also found different muscle force estimations during a single legged hop using 3 degrees of freedom (DOF) versus 1 DOF knee joint models. In addition, Dumas et al. (2012) showed that with more degrees of freedom in the model, the 3D joint reaction forces tend to increase along with alterations in estimated muscle forces. Finally, a 2D approach by neglecting out-of-sagittal plane moments in gait has been found to underestimate muscle forces and internal loads by as much as 60 % (Glitsch and Baumann 1997).

In the current work and using a hybrid lower extremity musculoskeletal model incorporating a detailed validated knee joint FE model (Marouane et al. 2016, 2015b), we aim to perform a much-needed comprehensive investigation on the effect of foregoing idealizations on muscle forces, knee joint contact forces/stresses/centers and ligament forces in gait. To develop the knee planar (2D) model, knee joint out-of-sagittal plane rotations (abduction-adduction and internal-external) and associated moment equilibrium equations are overlooked in the reference 3D model and analyses are repeated. Additional cases (referred to as 2.5D) are also considered with out-of-sagittal plane rotations prescribed but associated moment equilibrium constraints neglected. The models are all driven by identical sets of gait kinematics and kinetics collected on asymptomatic subjects in stance phase of gait (Astephen 2007; Hunt et al. 2001). Furthermore in the 2D model, tibial contact forces are alternatively calculated using equilibrium in the frontal plane with assumed fixed contact points (referred to as 1D model) (Gerus 2013; Winby et al. 2009). In accordance with earlier findings (Dumas et al. 2012; Glitsch and Baumann 1997; Valente et al. 2015), we hypothesize that the 2D approach markedly underestimates muscle and contact forces when compared to our 3D reference model considered as the gold standard.

7.3 Methods

A detailed FE model of the knee joint that consists of bony structures (tibia, femur and patella) and their compliant articular cartilage layers as well as menisci, major tibiofemoral (ACL, PCL, LCL, MCL) and patellofemoral (MPFL, LPFL) ligaments, patellar tendon (PT) and active musculature of the lower extremity is employed (Marouane et al. 2014, 2015b) (Figure 7.1). We have extensively validated this model with available in vitro and in vivo data under various passive and active load conditions over the last 20 years (e.g., Adouni et al. (2012); Adouni and Shirazi-Adl (2014a); Bendjaballah et al. (1995); Marouane et al. (2015b); Mesfar and Shirazi-Adl (2005); Moglo and Shirazi-Adl (2003); Shirazi et al. (2008)). The articular cartilage layers and menisci are simulated as non-homogeneous nonlinear depth-dependent composites of collagen fibrils and incompressible matrices. Cartilage layers are reinforced by fibril networks parallel to the articular surface in the superficial zone, randomly oriented in the middle zone and vertical in the deep zone. Ligaments are simulated by a number of nonlinear (tension only) axial elements with initial pre-strains (Mesfar and Shirazi-Adl 2005; Shirazi-Adl and Moglo 2005). This detailed knee model has been introduced within a musculoskeletal model of the lower extremity including hip and ankle joints as well as uni- and bi-articular muscles to analyze the stance phase of gait under mean in vivo kinematics/kinetics reported for asymptomatic subjects (Astephen 2007; Hunt et al. 2001).

In order to evaluate the effect of single and multi-DOF kinematics/kinetics constraints on knee joint biomechanics during the stance phase of gait, predictions of three different models are compared in this study: (1) The reference 3D model is our most accurate model that is fully driven by reported gait kinematics/kinetics in which muscle forces are iteratively evaluated by the minimization of cubic sum of muscle stresses and constraints on all moment equilibrium equations. Estimated muscle forces are applied, thereafter, along with gravity loads (foot and leg) and ground reaction forces (GRF) and iterations repeated till convergence (Marouane et al. 2016, 2015b). (2) In the 2D model, as a simplified version of foregoing 3D model, the knee joint is assumed as a hinge joint in the sagittal plane with abduction-adduction and internal-external rotations and moment equations overlooked. The model at the knee joint is hence driven only by the flexion-extension rotation and moment of gait data. (3) At 5 and 75 % stance periods, these analyses are repeated while applying all gait kinematics (i.e., rotations in 3 planes) but neglecting moment equations out-of-sagittal plane (identified hereafter as 2.5D model). In all

foregoing three models, the only difference from a model to another is in the extent of consideration of the knee joint moments and rotations, while the hip and ankle joints are simulated as 3D and 1D frictionless joints, respectively.

Following application of initial pre-strains in knee joint ligaments, the hip/knee/ankle rotations/moments and ground reaction forces (GRF) reported at each period of stance phase (0, 5, 25, 50, 75, 100 %) (Astephen 2007; Hunt et al. 2001) are applied and iterative nonlinear analyses carried out till convergence (i.e., unbalanced moments <0.1 Nm). The location of GRF at each period is determined so as to generate reported knee joint moments (Astephen et al. 2008) accounting for the leg/foot weights (29.78/7.98 N). Since our model is constructed based on a female knee, a body mass of 61.9 kg (606.6 N) and body height of 173 cm is considered (De Leva 1996). The nonlinear elastostatic analyses are carried out using ABAQUS (version 6.14, Simulia, Inc., Providence, RI, USA) finite element package program. MATLAB (R2013a Optimization Toolbox, genetic algorithms and Fmincon) is used in the optimization algorithm, and Python (3.3.5) is employed to locate the contact centers (CC) and forces (see Marouane et al. 2016).

To estimate tibial compartment contact forces, many MS model studies assume fixed medial-lateral locations for contact centers. These contact points are taken at the midpoints of condyles (Gerus 2013; Winby et al. 2009), 25 % of the tibial width on each side (Manal and Buchanan 2013), 25 % of the scaled intercondylar width (Kumar et al. 2012), the closest points between the femoral and tibial prosthesis components (Sandholm et al. 2011) or based on images using various approaches (Blagojevic et al. 2010; Lerner et al. 2015b, a; Li et al. 2005a; Miller et al. 2015). In our 2D and 3D models, contact forces and centers are accurately estimated using computed contact pressure distributions on each plateau (Marouane et al. 2016). In addition and in accordance with existing MS models (Gerus 2013; Kumar et al. 2012; Miller et al. 2015), contact forces are also recalculated using static equilibrium about the fixed medial and lateral contact points in the tibial frontal plane. Here, the external adduction/abduction moment (via inverse dynamics) determined at a contact point minus the associated moments of muscle forces (calculated in the 2D model) are used to evaluate the contact force on the opposing plateau. These results are identified hereafter as 1D contact forces.

7.4 Results

Forces in quadriceps, lateral/medial hamstrings and gastrocnemius substantially dropped (even at times to nil) in the 2D model when compared to the 3D reference one in many periods of stance (Figure 7.2). Overall, lower muscle forces were also noted in the 2.5D model at 5 and 75 % periods. Large unbalanced (required) out-of-sagittal plane moments, especially in the frontal plane, were computed in the 2D model reaching peaks of ~30 and 12 Nm abduction and internal moments, respectively, at 25 % stance (Figure 7.3). Unbalanced internal-external moments were smaller (<3 Nm) in remaining periods of stance. Unbalanced abduction-adduction moments were larger with ~24 Nm at mid-stance (50 %) and 75 % periods (Figure 7.3). Forces in ACL and PT also markedly reduced in the 2D model from peaks of 355 and 982 N to 217 and 823 N at 25 % stance, respectively (Figure 7.4). The use of the 2D model had negligible to small effects on forces in remaining ligaments except in the LCL ligament at toe-off (100 % period) where the force dropped from 208 to 25 N (Figure 7.4).

As a result of lower muscle forces, total tibiofemoral contact forces diminished in the 2D model at all stance periods (Table 7.1). The effect was, however, different on each plateau; the medial plateau experienced substantial decreases at later 25–100 % periods (by as much as 730 N or 92 % at toe-off), while on the contrary, lateral plateau was subjected to greater forces (by 366 N or 75 at 75 % period) in these periods except at 25 % where the lateral force was also decreased (Table 7.1; Figure 7.5). In contrast to the 3D model, larger share of contact forces were, however, computed on the lateral plateau at the mid-stance (58 %) and toe-off (74 %) in the 2D model. Overall, a larger portion of contact forces was transferred via uncovered areas on both plateaus (Figure 7.5). Changes in 2D model versus 3D model occurred, though to different extents, at both covered (via menisci) and uncovered (cartilage-cartilage) areas of contact (Figure 7.5). Along with foregoing alterations in contact forces, the location of contact centers on each plateau also markedly altered; at 25–100 % stance periods, the 2D model shifted contact centers laterally on both medial and lateral compartments (by as much as 5 mm) and anteriorly (by as much as 2 mm) on the lateral compartment, whereas posteriorly on the medial plateau (Figure 7.6). The TF and PF contact areas/pressures followed the same trends as their respective contact forces (Figure 7.7).

Substantial changes were found when comparing TF contact forces calculated accurately (though based on 2D muscle forces) in the 2D model to those calculated by the idealized 1D model; they generally decreased on both plateaus (Table 7.2). However, decreases were more pronounced in the lateral plateau rather than the medial plateau.

7.5 Discussion

Combining a MS model of the lower extremity with a detailed FE model of the knee joint and under reported kinetics-kinematics of gait collected on asymptomatic subjects, we aimed here to comprehensively investigate the effects of a number of common assumptions often made in MS models on predicted results. Analyses were carried out with out-of-sagittal plane rotations and moment equilibrium equations neglected (i.e., 2D model) and tibial compartmental forces estimated either accurately via predicated contact pressures at tibiofemoral articular surfaces (2D model) or using equilibrium in the frontal plane while disregarding passive resistance and assuming fixed contact centers (i.e., 1D model). Results were compared with our earlier predictions using a realistic 3D model (Adouni and Shirazi-Adl 2014a; Marouane et al. 2016) that accounts for all knee joint rotations and moments. Computed results confirm our hypothesis that, throughout stance phase and despite identical models, kinematics and kinetics, substantial differences are computed in all global and local results from muscle forces to knee joint contact forces/stresses/centers and ligament forces when the knee joint is idealized as a planar one and/or when contact centers are fixed.

In MS models of the lower extremity, the hip joint is generally modeled as a ball-and-socket joint (Arnold et al. 2010; Delp et al. 2007, 1990; Horsman et al. 2007) or simply as a planar hinge joint (Shelburne and Pandy 1998, 1997, 2002). The knee joint, on the other hand, is often assumed as a planar joint in MS models of the lower extremity (Delp et al. 1990; Horsman et al. 2007; Sandholm et al. 2011). While the ability of a 2D hip joint to reproduce similar kinematics and kinetics as a 3D hip joint has been indicated (Xiao and Higginson 2008), large differences have been found when idealizing the knee joint as a planar one (Glitsch and Baumann 1997; Kim et al. 2009; Taylor et al. 2004). A hybrid MS model of the lower extremity, similar to the one used in our earlier studies (Adouni and Shirazi-Adl 2014a; Marouane et al. 2015a, 2016), would circumvent inherent assumptions in such 2D models by a realistic detailed FE representation of the entire knee joint. Some earlier attempts to employ a detailed FE

model of the knee joint in gait have made substantial simplifying assumptions in muscle force estimation algorithm and consideration only of the flexion-extension moment (Yang et al. 2010a) or in limited loads/motions applied to the knee joint taken from reported gait data (Mononen et al. 2015). The ankle joint on the other hand is generally modeled as a revolute joint (Arnold et al. 2010; DeMers et al. 2014; Lerner et al. 2015a; Steele et al. 2012) or as a 2DOF universal joint (Shelburne et al. 2004).

Idealized 2D simulation of the knee joint with no consideration for out-of-sagittal plane rotations and moments equilibrium equations is found to substantially reduce forces estimated in all muscle groups and at most stance periods, in average by 48 % in quadriceps, 44 % in hamstrings and 16 % in gastrocnemius (Figure 7.2). Forces in quads even completely disappeared at 5 % period (Figure 7.2a). Less changes in muscle forces are, however, noted when neglecting only moment equilibrium equations out of the sagittal plane (2.5D model) at 5 and 75 % periods. Remaining muscles, not presented in Fig. 2, show slightly lower differences in forces (<10 N) with negligible contributions to the knee joint loading. Lower muscle forces in the 2D model are justified primarily due to the negligence of equilibrium equations of abduction-adduction and internal-external moments that relieve the additional burden on muscles crossing the knee joint (Glitsch and Baumann 1997; Valente et al. 2015). These neglected and unbalanced moments that are above and beyond the passive knee joint resistance moments (that are automatically and accurately accounted for here in this study when using detailed FE model of the knee joint in all 2D, 2.5D and 3D models) reach important values especially at 25–75 % periods of stance (see Figure 7.3). Neglecting out-of-sagittal plane moments in 2D models of gait has, in agreement with our results, been reported to underestimate muscle forces and internal loads by as much as 60 % (Glitsch and Baumann 1997).

In accordance with the lower activity computed in muscles, the total tibiofemoral contact forces diminish in the 2D model at all stance periods when compared to the reference 3D model (Table 1). Total tibiofemoral contact force peaks at 25 and 75 % stance periods with maximum of 4.2 BW at 25 % that substantially drops in the 2D model to 3.0 BW (Table 1). While the first peak in the tibiofemoral contact force occurs mainly due to high activation in quadriceps (Figure 7.2a), the second peak is due to gastrocnemius and hamstring exertions (Figure 7.2b, c). Valente et al. (2015) report greater contact force predictions (by 2.4 BW) when a frictionless spherical model is used instead of a hinge knee joint model. Interestingly and due to primarily neglecting

adduction rotations/moments, the 2D model markedly diminishes the compartmental load on the medial side at 25–100 % periods while in contrast increases that on the lateral side at 50–100 % periods. Reverse trends are noted at earlier 0–5 % periods. Foregoing changes result, in contrast to the 3D model, in the transmission of a larger portion of joint compression through the lateral plateau at 50 and 100 % periods (Table 7.1). Complete absence of the adduction rotation in the 2D model is the likely cause here (Adouni and Shirazi-Adl 2014b). At mid-stance period and in accordance with the current 2D model results, Adouni and Shirazi-Adl (2014b) reported that a 1.5°° drop in the adduction rotation (from a reference value of 1.6)°) significantly increased the lateral load by 346 % but reduced the medial load only by 12 % resulting in a more uniform distribution of load on both plateaus.

Along with foregoing alterations in contact forces, the location of contact centers on each plateau also markedly alters; at 25–100 % stance periods, the 2D model shifts the contact centers laterally on both medial and lateral compartments (by as much as 5 mm) and anteriorly (by as much as 2 mm) on the lateral compartment (Figure 7.6). These changes are caused by a combined effects of substantial alterations in both (1) knee joint kinematics where abduction rotation in early periods, adduction rotation later at 25–100 % periods and internal rotation at first half of stance are neglected, and (2) knee joint moments of abduction in early stance and adduction thereafter that are neglected while evaluating muscle forces. The extent of changes diminish, however, as the latter rotations are considered in the 2.5D model at 5 and 75 % periods. Lerner et al. (2015a), using the equilibrium model in the frontal plane to evaluate contact forces (similar to the approach sued here in 1D model), report that each one millimeter shift in the medial-lateral translation of the compartment contact point locations alters the first peak of medial compartment contact force by 41 N.

The knee joint passive structures play a significant role in supporting external loads and as a result in lowering demand on activity in muscles crossing the joint while enhancing joint stability (Bendjaballah et al. 1997; Marouane et al. 2015a). The knee joint passive stiffness further increases in the presence of larger compression forces that are omnipresent in most physiological activities as gait and stair ascent/descent (Marouane et al. 2015a). These passive moments of the knee joint that are automatically accounted in our hybrid model (in all 3D, 2.5D and 2D models) are in addition and above the unbalanced moments (Figure 7.3) that are also neglected in many earlier MS models. It is clear that neglecting passive moments results in

substantial increases in muscle activity and joint forces. In addition, assumption of fixed centers of contact in MS models further affects estimated compartmental forces. Comparing the joint contact forces calculated using the 1D model (taking equilibrium in the frontal plane with assumed fixed contact points under associated inverse dynamics moment, see Figure 7.6) with those predicted accurately by computed contact pressure distributions using the 2D model, also substantially affects tibiofemoral contact forces (Table 7.2). These differences are due both to the passive resistance of the knee joint in the frontal plane (Marouane et al. 2015a) as well as the idealization errors in assuming fixed centers of contact (Figure 7.6). Similar to the 3D and 2D models, the peak TF contact forces in the 1D model occur at 25 and 75 % stance periods. Calculated, in the 1D model, TF contact forces of 2 and 1.6 BW on the medial plateau and 1.6 and 0.8 BW on the lateral plateau at the first and second peaks, respectively, compared with the reported results of Winby et al. (2009); 2.5±0.52.5±0.5 and 1.9±0.31.9±0.3 BW on the medial and 1.5±0.51.5±0.5and 0.9±0.70.9±0.7 BW on the lateral plateau. It should be noted that results from the 1D model is very dependent in the position of the contact point (here, we have used values in accordance with Winby et al. (2009)). Taking different contact points on the frontal plane (Kumar et al. 2012; Lerner et al. 2015a; Manal and Buchanan 2013; Miller et al. 2015; Sandholm et al. 2011) can have significant effects on results of the 1D model (Lerner et al. 2015a). As compared to the reference 3D model, the use of 2D and 1D models reduces the mean or the peak (at 25 % stance) tibiofemoral force on the medial plateau by 34 and 42 % or 17 and 35 %, respectively. The mean differences on the lateral plateau were much greater at, respectively, 110 and 140 %.

In addition to foregoing concerns, musculoskeletal model studies of the trunk and lower extremity joints of human body commonly enforce the moment equilibrium equations at the origin of the joint coordinate system placed, for example, at the center of femoral epicondylar axis for the knee joint or the intervertebral disk center in the spinal column. Unknown muscle forces are subsequently estimated using the moment equations developed based on the assumption that this origin of axes coincides with the joint center of reaction known as the point where the (passive) joint reaction moments disappear. The estimated muscle forces and internal joint loads are hence markedly depend on the positioning of the origin of coordinate system and changes therein as demonstrated by earlier investigations (Li et al. 2006; Pierce and Li 2005; Zander et al. 2016). To obtain accurate results, the moment equilibrium equations should be

carried out about a point close enough to the knee center of reaction. But the position of this center of reaction is neither known a priori nor remains fixed as joint loads and motions vary that could further influence predictions of musculoskeletal model studies. This complexity is, however, taken into account in our hybrid model studies in which the knee joint is represented by a validated detailed FE model.

Our findings should be considered in the light of some limitations. All results and comparisons are based on a single model of a female cadaveric specimen (61.9 kg body mass). Though the input structural and material properties in the knee joint were taken from the literature and we have previously extensively validated this model with available in vitro and in vivo data, these properties could vary with age, sex and subjects. The musculature and input joint kinematics/kinetics were taken from the mean of male/female data reported in the literature. One is reminded that the current study focuses on the evaluation of the effect of various model assumptions when compared to our 3D model. For this purpose, identical gait data and musculoskeletal model plus FE knee model are used throughout. Alterations in these input data and models, though affecting the absolute estimations, are not expected to influence as much the relative findings and conclusions of this work. Antagonistic co-activity was not considered. The incompressible elastic response of soft tissues considered here is appropriate for the short-term loading present during gait.

In summary, individual or combined idealized considerations of the knee as a planar joint in the sagittal plane, of the joint with no passive resistance and of fixed centers of contact substantially alter muscle forces, ACL force, tibiofemoral contact forces, individual compartmental forces, contact pressures on cartilage and contact centers on each compartment. The detailed FE model of the entire knee joint combined with a MS model of the lower extremity (i.e., 3D model) yields the most accurate results (gold standard) by simultaneous considerations of synergies between both passive knee joint and active musculature as accurate as possible while driving the model by kinematics-kinetics of gait reported for normal subjects.

7.6 Acknowledgements

The current work is supported by a grant from the Natural Sciences and Engineering Research Council of Canada (NSERC). The partial scholarship of MUTAN-Tunisia to the first author is also gratefully acknowledged.

7.7 References

Adouni M, Shirazi-Adl A (2014b) Partitioning of knee joint internal forces in gait is dictated by the knee adduction angle and not by the knee adduction moment Journal of biomechanics 47:1696-1703

Adouni M, Shirazi-Adl A (2014a) Evaluation of knee joint muscle forces and tissue stresses-strains during gait in severe OA versus normal subjects Journal of Orthopaedic Research 32:69-78

Arnold EM, Ward SR, Lieber RL, Delp SL (2010) A model of the lower limb for analysis of human movement Annals of Biomedical Engineering 38:269-279

Astephen JL (2007) Biomechanical Factors in the Progression of Knee Osteoarthritis. Ph.D thesis. School of Biomedical Engineering, Dalhousie University, Halifax

Astephen JL, Deluzio KJ, Caldwell GE, Dunbar MJ (2008) Biomechanical changes at the hip, knee, and ankle joints during gait are associated with knee osteoarthritis severity Journal of Orthopaedic Research 26:332-341

Bendjaballah M, Shirazi-Adl A, Zukor D (1997) Finite element analysis of human knee joint in varus-valgus Clinical Biomechanics 12:139-148

Bendjaballah MZ, Shirazi-Adl A, Zukor D (1995) Biomechanics of the human knee joint in compression: reconstruction, mesh generation and finite element analysis The Knee 2:69-79

Blagojevic M, Jinks C, Jeffery A, Jordan K (2010) Risk factors for onset of osteoarthritis of the knee in older adults: a systematic review and meta-analysis Osteoarthritis and Cartilage 18:24-33

Bull AM, Kessler O, Alam M, Amis AA (2008) Changes in knee kinematics reflect the articular geometry after arthroplasty Clinical Orthopaedics and Related Research 466:2491-2499

De Leva P (1996) Adjustments to Zatsiorsky-Seluyanov's segment inertia parameters Journal of Biomechanics 29:1223-1230

Delp SL et al. (2007) OpenSim: open-source software to create and analyze dynamic simulations of movement Biomedical Engineering, IEEE Transactions on 54:1940-1950

Delp SL, Loan JP, Hoy MG, Zajac FE, Topp EL, Rosen JM (1990) An interactive graphics-based model of the lower extremity to study orthopaedic surgical procedures Biomedical Engineering, IEEE Transactions on 37:757-767

DeMers MS, Pal S, Delp SL (2014) Changes in tibiofemoral forces due to variations in muscle activity during walking Journal of Orthopaedic Research 32:769-776

Dumas R, Moissenet F, Gasparutto X, Cheze L (2012) Influence of joint models on lower-limb musculo-tendon forces and three-dimensional joint reaction forces during gait Proceedings of the Institution of Mechanical Engineers, Part H: Journal of Engineering in Medicine 226:146-160

Freeman M, Pinskerova V (2005) The movement of the normal tibio-femoral joint Journal of Biomechanics 38:197-208

Fregly BJ, Besier TF, Lloyd DG, Delp SL, Banks SA, Pandy MG, D'Lima DD (2012) Grand challenge competition to predict in vivo knee loads Journal of Orthopaedic Research 30:503-513

Gerus P et al. (2013) Subject-specific knee joint geometry improves predictions of medial tibiofemoral contact forces Journal of Biomechanics 46:2778-2786

Guilak F (2011) Biomechanical factors in osteoarthritis Best practice & research Clinical rheumatology 25:815-823

Horsman MK, Koopman H, Veeger H, van der Helm F (2007) The Twente Lower Extremity Model: a comparison of maximal isometric moment with the literature The Twente Lower Extremity Model:65

Hunt AE, M Smith R, Torode M, Keenan A-M (2001) Inter-segment foot motion and ground reaction forces over the stance phase of walking Clinical Biomechanics 16:592-600

Katz JN, Earp BE, Gomoll AH (2010) Surgical management of osteoarthritis Arthritis care & research 62:1220-1228

Kazemi M, Li L (2014) A viscoelastic poromechanical model of the knee joint in large compression Medical Engineering & Physics 36:998-1006

Kim HJ, Fernandez JW, Akbarshahi M, Walter JP, Fregly BJ, Pandy MG (2009) Evaluation of predicted knee-joint muscle forces during gait using an instrumented knee implant Journal of Orthopaedic Research 27:1326-1331

Kim S (2008) Changes in surgical loads and economic burden of hip and knee replacements in the US: 1997–2004 Arthritis Care & Research 59:481-488

Kumar D, Rudolph KS, Manal KT (2012) EMG-driven modeling approach to muscle force and joint load estimations: Case study in knee osteoarthritis Journal of Orthopaedic Research 30:377-383

Lerner ZF, Board WJ, Browning RC (2015b) Pediatric obesity and walking duration increase medial tibiofemoral compartment contact forces Journal of Orthopaedic Research

Lerner ZF, DeMers MS, Delp SL, Browning RC (2015a) How tibiofemoral alignment and contact locations affect predictions of medial and lateral tibiofemoral contact forces Journal of Biomechanics 48:644-650

Li G, DeFrate LE, Park SE, Gill TJ, Rubash HE (2005a) In Vivo Articular Cartilage Contact Kinematics of the Knee An Investigation Using Dual-Orthogonal Fluoroscopy and Magnetic Resonance Image–Based Computer Models The American Journal of Sports Medicine 33:102-107

Lloyd DG, Besier TF (2003) An EMG-driven musculoskeletal model to estimate muscle forces and knee joint moments in vivo Journal of Biomechanics 36:765-776

Losina E, Thornhill TS, Rome BN, Wright J, Katz JN (2012) The dramatic increase in total knee replacement utilization rates in the United States cannot be fully explained by growth in population size and the obesity epidemic J Bone Joint Surg Am 94:201-207

Manal K, Buchanan TS (2013) An electromyogram-driven musculoskeletal model of the knee to predict in vivo joint contact forces during normal and novel gait patterns Journal of Biomechanical Engineering 135:021014

Marouane H, Shirazi-Adl A, Adouni M (2015a) Knee joint passive stiffness and moment in sagittal and frontal planes markedly increase with compression Computer Methods in Biomechanics and Biomedical Engineering 18:339-350

Marouane H, Shirazi-Adl A, Adouni M (2015c) Alterations in knee contact forces and centers in stance phase of gait: A detailed lower extremity musculoskeletal model Journal of Biomechanics

Marouane H, Shirazi-Adl A, Adouni M, Hashemi J (2014) Steeper posterior tibial slope markedly increases ACL force in both active gait and passive knee joint under compression Journal of Biomechanics 47:1353-1359

Marouane H, Shirazi-Adl A, Hashemi J (2015b) Quantification of the role of tibial posterior slope in knee joint mechanics and ACL force in simulated gait Journal of Biomechanics

Mesfar W, Shirazi-Adl A (2005) Biomechanics of the knee joint in flexion under various quadriceps forces The Knee 12:424-434

Miller RH, Esterson AY, Shim JK (2015) Joint contact forces when minimizing the external knee adduction moment by gait modification: A computer simulation study The Knee

Mokhtarzadeh H, Perraton L, Fok L, Muñoz MA, Clark R, Pivonka P, Bryant AL (2014) A comparison of optimisation methods and knee joint degrees of freedom on muscle force predictions during single-leg hop landings Journal of Biomechanics 47:2863-2868

Mononen ME, Jurvelin JS, Korhonen RK (2015) Implementation of a gait cycle loading into healthy and meniscectomised knee joint models with fibril-reinforced articular cartilage Computer Methods in Biomechanics and Biomedical Engineering 18:141-152

Pena E, Calvo B, Martinez M, Doblare M (2006) A three-dimensional finite element analysis of the combined behavior of ligaments and menisci in the healthy human knee joint Journal of Biomechanics 39:1686-1701

Sandholm A, Schwartz C, Pronost N, de Zee M, Voigt M, Thalmann D (2011) Evaluation of a geometry-based knee joint compared to a planar knee joint The Visual Computer 27:161-171

Sartori M, Reggiani M, Farina D, Lloyd DG (2012) EMG-driven forward-dynamic estimation of muscle force and joint moment about multiple degrees of freedom in the human lower extremity PloS One 7:e52618

Shelburne K, Pandy M (1998) Determinants of cruciate-ligament loading during rehabilitation exercise Clinical Biomechanics 13:403-413

Shelburne KB, Pandy MG (1997) A musculoskeletal model of the knee for evaluating ligament forces during isometric contractions Journal of Biomechanics 30:163-176

Shelburne KB, Pandy MG (2002) A dynamic model of the knee and lower limb for simulating rising movements Computer Methods in Biomechanics & Biomedical Engineering 5:149-159

Shelburne KB, Pandy MG, Anderson FC, Torry MR (2004) Pattern of anterior cruciate ligament force in normal walking Journal of Biomechanics 37:797-805

Shelburne KB, Torry MR, Pandy MG (2006) Contributions of muscles, ligaments, and the ground-reaction force to tibiofemoral joint loading during normal gait Journal of Orthopaedic Research 24:1983-1990

Shirazi-Adl A, Moglo K (2005) Effect of changes in cruciate ligaments pretensions on knee joint laxity and ligament forces Computer methods in biomechanics and biomedical engineering 8:17-24

Steele KM, DeMers MS, Schwartz MH, Delp SL (2012) Compressive tibiofemoral force during crouch gait Gait & Posture 35:556-560

Taylor WR, Heller MO, Bergmann G, Duda GN (2004) Tibio-femoral loading during human gait and stair climbing Journal of Orthopaedic Research 22:625-632

Thelen DG, Anderson FC, Delp SL (2003) Generating dynamic simulations of movement using computed muscle control Journal of Biomechanics 36:321-328

Valente G, Pitto L, Stagni R, Taddei F (2015) Effect of lower-limb joint models on subject-specific musculoskeletal models and simulations of daily motor activities Journal of Biomechanics 48:4198-4205

Winby CR, Lloyd DG, Besier TF, Kirk TB (2009) Muscle and external load contribution to knee joint contact loads during normal gait Journal of Biomechanics 42:2294-2300

Xiao M, Higginson JS (2008) Muscle function may depend on model selection in forward simulation of normal walking Journal of Biomechanics 41:3236-3242

Yang N, Canavan P, Nayeb-Hashemi H, Najafi B, Vaziri A (2010a) Protocol for constructing subject-specific biomechanical models of knee joint Computer Methods in Biomechanics and Biomedical Engineering 13:589-603

Table 7.4: Predicted total compartmental contact forces (CF) on the medial (M) and lateral (L) plateaus in 2D and 3D models.

	0%		5%			25%		50%		75%			100%	
	3D	2D	3D	2D	2.5	3D	2D	3D	2D	3D	2D	2.5	3D	2D
L	495	325	1598	813	1022	628	272	116	465	488	845	355	0	131
M	210	202	444	460	287	1936	1602	1021	393	1828	1199	1927	792	62

Table 7.5: Predicted axial component of total contact forces on the medial (M) and lateral (L) plateaus when using idealized 1D model versus 2D model (same as in Table 7.1 except in the axial direction).

	0%		5%		25%		50%		75%		100%	
	2D	1D	2D	1D	2D	1D	2D	1D	2D	1D	2D	1D
L	242	19	607	87	218	966	414	526	758	480	104	0
M	160	103	357	319	1569	1217	376	504	1171	1006	49	147
M	160	103	357	319	1569	1217	376	504	1171	1006	49	147

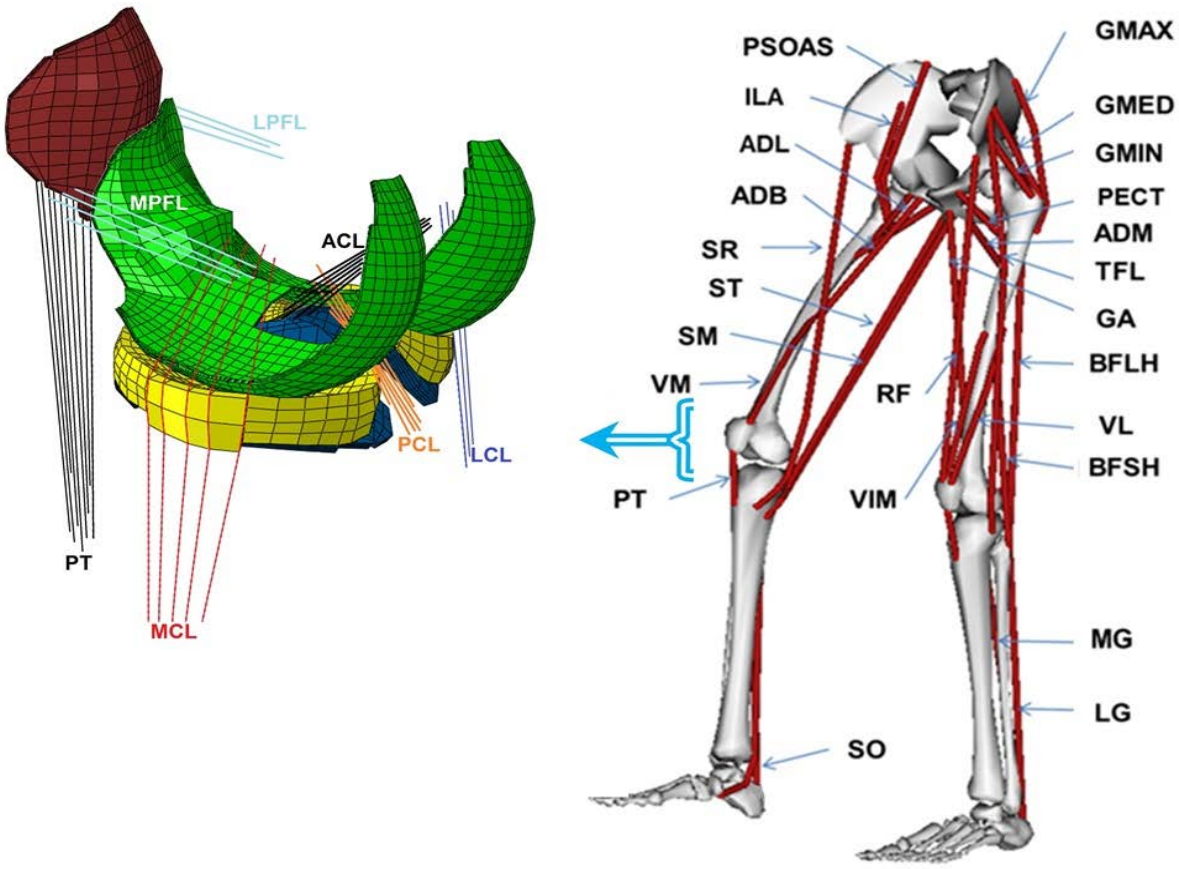

Figure 7.1: **(a)** Knee FE model; tibiofemoral (TF) and patellofemoral (PF) cartilage layers, menisci, patellar Tendon (PT). Joint ligaments include lateral patellofemoral (LPFL), medial patellofemoral (MPFL), anterior cruciate (ACL), posterior cruciate (PCL), lateral collateral (LCL) and medial collateral (MCL). **(b)** Schematic diagram showing the 34 muscles incorporated into the lower extremity model (Open Sim, Delp et al., [120]2007). Quadriceps components are vastus medialis obliqus (VMO), rectus femoris (RF), vastus intermidus medialis (VIM) and vastus lateralis (VL). Hamstrings components include biceps femoris long head (BFLH), biceps femoris short head (BFSH), semi membranous (SM) and TRIPOD made of sartorius (SR), gracilis (GA) and semitendinosus (ST). Gastrocnemius components are gastrocnemius medial (GM) and gastrocnemius lateral (GL). Soleus (SO) muscle is uni-articular ankle muscle. Hip joint muscles (not all shown) include adductor, long (ADL), mag (3 components ADM) and brev (ADB); gluteus max (3 components GMAX), med (3 components GMED) and min (3 components GMIN), iliacus (ILA), iliopsoas (PSOAS), quadriceps femoris; pectineus (PECT), tensor facia lata (TFL), periformis.

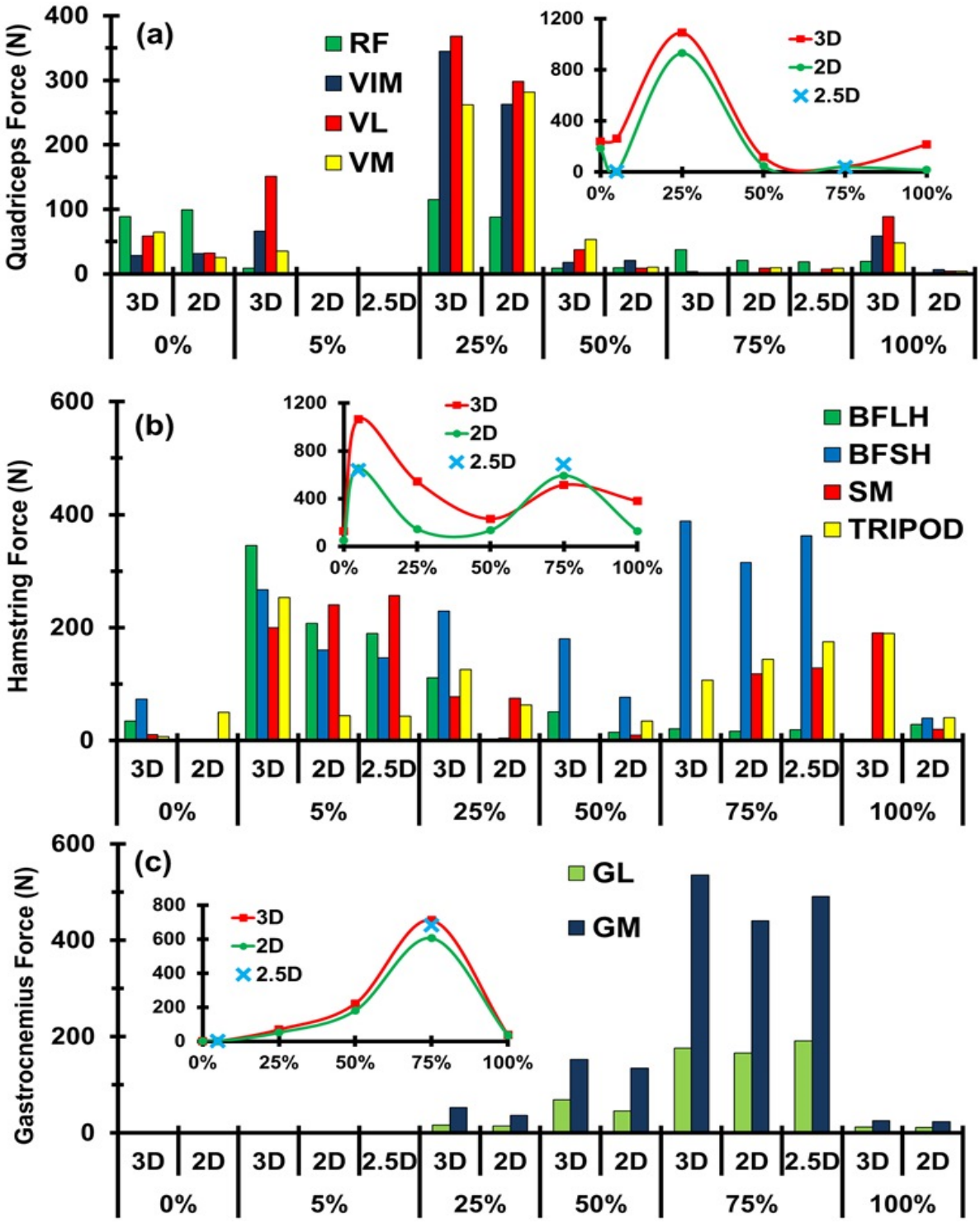

Figure 7.2: Predicted (a) quadriceps, (b) hamstrings and (c) gastrocnemius muscle forces (see Fig. 1 caption for muscle abbreviations) at various periods of stance in the 3D reference, 2.5D and 2D models. Inlay figures compare the vector sum of muscle forces in each group between these models.

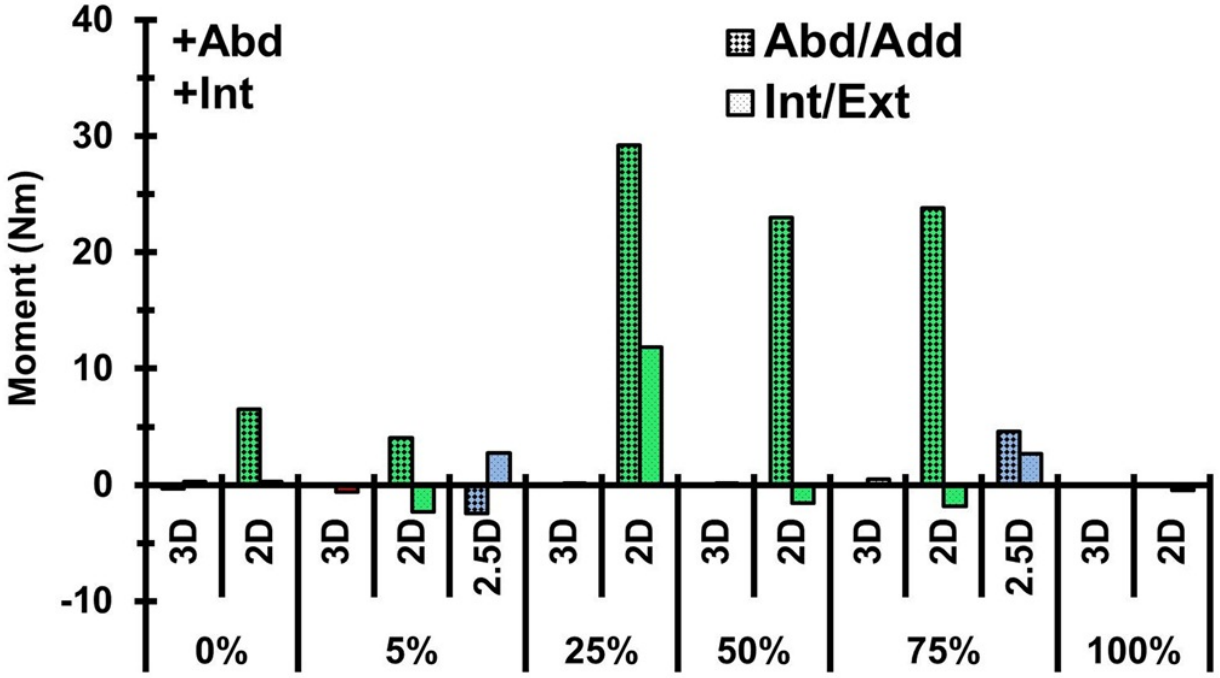

Figure 7.2: Neglected unbalanced abduction/adduction and internal/external resistance moments computed at various periods of stance in all models. The 2.5D model was analyzed only at 5% and 75% periods.

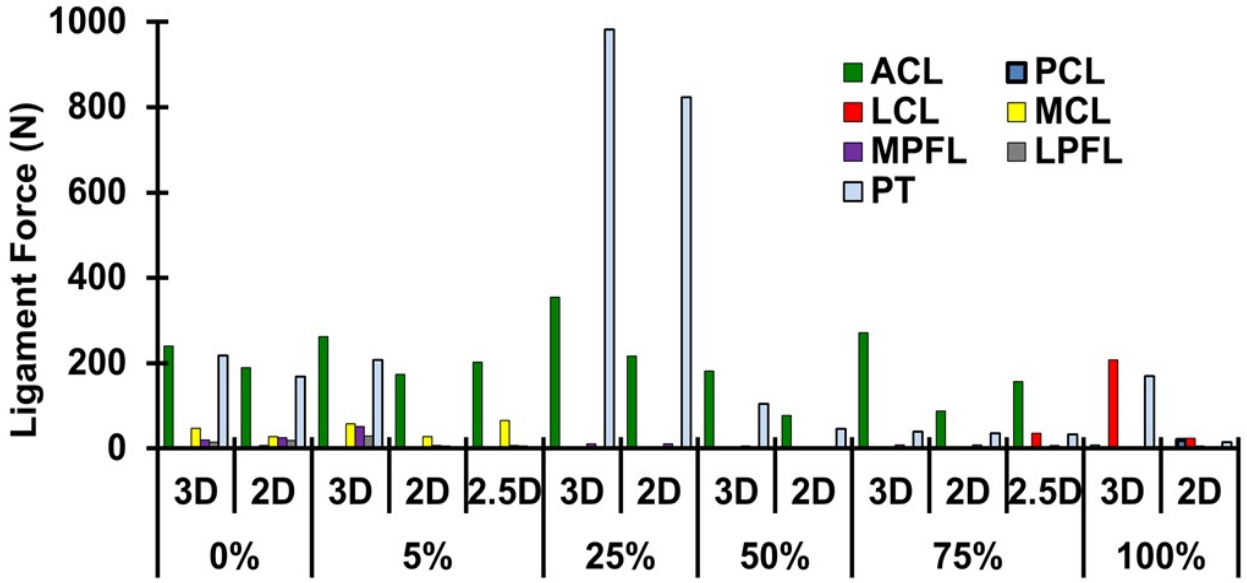

Figure 7.3: Total forces in various knee joint ligaments at various periods of stance in all models. The 2.5D model was analyzed only at 5% and 75% periods.

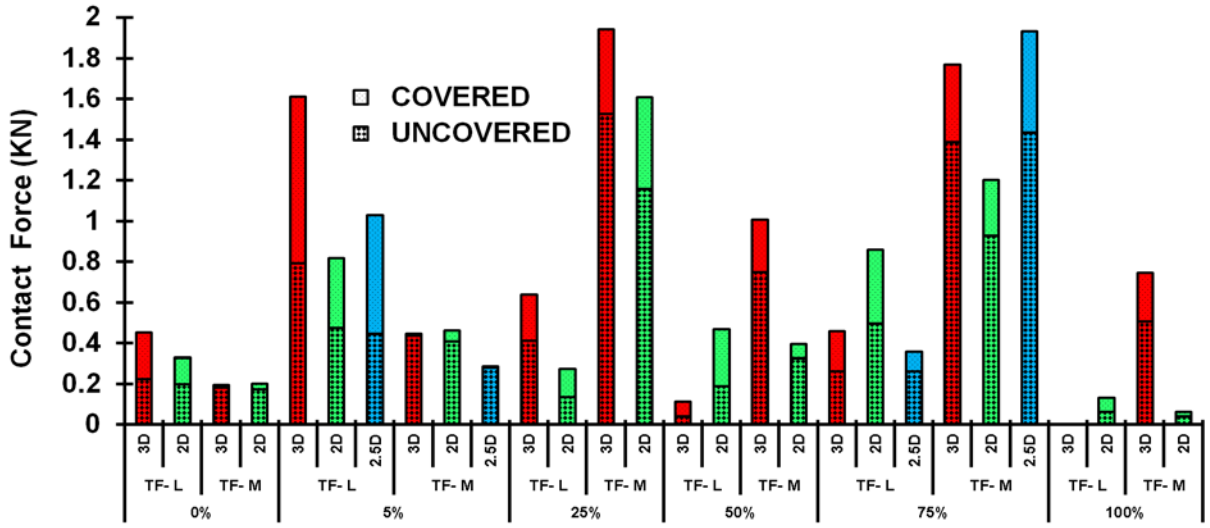

Figure 7.4: Total contact forces on tibiofemoral medial (M) and lateral (L) plateaus at covered (via menisci) and uncovered (via cartilage-cartilage) areas at various periods of stance in all models. The 2.5D model was analyzed only at 5% and 75% periods.

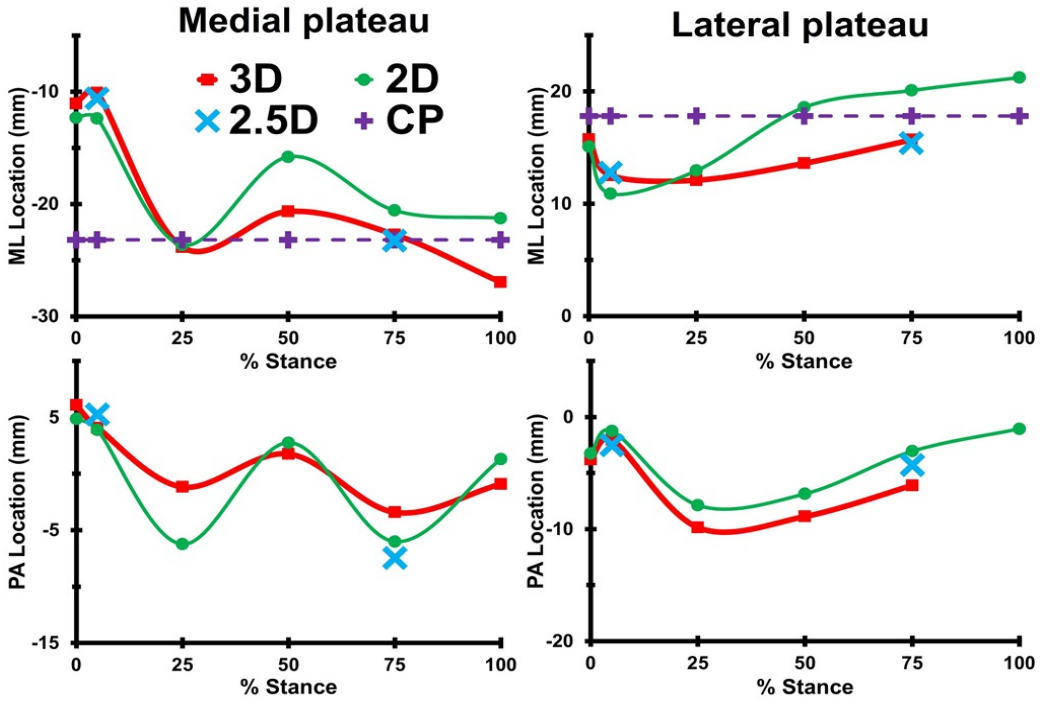

Figure 7.5: Posteroanterior (PA) and mediolateral (ML) locations of the estimated contact centers on the medial and lateral tibial plateaus at different stance periods in the 3D reference, 2.5D and 2D models. Lateral and anterior directions are positive here. The 2.5D model was analyzed only at 5% and 75% periods.

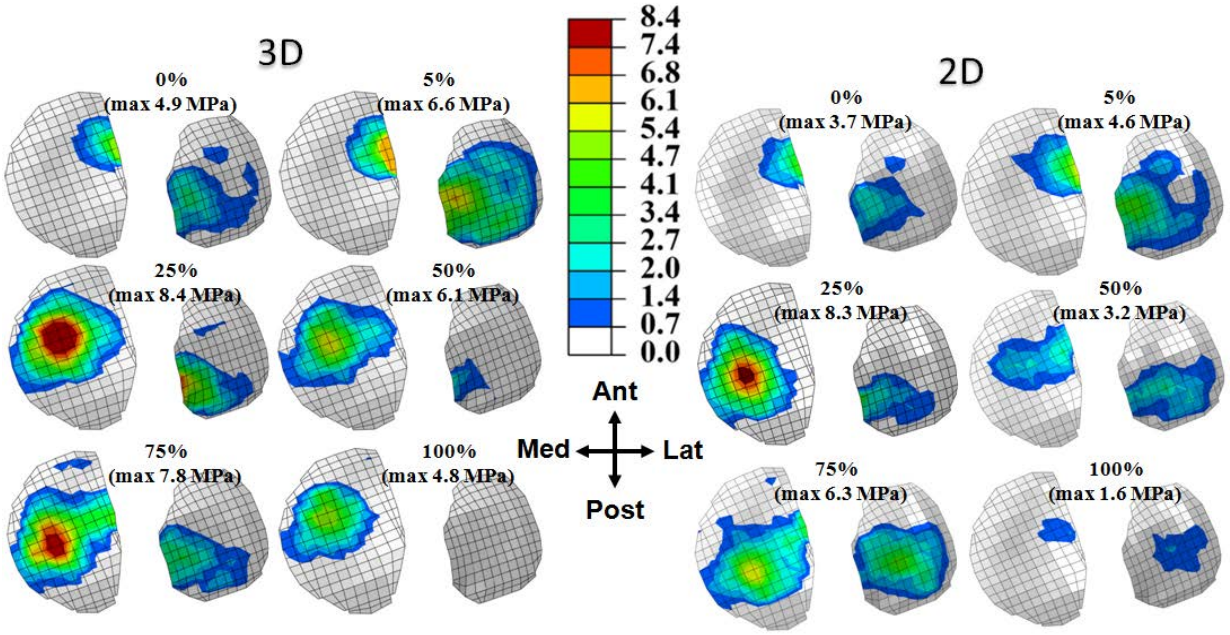

Figure 7.6: Predicted contact pressure distributions at articular surfaces of tibial plateaus at different stance periods in gait in the 3D reference and 2D models. Note that a common legend (in MPa) is used for ease in comparisons.

CHAPITRE 8 ARTICLE 5: MEDIAL-LATERAL LOAD DISTRIBUTION IN THE KNEE JOINT IS INFLUENCED BY CHANGES IN THE ADDUCTION ROTATION AND NOT IN THE ADDUCTION MOMENT

H. Marouane and A. Shirazi-Adl

Article submitted to

Biomechanics and Modeling in Mechanobiology December 2016

8.1 Abstract

Osteoarthritis (OA) of the knee joint is a common disease accompanied by pain and impaired mobility. Despite recent concerns on the lack of correlation between the medial load and the knee adduction moment (KAM), KAM is commonly considered as a surrogate measure of medial load and hence a marker where its reduction is the focus of preventive and treatment interventions. Using a lower extremity hybrid musculoskeletal model driven by gait kinematics-kinetics, we compute here, over the entire stance phase of gait, the relative effects of measured changes in the knee adduction rotation (KAR) by one standard deviation (SD) versus measured changes in KAM (also by one SD) on the knee joint response in general and medial/lateral load partitioning in particular.

As KAR increased (at constant KAM), so did the passive moment resistance of the knee joint which as a result substantially reduced forces in lateral hamstrings while increasing those in medial hamstrings. At 25/75% stance as two highly loaded periods of gait, the drop in KAR (from +SD to –SD while at constant KAM) drastically reduced the medial contact force by 44/30% and the medial over lateral contact load and area ratios by 92/79% and 64/51%, respectively. In contrast, the equivalent decrease in KAM (at constant KAR) had little effects (<7%) showing no sensitivity to changes in KAM alone. These findings clearly indicate a poor correlation between KAM and tibiofemoral load distribution suggesting instead that KAR should be the focus as the primary measure of knee joint load partitioning and associated prevention and treatment interventions.

Keywords: Musculoskeletal model; Finite element; Contact force; Adduction moment; Gait; Adduction rotation; Knee joint biomechanics

8.2 Introduction

Human knee joints experience loads and movements of substantial magnitudes during occupational, recreational and even regular daily living activities (Kutzner et al. 2010). This demanding mechanical environment exposes them to a host of painful and debilitating deformities, injuries and degenerations involving both patellofemoral (PF) and tibiofemoral (TF) articulations. Osteoarthritis (OA) is one of the most prevalent musculoskeletal disorders affecting approximately 27 million adults in the US alone (Lawrence et al. 2008) that is projected to further increase to 67 million by 2030 (Hootman and Helmick 2006). Incidence of knee OA, especially on the medial side that is often subject to a larger share of joint internal compression during gait (Adouni and Shirazi-Adl 2014a; Zhao et al. 2007b), rises hence at a marked rate hand in hand with ageing and obesity in general population (Harding et al. 2016; Hubertsson et al. 2012).

Knee adduction moment (KAM) as the net external knee joint torque in the frontal plane is commonly considered as a surrogate measure of loading on the medial compartment (Andriacchi and Mündermann 2006) and hence a marker where its reduction is the focus of interventions (e.g., orthoses, shoe insoles, gait modification, osteotomy, knee brace) to prevent the development and progression of medial OA (Gaasbeek et al. 2007; Simic et al. 2011). However, some recent in vivo studies using instrumented implants have questioned such association and qualified the correlation between KAM and the medial compartment load as poor to average (Meyer et al. 2013; Walter et al. 2010). Similarly, questions have been raised on the efficacy in reducing pain and symptoms of a reduction in KAM when wearing wedged insoles (Bennell et al. 2011; Jones et al. 2014) and braces (Gaasbeek et al. 2007).

Varus malalignment has however been identified as a significant risk factor in medial knee OA (Brouwer et al. 2007; Sharma et al. 2001; Tanamas et al. 2009; Zhao et al. 2007b). Peak knee varus angle was found at 4.8 ±6.1° in 44 patients with severe knee osteoarthritis as compared to 2.9 ±4.0° in 40 asymptomatic control subjects (Sosdian et al. 2016). Valgus high tibial osteotomy reduces the pain and progression of medial OA in patients (Huizinga et al. 2016). In vivo measurements show differences in the medial load of roughly one body weight (BW) between individuals with alignments of 4.5° abduction and 6.5° adduction (Trepczynski et al. 2014) and a significant correlation between the frontal plane alignment and the medial loading during early stance (Kutzner et al. 2013). Musculoskeletal model studies in gait have estimated

an alteration of ~51 N in peak medial force for each 1o change in the joint frontal alignment (Lerner et al. 2015). In a hybrid lower extremity model at mid-stance, a 1.5o drop in adduction angle was found much more effective in diminishing medial contact force and medial over lateral load ratio than a 50% reduction in KAM (Adouni and Shirazi-Adl 2014b).

Despite the foregoing sensitivity in the TF load partitioning to changes in the joint rotation and alignment in the frontal plane, there are major concerns regarding the relative accuracy in skin-marker based measurements of the adduction-abduction rotations (Gorton et al. 2009; Park et al. 2016). Mean errors of up to 4.4° in the adduction rotation are reported in gait when comparing skin markers versus intra-cortical pins (Benoit et al. 2006). The extent of such errors have also encouraged many researchers to consider the knee joint as a 2D structure while overlooking the crucial out-of-sagittal plane rotations and moment equilibria (Marouane et al. 2016a).

Using a lower extremity hybrid musculoskeletal model (Marouane et al. 2016b) driven by gait kinematics-kinetics (Astephen 2007; Hunt et al. 2001), we aim here to compute, over the entire stance phase of gait, the effects of changes in the measured knee adduction rotation (KAR) (by one standard deviation: ±SD) versus respective changes in measured KAM (also by one SD) (Astephen et al. 2014) on the knee joint response in general and medial/lateral load partitioning in particular. In accordance with earlier results, we hypothesize that the internal load distribution is influenced primarily by changes in KAR as compared to KAM. Such notion has important consequences in measurements as well as prevention, treatment, rehabilitation and evaluation of associated joint disorders.

8.3 Methods

8.3.1 Hybrid Musculoskeletal Model

A validated 3D FE model of the entire knee joint (Fig. 8.1) consisting of bony structures (tibia, femur and patella) and their compliant articular cartilage layers as well as menisci, major tibiofemoral (TF: ACL, PCL, CL, MCL) and patellofemoral (PF: MPFL, LPFL) ligaments, patellar tendon (PT), quadriceps (four components), hamstrings (six components) and gastrocnemius (two components) is employed (Adouni and Shirazi-Adl 2014a; Marouane et al. 2015b). This detailed knee model has been introduced within a musculoskeletal model of the

lower extremity including hip and ankle joints and associated uni- and bi-articular muscles (Fig. 8.1) to simulate the stance phase of gait under in vivo kinematics/kinetics reported for asymptomatic subjects (Astephen 2007; Hunt et al. 2001).

Bony structures are simulated as rigid bodies (Haut Donahue and Hull 2002) while the articular cartilage layers and menisci are represented as non-homogeneous nonlinear depth-dependent composites of collagen fibril networks and isotropic hyperelastic matrices. Ligaments are simulated by a number of nonlinear axial elements with initial pre-strains, non-linear (tension-only) material properties, and initial cross-sectional areas of 42, 60, 18, 25, 99, 42.7, and 28.5mm^2 respectively for ACL, PCL, LCL, MCL, PT, MPFL, and LPFL (Mesfar and Shirazi-Adl 2005).

8.3.2 Loading and Boundary Conditions

The femur is initially fixed in its instantaneous position recorded in gait while the tibia and patella are completely free except for the three prescribed TF rotations. Following application of initial prestrains in knee joint ligaments, the mean values of hip/knee/ankle rotations/moments and ground reaction forces (GRF) reported at each period of stance phase (HS 0%, 5%, 25%, 50%, 75% and TO 100%) (Astephen 2007; Hunt et al. 2001) are applied and iterative nonlinear analyses carried out till convergence (see section below). The location of GRF at each period is determined so as to generate reported knee joint moments accounting for the leg/foot weights (29.78/7.98 N). Since our model is constructed based on a female knee, a body weight of BW = 61.9 kg is considered (De Leva 1996). To investigate the effect of changes in KAR and KAM on results, analyses are repeated under identical kinematics and kinetics except that KAR or KAM is altered one at a time at each stance period by one standard deviation (±SD) based on reported measurements (Astephen et al. 2014). These changes cover most of datasets reported in the literature (Fig. 8.2) and hence the likely errors in measurements (Benoit et al. 2006; Leigh et al. 2014).

8.3.3 Muscle Force Estimation

Muscle forces are evaluated iteratively and applied as additional external forces along with ground reaction forces, leg/foot weights and in vivo kinematics/kinetics recorded on asymptomatic subjects (Astephen 2007; Astephen et al. 2014; Hunt et al. 2001) at each stance

period of gait. Static optimization along with a cost function of the sum of cubed stresses of all muscles, subject to reaction moment equilibrium equations (3 at the hip taken as a spherical joint, 3 at the knee simulated in details with validated passive properties and 1 at the ankle), and inequality equations on muscle forces, are used to iteratively estimate muscle forces at each instance. Details of the muscle force estimation are provided elsewhere (Adouni and Shirazi-Adl 2014a; Marouane et al. 2015b). The nonlinear elastostatic analyses are carried out using ABAQUS (version 6.12, Simulia, Inc., Providence, RI, USA) finite element package program. Matlab (R2013a Optimization Toolbox, genetic algorithms and Fmincon) was used in the optimization algorithm.

8.4 Results

Forces in hamstrings altered substantially as KAR varied by ±SD. Overall, larger KAR markedly increased forces in medial hamstrings but reduced those in lateral hamstrings at all periods of stance. Variations were, however, more pronounced in lateral hamstrings than in medial hamstrings (Fig. 8.3b). At 25% period, BFLH and BFSH decreased by 145N and 300N, respectively, when increasing KAR by -SD to +SD (Fig. 8.3b). Quadriceps forces also, though to a smaller degree, decreased with greater KAR (Fig. 8.3a). The effects were overall much less pronounced when KAM was altered by ±SD (Fig. 8.4).

Total force in ACL altered most at 25% stance reaching the peak of 418N at minimum KAR (Fig. 8.5a). It however increased with KAR at 75% stance. LCL force increased with KAR and reached its peak of ~469N at TO (100% period) under larger adduction rotation. Smaller changes were computed as KAM altered (Fig. 8.5b). Total force in PT closely followed activity levels in quadriceps muscles (Figs 8.3 and 8.4); it was much greater at 25% stance when compared to other periods and reached the peak of 1056 N under smaller KAR (R-SD).

Alterations in KAR, unlike KAM, had substantial effects on compartmental loads (Fig. 8.6a) and medial/lateral load partitioning ratio (Fig. 8.7); an increase in KAR drastically increased this ratio by substantially augmenting the load on the medial compartment while at the same time reducing that on the opposite lateral comportment (even to nil at 100%). Reverse trends were found when KAR decreased. Changes in KAM had however negligible effects (Figs 8.6b and 8.7). Contact areas on TF (Table 8.1) and PF joints followed nearly the same trends as their respective contact forces; lateral contact area substantially increased at lower KAR but

dropped at higher KAR to the extent that it even totally disappeared at the toe off (i.e., separation with no contact). Medial contact area followed reverse trends at early and late stance (0, 5 and 100%) with little changes at and around mid-stance (25-75%). TF contact pressures (Fig. 8.8) also followed similar trends as those in their respective contact forces (Fig. 8.6); peak contact pressures occurred on the medial side under larger KAR. The effect on contact stresses of changes in KAR was again much more pronounced when compared with changes in KAM (Fig. 8.8).

8.5 Discussion

Using a hybrid lower extremity musculoskeletal model including a detailed complex 3D FE model of the entire knee joint (Marouane et al. 2016a; Marouane et al. 2016b) driven by in vivo joint kinematics-kinetics recorded in gait of normal subjects (Astephen 2007; Hunt et al. 2001), we aimed here to quantify the effects of changes in measured KAR (by one standard deviation: ±SD) versus changes in measured KAM (±SD) (Astephen et al. 2014) on the knee joint response in general and medial-lateral load partitioning in particular. Computed results clearly support our hypothesis that, despite equivalent variations in prescribed adduction-abduction rotations (KAR) and moments (KAM) by one ±SD, the internal load distribution in the knee joint is influenced primarily by changes in KAR (or in the knee alignment in the frontal plane) with little sensitivity to changes in KAM.

At identical externally applied KAM, changes in KAR substantially altered forces in medial and lateral hamstrings; forces in lateral hamstrings markedly decreased at all stance periods with maximums of 145N in BFLH and 300N in BFSH when KAR increased from 2.38° valgus to 3.63° varus at 25% stance period. At the same time and with decreases in lateral hamstrings, forces in medial hamstrings followed opposite trends and increased (Fig. 8.3b). These trends are expected to continue under greater alterations in KAR. Foregoing concurrent opposite changes in hamstrings activation levels (demonstrating smaller adduction moment resistance by muscles) despite identical external KAM are due to the substantial increase in the knee joint passive resistant adduction moment at greater KAR. The knee passive structures play an important role in the joint equilibrium in the frontal plane (Lloyd and Buchanan 2001) especially at greater joint compression forces expected in gait (Marouane et al. 2015a). At full extension position, Marouane et al. (2015a) reported an increase of 20 Nm in the knee passive

adduction resistant moment when the adduction rotation rose only by ~1.2° under 1800N axial compression force. In contrast and at constant KAR, reverse changes though at much smaller magnitudes were overall noted when KAM increased (Fig. 8.4).

Forces in the joint ligaments altered with changes in KAM and KAR at different stance periods (Fig. 8.5). Though not resisting force at all stance periods, forces in LCL and MCL followed reverse trends; the former increased at larger KAR and KAM especially at the toe-off (100%) whereas the latter decreased at greater KAR in early stance. Changes in ACL force was less consistent; ACL reached its peak force under smaller KAR and KAM at 25% stance (Fig. 8.5).

As KAR increased within one standard deviation (from –SD to +SD) at constant KAM (Fig. 8.6a), the medial contact forces substantially increased whereas the lateral ones diminished. This occurred consistently at all stance periods, from HS (0%) to TO (100%), to the extent that the medial load in contrast to the reference condition exceeded the lateral one even at early stance periods (0% and 5%) and that the lateral plateau was completely unloaded at TO (100%). The medial over lateral contact force ratio substantially increased at greater adduction rotations and reached its extremes (minimum-maximum) values of 0.1-2.4, 0.2-1.2, 0.8-10.6, 1.7-90, 1.3-6.4 and 0.7-∞ (infinity) under min-max KAR values as the stance period progressed from HS to TO (Fig. 8.7). On the other hand and in clear contrast, as KAM increased at constant KAR (Fig. 8.6b & Table 8.1), much smaller and less consistent variations were found. These results clearly highlight the importance of KAR in dictating the load partitioning among the medial and lateral compartments of the knee joint. To reduce contact loads on the medial side, one should hence control the knee alignment through adduction-abduction rotations. Results indicate that a more uniform (i.e., balanced) contact load distribution between TF plateaus (ratios of ~1 in Fig. 8.7) can only be achieved, when compared to our reference rotations, at larger adduction rotations in early stance (0% and 5%) whereas at smaller adduction rotations thereafter in stance (25-100%). The effect of changes in KAM is far less pronounced in this respect.

At 25/75% stance as two highly loaded periods of gait, the drop in KAR (from +SD to –SD) reduced the medial contact force by 44/30% and the medial over lateral load and contact area ratios by 92/79% and 64/51%, respectively. In contrast, the equivalent decrease in KAM reduced those same measures at much smaller relative values by 7/-2%, 5/6% and -1/1%, respectively

(negative signs denote increases). Our results are in accordance with previous findings (Tetsworth and Paley 1994; Wong et al. 2011). Wong et al. (2011) reported that 3 to 5° of increased tibial varus alignment result in a 50 % increase in the force transmitted across the medial tibiofemoral compartment. Tetsworth and Paley (1994) reported a 20% increase in the medial compartment load with a 5° increase in varus alignment. Lerner et al. (2015) estimated an increase of 51 N in the peak medial contact force for each 1o rise in TF varus alignment. Our results, however, show more drastic changes with averaged increases of ~168N and 201N for each 1° increase in KAR at the first (25%) and second (75%) peaks, respectively. This difference might partly be due to the assumed fixed contact point algorithm used in Lerner et al. (2015) since according to our previous study (Marouane et al. 2016a) contact forces are sensitive to the location of contact points in the frontal plane. Such increases in the medial compartment load substantially augment stresses on articular cartilage (Fig. 8.8) and hence the risk to degenerative changes.

In accordance with the popular trend, numerous studies have focused on KAM and changes therein as a primary measure of loading on the knee medial plateau. External KAM has routinely been considered as a surrogate measure to estimate and control TF joint internal load distribution (Gaasbeek et al. 2007; Shakoor and Block 2006; Zhao et al. 2007b) and as a marker for the medial OA (Andriacchi 2013; Shelburne et al. 2008). Some findings however indicate no such effects (Hewett et al. 1998; Lindenfeld et al. 1997; Meyer et al. 2013). In corroboration with our current predictions, Meyer et al. (2013) and Walter et al. (2010), using instrumented implants, have questioned an association between KAM and medial-lateral load partitioning. Despite the expected drop in KAM when using lateral wedged footwear (Jones et al. 2014; Russell and Hamill 2011), reduction in pain and medial share of contact forces have remained less consistent (Hewett et al. 1998; Pollo et al. 2002).

Our study is unique in that it estimates for the first time the effect of reported changes during gait (by ±SD) in KAM and KAR on the joint medial-lateral load distribution during the entire stance phase of gait. The interpretations should, however, be made in the light of some limitations. We used a single knee geometry reconstructed from a female cadaveric specimen. Though the input structural and material properties in the knee joint are taken from the literature and could vary with age, sex and body weight, we have extensively validated this model with available in vitro and in vivo data (Adouni and Shirazi-Adl 2014a; Marouane et al. 2015a; Moglo

and Shirazi-Adl 2005; Shirazi et al. 2008). The lower extremity musculature as well as joint kinematics-kinetics were taken from the data in the literature. Antagonistic co-activity was not considered. The incompressible elastic response of soft tissues considered here is appropriate for short-term loading present during gait. Finally, limitations could affect the absolute magnitudes of predictions though the relative effects and conclusions as KAR and KAM vary are expected to remain valid.

In summary, results of the present study clearly demonstrate that the relative inter-compartmental partitioning of contact loads is substantially influenced by changes in KAR but remains hardly sensitive to alterations in KAM. These findings explain the poor correlation between KAM and TF compartment loading during gait suggesting that the internal load partitioning is dictated by changes in KAR. As a consequence and for effective assessments of various prevention and treatment managements, the present findings emphasize the importance of recording KAR and tibiofemoral alignment and changes therein in various interventions that aim to control the knee joint load distribution.

8.6 Acknowledgements

The current work was supported by a grant from the Natural Sciences and Engineering Research Council of Canada (NSERC). The partial scholarship of MUTAN-Tunisia to the first author is also gratefully acknowledged.

8.7 References

Adouni M, Shirazi-Adl A (2014b) Partitioning of knee joint internal forces in gait is dictated by the knee adduction angle and not by the knee adduction moment Journal of biomechanics 47:1696-1703

Adouni M, Shirazi-Adl A (2014a) Evaluation of knee joint muscle forces and tissue stresses-strains during gait in severe OA versus normal subjects Journal of Orthopaedic Research 32:69-78

Andriacchi TP (2013) Editorial: Valgus alignment and lateral compartment knee osteoarthritis: A biomechanical paradox or new insight into knee osteoarthritis? Arthritis & Rheumatism 65:310-313

Andriacchi TP, Mündermann A (2006) The role of ambulatory mechanics in the initiation and progression of knee osteoarthritis Current opinion in rheumatology 18:514-518

Astephen JL (2007) Biomechanical Factors in the Progression of Knee Osteoarthritis. Ph.D, School of Biomedical Engineering, Dalhousie University, Halifax.

Astephen JLW, Dunbar MJ, Hubley-Kozey CL (2014) Knee joint biomechanics and neuromuscular control during gait before and after total knee arthroplasty are sex-specific The Journal of arthroplasty 30:118-125

Bennell KL et al. (2011) Lateral wedge shoe insoles for medial knee osteoarthritis: a 12-month randomised controlled trial Journal of Foot and Ankle Research 4:1

Benoit DL, Ramsey DK, Lamontagne M, Xu L, Wretenberg P, Renström P (2006) Effect of skin movement artifact on knee kinematics during gait and cutting motions measured in vivo Gait & posture 24:152-164

Brouwer G et al. (2007) Association between valgus and varus alignment and the development and progression of radiographic osteoarthritis of the knee Arthritis & Rheumatism 56:1204-1211

Bulgheroni P, Bulgheroni M, Andrini L, Guffanti P, Giughello A (1997) Gait patterns after anterior cruciate ligament reconstruction Knee Surgery, Sports Traumatology, Arthroscopy 5:14-21

De Leva P (1996) Adjustments to Zatsiorsky-Seluyanov's segment inertia parameters Journal of Biomechanics 29:1223-1230

Delp SL et al. (2007) OpenSim: open-source software to create and analyze dynamic simulations of movement Biomedical Engineering, IEEE Transactions on 54:1940-1950

Gaasbeek RD, Groen BE, Hampsink B, Van Heerwaarden RJ, Duysens J (2007) Valgus bracing in patients with medial compartment osteoarthritis of the knee: a gait analysis study of a new brace Gait & posture 26:3-10

Gao B, Zheng NN (2010) Alterations in three-dimensional joint kinematics of anterior cruciate ligament-deficient and-reconstructed knees during walking Clinical Biomechanics 25:222-229

Geoffrey KS, Franz JR, Dicharry J, Della Croce U, Kerrigan DC (2011) Lower limb joint kinetics in walking: the role of industry recommended footwear Gait & posture 33:350-355

Gorton GE, Hebert DA, Gannotti ME (2009) Assessment of the kinematic variability among 12 motion analysis laboratories Gait & posture 29:398-402

Harding GT, Dunbar MJ, Hubley-Kozey CL, Stanish WD, Wilson JLA (2016) Obesity is associated with higher absolute tibiofemoral contact and muscle forces during gait with and without knee osteoarthritis Clinical Biomechanics 31:79-86

Haut Donahue TL, Hull M (2002) A finite element model of the human knee joint for the study of tibio-femoral contact Journal of Biomechanical Engineering 124:273

Hewett TE, Noyes FR, Barber-Westin SD, Hedcmann TP (1998) Decrease in knee joint pain and increase in function in patients with medial compartment arthrosis: a prospective analysis of valgus bracing Orthopedics 21:131-138

Hootman JM, Helmick CG (2006) Projections of US prevalence of arthritis and associated activity limitations Arthritis & Rheumatism 54:226-229

Hubertsson J, Petersson IF, Thorstensson CA, Englund M (2012) Risk of sick leave and disability pension in working-age women and men with knee osteoarthritis Annals of the rheumatic diseases:annrheumdis-2012-201472

Huizinga M, Gorter J, Demmer A, Bierma-Zeinstra S, Brouwer R (2016) Progression of medial compartmental osteoarthritis 2–8 years after lateral closing-wedge high tibial osteotomy Knee Surgery, Sports Traumatology, Arthroscopy:1-8

Hunt AE, Smith RM, Torode M, Keenan A-M (2001) Inter-segment foot motion and ground reaction forces over the stance phase of walking Clinical Biomechanics 16:592-600

Jones RK, Chapman GJ, Forsythe L, Parkes MJ, Felson DT (2014) The relationship between reductions in knee loading and immediate pain response whilst wearing lateral wedged insoles in knee osteoarthritis Journal of Orthopaedic Research 32:1147-1154

Kadaba MP, Ramakrishnan H, Wootten M (1990) Measurement of lower extremity kinematics during level walking Journal of orthopaedic research 8:383-392

Kozanek M, Hosseini A, Liu F, Van de Velde SK, Gill TJ, Rubash HE, Li G (2009) Tibiofemoral kinematics and condylar motion during the stance phase of gait Journal of biomechanics 42:1877-1884

Kutzner I et al. (2010) Loading of the knee joint during activities of daily living measured in vivo in five subjects Journal of biomechanics 43:2164-2173

Kutzner I, Trepczynski A, Heller MO, Bergmann G (2013) Knee adduction moment and medial contact force–facts about their correlation during gait PloS one 8:e81036

Lawrence RC et al. (2008) Estimates of the prevalence of arthritis and other rheumatic conditions in the United States: Part II Arthritis & Rheumatism 58:26-35

Leigh RJ, Pohl MB, Ferber R (2014) Does tester experience influence the reliability with which 3D gait kinematics are collected in healthy adults? Physical Therapy in Sport 15:112-116

Lerner ZF, DeMers MS, Delp SL, Browning RC (2015) How tibiofemoral alignment and contact locations affect predictions of medial and lateral tibiofemoral contact forces Journal of biomechanics 48:644-650

Lindenfeld TN, Hewett TE, Andriacchi TP (1997) Joint loading with valgus bracing in patients with varus gonarthrosis Clinical orthopaedics and related research 344:290-297

Lloyd DG, Buchanan TS (2001) Strategies of muscular support of varus and valgus isometric loads at the human knee Journal of biomechanics 34:1257-1267

Marouane H, Shirazi-Adl A, Adouni M (2015a) Knee joint passive stiffness and moment in sagittal and frontal planes markedly increase with compression Computer Methods in Biomechanics and Biomedical Engineering 18:339-350

Marouane H, Shirazi-Adl A, Adouni M (2016a) 3D Active-Passive Response of Human Knee Joint in Gait is Markedly Altered When Simulated as a Planar 2D Joint Biomechanics and Modeling in Mechanobiology:1-11

Marouane H, Shirazi-Adl A, Adouni M (2016b) Alterations in knee contact forces and centers in stance phase of gait: A detailed lower extremity musculoskeletal model Journal of biomechanics 49:185-192

Marouane H, Shirazi-Adl A, Hashemi J (2015b) Quantification of the role of tibial posterior slope in knee joint mechanics and ACL force in simulated gait Journal of Biomechanics

Mesfar W, Shirazi-Adl A (2005) Biomechanics of the knee joint in flexion under various quadriceps forces The Knee 12:424-434

Meyer AJ, D'Lima DD, Besier TF, Lloyd DG, Colwell CW, Fregly BJ (2013) Are external knee load and EMG measures accurate indicators of internal knee contact forces during gait? Journal of Orthopaedic Research 31:921-929

Moglo K, Shirazi-Adl A (2005) Cruciate coupling and screw-home mechanism in passive knee joint during extension–flexion Journal of biomechanics 38:1075-1083

Park S-K, Kobsar D, Ferber R (2016) Relationship between lower limb muscle strength, self-reported pain and function, and frontal plane gait kinematics in knee osteoarthritis Clinical Biomechanics 38:68-74

Pollo FE, Otis JC, Backus SI, Warren RF, Wickiewicz TL (2002) Reduction of medial compartment loads with valgus bracing of the osteoarthritic knee The American Journal of Sports Medicine 30:414-421

Roda RD, Wilson JLA, Wilson DA, Richardson G, Dunbar MJ (2012) The knee adduction moment during gait is associated with the adduction angle measured during computer-assisted total knee arthroplasty The Journal of arthroplasty 27:1244-1250

Russell EM, Hamill J (2011) Lateral wedges decrease biomechanical risk factors for knee osteoarthritis in obese women Journal of biomechanics 44:2286-2291

Schmalz T, Blumentritt S, Drewitz H, Freslier M (2006) The influence of sole wedges on frontal plane knee kinetics, in isolation and in combination with representative rigid and semi-rigid ankle–foot-orthoses Clinical Biomechanics 21:631-639

Shakoor N, Block JA (2006) Walking barefoot decreases loading on the lower extremity joints in knee osteoarthritis Arthritis & Rheumatism 54:2923-2927

Sharma L, Song J, Felson DT, Shamiyeh E, Dunlop DD (2001) The role of knee alignment in disease progression and functional decline in knee osteoarthritis Jama 286:188-195

Shelburne KB, Torry MR, Steadman JR, Pandy MG (2008) Effects of foot orthoses and valgus bracing on the knee adduction moment and medial joint load during gait Clinical Biomechanics 23:814-821

Shirazi R, Shirazi-Adl A, Hurtig M (2008) Role of cartilage collagen fibrils networks in knee joint biomechanics under compression Journal of biomechanics 41:3340-3348

Simic M, Hinman RS, Wrigley TV, Bennell KL, Hunt MA (2011) Gait modification strategies for altering medial knee joint load: a systematic review Arthritis care & research 63:405-426

Sosdian L, Hinman R, Wrigley T, Paterson K, Dowsey M, Choong P, Bennell K (2016) Quantifying varus and valgus thrust in individuals with severe knee osteoarthritis Clinical Biomechanics 39:44-51

Tanamas S, Hanna FS, Cicuttini FM, Wluka AE, Berry P, Urquhart DM (2009) Does knee malalignment increase the risk of development and progression of knee osteoarthritis? A systematic review Arthritis care & research 61:459-467

Tetsworth K, Paley D (1994) Malalignment and degenerative arthropathy Orthopedic Clinics of North America 25:367-378

Trepczynski A, Kutzner I, Bergmann G, Taylor WR, Heller MO (2014) Modulation of the relationship between external knee adduction moments and medial joint contact forces across subjects and activities Arthritis & Rheumatology 66:1218-1227

Walter JP, D'Lima DD, Colwell CW, Fregly BJ (2010) Decreased knee adduction moment does not guarantee decreased medial contact force during gait Journal of Orthopaedic Research 28:1348-1354

Winby C, Gerus P, Kirk T, Lloyd DG (2013) Correlation between EMG-based co-activation measures and medial and lateral compartment loads of the knee during gait Clinical Biomechanics 28:1014-1019

Wong J, Steklov N, Patil S, Flores-Hernandez C, Kester M, Colwell CW, D'Lima DD (2011) Predicting the effect of tray malalignment on risk for bone damage and implant subsidence after total knee arthroplasty Journal of Orthopaedic Research 29:347-353

Zhang L-Q, Shiavi RG, Limbird TJ, Minorik JM (2003) Six degrees-of-freedom kinematics of ACL deficient knees during locomotion—compensatory mechanism Gait & posture 17:34-42

Zhao D, Banks SA, Mitchell KH, D'Lima DD, Colwell CW, Fregly BJ (2007b) Correlation between the knee adduction torque and medial contact force for a variety of gait patterns Journal of Orthopaedic Research 25:789-797

Table 8.6: Predicted total compartmental contact area on the lateral (Lat) and medial (Med) plateaus in different add/abd conditions at various stance periods.

		Total Contact Area (mm^2)				
		R-SD	**M-SD**	**Ref**	**M+SD**	**R+SD**
0%	L	517	477	477	477	179
	M	42	136	136	143	371
5%	L	653	616	620	622	448
	M	76	134	135	136	494
25%	L	425	319	325	326	144
	M	592	603	606	607	550
50%	L	379	237	226	268	62
	M	505	524	524	558	522
75%	L	566	422	394	416	298
	M	560	622	630	618	606
100%	L	295	0	0	0	0
	M	223	405	405	428	465

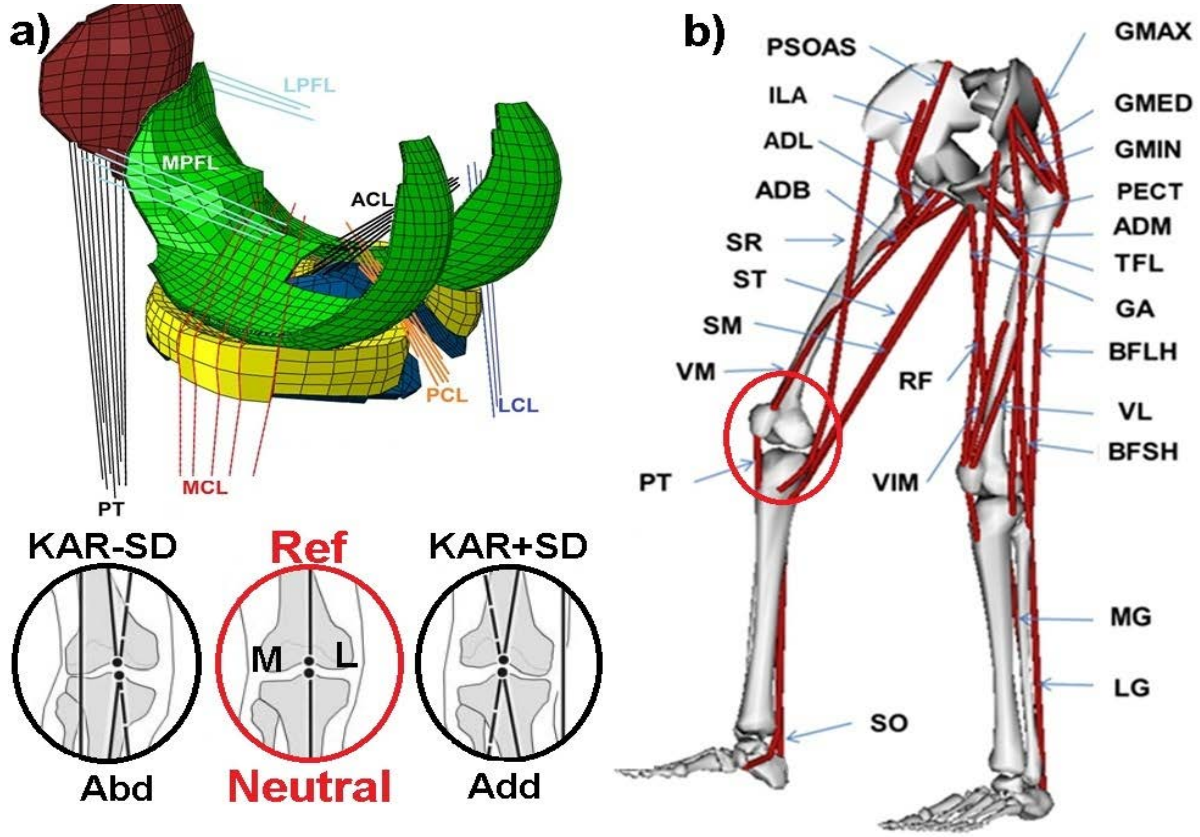

Figure 8.1: (a) (Top left) Detailed knee FE model; tibiofemoral (TF) and patellofemoral (PF) cartilage layers, menisci, patellar Tendon (PT). Joint ligaments include lateral patellofemoral (LPFL), medial patellofemoral (MPFL), anterior cruciate (ACL), posterior cruciate (PCL), lateral collateral (LCL) and medial collateral (MCL). (Bottom left) schematic representation of changes in the mean knee adduction rotation (KAR) by one standard deviation (±SD). (b) (Right) Schematic diagram showing the 34 muscles incorporated into the lower extremity model (Open Sim, Delp et al., 2007). Quadriceps components are vastus medialis obliqus (VMO), rectus femoris (RF), vastus intermidus medialis (VIM) and vastus lateralis (VL). Hamstrings components include biceps femoris long head (BFLH), biceps femoris short head (BFSH), semi membranous (SM) and TRIPOD made of sartorius (SR), gracilis (GA) and semitendinosus (ST). Gastrocnemius components are gastrocnemius medial (GM) and gastrocnemius lateral (GL). Soleus (SO) muscle is uni-articular ankle muscle. Hip joint muscles (not all shown) include adductor, long (ADL), mag (3 components ADM) and brev (ADB); gluteus max (3 components GMAX), med (3 components GMED) and min (3 components GMIN), iliacus (ILA), iliopsoas (PSOAS), quadriceps femoris; pectineus (PECT), tensor facia lata (TFL), periformis.

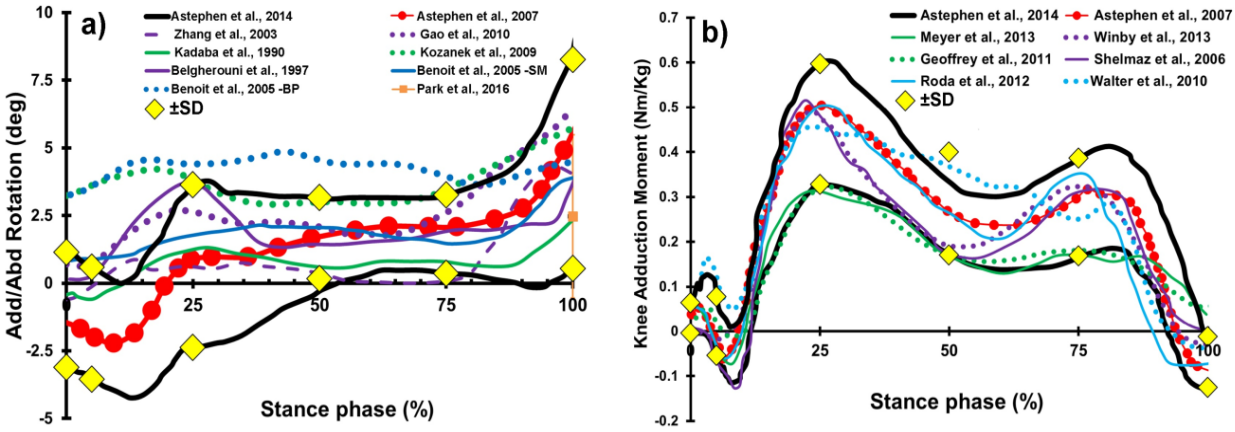

Figure 8.2: Knee joint adduction rotations (a) and moments (b) reported as mean values for asymptomatic subjects during the stance phase of gait. The values taken in our study at the stance phase are depicted by yellow diamonds based on reported mean±SD measurements of asymptomatic subjects (Astephen et al. 2014). These changes cover most of major datasets reported in the literature and the likely errors in measurements (Astephen 2007; Benoit et al. 2006; Bulgheroni et al. 1997; Gao and Zheng 2010; Geoffrey et al. 2011; Kadaba et al. 1990; Kozanek et al. 2009; Meyer et al. 2013; Park et al. 2016; Roda et al. 2012; Schmalz et al. 2006; Walter et al. 2010; Winby et al. 2013; Zhang et al. 2003). Note that moments are reported normalized to BW (kg). Positive rotations/moments denote adduction.

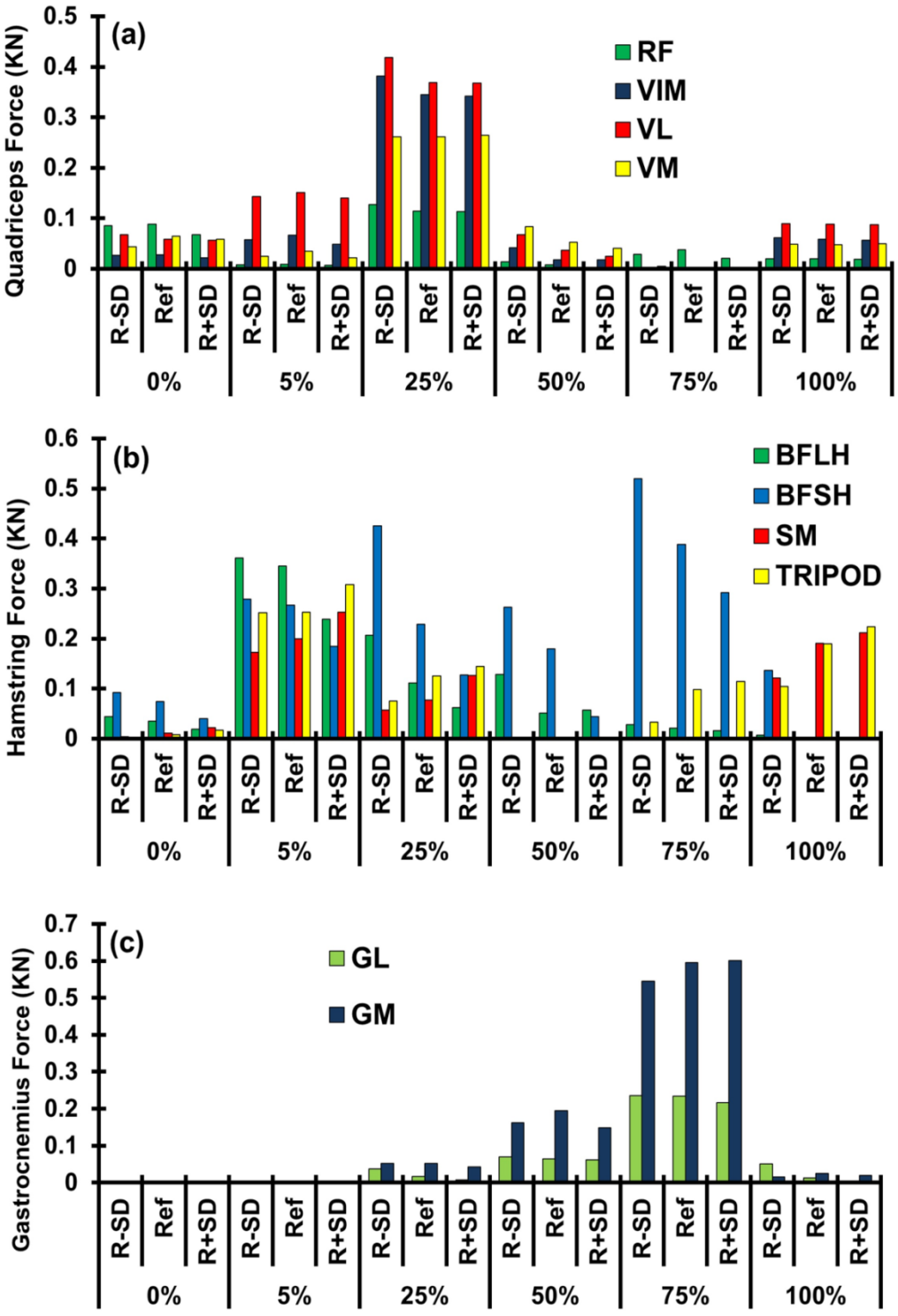

Figure 8.3: Predicted (a) quadriceps, (b) hamstrings and (c) gastrocnemius muscle forces (see Fig. 1 caption for muscle abbreviations) at various periods of stance under reference mean (Ref), mean+SD (R+SD) and mean-SD (R-SD) KAR cases (at constant KAM).

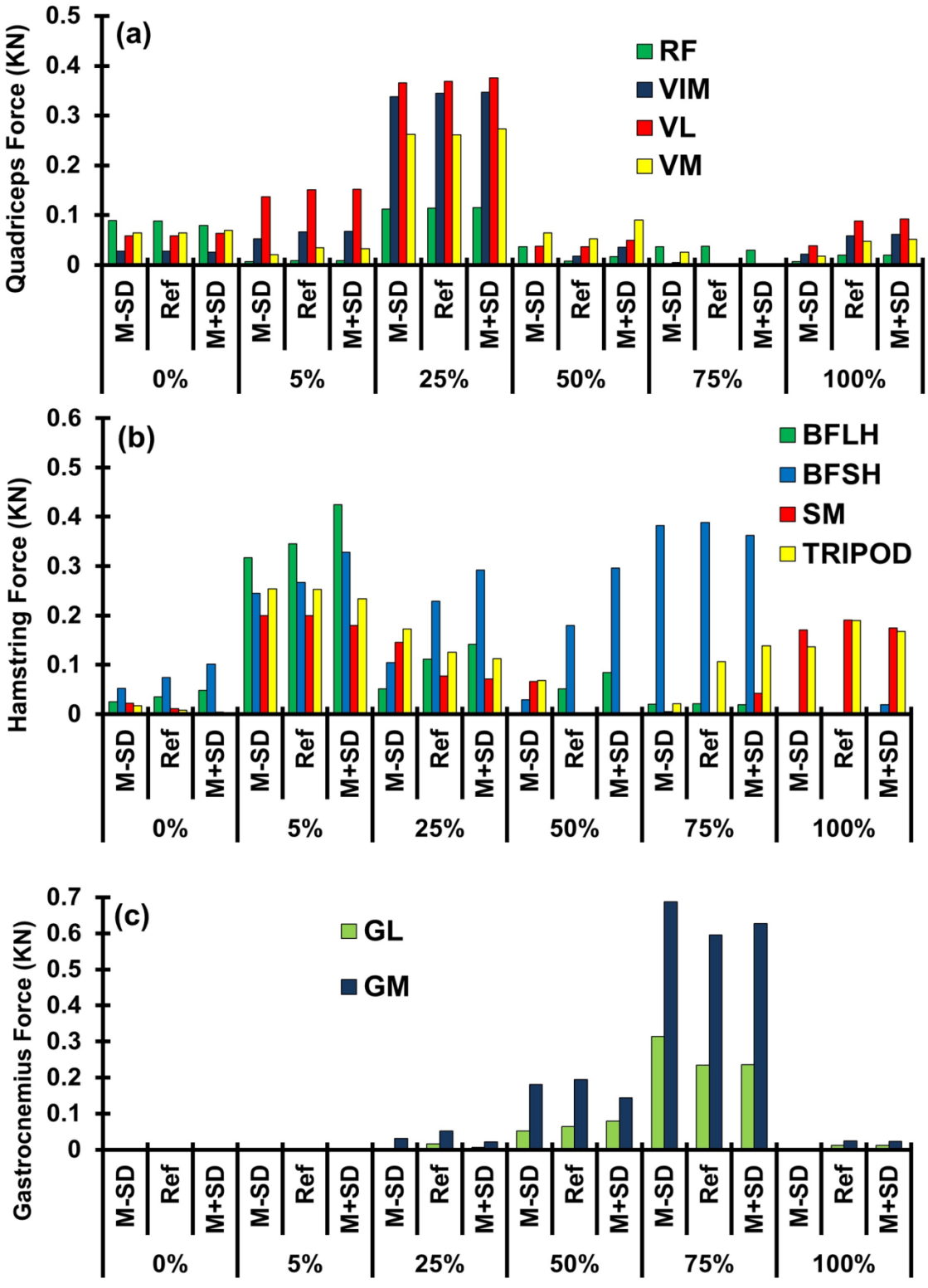

Figure 8.4: Predicted (a) quadriceps, (b) hamstrings and (c) gastrocnemius muscle forces (see Fig. 1 caption for muscle abbreviations) at various periods of stance under reference mean (Ref), mean+SD (M+SD) and mean-SD (M-SD) KAM cases (at constant KAR).

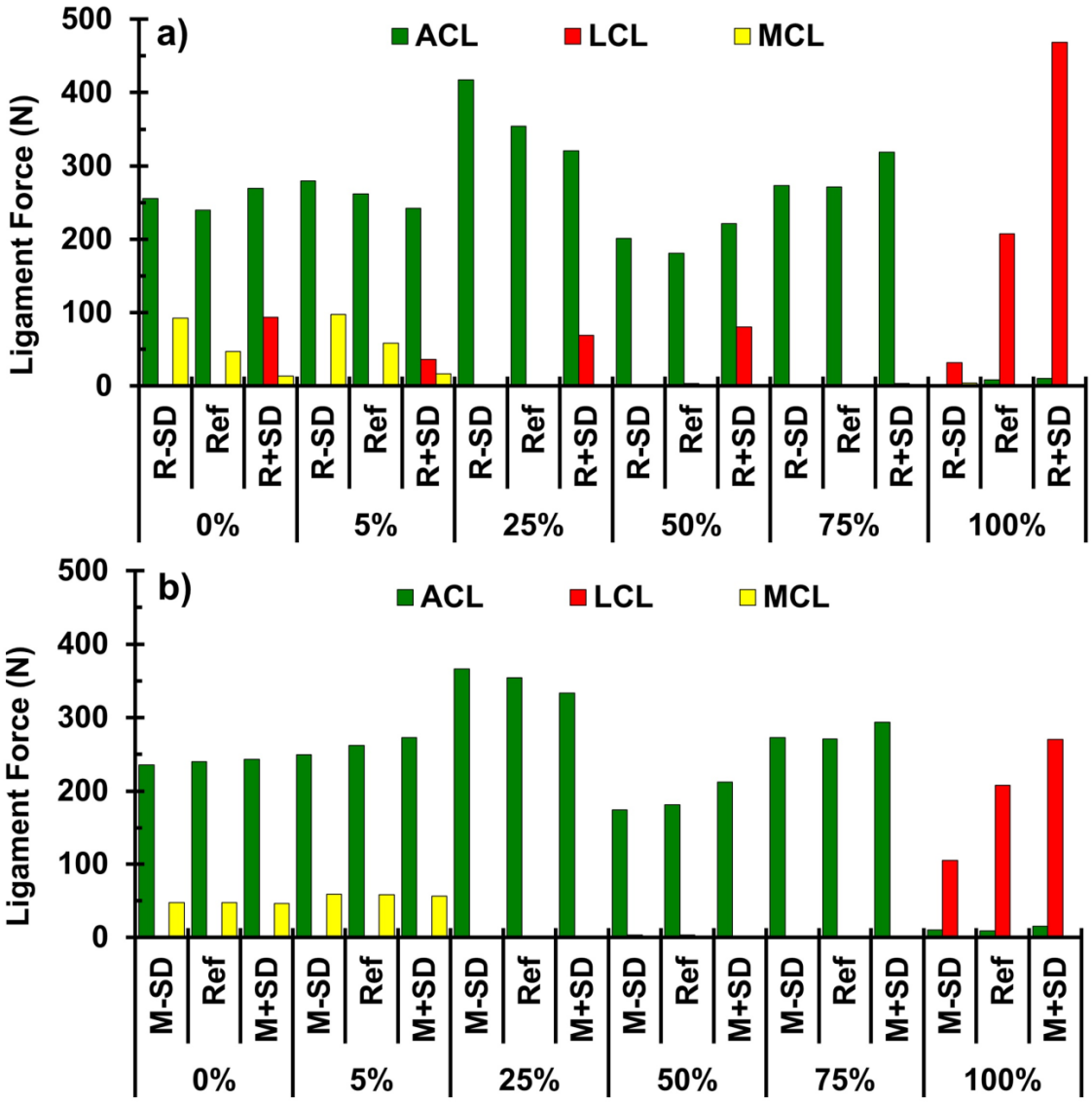

Figure 8.5: Predicted variation of total ACL, LCL and MCL forces during the stance phase of gait under mean (Ref) and mean±SD add/abd (a) rotations (R±SD at constant KAM) and (b) moments (M±SD at constant KAR). Forces in PCL, MPFL and LPFL remained negligible and those in PT followed forces in quadriceps.

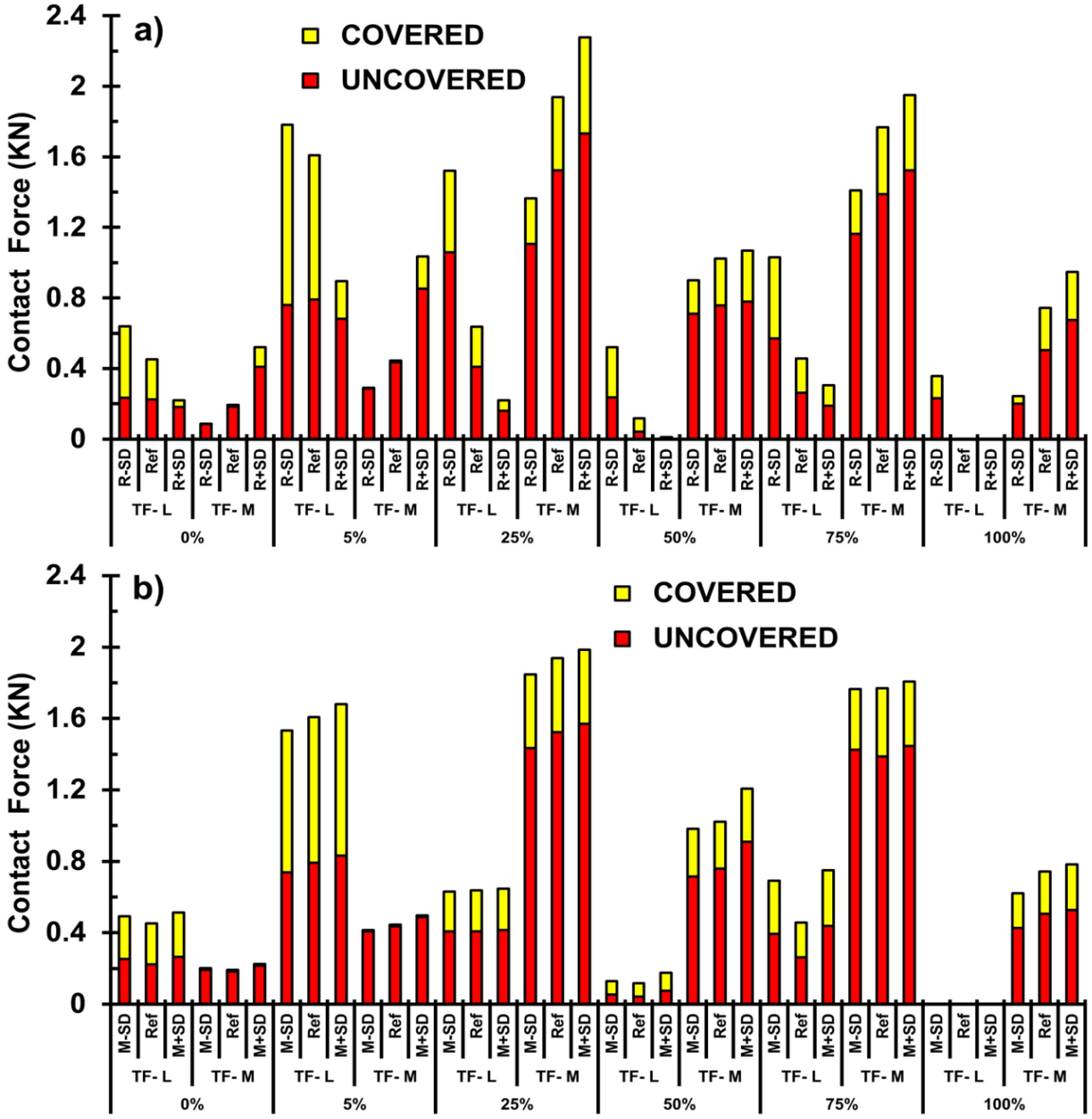

Figure 8.6: Total contact forces on tibiofemoral lateral (L) and medial (M) plateaus at covered (via menisci) and uncovered (via cartilage-cartilage) areas at various periods of stance under mean (Ref) and mean±SD add/abd (a) rotations (R±SD at constant KAM) and (b) moments (M±SD at constant KAR).

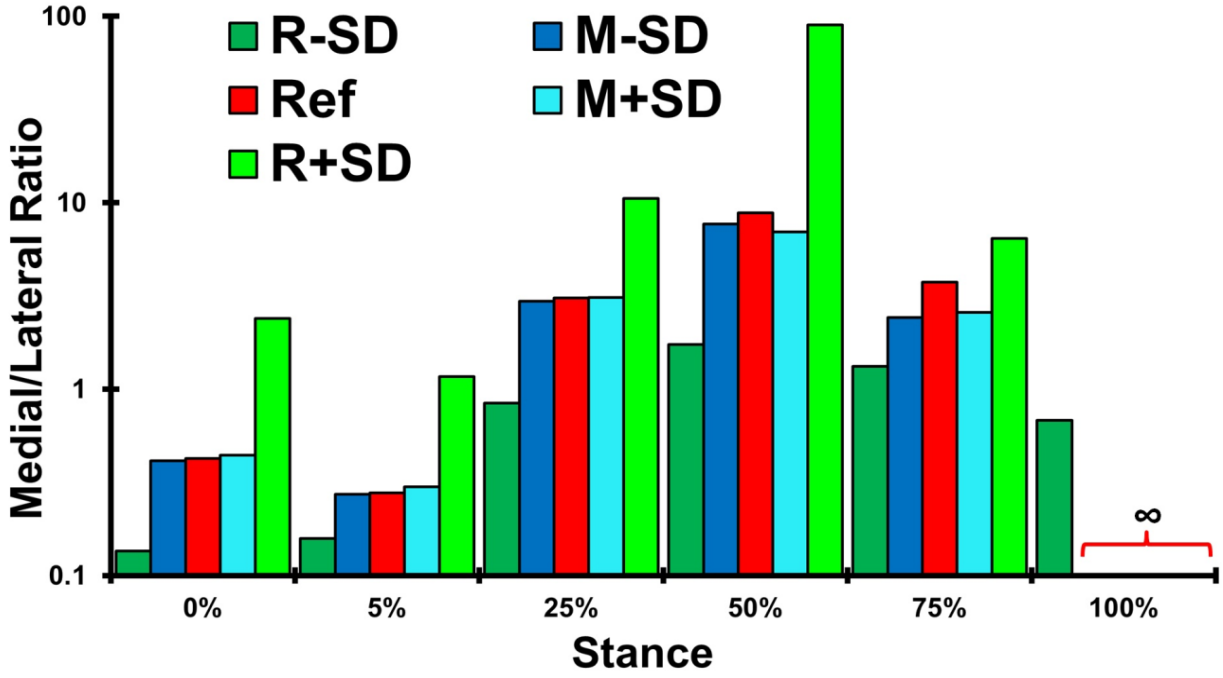

Figure 8.7: Variation (logarithmic) of medial/lateral contact force ratio at various periods of stance under mean (Ref) and mean±SD add/abd rotation (R±SD) and moment (M±SD) conditions. At TO, lateral plateau is completely unloaded except for the R-SD condition.

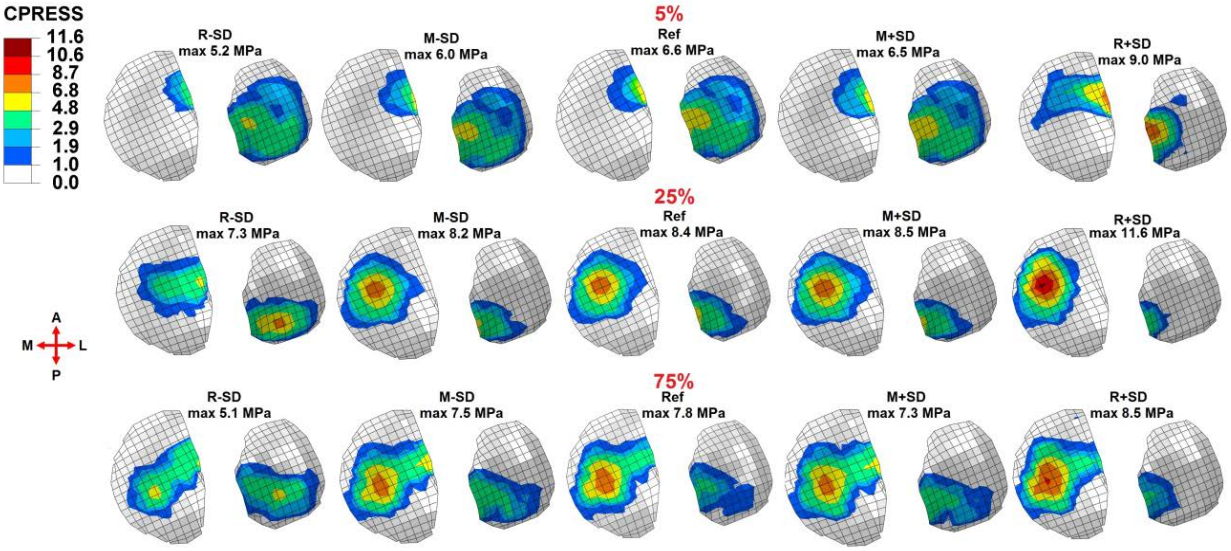

Figure 8.8: Predicted contact pressure distributions (MPa) at the tibial articular surfaces at 5, 25 and 75% stance periods under mean (Ref) and mean±SD add/abd rotation (R±SD) and moment (M±SD) conditions. Lateral and anterior directions are positive here. Note that a common legend is used for ease in comparisons.

CHAPITRE 9 DISCUSSION GÉNÉRALE

9.1 Simulations

9.1.1 Modèles

Dans ce travail on utilise deux modèles; (1) un modèle hybride musclo-squelettique (MS) des membres inférieurs comprenant un modèle EF de l'articulation du genou (modèle MS) (M Adouni, Shirazi-Adl, & Shirazi, 2012a) contrôlé par les données cinématiques et cinétiques provenant des sujets asymptomatiques durant la marche (Astephen, Deluzio, Caldwell, & Dunbar, 2008; A. E. Hunt, M Smith, et al., 2001) et (2) l'articulation passive tibio-fémorale (TF) isolée de ce modèle (modèle TF) (H Marouane et al., 2015a; R. Shirazi et al., 2008).

Le modèle du genou utilisé dans cette étude est le modèle initialement développé par Bendjaballah et al. (1995), dont sa reconstruction a été basée sur un échantillon cadavérique d'un genou humain normal provenant d'un donneur féminin de 27 ans. Ce modèle 3D non-linéaire comprend les deux ménisques médial et latéral, les couches de cartilage des trois structures osseuses (tibia, fémur et patella) ainsi que les cinq ligaments principaux (collatéraux, croisés et le tendon rotulien). Les parties osseuses ont été considérées comme des corps rigides (Haut Donahue & Hull, 2002). Un choix justifié vu la rigidité relative des parties osseuses et également en raison du fait qu'on n'est pas à la recherche de l'état de déformations dans ces structures. Chaque structure osseuse a été représentée par un noeud primaire (point de référence, PR), situé au centre, et par un ensemble de système de coordonnées locales qui tournent en suivant le corps rigide.

Les ménisques ont été modélisés comme un matériau composite avec une matrice renforcée par des réseaux de fibres de collagène dans les deux directions radiale et circonférentielle (R. Shirazi et al., 2008). Les ligaments ont été modélisés comme des ressorts non-linéaires avec des déformations initiales. Ce modèle a été validé dans différentes conditions de chargement (M. Adouni & Shirazi-Adl, 2009; M Adouni & Shirazi-Adl, 2012b; M Adouni et al., 2012a; Mohamed Z Bendjaballah et al., 1995; M. Z. Bendjaballah, A. Shirazi-Adl, & D. Zukor, 1997; M.Z. Bendjaballah et al., 1998; Hafedh Marouane, 2012; H Marouane et al., 2013; W. Mesfar & Shirazi-Adl, 2005, 2006a, 2006b, 2008a, 2008b; KE Moglo & A. Shirazi-Adl,

2003; Moglo & Shirazi-Adl, 2005; R. Shirazi et al., 2008) et a subit des améliorations toute au long de son utilisation par l'addition des mécanismes extenseurs et fléchisseurs et les muscles des gastrocnemii. Une amélioration au niveau de la propriété mécanique des matériaux des cartilages et le niveau de raffinement des couches des cartilages a été faite dans les travaux de Shirazi et al. (2008) sur ce modèle où une implémentation des réseaux des fibres de collagène avec des fractions volumiques appropriées dans le cartilage articulaire et les ménisques a été mise en évidence (voir annexe A).

9.1.2 Méthodologies

a. PTP

Dans un premier temps, le modèle passif TF a été utilisé pour évaluer l'effet de la PTP en flexion et sous l'action d'une force de compression allant jusqu'à 1400N sur la réponse globale de l'articulation du genou et particulièrement la réponse du LCA. La PTP a été modifiée par ±5° et les résultats ont été comparés avec le cas de référence (Hafedh Marouane, 2012; H Marouane et al., 2015a). Une étape nécessaire est de trouver les PTP de référence des plateaux médial et latéral.

Pour définir la PTP de référence sur chacun des deux plateaux du tibia, nous avons choisi 3 plans de coupe (M1, M2 et M3 pour le plateau médial et L1, L2 et L3 pour le plateau latéral). Les plans M1, M2 et M3 (L1, L2 et L3) coupent respectivement le plateau médial (latéral) à 25%, 50% et 75% de son largueur total (Figure 9.1). Ainsi, la pente est l'angle entre la perpendiculaire à l'axe vertical (l'axe des z en position de pleine extension) et la ligne qui représente l'inclinaison du plateau dans le plan de coupe choisi (la ligne reliant les deux extrémités du tibia dans le plan sagittal). La pente finale est ainsi trouvée en faisant la moyenne des trois pentes trouvées en utilisant les trois plans de coupe. Les PTPs de références sont respectivement 9.76° pour le plateau médial et 5° pour le plateau latéral (voir Tableau 2.1 pour une comparaison). Cette différence entre la pente tibiale médiale et celle latérale est en accord avec la récente étude de Weinberg et al (2017) qui ont rapportés en moyenne une PTP médiale de 6.9°±3.7° et une PTP latérale de 4.7°± 3.6° en analysant 1090 genoux cadavériques.

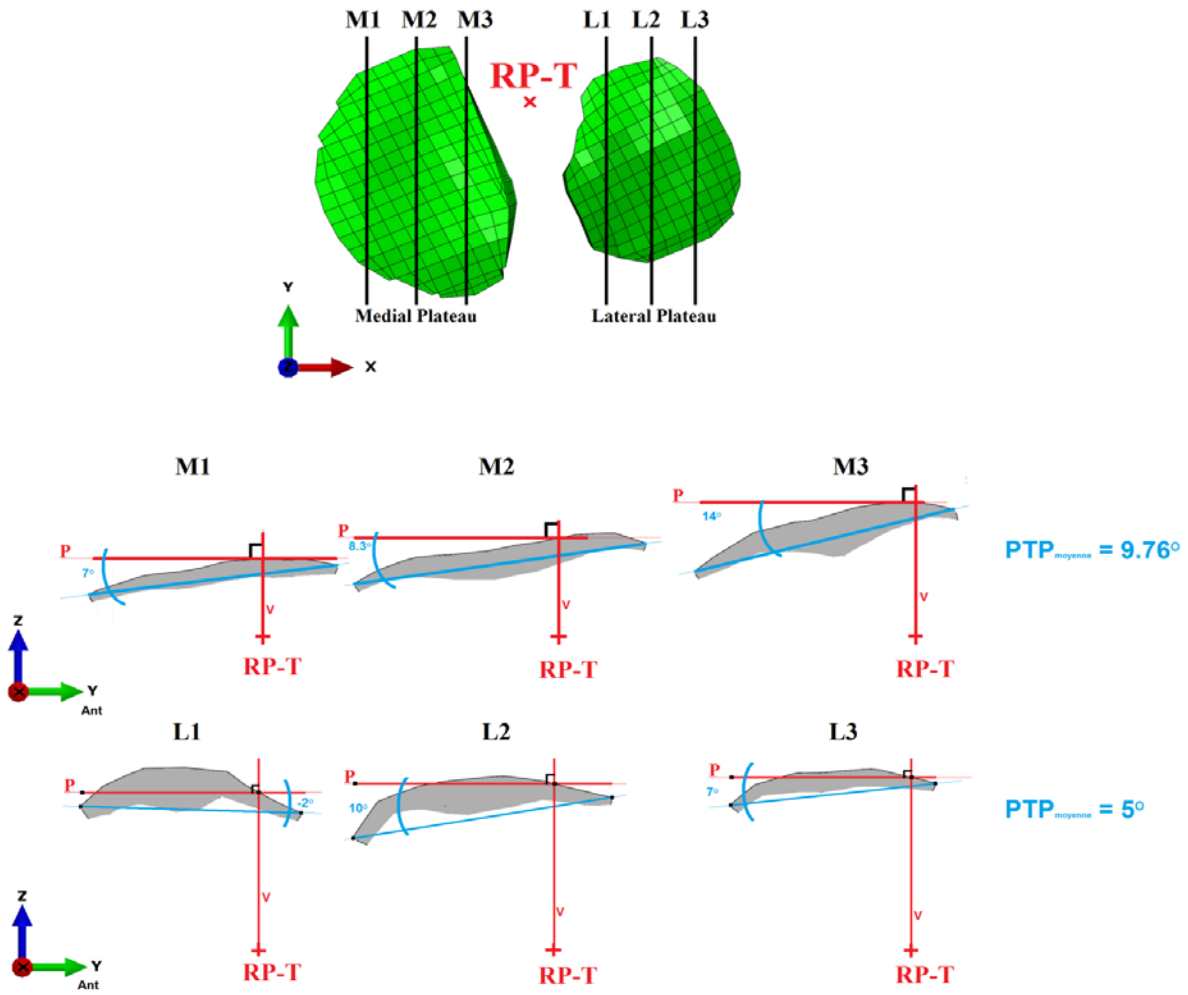

Figure 9.1: Pente tibiale postérieure de référence pour notre modèle d'EF

Pour étudier les effets de la variation de la PTP sur la translation tibiale antérieure (ATT) et la force/déformation du LCA, les études in vitro ont simulé la variation de la PTP par une ostéotomie antérieure (Agneskirchner, Hurschler, Stukenborg-Colsman, Imhoff, & Lobenhoffer, 2004; Fening et al., 2008; Giffin et al., 2004; Nelitz et al., 2013). Toutefois, cette technique modifie entièrement la configuration articulaire et ne tient pas compte ni des déformations initiales des ligaments ni de leurs points d'insertions. Notre but est donc; pouvoir altérer la PTP sans toucher le reste de la structure articulaire. Dans ce contexte, les PTPs de référence des deux plateaux (médial et latéral) ont été variées ensemble ou séparément par +5° ou par -5° en effectuant une rotation rigide des couches de cartilage autour des axes médial-latéral (M-L) placés au centre de chaque plateau respectif (Figure 9.2). De cette manière, la géométrie articulaire reste presque la même et les points d'insertions ligamentaires (et donc les longueurs

des ligaments et de leurs orientations) restent inchangés. En plus du modèle de référence, six modèles ont été créés en faisant les différentes combinaisons (+5ML, -5ML, +5M, -5M, +5L et -5L; L : Latéral, M: Médial, ML: Médial et Latéral).

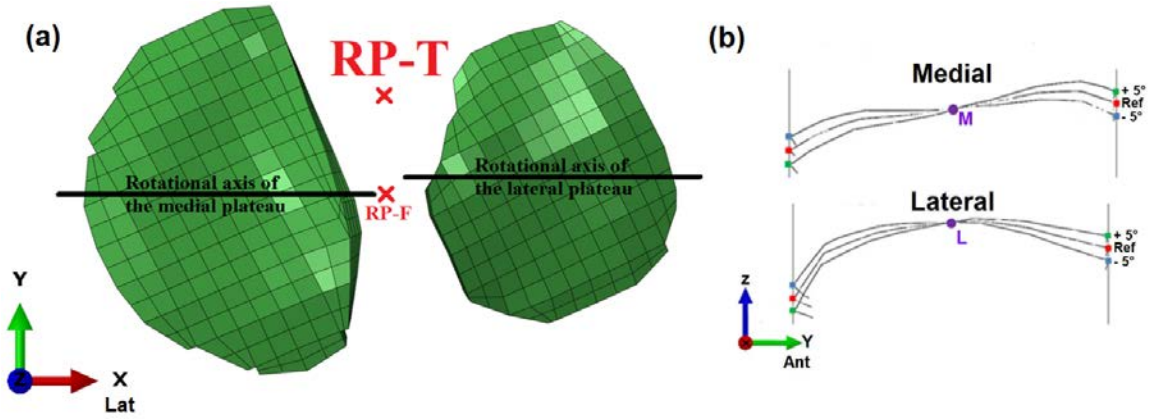

Figure 9.2: (a) Axes de rotation utilisés pour (b) varier la PTP de référence par ±5°

En utilisant le modèle TF de référence et les six modèles développés pour simuler la variation de la PTP (+5, -5, +5M, -5M, +5L et -5L), la réponse passive de l'articulation du genou a été étudiée dans quatre angles de flexion (0°, 15°, 30° et 45°) sous l'action d'une force de compression de 1400 N. Similairement à notre étude antérieure (Hafedh Marouane, 2012; H Marouane et al., 2015a) et afin d'éviter les moments d'artefact (artifact moments) la force de compression sera appliquée au point d'équilibre mécanique (MBP: Mechanical Balance Point). Cette position est la position où l'application de la force de compression ne doit générer aucune rotation ni dans le plan frontal ni dans le plan sagittal (Figure 2.21). La position du MBP varie avec la force de compression, l'angle de flexion et la PTP. Ahmed et Burke (1983) ont rapporté que jusqu'à un déplacement postérieur de 1 cm dans la position de la force de compression appliquée était nécessaire pour l'équilibre à un angle de flexion articulaire désiré lorsque l'articulation tournait de 0° à 90° de flexion.

b. Durant la marche

Six périodes de la phase d'appui de la marche ont été étudiées dans le présent travail; à savoir 0% (HS), 5%, 25%, 50% (mid-stance), 75% et 100% (TO). Les conditions aux limites ont été choisies de manière à représenter le plus fidèlement le cycle de la marche d'un sujet normal. Pour ce faire, on utilise les données cinématiques et cinétiques provenant des sujets sains utilisées déjà dans nos études antérieures (M Adouni & Shirazi-Adl, 2014a). Pour la cinématique, les

études de Astephan et al., (2007; 2008) réalisées sur 60 personnes saines, sans aucun historique pathologique, nous donnent les rotations et les moments de la hanche, du genou et de la cheville (Figures 2.12-2.14) dont on a besoin. Également, avec le même nombre des sujets, l'étude de Hunt et al. (2001) nous donne les forces de réaction au sol (GRF) durant la phase d'appui de la marche (Figure 2.13).

Une étape nécessaire dans notre étude de la marche humaine est la transformation du système d'axe. Tout comme la majorité des études expérimentales, les données cinématiques et cinétiques des membres inférieurs dans l'étude d'Astephen et al. (2007) ont été définies dans le système d'axe de Grood et Santy (1983). Ces données ont été transformées alors dans le système d'axe global de notre modèle EF. Le détail de cette transformation ont été précisé dans nos études antérieures (Malek Adouni, 2014; Wissal Mesfar, 2005) et dans l'étude de Grood et Santy (1983).

La première étape de chaque analyse consiste à placer l'articulation du genou dans sa position désirée relativement à l'articulation de la hanche. Ici les membres inférieurs ont été considérés comme un seul corps rigide et les rotations ont été appliquées au niveau du centre de la hanche. Le centre initialement défini dans les études de Adouni et al., (2014) basé sur le modèle de OpenSim (Delp et al., 2007) après calibration avec notre modèle féminin. Pour chaque analyse une configuration de référence est initialement produite en considérant la réponse du joint du genou sous l'action de pré-tensions ligamentaires. Ainsi, le fémur est fixé dans sa position instantanée tandis que le tibia et la rotule sont libres à l'exception des rotations TF prescrites qui ont été appliquées. La localisation du GRF à chaque période est déterminée de manière à générer les moments rapportés par Astephen et al. (2007; 2008). Puisque notre modèle d'éléments finis représente la géométrie d'un sujet féminin, les poids au centre de la jambe et du pied sont respectivement 29.3 N et 7.85N (De Leva, 1996).Une fois que la position du GRF est trouvée, une optimisation est nécessaire pour contrebalancer les moments autours les joints après un nombre d'itérations bien défini.

Les forces musculaires ont été évaluées par la technique d'optimisation. La somme des contraintes musculaires cubiques a été minimisée en considérant sept équations d'équilibre des moments (3 au niveau de la hanche, 3 au niveau du genou et 1 au niveau de la cheville) et une équation d'inégalités, dont la contrainte musculaire est comprise entre la contrainte passive et la

contrainte maximale. Les contraintes passives ont été négligées à cause des changements négligeables dans la longueur des muscles, et les contraintes maximales (0,6 MPa) ont été basées sur les travaux de Arjmand et Shirazi-Adl (2006). Ces calculs d'optimisations sont exécutés avec MATLAB® (the MathWorks Inc., Natick, MA, USA, version 2013) et l'algorithme génétique ainsi que la fonction Fmincon ont été utilisés. Pour tendre le moment au niveau du joint vers zéro, un nombre d'itérations bien défini est nécessaire (entre 6 et 14 itérations pour avoir ~0.1Nm).

En utilisant le modèle MS, l'effet de la PTP a été étudié également durant la phase d'appui de la marche. La même méthodologie a été suivie pour changer la PTP par ±5° et ±10° (voir section a). De même nos résultats ont été comparées avec le cas de référence (M Adouni & Shirazi-Adl, 2014a). Le modèle MS a été également utilisé pour étudier l'effet de la variation de la rotation varus/valgus versus l'effet de la variation du moment varus/valgus durant la phase d'appui de la marche, servant à détecter la relation entre ces paramètres externes et la répartition de charge sur les deux plateaux du tibia. Ensuite, l'idéalisation du joint du genou comme une articulation 2D et 1D a été étudiée et comparée avec le cas de référence (genou 3D). Finalement, les résultats de référence durant la phase d'appui de la marche normale et avec OA sévère (M Adouni & Shirazi-Adl, 2014a), ainsi que les résultats de nos études sur l'effet de la variation de la PTP et de l'angle/moment VV, ont été utilisés pour localiser le centre de contact avec différentes méthodes.

9.2 Analyse des résultats

Les forces musculaires trouvées durant le cas de référence (modèle 3D et PTP de référence) sont en accord avec les activités EMG mesurées durant la marche (Janie L Astephen, 2007). Bien que le premier pic de la force de contact TF survienne principalement en raison d'une forte activation dans les quadriceps, le deuxième pic est dû à l'activation des gastrocnemii. Une activité EMG minimale est rapportée pour les gastrocnemii (médial et latéral) au début de la phase d'appui qui augmente continuellement vers la fin de la phase en accord avec les études antérieures (Janie L Astephen, 2007). De plus, la baisse importante de l'activité de RF, associée à une augmentation à peu près égale à l'activité de VIM, corrobore bien avec les données EMG (Janie L Astephen, 2007; Sasaki & Neptune, 2010) qui montrent une activité EMG minimale dans la RF par rapport aux composantes VL et VM. De même pour les hamstrings, dont la

majorité de forces de la partie latérale est transférée par la composante interne BFSH à la fin de la phase d'appui avec une contribution presque nulle de son homologue externe BFLH.

Les grandes forces estimées dans les hamstrings latéraux expliquent leur importance dans la résistance au moment d'adduction et au moment d'extension du joint de genou durant la marche normale (cas de référence). Ce rôle qui a été négligé dans la majorité des travaux antérieurs par la limitation du rôle des Ischio-jambiers au plan sagittal (Anderson & Pandy, 2001; Messier et al., 2011; KB. Shelburne, Torry, & Pandy, 2005; K.B. Shelburne et al., 2006) a sans doute un effet sur les forces musculaires estimées. En effet, en simulant l'articulation du genou comme un joint 2D, sans considérer les rotations et les équations d'équilibre dans les plans frontal et transversal, les forces musculaires diminuent considérablement, en moyenne par 48, 44 et 16% pour les quadriceps, les Ischio-jambiers et les gastrocnemii, respectivement.

En variant la PTP durant la phase d'appui, des variations minimes dans les forces musculaires ont été estimées avec le modèle MS. Un changement justifié vue que la variation de la géométrie tibiale n'a aucun effet sur les insertions musculaires. La seule différence est donc causée par la contribution passive du joint suite à la variation de la PTP. Par contre, la variation de la rotation varus / valgus (avec moment varus/valgus constant) a un effet considérable sur la répartition des forces musculaires. Durant toute la phase d'appui, les forces des hamstrings latéraux diminuent et celles des hamstrings médiaux augmentent en augmentant la rotation varus en accord avec les simulations de Adouni et al., (2014b) faites à 50% de la phase d'appui. Ceci est lié principalement à la contribution passive dans l'équilibre total de l'articulation du genou dans le plan frontal (Lloyd & Buchanan, 2001). En outre, la diminution massive de l'activité musculaire des hamstrings latéraux avec l'augmentation de l'angle d'adduction peut expliquer les réponses silencieuses de ces muscles rapportées dans plusieurs travaux (Besier, Fredericson, Gold, Beaupré, & Delp, 2009; K.B. Shelburne et al., 2006; C. R. Winby et al., 2009).

Toutefois, les comparaisons entre les forces musculaires estimées et les données EMG enregistrées doivent, cependant, tenir compte de l'absence de co-activité dans le modèle qui a un effet majeur sur la stabilité de l'articulation, et aussi la limitation de mesure EMG aux composantes musculaires superficielles. Ces limitations, expliquent entre autre, le désaccord entre les forces musculaires des hamstrings estimées et la mesure EMG au début de la phase d'appui.

Dans les sous-sections suivantes, une analyse, une comparaison et une discussion des résultats sont présentées.

9.2.1 PTP

Nos prédictions avec les deux modèles TF et MS supportent clairement notre hypothèse; qu'une PTP plus grande augmente la force du LCA. Nos résultats du modèle TF montrent que la force du LCA en pleine extension est supportée principalement par le faisceau LCA-pl. En outre, la force du faisceau LCA-am augmente avec la flexion du genou et avec une PTP plus grande. De même, durant la phase d'appui de la marche, la force du LCA est principalement supportée par le faisceau LCA-pl avec une contribution minime de son homologue LCA-am. Ce transfert entre les deux faisceaux du LCA avec la flexion du genou; du LCA-pl au LCA-am, a été également rapporté dans des études in-vitro (Woo et al., 1998) et des études numériques (Moglo & Shirazi-Adl, 2005). Ceci suggère que la mesure d'une diminution de la déformation du LCA-am à un angle de flexion de 15° après une ostéotomie (Fening et al., 2008) ne peut pas représenter une image fidèle de la déformation du LCA entière et donc de sa force. De plus, une ostéotomie antérieure lors d'une tentative de modification de la PTP cause des modifications importantes au niveau de l'orientation et de la longueur de la structure ligamentaire, et a probablement une influence sur la réponse de l'articulation et rend les conclusions de certaines études cadavériques douteuses (Fening et al., 2008; Giffin et al., 2004). L'application d'une force de compression relativement faible dans ces études peut également être une raison pour ne pas détecter l'effet de la variation de la PTP sur la réponse de l'articulation du genou. Dans nos études actuelles avec le modèle EF, les plateaux médial et latéral ont été tournés par ± 5° (et ± 10°) autour des axes médial-latéral passant par les centroïdes de ces surfaces placées de manière à minimiser les changements de la géométrie articulaire tibiale. De plus, les points d'insertions de tous les ligaments, y inclus le LCA, sont restés inchangés. Toute différence avec le cas de référence est donc l'effet unique de la variation de la PTP.

Des études radiographiques faites sur des sujets normaux et avec déchirure du LCA (Bojicic, Beaulieu, Imaizumi Krieger, Ashton-Miller, & Wojtys, 2017; Dejour & Bonnin, 1994) ont rapporté une augmentation significative de la translation antérieure du tibia avec une PTP plus grande. Dans nos études sur l'effet de la PTP, la TTA augmente par 2.3mm à 50% de la phase d'appui de la marche et par 4.4mm sous l'action d'une force de compression de 1400N. En

association avec les changements calculés de la cinématique, les deux modèles estiment des forces LCA beaucoup plus grandes à tous les angles de flexion avec une PTP plus grande tandis que des forces plus petite avec une PTP plus petite. Par exemple la force du LCA change de 181 N dans le cas de référence à la phase 50% à 102 N et 317 N lorsque PTP change de -5° et + 5°, respectivement. Ces résultats corroborent les observations in vivo antérieures indiquant une PTP plus importante comme un facteur de risque majeur pour les lésions du LCA (Sonnery-Cottet et al., 2011; Todd et al., 2010). Le chargement du LCA avec l'augmentation de la PTP sous l'action d'une force de compression de 1400N, montre également la vulnérabilité du LCA à la rupture sous des forces de compression importantes en concordance avec les études in vitro (E. G. Meyer et al., 2008; E. G. Meyer & Haut, 2005, 2008b; Wall et al., 2012; Yeow, Cheong, Ng, Lee, & Goh, 2008).

Un aspect intéressant de ce travail a été la nouvelle simulation de variation de la PTP dans chaque plateau médial et latéral séparément afin d'identifier le rôle relatif de chaque plateau. Les modifications de la PTP séparément dans chaque plateau à la fois ont démontré que la force du LCA et la TTA étaient principalement influencées par les changements du plateau supportant une plus grande proportion de la force de compression articulaire. De cette manière, la TTA et la force du LCA ont été influencées par des changements de la PTP au niveau du plateau latéral à 5% de la phase d'appui, alors qu'au niveau du plateau médial à 50%. En effet, les forces de contact étaient beaucoup plus grandes dans le plateau latéral seulement au début de la phase d'appui et deviennent plutôt grandes sur le plateau médial durant le reste de la phase d'appui de la marche. Ces résultats soulignent en outre l'importance de la force de compression sur l'amplitude de la variation de la TTA et de la force du LCA suite aux variations de la PTP.

Les études antérieures qui ont modélisé l'extrémité inférieure durant la marche, malgré les simplifications dont la négligence des couches de cartilage et des ménisques, et de considérer l'équilibre seulement dans le plan sagittal (Kevin B Shelburne, Kim, Sterett, & Pandy, 2011) ou la représentation sagittale 2D de l'articulation (Liu & Maitland, 2003; Shao, MacLeod, Manal, & Buchanan, 2011) concordent avec nos prédictions sur l'augmentation substantielle de la translation tibial antérieure, TTA, (Liu & Maitland, 2003) et de la force du LCA (Shao et al., 2011; Kevin B Shelburne et al., 2011) avec une PTP plus grande. Dans l'étude de Shelburne et al. (2011), la variation de la PTP de + 5° et -5° durant la marche résulte respectivement en des changements de + 80 N et -75 N dans la force du LCA et +2,4 et -2,3 mm dans la TTA par

rapport aux valeurs de référence qui sont en accord avec des changements de + 136N et -79N de la force du LCA et +1.2 et -1.2 mm de la TTA calculés dans notre modèle actif à 50%. En outre, nos prédictions de l'augmentation de la translation tibiale antérieure (TTA) et de la rotation interne du tibia avec l'augmentation de la PTP concordent avec les études in-vitro en compression (Agneskirchner et al., 2004; K. L. Markolf et al., 2013; E. G. Meyer et al., 2008; E. G. Meyer & Haut, 2005, 2008b). Cependant, durant la marche avec le modèle MS, la rotation interne-externe du genou, ainsi que les rotations flexion-extension et de varus-valgus ont été prescrites tout au long de la phase d'appui selon les données cinématiques d'Astephen et al. (2007). Les variations de la force du LCA et de la TTA avec la variation de la PTP ont été donc calculées sous des rotations interne-externe identiques. Comme le LCA est connue comme une contrainte majeure en rotation axiale (Fleming et al., 2001; K. L. Markolf et al., 2013; 2009), des changements plus importants de la force du LCA auraient pu être estimés si nous avions varié les rotations tibiales internes conformément à nos études en compression.

La PTP étant plus importante chez les femmes que chez les hommes, elle pourrait aussi jouer, en tant que paramètre intrinsèque, un rôle crucial dans cette disparité (Hashemi et al., 2008; Hashemi et al., 2009, 2010; Hohmann et al., 2010; Todd et al., 2010). Un tel paramètre peut donc être utilisé comme marqueur pour identifier les individus à risque plus élevé et pour une prévention et une gestion plus efficaces des lésions du LCA.

9.2.2 Centre de contact

Outre la période de réception au début de la phase d'appui (0 et 5%) et due principalement aux rotations d'adduction, le plateau médial est le plateau qui supporte le plus de charge avec une contribution plus prononcée de la partie non-couverte par les ménisques (cartilage-cartilage). Une constations qui est en accord avec les études antérieures (Kumar, Manal, & Rudolph, 2013; Kutzner et al., 2010; Neptune et al., 2004; K.B. Shelburne et al., 2006; Zhao et al., 2007b). Deux pics de contact ont eu lieu à 25 et à 75% de la phase d'appui atteignant un maximum de 4 fois le poids du corps, une valeur supérieure à celles mesurées in vivo (2,5 à 3 fois le poids du corps) chez des patients avec des implants de genou instrumenté (Kutzner et al., 2010).

Dans les modèles intacts et OA à des périodes de 25 à 100%, la position du centre de contact (CC-Ref) par rapport au début de la phase (0 et 5%) se déplace médialement et postérieurement en accord aux rotations d'adduction et de flexion, respectivement. De plus, en

raison de la rotation interne du tibia, durant la phase d'appui de la marche, les CC sont plus antérieurs sur le plateau médial par rapport au plateau latéral. Il convient de souligner que les valeurs des FC et CC sur chaque plateau tibial et les changements qui y sont liés sont directement dues à la contribution passive du genou dans le soutien des moments externes de l'articulation (H Marouane et al., 2015a). Une résistance passive plus élevée diminue les forces musculaires qui traversent l'articulation et donc les forces de contacts articulaires.

Durant la phase d'appui de la marche, le déplacement global du CC-Ref est beaucoup plus important sur le plateau médial que sur le plateau latéral dans les deux directions ML (17mm contre <4 mm) et AP (10 mm vs 8 mm). Ces excursions plus grandes sur le plateau médial, comparativement à son homologue latéral, concordent avec les travaux antérieurs; selon lesquels le centre de rotation du genou est sur le côté latéral pendant la plupart du temps pendant la phase d'appui de la marche (Koo & Andriacchi, 2008; Wang et al., 2014).

L'excursion ML substantielle de CC-Ref durant la phase d'appui de la marche, en particulier sur le plateau médial, suscite l'inquiétude sur l'hypothèse d'une localisation ML fixe faite dans les modèles MS d'OpenSim initialement développés par Delp et al., (1990). L'écart entre la position ML du CC-Ref et celle du CP sur le plateau latéral est d'environ 6 mm (avec une moyenne de ~ 4 mm sur les deux plateaux). Des études antérieures ont rapporté des changements importants (jusqu'à 63%) dans les FC, calculées sur les deux plateaux médial et latéral, lorsqu'on utilise des CC plus précis plutôt qu'un emplacement ML fixe comme celui utilisé dans le modèle CP de Lerner et al., (2015). Les résultats actuels ainsi que les résultats antérieurs (Lerner et al., 2015) remettent en question l'utilisation d'un emplacement ML fixe de CC dans l'algorithme CP lorsqu'on estime des FC médiales et latérales (Gerus et al., 2013; Zhao, Banks, D'Lima, Colwell, & Fregly, 2007a).

9.2.3 Modèles 3D contre 2D

Dans les modèles MS de l'extrémité inférieure, l'articulation de la hanche est généralement modélisée comme une rotule 3D (Arnold et al., 2010; Delp et al., 2007; Horsman et al., 2007) ou plus simplement comme une articulation charnière dans le plan (KB Shelburne & Pandy, 1998; Kevin B Shelburne & Pandy, 1997, 2002). L'articulation du genou, quant à elle, est souvent considérée comme une articulation planaire dans les modèles MS de l'extrémité inférieure (Delp et al., 1990; Horsman et al., 2007; Sandholm et al., 2011). Bien que la capacité

d'une articulation charnière de la hanche à reproduire la même cinématique et cinétique comme celle d'une articulation 3D a été indiquée (Xiao & Higginson, 2008), des grandes différences ont été trouvées lors de l'idéalisation de l'articulation du genou comme une simple articulation dans le plan (Kim et al., 2009; Taylor et al., 2004). Un modèle hybride MS de l'extrémité inférieure, semblable à celui utilisé dans nos études, possède la puissance de contourner les hypothèses inhérentes de ces modèles planaires par une représentation détaillée de l'articulation du genou.

En simulant l'articulation du genou comme un joint 2D, sans considérer les rotations et les équations d'équilibre dans les plans frontal et transversal, les forces musculaires diminuent considérablement, en moyenne par 48, 44 et 16% pour les quadriceps, les Ischio-jambiers et les gastrocnemii, respectivement. En accordance, les forces totales de contact TF diminuent dans le modèle 2D à toutes les périodes de posture comparativement au modèle 3D de référence. Valente et al. (2015) ont rapporté des valeurs plus grande de la force de contact, avec un maximum de 2.4BW, lorsque une articulation sphérique 3D a été employée au lieu d'une articulation charnière. Ceci est dû principalement au fait qu'à la fois les rotations et les moments varus/valgus et interne/externe ont été négligés dans le modèle 2D.

Les fores de contact TF ont été affectées considérablement en utilisant le modèle 1D, comparativement au modèle 2D. Ces différences sont dues à la fois à la résistance passive de l'articulation du genou dans le plan frontal (H Marouane et al., 2015a) ainsi qu'à l'erreur d'idéalisation en supposant des centres de contact fixes. En utilisant le modèle 1D nos forces de contact à 25 et à 75% (les deux pics de contact) de la phase d'appui sont respectivement 2BW et 1,6BW sur le plateau médial et 1,6BW et 0,8BW sur le plateau latéral, ce qui est en accord avec les prédictions de Winby et al., (2009) qui ont rapporté des forces de contact de 2,5 ± 0,5BW et 1,9 ± 0,3BW sur le plateau médial et 1,5 ± 0,5BW et 0,9 ± 0,7BW sur le plateau latéral à 25 et 75% de la phase d'appui, respectivement. Toutefois, les résultats du modèle 1D sont assez dépendants à la position des points de contact. Ici nous avons utilisé la même méthodologie que Winby et al., (2009). La prise de différents points de contact sur le plan frontal (Kumar et al., 2012; Lerner et al., 2015; Manal & Buchanan, 2013; Miller et al., 2015; Sandholm et al., 2011) peut avoir des effets significatifs sur les résultats du modèle 1D.

9.2.4 Rotations versus moments Varus Valgus

La variation de la rotation varus / valgus (avec moment varus/valgus constant) a un effet considérable sur la répartition des forces musculaires et des forces de contact. Durant toute la phase d'appui, les forces des hamstrings latéraux diminuent et celles des hamstrings médiaux augmentent en augmentant la rotation varus. En accordance, les forces de contact médial augmentent et celles latérales diminuent avec une rotation varus plus grande. Une tendance inverse est observée en diminuant la rotation varus. Ces changements étant suite à des variations de la contribution du moment passif dans l'équilibre total de l'articulation du genou dans le plan frontal (Lloyd & Buchanan, 2001) pourront expliquer la réponse silencieuse des hamstrings latéraux rapporté dans les études antérieures (Besier et al., 2009; K.B. Shelburne et al., 2006; C. R. Winby et al., 2009). La variation du moment adduction/abduction (avec rotations constantes) a causé des variations beaucoup plus petites et moins cohérentes.

Le rapport de la force de contact médial/latéral augmente considérablement avec la rotation varus et a atteint ses valeurs extrêmes (minimum-maximum) de 0,1-2,4 à 0% (HS), 0,2-1,2 à 5%, 0,8-10,6 à 25%, 1,7-90 à 50%, 1,3-6,4 à 75% et finalement 0,7-∞ (infini) a 100% (TO) de la phase d'appui de la marche sous les valeurs min-max de la rotation varus (avec moments constants). Ces résultats soulignent clairement l'importance de la rotation adduction dans la détermination de la répartition de la charge entre les plateaux médial et latéral de l'articulation du genou. Pour réduire les charges de contact du côté médial, il faut donc contrôler l'alignement du genou par des rotations d'adduction-abduction. Les résultats indiquent qu'une distribution de charge de contact plus uniforme entre les plateaux TF ne peut être atteinte qu'en augmentant la rotation adduction au début de la phase d'appui (0 et 5%) et en diminuant cette rotation par la suite (de 25 à 100%). Ceci pourrait expliquer la répartition équilibrée entre les deux plateaux du tibia dans les études de Mononen et al., (2013, 2015). L'effet du changement du moment adduction/abduction est beaucoup moins prononcé à cet égard. Les présents résultats soulignent également l'importance d'une acquisition précise de la rotation adduction / abduction de l'articulation du genou dans diverses activités.

Nos résultats sont en accord avec les résultats antérieurs (Lerner et al., 2015; Tetsworth & Paley, 1994; Wong et al., 2011). Wong et al. (2011) ont rapporté qu'une augmentation par 3 à 5° de l'alignement varus entraîne une augmentation de 50% de la force transmise à travers le plateau médial. Tetsworth et Paley (1994) ont rapporté une augmentation de 20% de la charge du plateau

médial avec une augmentation de 5° de l'alignement varus. Lerner et al. (2015) ont estimé une augmentation de 51 N dans le pic de la force de contact médiale pour chaque augmentation de 1° de l'alignement varus. Nos résultats montrent toutefois des changements plus drastiques avec des augmentations moyennes de ~ 168N et de 201N pour chaque augmentation de 1° de la rotation varus au premier (25%) et au second (75%) pic, respectivement. Cette différence pourrait être en partie due à l'algorithme de point de contact fixe utilisé dans l'étude de Lerner et al. (2015) puisque selon notre étude précédente, les forces de contact sont sensibles à l'emplacement des points de contact dans le plan frontal.

Le moment varus du genou est généralement considéré comme la cause primaire pour le chargement du plateau médial et ainsi sa réduction permet de contrôler la distribution de charge sur le plateau TF (Gaasbeek, Groen, Hampsink, Van Heerwaarden, & Duysens, 2007; Shakoor & Block, 2006; Zhao et al., 2007b). À l'aide d'implants instrumentés du genou, Meyer et al. (2013) et Walter et al. (2010), ont remis en question une telle association entre le moment varus et la répartition de la charge médiale-latérale. Ainsi, nos prédictions concordent avec d'autres études (Hewett, Noyes, Barber-Westin, & Hedcmann, 1998; Lindenfeld, Hewett, & Andriacchi, 1997; A. J. Meyer et al., 2013; Walter, D'Lima, Colwell, & Fregly, 2010) pour refuser cette hypothèse.

9.3 Limitations

La méthode des éléments finis offre une méthode polyvalente pour analyser les problèmes biomécaniques complexes. Cependant, les modèles MS et éléments finis nécessitent certaines hypothèses et ont des limitations qui doivent être considérés et reconnus lors de l'interprétation des résultats. Par exemple, certaines hypothèses ont été faites sur les lois de comportement régissant le comportement des différentes structures. Ces hypothèses sont assez communes dans les modèles d'éléments finis et sont jugées acceptables, mais cela n'empêche pas que lors de l'évaluation des résultats du présent travail, les limites inhérentes à l'utilisation du modèle EF doivent être prises en compte. Par exemple:

- Ce travail étudie la réponse statique et à court terme du joint. Malgré le fait que les moments externes des joints sont évalués avec la méthode de dynamique inverse et donc tient compte de l'inertie du corps en mouvement, le modèle des éléments finis est statique. La réponse est applicable et bonne à court terme en phase transitoire de ce qu'on attend durant la marche.

Dans ce cas, les cartilages et les ménisques peuvent être représentés par des matériaux élastiques incompressibles au lieu des matériaux poroélastiques (biphasiques).

- La géométrie et l'anatomie musculaire du genou, variables d'un sujet à l'autre selon le sexe, l'âge, la taille, le poids, l'activité physique et aussi selon le degré de dégénérescence de l'articulation, influencent les résultats d'une manière quantitative mais pas les conclusions.
- Lors de l'analyse de l'effet de la géométrie tibiale (PTP) et les moments/rotations varus/valgus, le reste de la structure et les données cinématiques ainsi que cinétiques ont été laissés inchangés entre les différentes conditions d'essai pour faire sortir l'effet d'un seul paramètre à la fois.
- À noter aussi que toute variation des propriétés mécaniques des matériaux, prise dans la littérature pour les couches de cartilage, la matrice méniscale et les ligaments, peut affecter les résultats d'une manière quantitative.
- Les données cinématiques et cinétiques de la marche utilisées dans ce modèle hybride MS étaient basées sur les valeurs moyennes des résultats rapportés par Astephen et al., (2007); une étude jugé la plus complète dans la littérature (60 sujets asymptomatiques/OA cinématique/cinétique de la hanche/genou/cheville, EMG). Uniquement la force de réaction du sol provient d'une autre étude. Toutefois, la concordance entre les deux études est assurée par le fait que la force de réaction est appliquée à la position où on génère les moments de la première étude.

CHAPITRE 10 CONCLUSION ET RECOMMANDATIONS

10.1 Conclusion

L'effet de la PTP sur la biomécanique de l'articulation du genou et sur le chargement du LCA a été étudié par un modèle hybride MS durant la phase d'appui de la marche et par un modèle passif sous l'action d'une force de compression allant jusqu'à 1400N appliquée à différents angles de flexion. Le modèle MS est aussi utilisé pour étudier l'effet de la représentation 2D du joint du genou sur la réponse de l'articulation durant la marche en comparant cela avec la réponse 3D. L'effet de la variation de la rotation ou du moment varus/valgus sur les chargements internes et les forces de contact a été étudié également durant la marche. Finalement, la position du centre de contact du genou durant la marche a été recherchée. Plusieurs conclusions peuvent être tirées de ces travaux:

- La pente tibiale postérieure est un facteur de risque pour la lésion du LCA. Une PTP plus grande en présence d'une force de compression importante favorise une translation antérieure plus grande du tibia par rapport au fémur et donc augmente la force du LCA et ainsi sa vulnérabilité aux blessures. Cette constatation pourrait expliquer le pourcentage élevé de la lésion du LCA chez les femmes, qui ont une PTP plus grande, comparativement aux hommes.
- Durant la phase d'appui de la marche, une augmentation de la PTP des deux plateaux tibiaux ou du plateau qui porte le plus de charge (plateau latéral à 0 et 5%; plateau médial de 25 à 100%), augmente significativement la translation antérieur du tibia par rapport au fémur et donc la force du LCA (principalement le faisceau LCA-pl). Au contraire, une diminution de la PTP protège le LCA; en diminuant à la fois la translation antérieure du tibia et la force du LCA.
- La PTP est un facteur de risque important, en particulier chez les femmes et dans les activités avec de fortes forces de compression, ce qui augmente considérablement la force du LCA et sa vulnérabilité aux blessures. Les futurs programmes de formation et de prévention des blessures du LCA pourraient bénéficier de ces résultats.
- Les forces de contact sont plus élevées sur le plateau latéral au début de la phase d'appui de la marche, et sur le plateau médial pour le reste (du 25 à 100%). La position du centre de contact change significativement durant la marche, en particulier sur le plateau médial dans la direction medio-latéral.

- La considération du genou comme une articulation plane dans le plan sagittal, sans résistance passive et avec des centres de contact fixes modifient substantiellement les forces musculaires, la force du LCA, les forces de contact TF, la pression de contact sur les cartilages et les centres de contact sur chaque plateau.
- Le partage inter-compartimental relatif des charges de contact est fortement influencé par les changements de la rotation varus/valgus, mais reste peu sensible aux variations du moment varus/valgus. Ces résultats expliquent la mauvaise corrélation entre le moment varus et le déchargement du plateau médial pendant la marche suggérant que le partage de la charge interne est dicté par les changements de la rotation varus/valgus et non pas par le moment varus/valgus. Un enregistrement précis des rotations varus/valgus est assez important.
- Et comme conclusion générale des travaux menés: un modèle EF détaillé de l'articulation du genou combiné avec un modèle MS des membres inférieurs (c.-à-d. le modèle 3D hybride MS) donne les résultats les plus précis en considérant à la fois la structure passive et active de l'articulation.

10.2 Recommandations

Comme déjà mentionné, les risques de blessure du LCA liées à la morphologie articulaire suscitent de plus en plus l'attention des chercheurs. Récemment, Wahl et al. (2012) ont identifié d'une façon quantitative et qualitative les différences dans la géométrie de la surface articulaire fémoro-tibiale latérale (le rayon de courbure du plateau tibial, le rayon de courbure de la partie distale du fémur et la longueur maximale antéro-postérieure du fémur et du tibia) qui peuvent aider à expliquer le risque de lésion du LCA. Les résultats suggèrent qu'il existe un phénotype géométrique à risque de la surface articulaire fémoro-tibiale latérale, caractérisé par un plateau tibial court et plus convexe relativement au fémur et par une surface plus petite et plus convexe du fémur distal, ce qui peut rendre le genou plus sensible à la lésion du LCA. Dans ce contexte également, Hashemi et al. (2010) ont trouvé qu'une PTP (médiale et latérale à la fois) plus grande, ainsi qu'une profondeur tibiale médiale plus petite peuvent être associées à un risque de blessure du LCA. Toutefois, une modélisation numérique est encore nécessaire pour étudier l'effet de la concavité médiale sur la réponse de l'articulation du genou en général et sur le chargement du LCA en particulier. Les différentes combinaisons entre PTP et concavité médiale

devront être étudiées. En outre, basé sur nos résultats de l’article varus/valgus (chapitre huit), l’effet de la pente coronale sur la réponse de l’articulation est une étude à faire.

Dans les modèles musculosquelettiques, les équations d'équilibre des moments sont généralement maintenues à l'origine du système de coordonnées articulaires placées par exemple au centre de l'axe épicondylaire fémoral pour l'articulation du genou. Les forces musculaires inconnues sont ensuite estimées à l'aide d'équations d'optimisation et de moment basés sur l'hypothèse que cette origine des axes coïncide avec le centre de réaction du joint (CoR) connu comme le point où les moments des réactions passifs disparaissent. Les forces musculaires estimées et les charges articulaires internes sont donc fortement dépendantes à la position du système de coordonnées, comme cela a été clairement démontré par des études antérieures (Guoan Li, Pierce, & Herndon, 2006; Pierce & Li, 2005). Semblable au point d'équilibre mécanique du genou (Hafedh Marouane, 2012; H Marouane et al., 2015a), le CoR n'est ni connu ni fixe car les charges et les mouvements articulaires varient, ce qui pourrait influencer d’avantage les prédictions des modèles MS. Pour obtenir des résultats précis, les équations d'équilibre des moments de réactions doivent cependant être effectuées au vrais CoR du genou, où les moments passifs sont nuls. Une étude qui nous permet de trouver ce CoR est donc nécessaire.

Enfin, la quantification de la marge de stabilité des systèmes MS humains intacts et pathologiques est cruciale dans l'évaluation du rendement, la prévention des blessures et la gestion des traitements. La stabilité dynamique de l'articulation du genou dans les activités quotidiennes est maintenue par une relation délicate entre les tissus passifs et la structure active. Dans le contexte clinique, la stabilité mécanique d'un système biologique est habituellement évaluée par son hypermobilité lorsque des laxités excessives sont détectées sous des charges et des perturbations externes. L'hypermobilité articulaire a été associée à la douleur et à l'arthrose (Mulvey et al., 2013). Quantifier la stabilité mécanique de l'articulation du genou humain durant la phase debout ou encore durant l’exercice de certaines activités physiologiques (marche, sport) est promoteusse.

BIBLIOGRAPHIE

Adouni M (2014) ANALYSE BIOMÉCANIQUE DE L'ARTICULATION DE GENOU DURANT LA BIPÉDIE HUMAINE École Polytechnique de Montréal

Adouni M, Shirazi-Adl A (2009) Knee joint biomechanics in closed-kinetic-chain exercises Computer Methods in Biomechanics and Biomedical Engineering 12:661-670

Adouni M, Shirazi-Adl A (2012b) Consideration of equilibrium equations at the hip joint alongside those at the knee and ankle joints has mixed effects on knee joint response during gait Journal of biomechanics

Adouni M, Shirazi-Adl A, Shirazi R (2012) Computational biodynamics of human knee joint in gait: From muscle forces to cartilage stresses Journal of biomechanics

Adouni M, Shirazi-Adl A, Shirazi R (2012a) Computational biodynamics of human knee joint in gait: from muscle forces to cartilage stresses Journal of biomechanics 45:2149-2156

Adouni M, Shirazi-Adl A (2014a) Evaluation of knee joint muscle forces and tissue stresses-strains during gait in severe OA versus normal subjects Journal of Orthopaedic Research 32:69-78

Agel J, Arendt EA, Bershadsky B (2005) Anterior cruciate ligament injury in National Collegiate Athletic Association basketball and soccer a 13-year review The American journal of sports medicine 33:524-531

Agneskirchner J, Hurschler C, Stukenborg-Colsman C, Imhoff A, Lobenhoffer P (2004) Effect of high tibial flexion osteotomy on cartilage pressure and joint kinematics: a biomechanical study in human cadaveric knees Archives of orthopaedic and trauma surgery 124:575-584

Ahmed A, Burke D (1983) In-vitro measurement of static pressure distribution in synovial joints--Part I: Tibial surface of the knee Journal of biomechanical engineering 105:216

Akbarshahi M, Schache AG, Fernandez JW, Baker R, Banks S, Pandy MG (2010) Non-invasive assessment of soft-tissue artifact and its effect on knee joint kinematics during functional activity Journal of Biomechanics 43:1292-1301

Alhalki MM, Howell SM, Hull ML (1999) How three methods for fixing a medial meniscal autograft affect tibial contact mechanics The American Journal of Sports Medicine 27:320-328

Allaire R, Muriuki M, Gilbertson L, Harner CD (2008) Biomechanical consequences of a tear of the posterior root of the medial meniscusSimilar to total meniscectomy The Journal of Bone & Joint Surgery 90:1922-1931

Amis A, Dawkins G (1991) Functional anatomy of the anterior cruciate ligament. Fibre bundle actions related to ligament replacements and injuries Bone & Joint Journal 73:260-267

Amis AA (2012) The functions of the fibre bundles of the anterior cruciate ligament in anterior drawer, rotational laxity and the pivot shift Knee surgery, sports traumatology, arthroscopy 20:613-620

Anderson FC, Pandy MG (2001) Dynamic optimization of human walking Journal of biomechanical engineering 123:381-390

Anderson FC, Pandy MG (2003) Individual muscle contributions to support in normal walking Gait & posture 17:159-169

Andriacchi T, Alexander E, Toney M, Dyrby C, Sum J (1998) A point cluster method for in vivo motion analysis: applied to a study of knee kinematics Journal of biomechanical engineering 120:743-749

Andriacchi TP, Alexander EJ (2000) Studies of human locomotion: past, present and future Journal of Biomechanics 33:1217-1224

Andriacchi TP, Hurwitz DE (1997) Gait biomechanics and the evolution of total joint replacement Gait & posture 5:256-264

Arendt E, Dick R (1995) Knee injury patterns among men and women in collegiate basketball and soccer NCAA data and review of literature The American journal of sports medicine 23:694-701

Arendt EA, Agel J, Dick R (1999) Anterior cruciate ligament injury patterns among collegiate men and women Journal of Athletic Training 34:86

Arjmand N, Shirazi-Adl A (2006) Sensitivity of kinematics-based model predictions to optimization criteria in static lifting tasks Medical engineering & physics 28:504-514

Arnason A, Gudmundsson A, Dahl H, Johannsson E (1996) Soccer injuries in Iceland Scandinavian journal of medicine & science in sports 6:40-45

Arnold EM, Ward SR, Lieber RL, Delp SL (2010) A model of the lower limb for analysis of human movement Annals of Biomedical Engineering 38:269-279

Astephen JL (2007a) Biomechanical Factors in the Progression of Knee Osteoarthritis. Ph.D, School of Biomedical Engineering, Dalhousie University, Halifax.

Astephen JL (2007b) Biomechanical Factors in the Progression of Knee Osteoarthritis. School of Biomedical Engineering, Dalhousie University, Halifax

Astephen JL, Deluzio KJ, Caldwell GE, Dunbar MJ (2008) Biomechanical changes at the hip, knee, and ankle joints during gait are associated with knee osteoarthritis severity Journal of Orthopaedic Research 26:332-341

Atkinson P, Atkinson T, Huang C, Doane R A comparison of the mechanical and dimensional properties of the human medial and lateral patellofemoral ligaments. In, 2000.

Bendjaballah MZ, Shirazi-Adl A, Zukor D (1995) Biomechanics of the human knee joint in compression: reconstruction, mesh generation and finite element analysis The Knee 2:69-79

Bendjaballah MZ, Shirazi-Adl A, Zukor D (1997) Finite element analysis of human knee joint in varus-valgus Clinical Biomechanics 12:139-148

Bendjaballah MZ, Shirazi-Adl A, Zukor D (1998) Biomechanical response of the passive human knee joint under anterior-posterior forces Clinical Biomechanics 13:625-633

Blagojevic M, Jinks C, Jeffery A, Jordan K (2010) Risk factors for onset of osteoarthritis of the knee in older adults: a systematic review and meta-analysis Osteoarthritis and Cartilage 18:24-33

Blankevoort L, Huiskes R (1991c) Ligament-bone interaction in a three-dimensional model of the knee J Biomech Eng 113:263-269

Blankevoort L, Kuiper J, Huiskes R, Grootenboer H (1991a) Articular contact in a three-dimensional model of the knee Journal of biomechanics 24:1019-1031

Boakes JL, Rab GT (2006) Muscle activity during walking Human Walking Lippincott Williams and Wilkins

Boden BP, Breit I, Sheehan FT (2009a) Tibiofemoral alignment: contributing factors to noncontact anterior cruciate ligament injury The Journal of Bone & Joint Surgery 91:2381-2389

Bouisset S (2002) Biomécanique et physiologie du mouvement. Elsevier Masson,

Brandon ML, Haynes PT, Bonamo JR, Flynn MI, Barrett GR, Sherman MF (2006) The association between posterior-inferior tibial slope and anterior cruciate ligament insufficiency Arthroscopy: The Journal of Arthroscopic & Related Surgery 22:894-899

Brazier J, Migaud H, Gougeon F, Cotten A, Fontaine C, Duquennoy A (1996) Evaluation of methods for radiographic measurement of the tibial slope. A study of 83 healthy knees] Revue de chirurgie orthopédique et réparatrice de l'appareil moteur 82:195

Brinckmann P, Frobin W, Leivseth G (2002) Musculoskeletal biomechanics. Thieme,

Broom N, Marra D (1986) Ultrastructural evidence for fibril-to-fibril associations in articular cartilage and their functional implication Journal of anatomy 146:185

Brown TD, Shaw DT (1984) In vitro contact stress distribution on the femoral condyles Journal of orthopaedic research 2:190-199

Calmbach WL, Hutchens M (2003) Evaluation of patients presenting with knee pain: Part I. History, physical examination, radiographs, and laboratory tests American family physician 68:907-912

Cappozzo A, Marchetti M, Tosi V (1992) Biolocomotion: a century of research using moving pictures vol 1. Promograph,

Chao E, Laughman R, Schneider E, Stauffer R (1983) Normative data of knee joint motion and ground reaction forces in adult level walking Journal of Biomechanics 16:219-233

Chaudhari AM, Zelman EA, Flanigan DC, Kaeding CC, Nagaraja HN (2009) Anterior Cruciate Ligament–Injured Subjects Have Smaller Anterior Cruciate Ligaments Than Matched

Controls A Magnetic Resonance Imaging Study The American Journal of Sports Medicine 37:1282-1287

Chen C-H, Li J-S, Hosseini A, Gadikota HR, Kozanek M, Gill TJ, Li G Tibiofemoral Kinematics of the Knee During the Stance Phase of Gait After ACL Deficiency. In: ASME 2011 Summer Bioengineering Conference, 2011. American Society of Mechanical Engineers, pp 663-664

Chiu K, Zhang S, Zhang G (2000) Posterior slope of tibial plateau in Chinese The Journal of arthroplasty 15:224-227

Clarke I (1974) Articular cartilage: a review and scanning electron microscope study. II. The territorial fibrillar architecture Journal of anatomy 118:261

Crowninshield R, Pope M, Johnson R (1976) An analytical model of the knee Journal of biomechanics 9:397-405

Dahlstedt S (1978) Slow pedestrians: walking speeds and walking habits of old aged people Stockholm: The Swedish Council for Building Researd, Report 2:1977

Daniel DM, Stone ML, Dobson BE, Fithian DC, Rossman DJ, Kaufman KR (1994) Fate of the ACL-injured patient a prospective outcome study The American journal of sports medicine 22:632-644

de Boer JJ, Blankevoort L, Kingma I, Vorster W (2009) In vitro study of inter-individual variation in posterior slope in the knee joint Clinical Biomechanics 24:488-492

De Leva P (1996) Adjustments to Zatsiorsky-Seluyanov's segment inertia parameters Journal of Biomechanics 29:1223-1230

Dejour H, Bonnin M (1994) Tibial translation after anterior cruciate ligament rupture. Two radiological tests compared Journal of Bone & Joint Surgery, British Volume 76:745-749

Delp SL et al. (2007) OpenSim: open-source software to create and analyze dynamic simulations of movement Biomedical Engineering, IEEE Transactions on 54:1940-1950

Delp SL, Loan JP, Hoy MG, Zajac FE, Topp EL, Rosen JM (1990) An interactive graphics-based model of the lower extremity to study orthopaedic surgical procedures Biomedical Engineering, IEEE Transactions on 37:757-767

DeMers MS, Pal S, Delp SL (2014) Changes in tibiofemoral forces due to variations in muscle activity during walking Journal of Orthopaedic Research 32:769-776

Dennis DA, Mahfouz MR, Komistek RD, Hoff W (2005) In vivo determination of normal and anterior cruciate ligament-deficient knee kinematics Journal of biomechanics 38:241-253

Dujardin F, Roussignol X, Mejjad O, Weber J, Thomine J (1997) Interindividual variations of the hip joint motion in normal gait Gait & posture 5:246-250

Duthon V, Barea C, Abrassart S, Fasel J, Fritschy D, Ménétrey J (2006) Anatomy of the anterior cruciate ligament Knee surgery, sports traumatology, arthroscopy 14:204-213

Dyrby CO, Andriacchi TP (2004) Secondary motions of the knee during weight bearing and non-weight bearing activities Journal of Orthopaedic Research 22:794-800

Eng JJ, Winter DA (1995) Kinetic analysis of the lower limbs during walking: what information can be gained from a three-dimensional model? Journal of Biomechanics 28:753-758

Fairbank T (1948) Knee joint changes after meniscectomy Journal of Bone & Joint Surgery, British Volume 30:664-670

Fening SD, Kovacic J, Kambic H, McLean S, Scott J, Miniaci A (2008) The effects of modified posterior tibial slope on acl strain and knee kinematics: a human cadaveric study The journal of knee surgery 21:205

Fithian DC, Kelly MA, Mow VC (1990) Material properties and structure-function relationships in the menisci Clinical orthopaedics and related research:19

Fleming BC, Renstrom PA, Beynnon BD, Engstrom B, Peura GD, Badger GJ, Johnson RJ (2001) The effect of weightbearing and external loading on anterior cruciate ligament strain Journal of biomechanics 34:163-170

Fraysse F (2009) Estimation des activités musculaires au cours du mouvement en vue d'applications ergonomiques. Université Claude Bernard-Lyon I

Fukubayashi T, Kurosawa H (1980) The contact area and pressure distribution pattern of the knee: a study of normal and osteoarthrotic knee joints Acta Orthopaedica 51:871-879

Gao B, Zheng NN (2010) Alterations in three-dimensional joint kinematics of anterior cruciate ligament-deficient and -reconstructed knees during walking Clinical Biomechanics 25:222-229

Genin P, Weill G, Julliard R (1993) [The tibial slope. Proposal for a measurement method] Journal de radiologie 74:27

Geoffrey K, Franz JR, Dicharry J, Croce UD, Kerrigan DC (2011) Lower limb joint kinetics in walking: The role of industry recommended footwear Gait & posture 33:350-355

Gerus P et al. (2013) Subject-specific knee joint geometry improves predictions of medial tibiofemoral contact forces Journal of Biomechanics 46:2778-2786

Giffin JR, Vogrin TM, Zantop T, Woo SL, Harner CD (2004) Effects of increasing tibial slope on the biomechanics of the knee The American Journal of Sports Medicine 32:376-382

Grood E, Hefzy M (1982) An analytical technique for modeling knee joint stiffness--Part I: Ligamentous forces Journal of biomechanical engineering 104:330

Grood ES, Suntay WJ (1983a) A joint coordinate system for the clinical description of three-dimensional motions: application to the knee Journal of biomechanical engineering 105:136-144

Grood ES, Suntay WJ (1983b) A joint coordinate system for the clinical description of three-dimensional motions: application to the knee Journal of biomechanical engineering 105:136

Guilak F (2011) Biomechanical factors in osteoarthritis Best practice & research Clinical rheumatology 25:815-823

Halonen K, Mononen M, Töyräs J, Kröger H, Joukainen A, Korhonen R (2016) Optimal graft stiffness and pre-strain restore normal joint motion and cartilage responses in ACL reconstructed knee Journal of Biomechanics

Hashemi J et al. (2008) The geometry of the tibial plateau and its influence on the biomechanics of the tibiofemoral joint The Journal of Bone & Joint Surgery 90:2724-2734

Hashemi J et al. (2009) Shallow Medial Tibial Plateau and Steep Medial and Lateral Tibial Slopes New Risk Factors for Anterior Cruciate Ligament Injuries The American Journal of Sports Medicine 38:54-62

Hashemi J et al. (2010) Shallow medial tibial plateau and steep medial and lateral tibial slopes new risk factors for anterior cruciate ligament injuries The American journal of sports medicine 38:54-62

Haut Donahue TL, Hull M (2002) A finite element model of the human knee joint for the study of tibio-femoral contact Journal of Biomechanical Engineering 124:273

Haut Donahue TL, Hull M, Rashid MM, Jacobs CR (2003) How the stiffness of meniscal attachments and meniscal material properties affect tibio-femoral contact pressure computed using a validated finite element model of the human knee joint Journal of biomechanics 36:19-34

Hernigou P, Goutallier D (1990) Usure osseuse sous-chondrale des plateaux tibiaux dans les gonarthroses fémoro-tibiales Rev du Rhumat 57:67-72

HOFMANN AA, BACHUS KN, WYATT RW (1991) Effect of the tibial cut on subsidence following total knee arthroplasty Clinical orthopaedics and related research 269:63-69

Hohmann E, Bryant A, Reaburn P, Tetsworth K (2010) Does Posterior Tibial Slope Influence Knee Functionality in the Anterior Cruciate Ligament–Deficient and Anterior Cruciate Ligament–Reconstructed Knee? Arthroscopy: The Journal of Arthroscopic & Related Surgery 26:1496-1502

Horsman MK, Koopman H, Veeger H, van der Helm F (2007) The Twente Lower Extremity Model: a comparison of maximal isometric moment with the literature The Twente Lower Extremity Model:65

Huang A, Hull M, Howell SM (2003) The level of compressive load affects conclusions from statistical analyses to determine whether a lateral meniscal autograft restores tibial contact pressure to normal: a study in human cadaveric knees Journal of orthopaedic research 21:459-464

Hughes PE, Hsu JC, Matava MJ (2002) Hip anatomy and biomechanics in the athlete Sports medicine and arthroscopy review 10:103-114

Hunt AE, M Smith R, Torode M, Keenan A-M (2001a) Inter-segment foot motion and ground reaction forces over the stance phase of walking Clinical Biomechanics 16:592-600

Hunt AE, Smith RM, Torode M, Keenan A-M (2001b) Inter-segment foot motion and ground reaction forces over the stance phase of walking Clinical Biomechanics 16:592-600

Hunt MA, Birmingham TB, Giffin JR, Jenkyn TR (2006) Associations among knee adduction moment, frontal plane ground reaction force, and lever arm during walking in patients with knee osteoarthritis Journal of Biomechanics 39:2213-2220

Hurwitz DE, Sumner DR, Andriacchi TP, Sugar DA (1998) Dynamic knee loads during gait predict proximal tibial bone distribution Journal of Biomechanics 31:423-430

Hutchinson MR, Ireland ML (1995) Knee injuries in female athletes Sports medicine 19:288-302

Jiang C, Yip K, Liu T (1994) Posterior slope angle of the medial tibial plateau Journal of the Formosan Medical Association 93:509-512

Jones H, Rocha PC (2012) Prevention in ACL Injuries. In: Sports Injuries. Springer, pp 33-42

Julliard R, Genin P, Weil G, Palmkrantz P (1993) The median functional slope of the tibia. Principle. Technique of measurement. Value. Interest Rev Chir Orthop Reparatrice Appar Mot 79:625-634

Kääb M, Ap Gwynn I, Nötzli H (1998) Collagen fibre arrangement in the tibial plateau articular cartilage of man and other mammalian species Journal of anatomy 193:23-34

Kadaba MP, Ramakrishnan H, Wootten M (1990) Measurement of lower extremity kinematics during level walking Journal of orthopaedic research 8:383-392

Kapandji A (1994) Physiologie articulaire. Tome 2, schémas commentés de mécanique humaine, le membre inférieur. Edition Maloine,

Kaufman KR, Sutherland DH (2006) Kinematics of normal human walking Human walking 3:33-52

Kawamura S, Lotito K, Rodeo SA (2003) Biomechanics and healing response of the meniscus Operative Techniques in Sports Medicine 11:68-76

Kazemi M, Li L (2014) A viscoelastic poromechanical model of the knee joint in large compression Medical Engineering & Physics 36:998-1006

Keller T, Weisberger A, Ray J, Hasan S, Shiavi R, Spengler D (1996) Relationship between vertical ground reaction force and speed during walking, slow jogging, and running Clinical Biomechanics 11:253-259

Kim HJ, Fernandez JW, Akbarshahi M, Walter JP, Fregly BJ, Pandy MG (2009) Evaluation of predicted knee-joint muscle forces during gait using an instrumented knee implant Journal of Orthopaedic Research 27:1326-1331

Koay E, Athanasiou K (2009) ARTICULAR CARTILAGE BIOMECHANICS, MECHANOBIOLOGY, AND TISSUE ENGINEERING. In: Biomechanical Systems Technology: Volume 3: Muscular Skeletal Systems. pp 1-37

Koo S, Andriacchi TP (2008) The knee joint center of rotation is predominantly on the lateral side during normal walking Journal of biomechanics 41:1269-1273

Kozanek M, Hosseini A, Liu F, Van de Velde SK, Gill TJ, Rubash HE, Li G (2009) Tibiofemoral kinematics and condylar motion during the stance phase of gait Journal of biomechanics 42:1877-1884

Krause W, Pope M, Johnson R, Wilder D (1976) Mechanical changes in the knee after meniscectomy The Journal of bone and joint surgery American volume 58:599

Kumar D, Rudolph KS, Manal KT (2012) EMG-driven modeling approach to muscle force and joint load estimations: Case study in knee osteoarthritis Journal of Orthopaedic Research 30:377-383

Kurosawa H, Fukubayashi T, Nakajima H (1980) Load-bearing mode of the knee joint: physical behavior of the knee joint with or without menisci Clinical orthopaedics and related research:283

Kutzner I et al. (2010) Loading of the knee joint during activities of daily living measured in vivo in five subjects Journal of biomechanics 43:2164-2173

Kuwano T et al. (2005) Importance of the lateral anatomic tibial slope as a guide to the tibial cut in total knee arthroplasty in Japanese patients Journal of Orthopaedic Science 10:42-47

Lafortune M, Cavanagh P, Sommer Iii H, Kalenak A (1992) Three-dimensional kinematics of the human knee during walking Journal of Biomechanics 25:347-357

Landry SC, McKean KA, Hubley-Kozey CL, Stanish WD, Deluzio KJ (2007) Knee biomechanics of moderate OA patients measured during gait at a self-selected and fast walking speed Journal of Biomechanics 40:1754-1761

Lee SJ et al. (2006) Tibiofemoral contact mechanics after serial medial meniscectomies in the human cadaveric knee The American Journal of Sports Medicine 34:1334-1344

Lephart S, Ferris C, Fu F (2002) Risk factors associated with noncontact anterior cruciate ligament injuries in female athletes INSTRUCTIONAL COURSE LECTURES-AMERICAN ACADEMY OF ORTHOPAEDIC SURGEONS 51:307-310

Lerner ZF, Board WJ, Browning RC (2015b) Pediatric obesity and walking duration increase medial tibiofemoral compartment contact forces Journal of Orthopaedic Research

Lerner ZF, DeMers MS, Delp SL, Browning RC (2015) How tibiofemoral alignment and contact locations affect predictions of medial and lateral tibiofemoral contact forces Journal of biomechanics 48:644-650

Lerner ZF, Haight DJ, DeMers MS, Board WJ, Browning RC (2014) The effects of walking speed on tibiofemoral loading estimated via musculoskeletal modeling Journal of applied biomechanics 30:197

Levy IM, Torzilli P, Gould J, Warren R (1989) The effect of lateral meniscectomy on motion of the knee J Bone Joint Surg Am 71:401-406

Levy IM, Torzilli P, Warren R (1982) The effect of medial meniscectomy on anterior-posterior motion of the knee J Bone Joint Surg Am 64:883-888

Li G, DeFrate LE, Park SE, Gill TJ, Rubash HE (2005) In Vivo Articular Cartilage Contact Kinematics of the Knee An Investigation Using Dual-Orthogonal Fluoroscopy and Magnetic Resonance Image–Based Computer Models The American Journal of Sports Medicine 33:102-107

Li G, Gil J, Kanamori A, Woo S-Y (1999) A validated three-dimensional computational model of a human knee joint Journal of biomechanical engineering 121:657-662

Li G, Kozanek M, Hosseini A, Liu F (2009) New fluoroscopic imaging technique for investigation of 6DOF knee kinematics during treadmill gait Journal of Orthopaedic Surgery and Research 4:1-5

Li G, Moses JM, Papannagari R, Pathare NP, DeFrate LE, Gill TJ (2006a) Anterior cruciate ligament deficiency alters the in vivo motion of the tibiofemoral cartilage contact points in both the anteroposterior and mediolateral directions The Journal of Bone & Joint Surgery 88:1826-1834

Li G, Pierce JE, Herndon JH (2006b) A global optimization method for prediction of muscle forces of human musculoskeletal system Journal of biomechanics 39:522-529

Li G, Suggs J, Gill T (2002) The effect of anterior cruciate ligament injury on knee joint function under a simulated muscle load: a three-dimensional computational simulation Annals of biomedical engineering 30:713-720

Liu-Barba D, Hull M, Howell S (2007) Coupled motions under compressive load in intact and ACL-deficient knees: a cadaveric study TRANSACTIONS-AMERICAN SOCIETY OF MECHANICAL ENGINEERS JOURNAL OF BIOMECHANICAL ENGINEERING 129:818

Liu W, Maitland ME (2003) Influence of anthropometric and mechanical variations on functional instability in the ACL-deficient knee Annals of biomedical engineering 31:1153-1161

Lloyd DG, Besier TF (2003) An EMG-driven musculoskeletal model to estimate muscle forces and knee joint moments in vivo Journal of Biomechanics 36:765-776

Logan M, Dunstan E, Robinson J, Williams A, Gedroyc W, Freeman M (2004) Tibiofemoral kinematics of the anterior cruciate ligament (ACL)-deficient weightbearing, living knee employing vertical access open “interventional” multiple resonance imaging The American journal of sports medicine 32:720-726

Lohmander L, Östenberg A, Englund M, Roos H (2004) High prevalence of knee osteoarthritis, pain, and functional limitations in female soccer players twelve years after anterior cruciate ligament injury Arthritis & Rheumatism 50:3145-3152

Manal K, Buchanan TS (2013) An electromyogram-driven musculoskeletal model of the knee to predict in vivo joint contact forces during normal and novel gait patterns Journal of Biomechanical Engineering 135:021014

Marey E (1884) Analyse cinématique de la marche [chronophotograph] CR Séances Acad Sci:2

Markolf K, Mensch J, Amstutz H (1976) Stiffness and laxity of the knee--the contributions of the supporting structures. A quantitative in vitro study The Journal of bone and joint surgery American volume 58:583

Markolf KL, Burchfield DM, Shapiro MM, Shepard MF, Finerman GAM, Slauterbeck JL (1995) Combined knee loading states that generate high anterior cruciate ligament forces Journal of Orthopaedic Research 13:930-935

Markolf KL, Gorek JF, Kabo JM, Shapiro MS (1990) Direct measurement of resultant forces in the anterior cruciate ligament J Bone Joint Surg Am 72:557-567

Markolf KL, Jackson SR, Foster B, McAllister DR (2013) ACL forces and knee kinematics produced by axial tibial compression during a passive flexion–extension cycle Journal of Orthopaedic Research

Markolf KL, Park S, Jackson SR, McAllister DR (2009) Anterior-posterior and rotatory stability of single and double-bundle anterior cruciate ligament reconstructions The Journal of Bone & Joint Surgery 91:107-118

Marouane H (2012) Effet de la force de compression sur la réponse passive de l'articulation du genou: une étude numérique non-linéaire. École Polytechnique de Montréal

Marouane H, Shirazi-Adl A, Adouni M (2013) Knee joint passive stiffness and moment in sagittal and frontal planes markedly increase with compression Computer methods in biomechanics and biomedical engineering:1-12

Marouane H, Shirazi-Adl A, Adouni M (2015a) Knee joint passive stiffness and moment in sagittal and frontal planes markedly increase with compression Computer Methods in Biomechanics and Biomedical Engineering 18:339-350

Marouane H, Shirazi-Adl A, Adouni M (2016a) 3D Active-Passive Response of Human Knee Joint in Gait is Markedly Altered When Simulated as a Planar 2D Joint Biomechanics and Modeling in Mechanobiology:1-11

Marouane H, Shirazi-Adl A, Adouni M (2016b) Alterations in knee contact forces and centers in stance phase of gait: A detailed lower extremity musculoskeletal model Journal of biomechanics 49:185-192

Marouane H, Shirazi-Adl A, Hashemi J (2015b) Quantification of the role of tibial posterior slope in knee joint mechanics and ACL force in simulated gait Journal of Biomechanics

Marzo JM, Gurske-DePerio J (2009) Effects of medial meniscus posterior horn avulsion and repair on tibiofemoral contact area and peak contact pressure with clinical implications The American journal of sports medicine 37:124-129

Matsuda S, Miura H, Nagamine R, Urabe K, Ikenoue T, Okazaki K, Iwamoto Y (1999) Posterior tibial slope in the normal and varus knee The American journal of knee surgery 12:165

McLean SG, Lucey SM, Rohrer S, Brandon C (2010) Knee joint anatomy predicts high-risk in vivo dynamic landing knee biomechanics Clinical Biomechanics 25:781-788

Meister K, Talley MC, Horodyski MB, Indelicato PA, Hartzel JS, Batts J (1998) Caudal slope of the tibia and its relationship to noncontact injuries to the ACL The American journal of knee surgery 11:217

Mellal A (2010) Application pratique de l'anatomie humaine-Tome 2 vol 2. Editions Publibook,

Mesfar W (2005) Biomecanique du genou humain en flexion sous les activites musculaires: Modelisation par la methode des elements finis. École Polytechnique de Montréal

Mesfar W, Shirazi-Adl A (2005) Biomechanics of the knee joint in flexion under various quadriceps forces The knee 12:424-434

Mesfar W, Shirazi-Adl A (2006a) Biomechanics of changes in ACL and PCL material properties or prestrains in flexion under muscle force-implications in ligament reconstruction Computer Methods in Biomechanics and Biomedical Engineering 9:201-209

Mesfar W, Shirazi-Adl A (2006b) Knee joint mechanics under quadriceps-hamstrings muscle forces are influenced by tibial restraint Clinical Biomechanics 21:841-848

Mesfar W, Shirazi-Adl A (2008a) Computational biomechanics of knee joint in open kinetic chain extension exercises Computer methods in biomechanics and biomedical engineering 11:55-61

Mesfar W, Shirazi-Adl A (2008b) Knee joint biomechanics in open-kinetic-chain flexion exercises Clinical Biomechanics-Kidlington 23:477-482

Meyer EG, Baumer TG, Slade JM, Smith WE, Haut RC (2008) Tibiofemoral contact pressures and osteochondral microtrauma during anterior cruciate ligament rupture due to excessive compressive loading and internal torque of the human knee The American journal of sports medicine 36:1966-1977

Meyer EG, Haut RC (2005) Excessive compression of the human tibio-femoral joint causes ACL rupture Journal of biomechanics 38:2311-2316

Meyer EG, Haut RC (2008b) Anterior cruciate ligament injury induced by internal tibial torsion or tibiofemoral compression Journal of biomechanics 41:3377-3383

Miller RH, Esterson AY, Shim JK (2015) Joint contact forces when minimizing the external knee adduction moment by gait modification: A computer simulation study The Knee

Minns R, Steven F (1977) The collagen fibril organization in human articular cartilage Journal of Anatomy 123:437

Moglo K, Shirazi-Adl A (2003) Biomechanics of passive knee joint in drawer: load transmission in intact and ACL-deficient joints The Knee 10:265-276

Moglo K, Shirazi-Adl A (2005) Cruciate coupling and screw-home mechanism in passive knee joint during extension–flexion Journal of biomechanics 38:1075-1083

Moller JT, Weeth RE, Keller JO (1985) Unicompartmental arthroplasty of the knee: cadaver study of tibial component placement Acta Orthopaedica 56:115-119

Moore TM, HARVEYJR JP (1974) Roentgenographic measurement of tibial-plateau depression due to fracture The Journal of Bone and Joint Surgery (American) 56:155-160

Mow VC, Guo XE (2002) Mechano-electrochemical properties of articular cartilage: their inhomogeneities and anisotropies Annual Review of Biomedical Engineering 4:175-209

Mow VC, Holmes MH, Michael Lai W (1984) Fluid transport and mechanical properties of articular cartilage: a review Journal of biomechanics 17:377-394

Mulvey MR et al. (2013) Modest Association of Joint Hypermobility With Disabling and Limiting Musculoskeletal Pain: Results From a Large-Scale General Population–Based Survey Arthritis care & research 65:1325-1333

Muybridge E (1883) The attitudes of animals in motion Journal of the Franklin Institute 115:260-274

Nelitz M, Seitz AM, Bauer J, Reichel H, Ignatius A, Dürselen L (2013) Increasing posterior tibial slope does not raise anterior cruciate ligament strain but decreases tibial rotation ability Clinical Biomechanics

Neptune R, Zajac F, Kautz S (2004) Muscle force redistributes segmental power for body progression during walking Gait & posture 19:194-205

Nielsen S, Rasmussen O, Ovesen J, Andersen K (1984) Rotatory instability of cadaver knees after transection of collateral ligaments and capsule Archives of Orthopaedic and Trauma Surgery 103:165-169

Paci JM, Scuderi MG, Werner FW, Sutton LG, Rosenbaum PF, Cannizzaro JP (2009) Knee medial compartment contact pressure increases with release of the type I anterior intermeniscal ligament The American Journal of Sports Medicine 37:1412-1416

Paletta GA, Manning T, Snell E, Parker R, Bergfeld J (1997) The effect of allograft meniscal replacement on intraarticular contact area and pressures in the human knee a biomechanical study The American journal of sports medicine 25:692-698

Pandy MG, Andriacchi TP (2010) Muscle and joint function in human locomotion Annual review of biomedical engineering 12:401-433

Pena E, Calvo B, Martinez M, Doblare M (2006) A three-dimensional finite element analysis of the combined behavior of ligaments and menisci in the healthy human knee joint Journal of Biomechanics 39:1686-1701

Perron M, Malouin F, Moffet H, McFadyen BJ (2000) Three-dimensional gait analysis in women with a total hip arthroplasty Clinical Biomechanics 15:504-515

Perry J, Davids JR (1992) Gait analysis: normal and pathological function Journal of Pediatric Orthopaedics 12:815

Pierce JE, Li G (2005) Muscle forces predicted using optimization methods are coordinate system dependent Journal of biomechanics 38:695-702

Plas F, Viel É, Blanc Y (1989) La marche humaine: kinésiologie dynamique, biomécanique et pathomécanique. Masson,

Poh SY, Yew KSA, Wong PLK, Koh SBJ, Chia SL, Fook-Chong S, Howe TS (2011) Role of the anterior intermeniscal ligament in tibiofemoral contact mechanics during axial joint loading The Knee

Radin EL, de Lamotte F, Maquet P (1984) Role of the Menisci in the Distribution of Stress in the Knee Clinical orthopaedics and related research 185:290-294

Ramakrishnan H, Kadaba M (1991) On the estimation of joint kinematics during gait Journal of Biomechanics 24:969-977

Ratcliffe A, Fryer PR, Hardingham TE (1984) The distribution of aggregating proteoglycans in articular cartilage: comparison of quantitative immunoelectron microscopy with radioimmunoassay and biochemical analysis Journal of Histochemistry & Cytochemistry 32:193

Renstrom P et al. (2008) Non-contact ACL injuries in female athletes: an International Olympic Committee current concepts statement British Journal of Sports Medicine 42:394-412

Riley PO, Paolini G, Della Croce U, Paylo KW, Kerrigan DC (2007) A kinematic and kinetic comparison of overground and treadmill walking in healthy subjects Gait & posture 26:17-24

Sakane M, Fox RJ, Glen SLYW, Livesay A, Li G, Fu FH (1997) In situ forces in the anterior cruciate ligament and its bundles in response to anterior tibial loads Journal of Orthopaedic Research 15:285-293

Sandholm A, Schwartz C, Pronost N, de Zee M, Voigt M, Thalmann D (2011) Evaluation of a geometry-based knee joint compared to a planar knee joint The Visual Computer 27:161-171

Seedhom B (1979) Transmission of the load in the knee joint with special reference to the role of the menisci part I: anatomy, analysis and apparatus Engineering in Medicine 8:207-219

Seitz AM, Lubomierski A, Friemert B, Ignatius A, Dürselen L (2012) Effect of partial meniscectomy at the medial posterior horn on tibiofemoral contact mechanics and meniscal hoop strains in human knees Journal of Orthopaedic Research 30:934-942

Sekaran SV, Hull ML, Howell SM (2002) Nonanatomic location of the posterior horn of a medial meniscal autograft implanted in a cadaveric knee adversely affects the pressure distribution on the tibial plateau The American Journal of Sports Medicine 30:74-82

Shao Q, MacLeod TD, Manal K, Buchanan TS (2011) Estimation of ligament loading and anterior tibial translation in healthy and ACL-deficient knees during gait and the influence of increasing tibial slope using EMG-driven approach Annals of biomedical engineering 39:110-121

Shelburne K, Pandy M (1998) Determinants of cruciate-ligament loading during rehabilitation exercise Clinical Biomechanics 13:403-413

Shelburne KB, Kim HJ, Sterett WI, Pandy MG (2011) Effect of posterior tibial slope on knee biomechanics during functional activity Journal of Orthopaedic Research 29:223-231

Shelburne KB, Pandy MG (1997) A musculoskeletal model of the knee for evaluating ligament forces during isometric contractions Journal of Biomechanics 30:163-176

Shelburne KB, Pandy MG (2002) A dynamic model of the knee and lower limb for simulating rising movements Computer Methods in Biomechanics & Biomedical Engineering 5:149-159

Shelburne KB, Pandy MG, Anderson FC, Torry MR (2004) Pattern of anterior cruciate ligament force in normal walking Journal of Biomechanics 37:797-805

Shelburne KB, Torry MR, Pandy MG (2006) Contributions of muscles, ligaments, and the ground-reaction force to tibiofemoral joint loading during normal gait Journal of Orthopaedic Research 24:1983-1990

Shepherd D, Seedhom B (1999) Thickness of human articular cartilage in joints of the lower limb Annals of the rheumatic diseases 58:27-34

Shim VB, Besier TF, Lloyd DG, Mithraratne K, Fernandez JF (2016) The influence and biomechanical role of cartilage split line pattern on tibiofemoral cartilage stress distribution during the stance phase of gait Biomechanics and modeling in mechanobiology 15:195-204

Shirazi R, Shirazi-Adl A, Hurtig M (2008) Role of cartilage collagen fibrils networks in knee joint biomechanics under compression Journal of biomechanics 41:3340-3348

Shumway-Cook A, Woollacott MH (2007) Motor control: translating research into clinical practice. Lippincott Williams & Wilkins,

Simon R, Everhart J, Nagaraja H, Chaudhari A (2010) A case-control study of anterior cruciate ligament volume, tibial plateau slopes and intercondylar notch dimensions in ACL-injured knees Journal of biomechanics 43:1702-1707

Sonnery-Cottet B et al. (2011) The influence of the tibial slope and the size of the intercondylar notch on rupture of the anterior cruciate ligament Journal of Bone & Joint Surgery, British Volume 93:1475-1478

Spyropoulos P, Pisciotta JC, Pavlou KN, Cairns M, Simon SR (1991) Biomechanical gait analysis in obese men Archives of physical medicine and rehabilitation 72:1065-1070

Stijak L, Herzog RF, Schai P (2008) Is there an influence of the tibial slope of the lateral condyle on the ACL lesion? Knee Surgery, Sports Traumatology, Arthroscopy 16:112-117

Sutherland DH (2001) The evolution of clinical gait analysis: Part II Kinematics Gait & posture 16:159-179

Taylor WR, Heller MO, Bergmann G, Duda GN (2004) Tibio-femoral loading during human gait and stair climbing Journal of Orthopaedic Research 22:625-632

Tetsworth K, Paley D (1994) Malalignment and degenerative arthropathy Orthopedic Clinics of North America 25:367-378

Thelen DG, Anderson FC, Delp SL (2003) Generating dynamic simulations of movement using computed muscle control Journal of Biomechanics 36:321-328

Titianova EB, Mateev PS, Tarkka IM (2004) Footprint analysis of gait using a pressure sensor system Journal of Electromyography and Kinesiology 14:275-281

Todd MS, Lalliss S, Garcia ES, DeBerardino TM, Cameron KL (2010) The relationship between posterior tibial slope and anterior cruciate ligament injuries The American Journal of Sports Medicine 38:63-67

Viel E (2000) La marche humaine, la course et le saut: biomécanique, explorations, normes et dysfonctionnements vol 9. Elsevier Masson,

Wahl CJ, Westermann RW, Blaisdell GY, Cizik AM (2012) An association of lateral knee sagittal anatomic factors with non-contact ACL injury: sex or geometry? The Journal of Bone & Joint Surgery 94:217-226

Walker P, Hajek J (1972) The load-bearing area in the knee joint Journal of biomechanics 5:581-589

Walker PS, Erkman MJ (1975) The role of the menisci in force transmission across the knee Clinical orthopaedics and related research 109:184

Wall SJ, Rose DM, Sutter EG, Belkoff SM, Boden BP (2012) The Role of Axial Compressive and Quadriceps Forces in Noncontact Anterior Cruciate Ligament Injury A Cadaveric Study The American journal of sports medicine 40:568-573

Wang H et al. (2014) Image based weighted center of proximity versus directly measured knee contact location during simulated gait Journal of biomechanics 47:2483-2489

Weber W, Weber EF (1836) Mechanik der menschlichen Gehwerkzeuge: eine anatomisch-physiologische Untersuchung vol 1. Dietrich,

White R, Agouris I, Selbie R, Kirkpatrick M (1999) The variability of force platform data in normal and cerebral palsy gait Clinical Biomechanics 14:185-192

Whittle MW (1996) Clinical gait analysis: A review Human Movement Science 15:369-387

Wilson W, Huyghe J, Van Donkelaar C (2007) Depth-dependent compressive equilibrium properties of articular cartilage explained by its composition Biomechanics and modeling in mechanobiology 6:43-53

Winby C, Gerus P, Kirk T, Lloyd D (2013) Correlation between EMG-based co-activation measures and medial and lateral compartment loads of the knee during gait Clinical Biomechanics 28:1014-1019

Winby CR, Lloyd DG, Besier TF, Kirk TB (2009) Muscle and external load contribution to knee joint contact loads during normal gait Journal of biomechanics 42:2294-2300

Wong J, Steklov N, Patil S, Flores-Hernandez C, Kester M, Colwell CW, D'Lima DD (2011) Predicting the effect of tray malalignment on risk for bone damage and implant subsidence after total knee arthroplasty Journal of Orthopaedic Research 29:347-353

Woo SL, Fox RJ, Sakane M, Livesay GA, Rudy TW, Fu FH (1998) Biomechanics of the ACL: measurements of in situ force in the ACL and knee kinematics The Knee 5:267-288

Xiao M, Higginson JS (2008) Muscle function may depend on model selection in forward simulation of normal walking Journal of Biomechanics 41:3236-3242

Yang N, Canavan P, Nayeb-Hashemi H, Najafi B, Vaziri A (2010a) Protocol for constructing subject-specific biomechanical models of knee joint Computer Methods in Biomechanics and Biomedical Engineering 13:589-603

Yang NH, Nayeb-Hashemi H, Canavan PK, Vaziri A (2010b) Effect of frontal plane tibiofemoral angle on the stress and strain at the knee cartilage during the stance phase of gait Journal of Orthopaedic Research 28:1539-1547

Yeow CH, Cheong CH, Ng KS, Lee PVS, Goh JCH (2008) Anterior Cruciate Ligament Failure and Cartilage Damage During Knee Joint Compression A Preliminary Study Based on the Porcine Model The American Journal of Sports Medicine 36:934-942

Zajac FE, Neptune RR, Kautz SA (2002) Biomechanics and muscle coordination of human walking: Part I: Introduction to concepts, power transfer, dynamics and simulations Gait & posture 16:215-232

Zajac FE, Neptune RR, Kautz SA (2003) Biomechanics and muscle coordination of human walking: part II: lessons from dynamical simulations and clinical implications Gait & posture 17:1-17

Zatsiorky V, Werner S, Kaimin M (1994) Basic kinematics of walking: step length and step frequency: a review Journal of sports medicine and physical fitness 34:109-134

Zhang L-Q, Shiavi RG, Limbird TJ, Minorik JM (2003) Six degrees-of-freedom kinematics of ACL deficient knees during locomotion—compensatory mechanism Gait & posture 17:34-42

Zhao D, Banks SA, D'Lima DD, Colwell CW, Fregly BJ (2007a) In vivo medial and lateral tibial loads during dynamic and high flexion activities Journal of orthopaedic research 25:593-602

ANNEXE A - BOOK CHAPTER: COMPUTATIONAL BIOMECHANICS OF THE KNEE JOINT

Hafedh Marouane and Aboulfazl Shirazi-Adl

Submitted for Elsevier book on Computational Mechanics of Musculoskeletal Tissues 2016

Editor: Amir A. Zadpoor

Abstract

Activation in musculature as well as passive properties both govern the complex response of the human knee joint under large loads and motions in various activities of daily living. Knowledge of knee joint biomechanics is essential in improved prevention and treatment managements of numerous joint disorders. In the current work, we present passive finite element and active hybrid musculoskeletal model investigations of the knee joint in different tasks such as gait. In particular, attention is made on the details of the knee joint model, boundary conditions, loadings and validation of estimations in such model studies. It is demonstrated that proper representation of boundary conditions and loads are essential in order to avoid instability (hypermobility), over-constraint and large errors in the model response. This review presents the current knowledge on knee biomechanics, some crucial issues necessary to estimate accurate results and future directions.

Keywords: Knee Joint, Finite element, Gait, Boundary Conditions, Load, Biomechanics, Lower limb, Muscles

1. Introduction

Due to large relative movements and distal location in the body, human knee joints experience loads and movements of substantial magnitude during various occupational, recreational and regular daily living activities (Kutzner et al., 2010). This demanding mechanical environment exposes knee joints to a host of painful deformities, injuries and degenerations involving both patellofemoral (PF) and tibiofemoral (TF) articulations. With the osteoarthritis (OA) as a painful and debilitating disease (present in ~10% of the general population and >70% of those over age 65) that affects the knee more than any other weight bearing joint in the human body, total knee replacements approaching one million per year in US, anterior cruciate ligament

(ACL) damage as the most common sports injury with ~100k new injuries per year in US at ~50% reconstruction rate, >500k per year arthroscopic partial meniscectomy in US and finally also with millions of corrective/preventive osteotomy surgeries and biologic repairs (tissue engineering), the knee joint is at the spotlight in immediate need for more effective preventive and treatment programs (Guilak, 2011, Murphy et al., 2008, Katz et al., 2010, Kim, 2008, Losina et al., 2012, Jones and Rocha, 2012). The situation is alarming due both to the dramatic increase in these interventions especially in younger and more active age groups that expect to remain active even after surgery and to the ever-growing portion of the population with obesity and ageing that are common OA risk factors.

An improved in-depth understanding of the biomechanics of the knee joint is therefore necessary for improved design and management of preventive and treatment programs for these injuries. In response, several finite element (FE) models with different degrees of precision and refinement have been developed (Yang et al., 2010a, Kazemi and Li, 2014, Pena et al., 2006, Bendjaballah et al., 1995, Halonen et al., 2016, Shim et al., 2016, Mesfar and Shirazi-Adl, 2006b). Likewise, various musculoskeletal (MS) models of the lower extremity have been constructed with the objective to further existing understanding of the knee joint functional biomechanics in normal and disturbed conditions under more physiological load and movement conditions (Adouni and Shirazi-Adl, 2014a, Delp et al., 1990, Lloyd and Besier, 2003, Manal and Buchanan, 2013, Marouane et al., 2015b, Adouni et al., 2012, Lerner et al., 2014, Marouane et al., 2016b, Marouane et al., 2016a, Yang et al., 2010b). While former FE models provide valuable detailed information (i.e., tissue stresses and strains) in joint constituent materials, MS models offer crucial results on activation patterns in musculature and resulting global joint loads in complex physiological activities such as gait (Kim et al., 2009, Taylor et al., 2004, Winby et al., 2009). Our recent lower extremity hybrid kinematics-driven MS model investigations, by explicit incorporation of a validated detailed FE model of the entire knee joint, offer however improved estimations both at the global (muscle and joint forces) and local knee joint (tissue stresses and strains, contact pressure and center) levels (Adouni et al., 2012, Adouni and Shirazi-Adl, 2014a, Adouni and Shirazi-Adl, 2014b, Marouane et al., 2014, Marouane et al., 2015a, Marouane et al., 2015b, Marouane et al., 2016b, Marouane et al., 2016a) by full consideration of the active-passive synergy though only at the crucial knee joint. A short description of the joint

passive tissues, our knee joint FE and lower extremity MS models will be provided in the next sections followed by some sample results and validation of model predictions.

2. Method and Passive-Active Models

2.1. Passive Tissues

2.1.1. Cartilage

As a fluid-saturated nonhomogeneous composite tissue, articular cartilage provides smooth articulation at joint surfaces, absorbs impacts and redistributes applied stresses to underlying bone. Articular cartilage is made mainly of collagen (type II) (50-73% dry weight), proteoglycans (15-30% dry weight) and water (58-78% weight). The composition and structure of articular cartilage change with depth from the joint surface (Koay and Athanasiou, 2009, Clarke, 1974, Kääb et al., 1998, Mow and Guo, 2002, Mow et al., 1984, Ratcliffe et al., 1984, Shepherd and Seedhom, 1999, Wilson et al., 2007). At the superficial zone, collagen fibrils are horizontally oriented parallel to the articular surface, whereas they become rather random in the transitional zone and finally turn perpendicular to the subchondral bone-cartilage interface in the deep zone (Kääb et al., 1998, Minns and Steven, 1977, Broom and Marra, 1986). Collagen content is highest in the superficial and deep zones of articular cartilage, and lowest in the middle zone (Mow and Guo, 2002). With proteoglycan content, the equilibrium modulus of nonfibrillar solid matrix increases downward along the depth from the articular surface to the subchondral junction (Mow and Guo, 2002).

This layered structure along with the nonlinearity and tension-compression differences in the collagen fibril properties result in a highly nonlinear, nonhomogeneous composite fibrous tissue (Huang et al., 2005, Mow and Guo, 2002). The tissue is saturated with water the inflow and outflow of which (mobile portion) give rise to the time-dependent viscoelastic behaviour leading to common stress-relaxation (drop in stress under constant strain) and creep (increase in deformation under constant loads) effects. The water content, as in other similar fibrous tissues such as the intervertebral disc and meniscus, vary with time depending on the tissue composition, external load and osmolality of surrounding media and as such play a crucial role in the load bearing especially in the transient (short term) loading periods where fluid pressurization plays a crucial role in non-degenerate conditions.

2.1.2. Ligaments

Similar to other biological soft tissues, the ligaments of the knee are made of a water-rich ground substance reinforced with collagen fibers (mainly type I) (Duthon et al., 2006). Four major ligaments (ACL, anterior cruciate ligament; PCL, posterior cruciate ligament; LCL, lateral collateral ligament; MCL, medial collateral ligament), among others, stiffen and control the relative movements of the tibiofemoral joint. ACL and PCL can each be separated into two bundles; anteromedial (am) and posterolateral (pl) in ACL whereas anterolateral (al) and posteromedial (pm) in PCL. These bundles experience different patterns of length changes during active/passive knee flexion (Hollis et al., 1991, Woo et al., 1998). Cadaver studies have confirmed the primary roles of ACL-am in high flexion and ACL-pl at near extension angles during passive knee flexion or under an anterior tibial load (Amis and Dawkins, 1991, Gabriel et al., 2004, Sakane et al., 1997). Depending on loading conditions, one or some of these ligaments act as primary restraints in the stability of the joint. Though modulated by joint flexion angle, MCL and LCL are primary constraints in adduction-abduction rotations whereas AP translations and internal-external rotations are resisted primarily by cruciate ligaments (Markolf et al., 1995b, Sakane et al., 1997).

2.1.3. Meniscus

Meniscus is a semi-lunar shaped fibrocartilaginous tissue with extremities inserted into the intercondylar eminence at the tibial plateau. It is composed mainly of a dense network of collagen fibrils (mainly type I), proteoglycans and water. Similar to cartilage, its fluid content gives rise to tissue time-dependent response. While the collagen fibrils at top, bottom and peripheral surfaces show no major preferred orientations, they are nevertheless circumferentially oriented in the bulk of the tissue in between these surfaces (Aspden, 1985). In addition, radial tie fibres are present that increase the tensile resistance of the meniscus (Skaggs et al., 1994). Similar to the articular cartilage, the structural inhomogeneity and anisotropy of menisci dominate its tensile behavior (Fithian et al., 1990).

Primary meniscal functions are to redistribute the load across the cartilage (Levy et al., 1982), provide shock absorption (Fithian et al., 1990, Voloshin and Wosk, 1983), stiffen and stabilize the joint (Radin et al., 1984, Levy et al., 1989), facilitate joint lubrication and articulation, prevent hyperextension and protect the joint (Seedhom, 1979, Kawamura et al., 2003). Pressure measurements have shown that 45% to 70% of the applied load is transmitted

through the menisci (Shrive et al., 1978, Seedhom, 1979, Ahmed and Burke, 1983, Fithian et al., 1990). In joints after total meniscectomy, contact stresses could double with a 50% to 70% reduction in contact areas (Baratz et al., 1986). A 10% reduction in meniscal contact area secondary to partial meniscectomy produces ~65% increase in peak contact stresses (Baratz et al., 1986), leading likely to an early development of OA (Caplan and Kader, 2014, Fairbank, 1948, Jones et al., 1978).

The mechanical properties of menisci have been extensively studied under compressive, tensile and shear load conditions (Fithian et al., 1990, Mow and Ratcliffe, 1997, Tissakht and Ahmed, 1995, Zhu et al., 1994). Tensile Properties, as in the articular cartilage, vary with tissue depth from a direction to another depending on the spatial organization of collagen fibrils within the tissue (Tissakht and Ahmed, 1995).

2.2. Knee Joint Passive Finite Element Model

Numerous FE models with different degrees of accuracy and complexity have been developed to study the knee joint biomechanics under various loads and movements. The first comprehensive model of the TF joint is that of Bendjaballah et al. (1995) with the model reconstructed from CT images and direct measurements of a cadaver knee. Menisci were simulated as a nonlinear nonhomogeneous composite of a an isotropic bulk reinforced by collagen fibrils with strain-dependent nonlinear material properties (Shiraz-Adl, 1989), ligaments as nonlinear elements with initial strains at different bundles and articular cartilage layers as a simple isotropic elastic material. Each bony structure was taken as a rigid body and represented by a primary reference node. The material properties were derived from the data available in the literature (Bendjaballah et al., 1995, Moglo and Shirazi-Adl, 2003a, Mesfar and Shirazi-Adl, 2005). Each meniscus matrix was stiffened by a higher modulus of 15 MPa at both ends (~5 mm length) where inserted into the tibial eminence to simulate its horns (Moglo and Shirazi-Adl, 2003b). Articulations at the cartilage–cartilage (i.e., uncovered areas) as well as cartilage–meniscus (i.e., covered areas) were simulated as large displacement frictionless contact (Moglo and Shirazi-Adl, 2005, Moglo and Shirazi-Adl, 2003b).

In later refinements and developments of this model, the articular cartilage layers at both TF and PF joints were also represented as a depth-dependent nonhomogeneous nonlinear composite of incompressible bulk matrices reinforced by collagen fibril networks, Figure X.1

(Shirazi and Shirazi-Adl, 2005, Shirazi and Shirazi-Adl, 2008, Shirazi et al., 2008). In superficial zones of all cartilage layers as well as bounding surfaces of menisci, membrane elements were used to represent homogeneous in-plane distribution of fibrils with random orientations (Figure X.1). Despite such isotropic distribution, however, a direction-dependent response prevails due to the strain-dependency in fibrils material properties and anisotropy in strain field. The collagen fibril properties (types I and II) were taken nonlinear based on earlier studies (Shirazi-Adl et al., 1984). In the transitional zone with random fibrils (i.e., no dominant orientations), continuum brick elements that take the principal strain directions as the material principal axes represent collagen fibrils (Figure A1.1). In the deep zone, however, vertical fibrils were modelled with vertical membrane elements similar to horizontal superficial ones except in offering resistance only in local fibrils directions (Shirazi and Shirazi-Adl, 2008). In the bulk region of each meniscus in between peripheral surfaces, collagen fibrils that are dominant in the circumferential direction were represented by membrane elements with local material principal axes defined initially in orthogonal circumferential and radial directions.

Thickness of membrane elements in different regions of cartilage and menisci was computed based on fibrils volume fraction in each zone. In cartilage, the equivalent collagen fibrils content at the superficial zone was estimated based on reported tissue properties in tension (Kempson et al., 1968, Kempson et al., 1973, Woo et al., 1976) and type II collagen stress–strain curve (Shirazi and Shirazi-Adl, 2005). A total volume fraction of 15% was estimated in the superficial zone in agreement with the mean value of 14% reported for its wet weight.

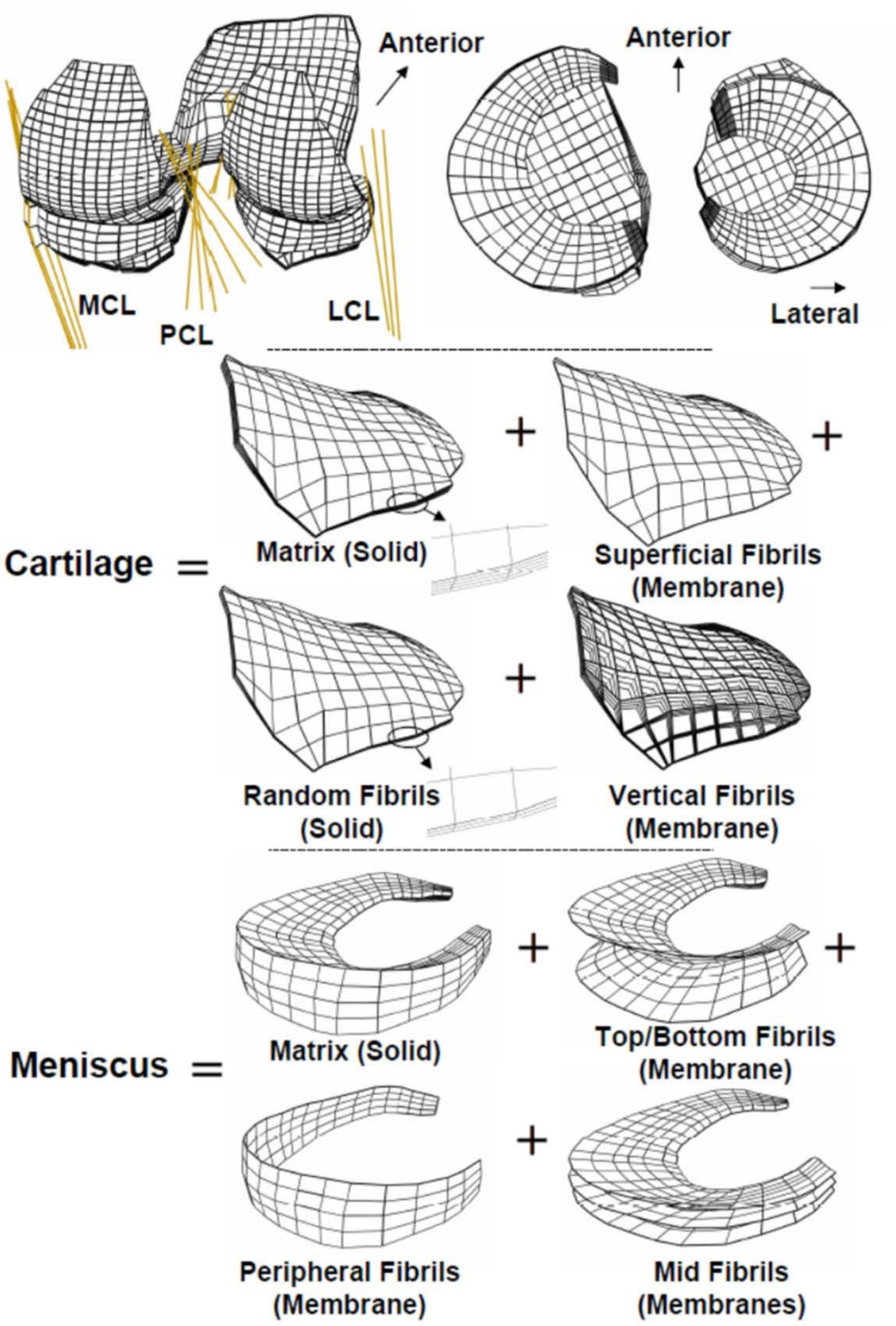

Figure A1.1: Nonhomogeneous composite model of the articular cartilage and menisci showing depth-dependent fibril networks (Shirazi et al., 2008).

In accordance with earlier investigations (Brown and Singerman, 1986, Ateshian et al., 2007), the transient response of water-saturated articular cartilage and meniscus under higher strain rates could be computed either by a biphasic approach or equivalently by an incompressible elastic analysis using bulk equilibrium moduli. Examining this equivalency at various Poisson's ratios using our earlier non-homogeneous axisymmetric model of cartilage (Shirazi and Shirazi-Adl, 2008), indentation results at 20% strain applied in 0.5 s demonstrated a significant sensitivity in transient reaction force (Shirazi and Shirazi-Adl, 2008, Shirazi et al., 2008). Nearly incompressible Poisson's ratios in the range of 0.4999-0.5 could yield results identical to those computed with biphasic simulations. Since loading cycles of daily activities like walking and running last for only a fraction of second, an incompressible elastic model can hence alternatively be employed with no loss of accuracy to compute the transient response. In this case the hydrostatic pressure in the elastic model represents the transient pore pressure in its equivalent poroelastic model. An equivalent compressible elastic material can also be employed in which case greater equilibrium moduli should be used depending on the Poisson's ratio considered.

Non-linear spring elements were employed to model various ligaments of the TF and PF joints. The MCL wrapped around the proximal medial bony edge of the tibia with peripheral attachments to the medial meniscus (Bendjaballah et al., 1995, Moglo and Shirazi-Adl, 2003a). Each ligament was simulated by a number of uniaxial elements with different cross-sectional areas (based on the literature) and initial strains (based on the literature and comparison of results with available measurements) (Mesfar and Shirazi-Adl, 2005, Mesfar and Shirazi-Adl, 2006a, Moglo and Shirazi-Adl, 2003b, Shirazi-Adl and Moglo, 2005). Overall, the FE model including both TF and PF joints and associated soft tissues is shown in Figure A1.2.

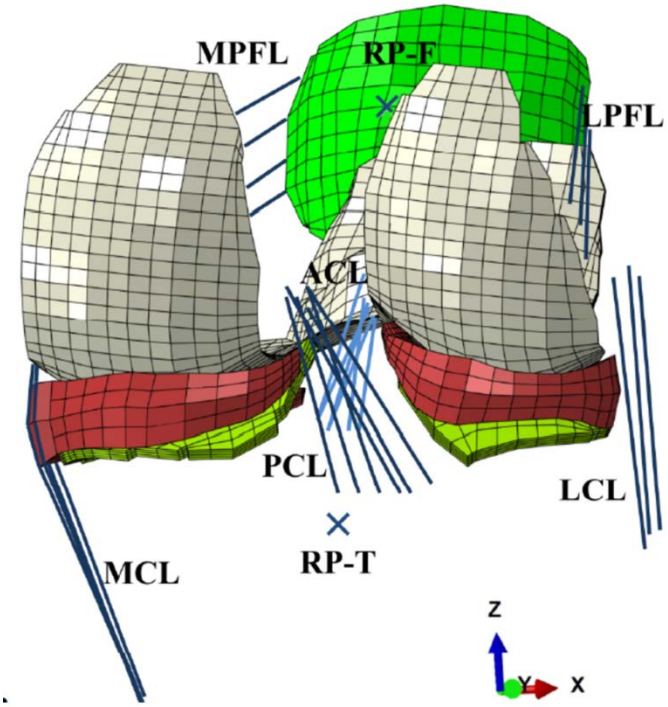

Figure A1.2: Posterior view of the knee joint FE model showing articular cartilage layers, menisci and ligaments. Rigid bony structures are represented by their reference primary nodes and are not shown.

2.3. Lower Extremity Musculoskeletal Model

Resolution of redundancy towards estimation of unknown muscle forces in MS models of human body during various activities remains a formidable challenge. Inverse dynamics is the common method of choice when compared with the forward dynamic simulations in which activity in muscles are prescribed, say based on measured activation via limited surface electromyography (EMG), and then continuously updated with constraints on some kinematics trajectories, measured contact forces and/or objective functions (Thelen et al., 2003). In the former, joint moments are initially evaluated (inverse dynamics) by equations of motion using measured joint kinematics, external loads and body anthropometric characteristics. The redundant muscle forces are subsequently estimated, either using an optimization (DeMers et al., 2014, Kim et al., 2009, Knarr and Higginson, 2015, Lerner et al., 2015, Lerner et al., 2014, Miller et al., 2015, Steele et al., 2012) or an EMG-driven (Besier et al., 2009, Gerus et al., 2013, Kumar et al., 2012, Lloyd and Besier, 2003, Manal and Buchanan, 2013, Sartori et al., 2012) method. There are also hybrid EMG-based optimization versions of these two approaches (Cholewicki and

McGill, 1994, Gagnon et al., 2011). In the optimization-based methods, muscle forces are estimated by minimizing a single or multiple objective functions, such as the sum of muscle forces, system margin of stability or muscle activations to different powers (Arjmand and Shirazi-Adl, 2006, Kim et al., 2009, Adouni et al., 2012, Mokhtarzadeh et al., 2014, Lerner et al., 2014, Adouni and Shirazi-Adl, 2014a, Adouni and Shirazi-Adl, 2013).

The predicted muscle forces are generally validated qualitatively by comparison of estimated muscle activation levels with normalized recorded EMG under the same activity (Adouni and Shirazi-Adl, 2013, Adouni et al., 2012) or the predicted contact forces with data from patients with instrumented knee implant (DeMers et al., 2014, Steele et al., 2012). Predictions have been found sensitive to many factors, such as muscle activation patterns (DeMers et al., 2014), muscle weighting (Lerner et al., 2015, Steele et al., 2012) and musculotendon properties. In a study on the sensitivity of muscle force estimations to changes in musculotendon properties, Redl et al. (2007) found that changes in the muscle-fiber length and tendon rest length of vasti were most critical to model force estimates in normal gait. EMG-driven models often use Hill-type muscle models (accounting for activation, fiber length/velocity and pennation angle) when estimating muscle forces (Lloyd and Besier, 2003, Arnold et al., 2010). Muscle gains are evaluated in a manner to match joint moments based on inverse dynamics (Besier et al., 2009, Lloyd and Besier, 2003, Manal and Buchanan, 2013, Winby et al., 2009) or to minimize error between predicted and measured (via instrumented implants) joint contact forces (Gerus et al., 2013). While EMG-driven approaches are biological in using recorded individual's muscle activity with inter- and intra-subject volitional variations, they remain susceptible to major assumptions and shortcomings in limited available surface EMG, cross-talk considerations, force-EMG relation, normalization, and introduction of gain factors (Arjmand et al., 2010, Gerus et al., 2013).

Using a hybrid MS model of the lower extremity with our detailed validated FE model of the knee joint, we resolve the redundancy and estimate muscle forces using a kinematics-driven optimization approach (Adouni et al., 2012, Adouni and Shirazi-Adl, 2014a, Adouni and Shirazi-Adl, 2014b, Marouane et al., 2014, Marouane et al., 2016b). In this way not only the passive properties of the knee joint are accurately represented but also both joint moments (from inverse dynamics) and joint kinematics (from gait data) are used to drive the model resulting in a

synergistic passive-active simulation. By considering the measured kinematics, this kinematics-driven MS model is defined as a biological approach.

3. Applications: Boundary Conditions and Loading

In knee joint biomechanics, under both active and passive conditions, proper consideration of joint loading and boundary conditions are of prime importance as they both substantially affect results and subsequent comparisons and validations. Here as follows are samples of our model applications on boundary conditions and loading.

Careful selection of stable and fully unconstrained boundary conditions in experimental and model studies of any complex articulation such the knee joint is crucial. On the one hand, the constraints should be sufficient to avoid instability (hypermobility) while on the other hand they should not be excessive to artificially and inadvertently over-constraint and stiffen the response. In addition, if the intention is to represent and compare to an existing study, being in vivo, in vitro or in silico, the model should replicate as closely as possible the corresponding boundary conditions. For example to investigate the passive tibiofemoral response in full extension under 1000 N, Bendjaballah et al. ((1995) applied the force on the primary (reference) node of the femur with the tibia completely fixed. For a stable and unconstrained response, the femoral flexion-extension (F-E) and adduction-abduction (add-abd) rotations were also fixed while leaving internal-external (I-E) rotations and all three translations at the femur free. Additional constraint on I-E rotations was found to have a significant effect on knee biomechanics especially in the meniscectomized case; the knee became stiffer in the axial direction, the ratio of medial/lateral contact load increased and the coupled displacements decreased as coupled I-E rotations were fixed (Bendjaballah et al., 1995). In a similar study but with the refined and improved version of the model under up to 2000 N compression at full extension, Shirazi and Shirazi-Adl (2008) used equivalent but reversed boundary conditions with the femur fixed and tibia left free except in add-abd and F-E rotations. They also found much stiffer response as tibial coupled I-E rotations were also constrained. Foregoing boundary conditions in the knee joint under axial compression assure unconstrained motions with no interference with the natural biomechanical roles of menisci, ligaments and articular surfaces. Besides and equally important, the response is no more dependent on the location where the axial compression is applied on the femur or on the tibia.

Due to the joint instability as well as artefact moments caused by large compression forces, in vitro biomechanical investigations of the knee joint face the dilemma of how (joint constraints) and where (anterior–posterior, A–P and medial–lateral, M–L, locations) to apply compression forces of physiological magnitudes (Ahmed and Burke, 1983, Markolf et al., 1981b). To circumvent these difficulties under compression forces, in vitro studies impose additional constraints on rotations in sagittal and frontal planes (Kurosawa et al., 1980, Lee et al., 2006). A novel approach was proposed in our recent study (Marouane et al., 2015a) where the compression load was applied at the joint mechanical balance point (MBP) identified as a point at which the compression does not cause any coupled rotations in sagittal and frontal planes (Figure A1.3). Analyses were carried out at different flexion angles (0°, 15°, 30° and 45°) while the tibia was fully free (even in the F-E and add-abd rotations unlike earlier studies discussed in the foregoing paragraph) and the femur fixed at the desired flexion angle. For a robust approach to determine the unique location of the joint MBP under a specific axial compression force, tibial coupled rotations were initially constrained and the associated required reaction moments were estimated. Subsequently, the location of the compression force was shifted in A–P and M–L directions (by the ratio of these required moments divided by the applied compression force) in order to eliminate these undesired moments (Marouane et al., 2015a). The computed MBP location varied with the joint flexion angle and compression force magnitude (Figure A1.3).

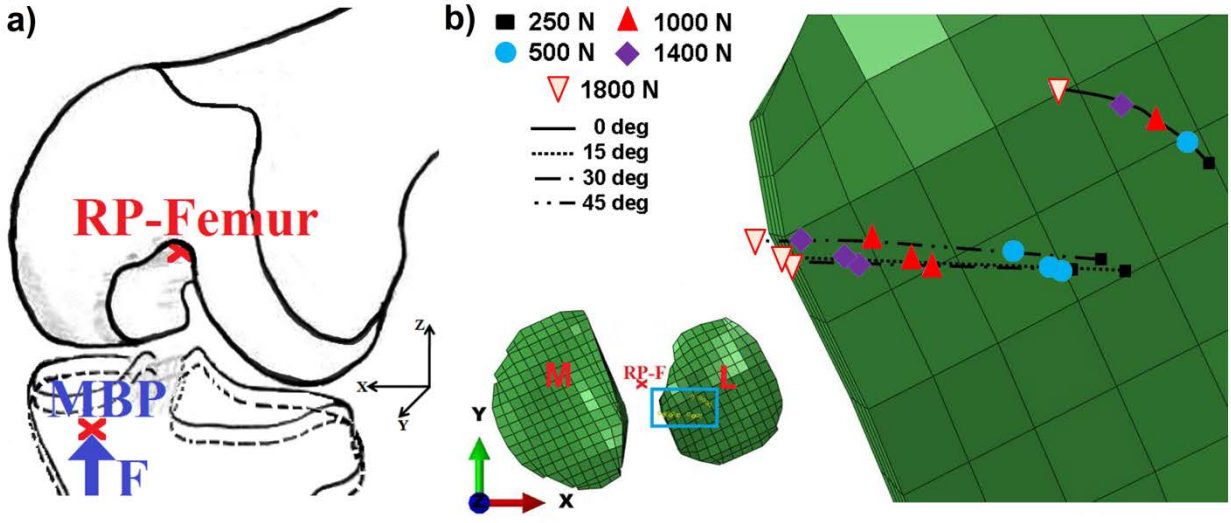

Figure A1.3: (a) MBP approach; when applied at these locations, the compression preloads do not cause any coupled sagittal and frontal rotations in the fully unconstrained tibia. (b) Shifts in

the location of the MBP superposed on the tibial plateau as a function of joint flexion angle and compression preload.

To study the passive tibiofemoral joint at full extension under add-abd moments of up to 15Nm (Bendjaballah et al., 1997), the femur was left free except in F-E rotations whereas the tibia was completely fixed. The joint laxity in this loading case is found to be relatively unaffected by additional restraint on the femoral I-E rotations. The joint is found much stiffer under adduction moment. Using an updated version of the model, Marouane et al., (2015a) carried out similar analyses under up to 20 Nm moments at various flexion angles and compression preloads (up to 1800 N) applied at MBP locations. The compression force substantially increased the joint moment bearing capacities and instantaneous angular rigidities in both frontal (add-abd) and sagittal (F-E) planes. The add-abd laxities diminished with compression preloads despite concomitant substantial reductions in collateral ligament forces. It was concluded that the augmented passive moment resistance under larger compression preloads as expected in daily activities such as gait should not be overlooked in the knee joint MS models.

The knee joint passive response was also studied at full extension under a femoral posterior drawer force up to 200 N acting alone or combined with a 1500 N compression preload (Shirazi and Shirazi-Adl, 2009). For an unconstrained response while avoiding the adverse effect of load positioning on joint kinematics (Rudy et al., 2000), the femur was left free in three translations while fixed in all three rotations. A posterior drawer force of 200 N was applied onto the femur with and without a 1500 N compression preload. For the tibia, on the other hand, I-E and add-abd rotations were left free while constraining F-E rotations and three translations. An equivalent reversed unconstrained set of boundary conditions was also examined, i.e. free rotations on the femur while loading the tibia with free translations, a different boundary condition that yielded almost the same results.

To apply quadriceps and hamstrings muscle forces, measurement studies restrain the tibial A-P translation at a point away from the joint to counterbalance the moment of muscle forces while preserving the joint flexion angle (Ahmed and Burke, 1983, Buff et al., 1988, Lee et al., 1994, Draganich et al., 1987, Senavongse et al., 2003, Farahmand et al., 2004)). This constraint, however apart from generating extensor/flexor moments, introduces artefact tibial A-P shear forces the magnitude of which depends on the distal location of restraint (i.e., lever arm) as well

as the joint moment (i.e., muscle forces) (Mesfar and Shirazi-Adl, 2006b). The likely effect of such constrain on the joint response in flexion-extension (0°–90°) under isolated and combined hamstrings (205.5N) and quadriceps (411N) activation was investigated (Mesfar and Shirazi-Adl, 2006b). The femur was completely fixed while the tibia and patella were left free in all directions. The effect of tibial restraint at two locations (20 cm or 30 cm distal to the joint level) on results was studied and compared with the reference boundary condition of the tibia constrained by pure moments (Figure A1.4). The tibial restraint by a force markedly influenced, depending on the joint moment and restraining lever arm, the tibial A-P translation, TF contact forces and forces in cruciate ligaments (Figure A1.4). The restraining forces, especially when placed closer to the joint (i.e., smaller lever arm), had reduced forces in cruciate ligaments at critical joint angles; in the ACL at near full extension and in the PCL at larger flexion angles. Ahmed et al. (1983) reported the effect of this restraint lever arm on results and estimated that any moment arm >40cm had no discernible effect on the pressure distribution on the patellar cartilage. Others reported that ACL force and tibial anterior translation significantly increased as the resisting force shifted distally from the joint (i.e., larger lever arm) (Jurist and Otis, 1985, Pandy and Shelburne, 1997).

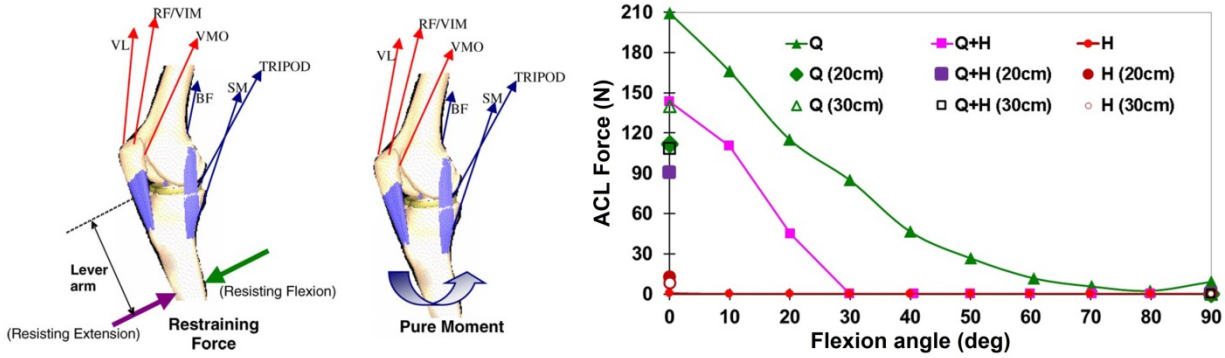

Figure A1.4: Schematic representations of muscle forces in two load conditions (left) and computed forces in ACL for cases with quadriceps activation alone (Q), hamstrings activation alone (H) and coactivation in both (Q+H) under pure moment (0°-90°) and restraining forces (only at 0° and 90 ° flexion angles (right) (Mesfar and Shirazi-Adl, 2006b).

The importance of loading was also demonstrated when simulating the closed-kinetic-chain squat exercises at different flexion angles (Adouni and Shirazi-Adl, 2009). The effect of two loading configurations generating identical joint moments was considered; a realistic vertical reaction force at foot and an idealised pure sagittal moment similar to that used by Cohen et al.

(2001). In corroboration of earlier studies (Mesfar and Shirazi-Adl, 2006b) described earlier, the pure moment loading markedly influenced TF and PF contact forces/areas and forces in cruciate ligaments.

Knee morphologic aspects have extensively been investigated in search for factors that could play a role in the risk of ACL rupture in both sexes as well as in higher prevalence of non-contact ACL ruptures in female athletes. Many image-based studies of patients with non-contact ACL rupture versus the control subjects have identified the higher posterior tibial slope (PTS) as a risk factor (Hashemi et al., 2010, Sonnery-Cottet et al., 2011). To simulate the effect of changes in PTS on tibial translation and ACL force under compression (Marouane et al., 2014) and during simulated gait (Marouane et al., 2015b), the initial medial and lateral PTSs were altered both by rigidly rotating tibial cartilage layers around lateral– medial axes at the center of the respective tibial articulations. In this manner, minimal changes were made in tibial articular geometries; ligaments footprints were not altered; their lengths and orientations remained unchanged. These changes in PTS hence affected only the tibial slope with minimal effects on the geometry of the articular cartilage layers and overlying menisci. In accordance with image-based studies, results showed that steeper PTS is a major risk factor in markedly increasing ACL force and its vulnerability to injury.

MS modeling of the lower extremity is promising to improve the current understanding of the knee joint function and injuries and associated prevention and treatment programs. Due to the complexity, numerous assumptions are often made when estimating muscle forces and joint contact loads. The knee is commonly idealized as a planar (2D) joint with its motion constrained to remain in the sagittal plane (Delp et al., 1990, DeMers et al., 2014, Shelburne and Pandy, 1998, Shelburne et al., 2004, Shelburne et al., 2006, Thelen et al., 2003, Fregly et al., 2012)), neglecting thus both displacements and equilibrium equations in remaining planes. With muscle forces predicted, the static equilibrium in the frontal plane is consequently considered to estimate tibial compartmental loads neglecting the knee joint passive resistance and assuming medial/lateral contact centers (Gerus et al., 2013, Winby et al., 2009, Miller et al., 2015). To evaluate the effects of such assumptions, a hybrid MS model of the lower extremity incorporating a detailed validated 3D knee FE model was used to simulate the stance phase of gait (Adouni and Shirazi-Adl, 2014a, Adouni et al., 2012, Marouane et al., 2016b). To drive the musculoskeletal model, kinetics (hip/knee/ankle joint moments and GRF) as well as kinematics (hip/knee/ankle

joint rotations) data were taken from the mean of asymptomatic subjects collected in gait (Astephen, 2007, Astephen et al., 2008). Ground reaction forces were based on measurements of Hunt et al. (2001). The consistency of these two datasets at various periods of gait were assured by applying the latter forces on the foot at locations that generate the knee joint moments reported in the former studies. In the 2D model, unbalanced knee joint moments reaching, at 25% stance, 30 Nm in abduction moment and 12 Nm in internal moment were neglected in the 2D model when estimating muscle forces. The model with an idealized planar 2D knee joint substantially diminished muscle forces, ACL force and TF contact forces/stresses when compared to the realistic 3D model, see Figure A1-5.

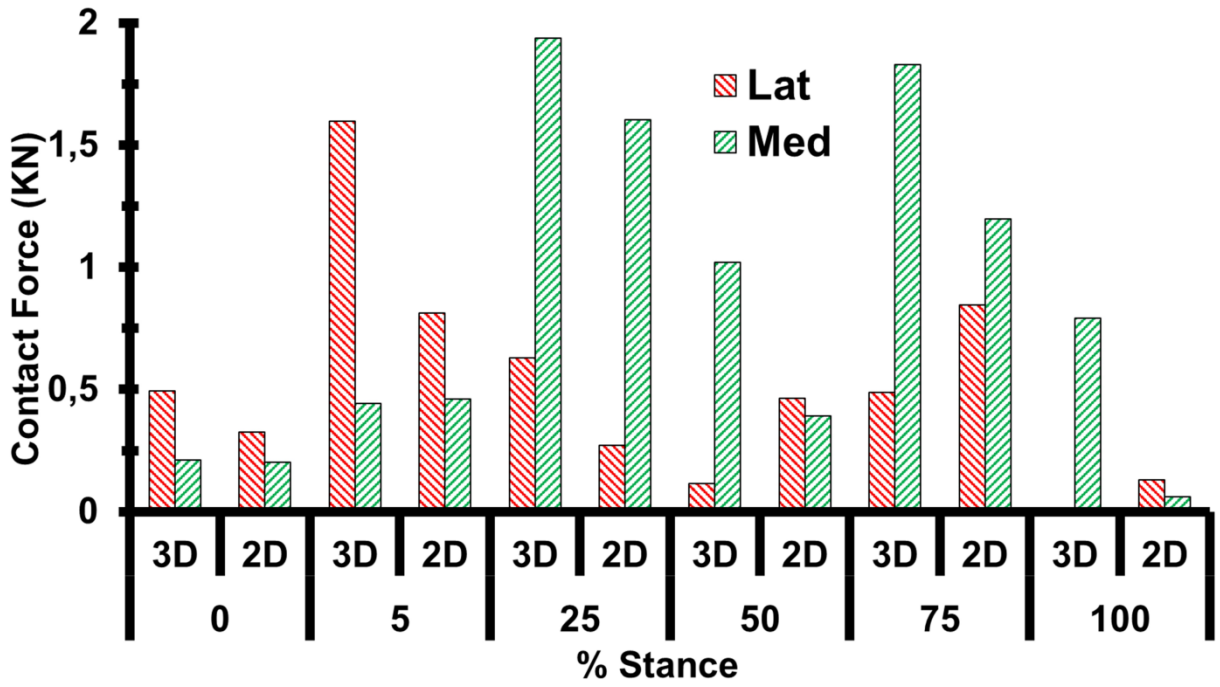

Figure A1.5: Computed compartmental contact forces on the medial and lateral plateaus in the 3D and 2D models. In the 2D model, the knee joint out-of-sagittal plane rotations and moments recorded in gait are neglected (Marouane et al., 2016a)

4. Validation

Computational models, if accurate and properly validated, are powerful and reliable tools in advancing our comprehension of joint functions in normal and perturbed conditions as well as in prevention and treatment programs (Henninger et al., 2010, Jones and Wilcox, 2008, Viceconti et al., 2005). Due to inherent challenges in experimental studies (in vivo and ex vivo) and the

associated burdens in time and cost, computational approaches have been recognized as a reliable and complementary method in the study of human biomechanics. The primary advantage of these numerical approaches lies in robust control over boundary conditions, loading, geometry and material properties allowing for sensitivity and statistical analyses in various input parameters. Moreover, internal forces, contact stresses/areas/centers and tissue stresses/strains are invaluable outputs that are difficult, if not impossible, to quantify in experimental investigations.

Our model of the knee joint has constantly and extensively been validated at different stages of its development over the last 20 years since mid-1990s (Bendjaballah et al., 1995) by comparison of its predictions with reported measurements under various loading and boundary conditions in passive (e.g., axial compression load (Marouane et al., 2015a, Shirazi et al., 2008, Marouane et al., 2014, Bendjaballah et al., 1995), F-E (Moglo and Shirazi-Adl, 2005), add-abd (Bendjaballah et al., 1997, Marouane et al., 2015a), A-P drawer (Bendjaballah et al., 1998, Moglo and Shirazi-Adl, 2003a, Moglo and Shirazi-Adl, 2003b, Shirazi and Shirazi-Adl, 2009) load-displacement conditions as well as active (e.g., F-E (Mesfar and Shirazi-Adl, 2006b, Mesfar and Shirazi-Adl, 2006a, Mesfar and Shirazi-Adl, 2005), open-closed kinetic-chain exercises (Adouni and Shirazi-Adl, 2009, Mesfar and Shirazi-Adl, 2008b, Mesfar and Shirazi-Adl, 2008a) and during gait (Adouni and Shirazi-Adl, 2014b, Adouni and Shirazi-Adl, 2014a, Adouni et al., 2012, Marouane et al., 2016b, Marouane et al., 2016a, Marouane et al., 2014)). Overall, satisfactory agreements were found that are presented here for some conditions.

Results of the TF model on the contact forces/pressures/areas under axial compression forces up to 1800 N has been compared with available measurements, see Table A1.1 (Marouane et al., 2015a) demonstrating good agreements. Despite differences in femoral constraints and loadings, in vitro studies of the TF joint at full extension under axial compression (Krause et al., 1976, Kurosawa et al., 1980, Seedhom, 1979, Shrive et al., 1978, Walker and Erkman, 1975) report similar nonlinear stiffening in the axial direction.

Table A1.1: Comparison of contact areas/pressures at different compression load and knee flexion angle (L: Lateral, M: Medial, T: Total).

Tibial Contact Area (mm^2)			**0N**	**400N**	**500N**	**800N**	**1000N**	**1200N**	**1400N**	**1500N**	**1800N**
Refined model (H Marouane et al., 2015a)	**0°** **15°** **30°** **45°**	L/M/**T** L/M L/M L/M	168/132/**300** - - -	- 344/199 363/170 376/151	484/208/**692** 380/232 382/196 396/188	544/237/**782** 423/301 440/264 426/265	570/260/**830** 460/342 466/335 446/281	580/269/**849** 486/374 475/366 458/324	586/300/**836** 505/404 491/382 472/343	- - - -	- - - -
Less refined model (H Marouane et al., 2015a)	**0°**	L/M/ **T**	169/100/ **270**	-	485/258/ **743**	526/327/ **853**	574/327/ **902**	585/351/ **937**	604/388/ **992**	604/378/ **982**	651/453/ **1104**
Shirazi et al (2008)	**0°**	**T**	**355**	-	**893**	-	**1083**	**-**	**-**	**1214**	**1253**
Poh et al. (2011)	**0°**	L/M/**T**	403 (±120) / 374 (±87) / **777 (±89)** (@ 1800N)								
Seitz et al. (2012)	**0°** **30°**	L/M	-	-	323±160/313±119 (@ 500N) 302±128/348±164 (@ 500N)			376±161/392±108 (@ 1200N) 364±148/410±92 (@ 1200N)			**-**
Marzo and Gurske-DePerio (2009)	**0°**	L/M	571±80 / 594±59 (@ 1800N)								
Paci et al. (2009)	**0°** **15°** **30°** **45°**	M	-	**-**	-	**-**	327 336 300 277	-	-	**-**	-
Brown and Shaw (1984)	**0°**	**T**	**-**	-	**1225±180**	**-**	**1250±100**	**-**	**-**	**1340±100**	**-**
Ahmed and Burke (1983)	**0°**	**T**	-	**1200** @ 445N	**-**	**1650** @ 890N	**-**	**-**	**1800** @ 1335N	**-**	**2000 @** 1779N
Huang et al. (2003)	**0°** **15°** **30°** **45°**	L	-	238±135280±120280±130300±120	-	-	-	300±100 300±95 330±130 310±120	-	-	-
Paletta et al. (1997)	**0°** **15°**	L	-	-	-	-	-		-	-	407 363
Lee et al. (2006)	**0°** **30°**	M	**-**	-	**-**	**-**	**-**	**-**	**-**	**-**	533±48 477±84
Fukubayashi and Kurosawa (1980)	**0°**	L/M/**T**	-	420±60/530±150/**960±170** (@ 500N)			510±70/640±180/**1150±200** (@ 1000N)			-	-
Kurosawa et al. (1980)	**0°**	**T**	**-**	**-**	**1130±250**	**-**	**1300±300**	**-**	**-**	**1410±320**	**-**
Krause et al. (1976)	**0°**	**T**	**-**	-	**-**	**-**	**2084**	**-**	-	**-**	**-**
Walker et al. (1972; 1975)	**0°**	**T**	**330**	**-**	**-**	**-**	**-**	**-**	-	**1514**	**-**
Mean Contact Pressure (MPa)			**200N**	**400N**	**500N**	**800N**	**1000N**	**1200N**	**1400N**	**1500N**	**1800N**
Refined Model (H Marouane et al., 2015a)	**0°** **15°** **30°** **45°**	L/M/**T** **L** **L** **L**	-	- 0.99 0.99 1.00	0.92/0.62/**0.78** 1.09 1.14 1.13	1.29/0.81/**1.08** - 1.46 1.53	1,53/0.91/**1,26** - 1.65 1.74	1.78/1.05/**1.46** 1.75 1.86 1.96	2.06/1.12/**1.64** 1.93 2.05 2.16	- - - -	- - - -
Less Refined Model (H Marouane et al., 2015a)	**0°**	L/M/**T**	-	**-**	0,87/0.48/**0.7**	1,26/0.58**0.95**	1,43/0.73/**1.11**	1,67/0.82/**1.28**	1.86/0.89/ **1.41**	1,98/0.99/**1.52**	2,16/1.03/**1.61**

Table A1.1 (suite): Comparison of contact areas/pressures at different compression load and knee flexion angle (L: Lateral, M: Medial, T: Total).

Poh et al. (2011)	**0°**	L/M/**T**	1.93 (±0.6) / 3.61 (±0.72) / **2.73 (±0.49)** (@ 1800N)								
Shirazi et al. (2008)	**0°**	**T**	**-**	**0.58**	**0.65**	**-**	**1.0**	**-**	**-**	**1.29**	**-**
Haut Donahue et al. (2002; 2003)	**0°**	L/M	-	-	-	0.94/0.72	-	1,59/1.36	**-**	-	-
Kurosawa et al. (1980)	**0°**	**T**	-	**-**	**0.47±0.12**	-	**0.8±0.2**	**-**	-	**1.1±0.28**	**-**
Krause et al. (1976)	**0°**	**T**	**-**	**-**	**-**	-	**0.48±0.08**	**-**	-	**-**	**-**
Huang et al. (2003)	**0°** **15°** **30°** **45°**	L	-	1.45±0.95 1.32±0.76 1±0.5 0.85±0.42	**-**	-	**-**	2.6±0.8 2.86±1.32 2.7±1 2.72±1.2	-	**-**	**-**

Under a small compression preload of 10 N, the TF FE model computed tangent add-abd angular stiffnesses of 5.38, 1.29, 1.13 and 0.83 Nm/deg in the frontal plane at 0°, 15°, 30° and 45° joint flexion angles, respectively (Marouane et al., 2015a). Presence of compression preload (up to 1800 N) applied at MBP substantially increased stiffnesses of the TF joint at all flexion angles (Marouane et al., 2015a), see Figure A1.6. With no joint compression, the femur fixed and the tibia under add-abd moments, Markolf et al. (1976) measured similar in vitro stiffness values (mean ± standard deviation) of 11.0 ± 7.5, 1.6 ± 1.2, 1.1 ± 0.8 and 0.8 ± 0.9 Nm/deg at 0°, 10°, 20° and 45° flexion angles, respectively. Moreover, Creaby et al. (2010) measured in vivo at 20° flexion the midrange angular stiffness of 1.62 ± 0.68 Nm/deg in asymptomatic controls, whereas Bendjaballah et al. (1997) computed the stiffness of ~4.5Nm/deg at full extension.

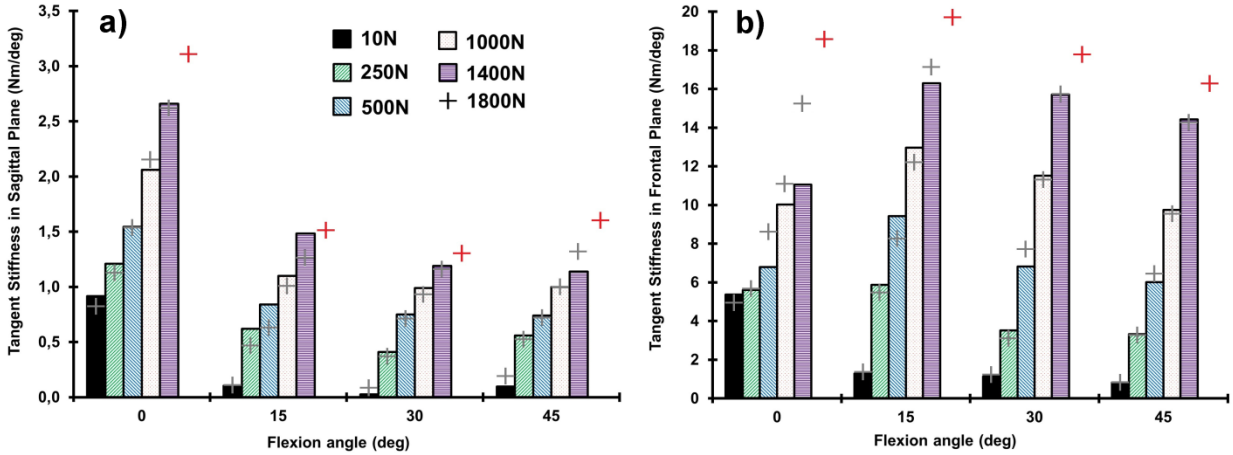

Figure A1.6: Instantaneous (tangent) F-E (a) and add-abd (b) angular rigidity of the TF joint as a function of compression preload and flexion angle (+: less refined model) (Marouane et al., 2015a).

Computed cruciate coupling and screw-home mechanism in passive TF joint during F-E was found in agreement with the literature (Moglo and Shirazi-Adl, 2005). Screw home motion of internal tibial rotation during joint flexion and external rotation during extension was computed. Prediction of ~16° internal tibial rotation at 90° femoral flexion is in the range of reported values of 6.5±4° (Markolf et al., 1976), 14.5° (Shoemaker and Markolf, 1985), 19.2±4° (Kurosawa et al., 1985) and 20±4° (Hsich and Draganich, 1997) at 90° flexion angle. In passive TF unconstrained F-E, ACL force diminished from 65N at 10° hyper-extension to 31N at 90° flexion. This change was found due to the shift in load resistance from ACL-pl bundle at hyper extension to ACL-am bundle in flexion angles, a trend in agreement with measurements (Woo et

al., 1998). The resistance in the PCL, on the other hand, initiated at flexion angles beyond 20–30° and reached 35N (by PCL-al bundle only) at 90° flexion. The foregoing predictions agree with others reporting increased force/strain in the PCL after 40–50° of flexion (Beynnon et al., 1996) and increased strain in ACL anteromedial bundles with flexion after 40° of flexion (Bach et al., 1997).

In the passive TF joint at full extension under single and combined femoral posterior drawer and axial compression forces, computed primary femoral laxity of 3.6 mm under 100 N posterior femoral force alone (Shirazi and Shirazi-Adl, 2009) compared well with the mean anterior tibial laxities of 2.8 mm to 6.7 mm reported under 100 N anterior tibial force at full extension (Markolf et al., 1981a, Rudy et al., 2000, Torzilli et al., 1994). The posterior translation of the femur relative to the tibia under pure compression, which is due to the posterior slope of the tibia (Torzilli et al., 1994) agreed with reported values (Torzilli et al., 1994, Markolf et al., 1981a). The relative magnitude and increases with compression preload of femoral translation in drawer were also in agreement with measurements (Torzilli et al., 1994, Hsieh and Walker, 1976, Markolf et al., 1981a, Li et al., 1998), Torzilli et al., 1994). The estimated force of 170 N in ACL matched with measured values of 75-162 N reported under ~100 N drawer at full extension (Takai et al., 1993, Markolf et al., 1995a). Addition of axial compression preload further increased ACL force under drawer from ~1.6 times, in agreement with 150% in measurements (Markolf et al., 1995a), to more than two-fold that of the applied drawer force. Prediction of the marked increase in ACL force in presence of compression preload (Marouane et al, 2014, 2015; Shirazi and Shirazi-Adl, 2009) corroborates well with earlier findings (Torzilli et al., 1994, Fleming et al., 2001, Li et al., 1998, Meyer and Haut, 2005, Meyer et al., 2008, Wall et al., 2012) but contradicts others suggesting that compression preload in drawer protects the ACL from damage (Markolf et al., 1990).

Our muscle force predictions during the stance phase of gait were also compared to available results in literature (Adouni et al., 2012, Adouni and Shirazi-Adl, 2014a). Predicted activation levels in quadriceps and gastrocnemius muscles were in satisfactory agreement with values in the literature (Besier et al., 2009, Shelburne et al., 2005, Winby et al., 2009, Lin et al., 2010, Neptune et al., 2004) and follow the same relative trends as measured EMG activities (Astephen, 2007, Astephen et al., 2008). The computed hamstring forces peaked right after the HS at 5% period (Adouni and Shirazi-Adl, 2014a, Adouni et al., 2012). Reported normalized

EMG activities in the superficial lateral and medial hamstrings (Astephen, 2007) are also highest right at the HS and decrease thereafter. On the other hand, apart from early periods of stance (0 and 5%) and due mainly to add-abd rotations, the medial plateau carried a larger portion of contact forces than did the lateral plateau (Adouni and Shirazi-Adl, 2014a, Adouni et al., 2012, Marouane et al., 2016b) which agrees with earlier estimates (Kumar et al., 2013, Kumar et al., 2012). In accordance with our predictions, others also reported small forces or none at all on the lateral compartment at the toe off phase (Shelburne et al., 2006, Guess et al., 2010).

5. Future directions

In our MS model of the lower extremity, only the knee joint was represented in details. On the other hand, hip and ankle joints were modeled as simple frictionless spherical joints. To improve the accuracy of estimations, it is appropriate to incorporate also the passive properties of these articulations as accurate as possible. In addition, due to expected variations in geometry, musculature and material properties, subject-specific models taking account of individual characteristics are recommended in order to predict the response in various activities (Kłodowski et al., 2016). The resulting predictions will help establish more subject-specific protocols for effective injury prevention and post-operative rehabilitation. Towards this goal, statistical modeling and sensitivity analyses are helpful.

With the rising incidence of medial knee joint OA, knee adduction moment (KAM) is commonly introduced as a surrogate measure of load on the medial plateau and hence as a marker where its reduction is the main focus of various interventions (e.g., orthoses, shoe insoles, gait modification, osteotomy) that aim to prevent the development and progression of OA. However, some recent in vivo studies using instrumented implants have questioned such direct relationship and qualified the correlation between KAM and the medial compartment load as poor to average (Walter et al., 2010). Similarly, questions have been raised on the association between pain/symptoms and reduction in KAM when wearing wedged insoles (Jones et al., 2014). The internal load distribution is however influenced mainly by changes in the knee adduction rotation than in KAM as reported in our previous work at mid-stance phase of gait (Adouni and Shirazi-Adl, 2014b). Confirmation this finding during the whole stance phase of gait is necessary. KAR and KAM should be altered one at a time at each stance period based on reported measurements (Wilson et al., 2014).

Quantification of stability reserve of intact/injured human musculoskeletal systems is crucial in performance evaluation, injury prevention and treatment managements. Dynamic stability of the knee joint in daily activities is maintained by a delicate interplay between the passive tissues and active musculature (voluntary and reflex). Joint hypermobility has been associated with pain and OA (Mulvey et al., 2013). Generally greater muscle antagonist contractions are recorded via surface EMG in OA patients. Future developments should hence quantify the mechanical stability of human knee joint in daily activities especially during gait and also investigate the role of muscle antagonistic coactivity at different levels on both the joint stability margin as well as muscle/contact/ligament forces.

ACCKNOWLEDGEMENTS

The current work was supported by a grant from the Natural Sciences and Engineering Research Council of Canada (RGPIN5596). The partial scholarship of MUTAN-Tunisia to the first author is also acknowledged.

REFERENCE

Adouni, M. (2014). *ANALYSE BIOMÉCANIQUE DE L'ARTICULATION DE GENOU DURANT LA BIPÉDIE HUMAINE* (Ph.D), École Polytechnique de Montréal.

Adouni, M., & Shirazi-Adl, A. (2009). Knee joint biomechanics in closed-kinetic-chain exercises. *Computer methods in biomechanics and biomedical engineering, 12*(6), 661-670.

Adouni, M., & Shirazi-Adl, A. (2012b). Consideration of equilibrium equations at the hip joint alongside those at the knee and ankle joints has mixed effects on knee joint response during gait. *Journal of Biomechanics*.

Adouni, M., & Shirazi-Adl, A. (2013). Consideration of equilibrium equations at the hip joint alongside those at the knee and ankle joints has mixed effects on knee joint response during gait. *Journal of biomechanics, 46*(3), 619-624.

Adouni, M., & Shirazi-Adl, A. (2014b). Partitioning of knee joint internal forces in gait is dictated by the knee adduction angle and not by the knee adduction moment. *Journal of biomechanics, 47*(7), 1696-1703.

Adouni, M., Shirazi-Adl, A., & Marouane, H. (2015). Role of gastrocnemius activation in knee joint biomechanics: gastrocnemius acts as an ACL antagonist. *Computer methods in biomechanics and biomedical engineering*(ahead-of-print), 1-10.

Adouni, M., Shirazi-Adl, A., & Shirazi, R. (2012). Computational biodynamics of human knee joint in gait: From muscle forces to cartilage stresses. *Journal of biomechanics*.

Adouni, M., Shirazi-Adl, A., & Shirazi, R. (2012a). Computational biodynamics of human knee joint in gait: from muscle forces to cartilage stresses. *Journal of Biomechanics, 45*(12), 2149-2156.

Adouni, M., & Shirazi-Adl, A. (2014a). Evaluation of knee joint muscle forces and tissue stresses-strains during gait in severe OA versus normal subjects. *Journal of Orthopaedic Research, 32*(1), 69-78.

Agel, J., Arendt, E. A., & Bershadsky, B. (2005). Anterior cruciate ligament injury in National Collegiate Athletic Association basketball and soccer a 13-year review. *The American Journal of Sports Medicine, 33*(4), 524-531.

Agneskirchner, J., Hurschler, C., Stukenborg-Colsman, C., Imhoff, A., & Lobenhoffer, P. (2004). Effect of high tibial flexion osteotomy on cartilage pressure and joint kinematics: a biomechanical study in human cadaveric knees. *Archives of orthopaedic and trauma surgery, 124*(9), 575-584.

Ahmed, A., & Burke, D. (1983). In-vitro measurement of static pressure distribution in synovial joints--Part I: Tibial surface of the knee. *Journal of biomechanical engineering, 105*(3), 216.

Akbarshahi, M., Schache, A. G., Fernandez, J. W., Baker, R., Banks, S., & Pandy, M. G. (2010). Non-invasive assessment of soft-tissue artifact and its effect on knee joint kinematics during functional activity. *Journal of Biomechanics, 43*(7), 1292-1301.

Alhalki, M. M., Howell, S. M., & Hull, M. L. (1999). How three methods for fixing a medial meniscal autograft affect tibial contact mechanics. *The American Journal of Sports Medicine, 27*(3), 320-328.

Allaire, R., Muriuki, M., Gilbertson, L., & Harner, C. D. (2008). Biomechanical consequences of a tear of the posterior root of the medial meniscusSimilar to total meniscectomy. *The Journal of Bone & Joint Surgery, 90*(9), 1922-1931.

Amis, A., & Dawkins, G. (1991). Functional anatomy of the anterior cruciate ligament. Fibre bundle actions related to ligament replacements and injuries. *Bone & Joint Journal, 73*(2), 260-267.

Amis, A. A. (2012). The functions of the fibre bundles of the anterior cruciate ligament in anterior drawer, rotational laxity and the pivot shift. *Knee Surgery, Sports Traumatology, Arthroscopy, 20*(4), 613-620.

Anderson, F. C., & Pandy, M. G. (2001). Dynamic optimization of human walking. *Journal of biomechanical engineering, 123*(5), 381-390.

Anderson, F. C., & Pandy, M. G. (2003). Individual muscle contributions to support in normal walking. *Gait & posture, 17*(2), 159-169.

Andriacchi, T., Alexander, E., Toney, M., Dyrby, C., & Sum, J. (1998). A point cluster method for in vivo motion analysis: applied to a study of knee kinematics. *Journal of biomechanical engineering, 120*(6), 743-749.

Andriacchi, T. P., & Alexander, E. J. (2000). Studies of human locomotion: past, present and future. *Journal of Biomechanics, 33*(10), 1217-1224.

Andriacchi, T. P., & Hurwitz, D. E. (1997). Gait biomechanics and the evolution of total joint replacement. *Gait & posture, 5*(3), 256-264.

Arendt, E., & Dick, R. (1995). Knee injury patterns among men and women in collegiate basketball and soccer NCAA data and review of literature. *The American Journal of Sports Medicine, 23*(6), 694-701.

Arendt, E. A., Agel, J., & Dick, R. (1999). Anterior cruciate ligament injury patterns among collegiate men and women. *Journal of Athletic Training, 34*(2), 86.

Arjmand, N., & Shirazi-Adl, A. (2006). Sensitivity of kinematics-based model predictions to optimization criteria in static lifting tasks. *Medical Engineering & Physics, 28*(6), 504-514.

Arnason, A., Gudmundsson, A., Dahl, H., & Johannsson, E. (1996). Soccer injuries in Iceland. *Scandinavian journal of medicine & science in sports, 6*(1), 40-45.

Arnold, E. M., Ward, S. R., Lieber, R. L., & Delp, S. L. (2010). A model of the lower limb for analysis of human movement. *Annals of biomedical engineering, 38*(2), 269-279.

Astephen, J. L. (2007). *Biomechanical Factors in the Progression of Knee Osteoarthritis.* (Ph.D), School of Biomedical Engineering, Dalhousie University, Halifax.

Astephen, J. L. (2007). *Biomechanical Factors in the Progression of Knee Osteoarthritis.* (Ph.D thesis), School of Biomedical Engineering, Dalhousie University, Halifax.

Astephen, J. L., Deluzio, K. J., Caldwell, G. E., & Dunbar, M. J. (2008). Biomechanical changes at the hip, knee, and ankle joints during gait are associated with knee osteoarthritis severity. *Journal of Orthopaedic Research, 26*(3), 332-341.

Atkinson, P., Atkinson, T., Huang, C., & Doane, R. (2000). *A comparison of the mechanical and dimensional properties of the human medial and lateral patellofemoral ligaments.*

Bendjaballah, M., Shirazi-Adl, A., & Zukor, D. (1997). Finite element analysis of human knee joint in varus-valgus. *Clinical Biomechanics, 12*(3), 139-148.

Bendjaballah, M. Z., Shirazi-Adl, A., & Zukor, D. (1995). Biomechanics of the human knee joint in compression: reconstruction, mesh generation and finite element analysis. *The Knee, 2*(2), 69-79.

Bendjaballah, M. Z., Shirazi-Adl, A., & Zukor, D. (1997). Finite element analysis of human knee joint in varus-valgus. *Clinical Biomechanics, 12*(3), 139-148.

Bendjaballah, M. Z., Shirazi-Adl, A., & Zukor, D. (1998). Biomechanical response of the passive human knee joint under anterior-posterior forces. *Clinical Biomechanics, 13*(8), 625-633.

Besier, T. F., Fredericson, M., Gold, G. E., Beaupré, G. S., & Delp, S. L. (2009). Knee muscle forces during walking and running in patellofemoral pain patients and pain-free controls. *Journal of biomechanics, 42*(7), 898-905.

Blagojevic, M., Jinks, C., Jeffery, A., & Jordan, K. (2010). Risk factors for onset of osteoarthritis of the knee in older adults: a systematic review and meta-analysis. *Osteoarthritis and cartilage, 18*(1), 24-33.

Blankevoort, L., & Huiskes, R. (1991c). Ligament-bone interaction in a three-dimensional model of the knee. *J Biomech Eng, 113*(3), 263-269.

Blankevoort, L., Kuiper, J., Huiskes, R., & Grootenboer, H. (1991a). Articular contact in a three-dimensional model of the knee. *Journal of biomechanics, 24*(11), 1019-1031.

Boakes, J. L., & Rab, G. T. (2006). Muscle activity during walking. *Human Walking. Lippincott Williams and Wilkins*.

Boden, B. P., Breit, I., & Sheehan, F. T. (2009a). Tibiofemoral alignment: contributing factors to noncontact anterior cruciate ligament injury. *The Journal of Bone & Joint Surgery, 91*(10), 2381-2389.

Bojicic, K. M., Beaulieu, M. L., Imaizumi Krieger, D. Y., Ashton-Miller, J. A., & Wojtys, E. M. (2017). Association Between Lateral Posterior Tibial Slope, Body Mass Index, and ACL Injury Risk. *Orthopaedic Journal of Sports Medicine, 5*(2), 2325967116688664.

Bouisset, S. (2002). *Biomécanique et physiologie du mouvement*: Elsevier Masson.

Bourne, R. B., Chesworth, B. M., Davis, A. M., Mahomed, N. N., & Charron, K. D. (2010). Patient satisfaction after total knee arthroplasty: who is satisfied and who is not? *Clinical Orthopaedics and Related Research®, 468*(1), 57-63.

Bourne, R. B., McCalden, R. W., MacDonald, S. J., Mokete, L., & Guerin, J. (2007). Influence of patient factors on TKA outcomes at 5 to 11 years followup. *Clinical orthopaedics and related research, 464*, 27-31.

Brandon, M. L., Haynes, P. T., Bonamo, J. R., Flynn, M. I., Barrett, G. R., & Sherman, M. F. (2006). The association between posterior-inferior tibial slope and anterior cruciate ligament insufficiency. *Arthroscopy: The Journal of Arthroscopic & Related Surgery, 22*(8), 894-899.

Brazier, J., Migaud, H., Gougeon, F., Cotten, A., Fontaine, C., & Duquennoy, A. (1996). Evaluation of methods for radiographic measurement of the tibial slope. A study of 83 healthy knees]. *Revue de chirurgie orthopédique et réparatrice de l'appareil moteur, 82*(3), 195.

Brinckmann, P., Frobin, W., & Leivseth, G. (2002). *Musculoskeletal biomechanics*: Thieme.

Broom, N., & Marra, D. (1986). Ultrastructural evidence for fibril-to-fibril associations in articular cartilage and their functional implication. *Journal of anatomy, 146*, 185.

Brown, T. D., & Shaw, D. T. (1984). In vitro contact stress distribution on the femoral condyles. *Journal of Orthopaedic Research, 2*(2), 190-199.

Calmbach, W. L., & Hutchens, M. (2003). Evaluation of patients presenting with knee pain: Part I. History, physical examination, radiographs, and laboratory tests. *American family physician, 68*(5), 907-912.

Cappozzo, A., Marchetti, M., & Tosi, V. (1992). *Biolocomotion: a century of research using moving pictures* (Vol. 1): Promograph.

Chao, E., Laughman, R., Schneider, E., & Stauffer, R. (1983). Normative data of knee joint motion and ground reaction forces in adult level walking. *Journal of Biomechanics, 16*(3), 219-233.

Chaudhari, A. M., Zelman, E. A., Flanigan, D. C., Kaeding, C. C., & Nagaraja, H. N. (2009). Anterior Cruciate Ligament–Injured Subjects Have Smaller Anterior Cruciate Ligaments Than Matched Controls A Magnetic Resonance Imaging Study. *The American journal of sports medicine, 37*(7), 1282-1287.

Chen, C.-H., Li, J.-S., Hosseini, A., Gadikota, H. R., Kozanek, M., Gill, T. J., & Li, G. (2011). *Tibiofemoral Kinematics of the Knee During the Stance Phase of Gait After ACL Deficiency.* Paper presented at the ASME 2011 Summer Bioengineering Conference.

Chiu, K., Zhang, S., & Zhang, G. (2000). Posterior slope of tibial plateau in Chinese. *The Journal of arthroplasty, 15*(2), 224-227.

Clarke, I. (1974). Articular cartilage: a review and scanning electron microscope study. II. The territorial fibrillar architecture. *Journal of anatomy, 118*(Pt 2), 261.

Crowninshield, R., Pope, M., & Johnson, R. (1976). An analytical model of the knee. *Journal of biomechanics, 9*(6), 397-405.

Dahlstedt, S. (1978). Slow pedestrians: walking speeds and walking habits of old aged people. *Stockholm: The Swedish Council for Building Researd, Report, 2*, 1977.

Daniel, D. M., Stone, M. L., Dobson, B. E., Fithian, D. C., Rossman, D. J., & Kaufman, K. R. (1994). Fate of the ACL-injured patient a prospective outcome study. *The American journal of sports medicine, 22*(5), 632-644.

de Boer, J. J., Blankevoort, L., Kingma, I., & Vorster, W. (2009). In vitro study of inter-individual variation in posterior slope in the knee joint. *Clinical Biomechanics, 24*(6), 488-492.

De Leva, P. (1996). Adjustments to Zatsiorsky-Seluyanov's segment inertia parameters. *Journal of biomechanics, 29*(9), 1223-1230.

Dejour, H., & Bonnin, M. (1994). Tibial translation after anterior cruciate ligament rupture. Two radiological tests compared. *Journal of Bone & Joint Surgery, British Volume, 76*(5), 745-749.

Delp, S. L., Anderson, F. C., Arnold, A. S., Loan, P., Habib, A., John, C. T., . . . Thelen, D. G. (2007). OpenSim: open-source software to create and analyze dynamic simulations of movement. *Biomedical Engineering, IEEE Transactions on, 54*(11), 1940-1950.

Delp, S. L., Loan, J. P., Hoy, M. G., Zajac, F. E., Topp, E. L., & Rosen, J. M. (1990). An interactive graphics-based model of the lower extremity to study orthopaedic surgical procedures. *Biomedical Engineering, IEEE Transactions on, 37*(8), 757-767.

DeMers, M. S., Pal, S., & Delp, S. L. (2014). Changes in tibiofemoral forces due to variations in muscle activity during walking. *Journal of Orthopaedic Research, 32*(6), 769-776.

Dennis, D. A., Mahfouz, M. R., Komistek, R. D., & Hoff, W. (2005). In vivo determination of normal and anterior cruciate ligament-deficient knee kinematics. *Journal of biomechanics, 38*(2), 241-253.

Dujardin, F., Roussignol, X., Mejjad, O., Weber, J., & Thomine, J. (1997). Interindividual variations of the hip joint motion in normal gait. *Gait & posture, 5*(3), 246-250.

Duthon, V., Barea, C., Abrassart, S., Fasel, J., Fritschy, D., & Ménétrey, J. (2006). Anatomy of the anterior cruciate ligament. *Knee Surgery, Sports Traumatology, Arthroscopy, 14*(3), 204-213.

Dyrby, C. O., & Andriacchi, T. P. (2004). Secondary motions of the knee during weight bearing and non-weight bearing activities. *Journal of Orthopaedic Research, 22*(4), 794-800.

Eng, J. J., & Winter, D. A. (1995). Kinetic analysis of the lower limbs during walking: what information can be gained from a three-dimensional model? *Journal of Biomechanics, 28*(6), 753-758.

Fairbank, T. (1948). Knee joint changes after meniscectomy. *Journal of Bone & Joint Surgery, British Volume, 30*(4), 664-670.

Fening, S. D., Kovacic, J., Kambic, H., McLean, S., Scott, J., & Miniaci, A. (2008). The effects of modified posterior tibial slope on acl strain and knee kinematics: a human cadaveric study. *The journal of knee surgery, 21*(3), 205.

Fithian, D. C., Kelly, M. A., & Mow, V. C. (1990). Material properties and structure-function relationships in the menisci. *Clinical orthopaedics and related research*(252), 19.

Fleming, B. C., Renstrom, P. A., Beynnon, B. D., Engstrom, B., Peura, G. D., Badger, G. J., & Johnson, R. J. (2001). The effect of weightbearing and external loading on anterior cruciate ligament strain. *Journal of Biomechanics, 34*(2), 163-170.

Fraysse, F. (2009). *Estimation des activités musculaires au cours du mouvement en vue d'applications ergonomiques.* Université Claude Bernard-Lyon I.

Fukubayashi, T., & Kurosawa, H. (1980). The contact area and pressure distribution pattern of the knee: a study of normal and osteoarthrotic knee joints. *Acta Orthopaedica, 51*(1-6), 871-879.

Gaasbeek, R. D., Groen, B. E., Hampsink, B., Van Heerwaarden, R. J., & Duysens, J. (2007). Valgus bracing in patients with medial compartment osteoarthritis of the knee: a gait analysis study of a new brace. *Gait & posture, 26*(1), 3-10.

Gao, B., & Zheng, N. N. (2010). Alterations in three-dimensional joint kinematics of anterior cruciate ligament-deficient and -reconstructed knees during walking. *Clinical Biomechanics, 25*, 222-229.

Genin, P., Weill, G., & Julliard, R. (1993). [The tibial slope. Proposal for a measurement method]. *Journal de radiologie, 74*(1), 27.

Geoffrey, K., Franz, J. R., Dicharry, J., Croce, U. D., & Kerrigan, D. C. (2011). Lower limb joint kinetics in walking: The role of industry recommended footwear. *Gait & posture, 33*(3), 350-355.

Gerus, P., Sartori, M., Besier, T. F., Fregly, B. J., Delp, S. L., Banks, S. A., . . . Lloyd, D. G. (2013). Subject-specific knee joint geometry improves predictions of medial tibiofemoral contact forces. *Journal of biomechanics, 46*(16), 2778-2786.

Giffin, J. R., Vogrin, T. M., Zantop, T., Woo, S. L., & Harner, C. D. (2004). Effects of increasing tibial slope on the biomechanics of the knee. *The American journal of sports medicine, 32*(2), 376-382.

Grood, E., & Hefzy, M. (1982). An analytical technique for modeling knee joint stiffness--Part I: Ligamentous forces. *Journal of biomechanical engineering, 104*(4), 330.

Grood, E. S., & Suntay, W. J. (1983). A joint coordinate system for the clinical description of three-dimensional motions: application to the knee. *Journal of biomechanical engineering, 105*(2), 136-144.

Grood, E. S., & Suntay, W. J. (1983). A joint coordinate system for the clinical description of three-dimensional motions: application to the knee. *Journal of biomechanical engineering, 105*(2), 136.

Guilak, F. (2011). Biomechanical factors in osteoarthritis. *Best practice & research Clinical rheumatology, 25*(6), 815-823.

Halonen, K., Mononen, M., Töyräs, J., Kröger, H., Joukainen, A., & Korhonen, R. (2016). Optimal graft stiffness and pre-strain restore normal joint motion and cartilage responses in ACL reconstructed knee. *Journal of biomechanics*.

Hashemi, J., Chandrashekar, N., Gill, B., Beynnon, B. D., Slauterbeck, J. R., SchuttJr, R. C., . . . Dabezies, E. (2008). The geometry of the tibial plateau and its influence on the biomechanics of the tibiofemoral joint. *The Journal of Bone & Joint Surgery, 90*(12), 2724-2734.

Hashemi, J., Chandrashekar, N., Mansouri, H., Gill, B., Slauterbeck, J. R., Schutt, R. C., . . . Beynnon, B. D. (2009). Shallow Medial Tibial Plateau and Steep Medial and Lateral

Tibial Slopes New Risk Factors for Anterior Cruciate Ligament Injuries. *The American journal of sports medicine, 38*(1), 54-62.

Hashemi, J., Chandrashekar, N., Mansouri, H., Gill, B., Slauterbeck, J. R., Schutt, R. C., . . . Beynnon, B. D. (2010). Shallow medial tibial plateau and steep medial and lateral tibial slopes new risk factors for anterior cruciate ligament injuries. *The American Journal of Sports Medicine, 38*(1), 54-62.

Haut Donahue, T. L., & Hull, M. (2002). A finite element model of the human knee joint for the study of tibio-femoral contact. *Journal of biomechanical engineering, 124*, 273.

Haut Donahue, T. L., Hull, M., Rashid, M. M., & Jacobs, C. R. (2003). How the stiffness of meniscal attachments and meniscal material properties affect tibio-femoral contact pressure computed using a validated finite element model of the human knee joint. *Journal of biomechanics, 36*(1), 19-34.

Hernigou, P., & Goutallier, D. (1990). Usure osseuse sous-chondrale des plateaux tibiaux dans les gonarthroses fémoro-tibiales. *Rev du Rhumat, 57*(1), 67-72.

Hewett, T. E., Noyes, F. R., Barber-Westin, S. D., & Hedcmann, T. P. (1998). Decrease in knee joint pain and increase in function in patients with medial compartment arthrosis: a prospective analysis of valgus bracing. *Orthopedics, 21*(2), 131-138.

HOFMANN, A. A., BACHUS, K. N., & WYATT, R. W. (1991). Effect of the tibial cut on subsidence following total knee arthroplasty. *Clinical orthopaedics and related research, 269*, 63-69.

Hohmann, E., Bryant, A., Reaburn, P., & Tetsworth, K. (2010). Does Posterior Tibial Slope Influence Knee Functionality in the Anterior Cruciate Ligament–Deficient and Anterior Cruciate Ligament–Reconstructed Knee? *Arthroscopy: The Journal of Arthroscopic & Related Surgery, 26*(11), 1496-1502.

Horsman, M. K., Koopman, H., Veeger, H., & van der Helm, F. (2007). The Twente Lower Extremity Model: a comparison of maximal isometric moment with the literature. *The Twente Lower Extremity Model*, 65.

Huang, A., Hull, M., & Howell, S. M. (2003). The level of compressive load affects conclusions from statistical analyses to determine whether a lateral meniscal autograft restores tibial

contact pressure to normal: a study in human cadaveric knees. *Journal of Orthopaedic Research, 21*(3), 459-464.

Hughes, P. E., Hsu, J. C., & Matava, M. J. (2002). Hip anatomy and biomechanics in the athlete. *Sports medicine and arthroscopy review, 10*(2), 103-114.

Hunt, A. E., M Smith, R., Torode, M., & Keenan, A.-M. (2001). Inter-segment foot motion and ground reaction forces over the stance phase of walking. *Clinical Biomechanics, 16*(7), 592-600.

Hunt, A. E., Smith, R. M., Torode, M., & Keenan, A.-M. (2001). Inter-segment foot motion and ground reaction forces over the stance phase of walking. *Clinical Biomechanics, 16*(7), 592-600.

Hunt, M. A., Birmingham, T. B., Giffin, J. R., & Jenkyn, T. R. (2006). Associations among knee adduction moment, frontal plane ground reaction force, and lever arm during walking in patients with knee osteoarthritis. *Journal of Biomechanics, 39*(12), 2213-2220.

Hurwitz, D. E., Sumner, D. R., Andriacchi, T. P., & Sugar, D. A. (1998). Dynamic knee loads during gait predict proximal tibial bone distribution. *Journal of Biomechanics, 31*(5), 423-430.

Hutchinson, M. R., & Ireland, M. L. (1995). Knee injuries in female athletes. *Sports medicine, 19*(4), 288-302.

Jiang, C., Yip, K., & Liu, T. (1994). Posterior slope angle of the medial tibial plateau. *Journal of the Formosan Medical Association, 93*(6), 509-512.

Jones, H., & Rocha, P. C. (2012). Prevention in ACL Injuries *Sports Injuries* (pp. 33-42): Springer.

Julliard, R., Genin, P., Weil, G., & Palmkrantz, P. (1993). The median functional slope of the tibia. Principle. Technique of measurement. Value. Interest. *Rev Chir Orthop Reparatrice Appar Mot, 79*(8), 625-634.

Kääb, M., Ap Gwynn, I., & Nötzli, H. (1998). Collagen fibre arrangement in the tibial plateau articular cartilage of man and other mammalian species. *Journal of anatomy, 193*(1), 23-34.

Kadaba, M. P., Ramakrishnan, H., & Wootten, M. (1990). Measurement of lower extremity kinematics during level walking. *Journal of Orthopaedic Research, 8*(3), 383-392.

Kapandji, A. (1994). Physiologie articulaire. Tome 2, schémas commentés de mécanique humaine, le membre inférieur: Edition Maloine.

Kaufman, K. R., & Sutherland, D. H. (2006). Kinematics of normal human walking. *Human walking, 3*, 33-52.

Kawamura, S., Lotito, K., & Rodeo, S. A. (2003). Biomechanics and healing response of the meniscus. *Operative Techniques in Sports Medicine, 11*(2), 68-76.

Kazemi, M., & Li, L. (2014). A viscoelastic poromechanical model of the knee joint in large compression. *Medical Engineering & Physics, 36*(8), 998-1006.

Keller, T., Weisberger, A., Ray, J., Hasan, S., Shiavi, R., & Spengler, D. (1996). Relationship between vertical ground reaction force and speed during walking, slow jogging, and running. *Clinical Biomechanics, 11*(5), 253-259.

Kim, H. J., Fernandez, J. W., Akbarshahi, M., Walter, J. P., Fregly, B. J., & Pandy, M. G. (2009). Evaluation of predicted knee-joint muscle forces during gait using an instrumented knee implant. *Journal of Orthopaedic Research, 27*(10), 1326-1331.

Koay, E., & Athanasiou, K. (2009). ARTICULAR CARTILAGE BIOMECHANICS, MECHANOBIOLOGY, AND TISSUE ENGINEERING *Biomechanical Systems Technology: Volume 3: Muscular Skeletal Systems* (pp. 1-37).

Koo, S., & Andriacchi, T. P. (2008). The knee joint center of rotation is predominantly on the lateral side during normal walking. *Journal of biomechanics, 41*(6), 1269-1273.

Kozanek, M., Hosseini, A., Liu, F., Van de Velde, S. K., Gill, T. J., Rubash, H. E., & Li, G. (2009). Tibiofemoral kinematics and condylar motion during the stance phase of gait. *Journal of biomechanics, 42*(12), 1877-1884.

Krause, W., Pope, M., Johnson, R., & Wilder, D. (1976). Mechanical changes in the knee after meniscectomy. *The Journal of bone and joint surgery. American volume, 58*(5), 599.

Kumar, D., Manal, K. T., & Rudolph, K. S. (2013). Knee joint loading during gait in healthy controls and individuals with knee osteoarthritis. *Osteoarthritis and cartilage, 21*(2), 298-305.

Kumar, D., Rudolph, K. S., & Manal, K. T. (2012). EMG-driven modeling approach to muscle force and joint load estimations: Case study in knee osteoarthritis. *Journal of Orthopaedic Research, 30*(3), 377-383.

Kurosawa, H., Fukubayashi, T., & Nakajima, H. (1980). Load-bearing mode of the knee joint: physical behavior of the knee joint with or without menisci. *Clinical orthopaedics and related research*(149), 283.

Kurtz, S., Ong, K., Lau, E., Mowat, F., & Halpern, M. (2007). Projections of primary and revision hip and knee arthroplasty in the United States from 2005 to 2030. *The Journal of Bone & Joint Surgery, 89*(4), 780-785.

Kutzner, I., Heinlein, B., Graichen, F., Bender, A., Rohlmann, A., Halder, A., . . . Bergmann, G. (2010). Loading of the knee joint during activities of daily living measured in vivo in five subjects. *Journal of biomechanics, 43*(11), 2164-2173.

Kuwano, T., Urabe, K., Miura, H., Nagamine, R., Matsuda, S., Satomura, M., . . . Iwamoto, Y. (2005). Importance of the lateral anatomic tibial slope as a guide to the tibial cut in total knee arthroplasty in Japanese patients. *Journal of Orthopaedic Science, 10*(1), 42-47.

Lafortune, M., Cavanagh, P., Sommer Iii, H., & Kalenak, A. (1992). Three-dimensional kinematics of the human knee during walking. *Journal of Biomechanics, 25*(4), 347-357.

Landry, S. C., McKean, K. A., Hubley-Kozey, C. L., Stanish, W. D., & Deluzio, K. J. (2007). Knee biomechanics of moderate OA patients measured during gait at a self-selected and fast walking speed. *Journal of Biomechanics, 40*(8), 1754-1761.

Lee, S. J., Aadalen, K. J., Malaviya, P., Lorenz, E. P., Hayden, J. K., Farr, J., . . . Cole, B. J. (2006). Tibiofemoral contact mechanics after serial medial meniscectomies in the human cadaveric knee. *The American journal of sports medicine, 34*(8), 1334-1344.

Lephart, S., Ferris, C., & Fu, F. (2002). Risk factors associated with noncontact anterior cruciate ligament injuries in female athletes. *INSTRUCTIONAL COURSE LECTURES-AMERICAN ACADEMY OF ORTHOPAEDIC SURGEONS, 51*, 307-310.

Lerner, Z. F., Board, W. J., & Browning, R. C. (2015b). Pediatric obesity and walking duration increase medial tibiofemoral compartment contact forces. *Journal of Orthopaedic Research*.

Lerner, Z. F., DeMers, M. S., Delp, S. L., & Browning, R. C. (2015). How tibiofemoral alignment and contact locations affect predictions of medial and lateral tibiofemoral contact forces. *Journal of biomechanics, 48*(4), 644-650.

Lerner, Z. F., Haight, D. J., DeMers, M. S., Board, W. J., & Browning, R. C. (2014). The effects of walking speed on tibiofemoral loading estimated via musculoskeletal modeling. *Journal of applied biomechanics, 30*(2), 197.

Levy, I. M., Torzilli, P., Gould, J., & Warren, R. (1989). The effect of lateral meniscectomy on motion of the knee. *J Bone Joint Surg Am, 71*(3), 401-406.

Levy, I. M., Torzilli, P., & Warren, R. (1982). The effect of medial meniscectomy on anterior-posterior motion of the knee. *J Bone Joint Surg Am, 64*(6), 883-888.

Li, G., DeFrate, L. E., Park, S. E., Gill, T. J., & Rubash, H. E. (2005). In Vivo Articular Cartilage Contact Kinematics of the Knee An Investigation Using Dual-Orthogonal Fluoroscopy and Magnetic Resonance Image–Based Computer Models. *The American Journal of Sports Medicine, 33*(1), 102-107.

Li, G., Gil, J., Kanamori, A., & Woo, S.-Y. (1999). A validated three-dimensional computational model of a human knee joint. *Journal of biomechanical engineering, 121*(6), 657-662.

Li, G., Kozanek, M., Hosseini, A., & Liu, F. (2009). New fluoroscopic imaging technique for investigation of 6DOF knee kinematics during treadmill gait. *Journal of Orthopaedic Surgery and Research, 4*(1), 1-5.

Li, G., Moses, J. M., Papannagari, R., Pathare, N. P., DeFrate, L. E., & Gill, T. J. (2006). Anterior cruciate ligament deficiency alters the in vivo motion of the tibiofemoral cartilage contact points in both the anteroposterior and mediolateral directions. *The Journal of Bone & Joint Surgery, 88*(8), 1826-1834.

Li, G., Pierce, J. E., & Herndon, J. H. (2006). A global optimization method for prediction of muscle forces of human musculoskeletal system. *Journal of biomechanics, 39*(3), 522-529.

Li, G., Suggs, J., & Gill, T. (2002). The effect of anterior cruciate ligament injury on knee joint function under a simulated muscle load: a three-dimensional computational simulation. *Annals of biomedical engineering, 30*(5), 713-720.

Lindenfeld, T. N., Hewett, T. E., & Andriacchi, T. P. (1997). Joint loading with valgus bracing in patients with varus gonarthrosis. *Clinical orthopaedics and related research, 344*, 290-297.

Liu-Barba, D., Hull, M., & Howell, S. (2007). Coupled motions under compressive load in intact and ACL-deficient knees: a cadaveric study. *TRANSACTIONS-AMERICAN SOCIETY OF MECHANICAL ENGINEERS JOURNAL OF BIOMECHANICAL ENGINEERING, 129*(6), 818.

Liu, W., & Maitland, M. E. (2003). Influence of anthropometric and mechanical variations on functional instability in the ACL-deficient knee. *Annals of biomedical engineering, 31*(10), 1153-1161.

Lloyd, D. G., & Besier, T. F. (2003). An EMG-driven musculoskeletal model to estimate muscle forces and knee joint moments in vivo. *Journal of biomechanics, 36*(6), 765-776.

Lloyd, D. G., & Buchanan, T. S. (2001). Strategies of muscular support of varus and valgus isometric loads at the human knee. *Journal of biomechanics, 34*(10), 1257-1267.

Logan, M., Dunstan, E., Robinson, J., Williams, A., Gedroyc, W., & Freeman, M. (2004). Tibiofemoral kinematics of the anterior cruciate ligament (ACL)-deficient weightbearing, living knee employing vertical access open “interventional” multiple resonance imaging. *The American journal of sports medicine, 32*(3), 720-726.

Lohmander, L., Östenberg, A., Englund, M., & Roos, H. (2004). High prevalence of knee osteoarthritis, pain, and functional limitations in female soccer players twelve years after anterior cruciate ligament injury. *Arthritis & Rheumatism, 50*(10), 3145-3152.

Manal, K., & Buchanan, T. S. (2013). An electromyogram-driven musculoskeletal model of the knee to predict in vivo joint contact forces during normal and novel gait patterns. *Journal of biomechanical engineering, 135*(2), 021014.

Marey, E. (1884). Analyse cinématique de la marche [chronophotograph]. *CR Séances Acad. Sci*, 2.

Markolf, K., Mensch, J., & Amstutz, H. (1976). Stiffness and laxity of the knee--the contributions of the supporting structures. A quantitative in vitro study. *The Journal of bone and joint surgery. American volume, 58*(5), 583.

Markolf, K. L., Burchfield, D. M., Shapiro, M. M., Shepard, M. F., Finerman, G. A. M., & Slauterbeck, J. L. (1995). Combined knee loading states that generate high anterior cruciate ligament forces. *Journal of Orthopaedic Research, 13*(6), 930-935.

Markolf, K. L., Gorek, J. F., Kabo, J. M., & Shapiro, M. S. (1990). Direct measurement of resultant forces in the anterior cruciate ligament. *J Bone Joint Surg Am, 72*, 557-567.

Markolf, K. L., Jackson, S. R., Foster, B., & McAllister, D. R. (2013). ACL forces and knee kinematics produced by axial tibial compression during a passive flexion–extension cycle. *Journal of Orthopaedic Research*.

Markolf, K. L., Park, S., Jackson, S. R., & McAllister, D. R. (2009). Anterior-posterior and rotatory stability of single and double-bundle anterior cruciate ligament reconstructions. *The Journal of Bone & Joint Surgery, 91*(1), 107-118.

Marouane, H. (2012). *Effet de la force de compression sur la réponse passive de l'articulation du genou: une étude numérique non-linéaire.* École Polytechnique de Montréal.

Marouane, H., Shirazi-Adl, A., & Adouni, M. (2013). Knee joint passive stiffness and moment in sagittal and frontal planes markedly increase with compression. *Computer methods in biomechanics and biomedical engineering*(ahead-of-print), 1-12.

Marouane, H., Shirazi-Adl, A., & Adouni, M. (2015a). Knee joint passive stiffness and moment in sagittal and frontal planes markedly increase with compression. *Computer methods in biomechanics and biomedical engineering, 18*(4), 339-350.

Marouane, H., Shirazi-Adl, A., & Adouni, M. (2016a). 3D Active-Passive Response of Human Knee Joint in Gait is Markedly Altered When Simulated as a Planar 2D Joint. *Biomechanics and modeling in mechanobiology*, 1-11.

Marouane, H., Shirazi-Adl, A., & Adouni, M. (2016b). Alterations in knee contact forces and centers in stance phase of gait: A detailed lower extremity musculoskeletal model. *Journal of biomechanics, 49*(2), 185-192.

Marouane, H., Shirazi-Adl, A., & Hashemi, J. (2015b). Quantification of the role of tibial posterior slope in knee joint mechanics and ACL force in simulated gait. *Journal of biomechanics*.

Marzo, J. M., & Gurske-DePerio, J. (2009). Effects of medial meniscus posterior horn avulsion and repair on tibiofemoral contact area and peak contact pressure with clinical implications. *The American Journal of Sports Medicine, 37*(1), 124-129.

Matsuda, S., Miura, H., Nagamine, R., Urabe, K., Ikenoue, T., Okazaki, K., & Iwamoto, Y. (1999). Posterior tibial slope in the normal and varus knee. *The American journal of knee surgery, 12*(3), 165.

McLean, S. G., Lucey, S. M., Rohrer, S., & Brandon, C. (2010). Knee joint anatomy predicts high-risk in vivo dynamic landing knee biomechanics. *Clinical Biomechanics, 25*(8), 781-788.

Meister, K., Talley, M. C., Horodyski, M. B., Indelicato, P. A., Hartzel, J. S., & Batts, J. (1998). Caudal slope of the tibia and its relationship to noncontact injuries to the ACL. *The American journal of knee surgery, 11*(4), 217.

Mellal, A. (2010). *Application pratique de l'anatomie humaine-Tome 2* (Vol. 2): Editions Publibook.

Mesfar, W. (2005). *Biomecanique du genou humain en flexion sous les activites musculaires: Modelisation par la methode des elements finis.* (Ph.D), École Polytechnique de Montréal.

Mesfar, W., & Shirazi-Adl, A. (2005). Biomechanics of the knee joint in flexion under various quadriceps forces. *The Knee, 12*(6), 424-434.

Mesfar, W., & Shirazi-Adl, A. (2006a). Biomechanics of changes in ACL and PCL material properties or prestrains in flexion under muscle force-implications in ligament reconstruction. *Computer methods in biomechanics and biomedical engineering, 9*(4), 201-209.

Mesfar, W., & Shirazi-Adl, A. (2006b). Knee joint mechanics under quadriceps-hamstrings muscle forces are influenced by tibial restraint. *Clinical Biomechanics, 21*(8), 841-848.

Mesfar, W., & Shirazi-Adl, A. (2008a). Computational biomechanics of knee joint in open kinetic chain extension exercises. *Computer methods in biomechanics and biomedical engineering, 11*(1), 55-61.

Mesfar, W., & Shirazi-Adl, A. (2008b). Knee joint biomechanics in open-kinetic-chain flexion exercises. *Clinical Biomechanics-Kidlington, 23*(4), 477-482.

Messier, S. P., Legault, C., Loeser, R. F., Van Arsdale, S. J., Davis, C., Ettinger, W. H., & DeVita, P. (2011). Does high weight loss in older adults with knee osteoarthritis affect bone-on-bone joint loads and muscle forces during walking? *Osteoarthritis and cartilage, 19*(3), 272-280.

Meyer, A. J., D'Lima, D. D., Besier, T. F., Lloyd, D. G., Colwell, C. W., & Fregly, B. J. (2013). Are external knee load and EMG measures accurate indicators of internal knee contact forces during gait? *Journal of Orthopaedic Research, 31*(6), 921-929.

Meyer, E. G., Baumer, T. G., Slade, J. M., Smith, W. E., & Haut, R. C. (2008). Tibiofemoral contact pressures and osteochondral microtrauma during anterior cruciate ligament rupture due to excessive compressive loading and internal torque of the human knee. *The American Journal of Sports Medicine, 36*(10), 1966-1977.

Meyer, E. G., & Haut, R. C. (2005). Excessive compression of the human tibio-femoral joint causes ACL rupture. *Journal of biomechanics, 38*(11), 2311-2316.

Meyer, E. G., & Haut, R. C. (2008b). Anterior cruciate ligament injury induced by internal tibial torsion or tibiofemoral compression. *Journal of biomechanics, 41*(16), 3377-3383.

Miller, R. H., Esterson, A. Y., & Shim, J. K. (2015). Joint contact forces when minimizing the external knee adduction moment by gait modification: A computer simulation study. *The Knee*.

Minns, R., & Steven, F. (1977). The collagen fibril organization in human articular cartilage. *Journal of anatomy, 123*(Pt 2), 437.

Moglo, K., & Shirazi-Adl, A. (2003). Biomechanics of passive knee joint in drawer: load transmission in intact and ACL-deficient joints. *The Knee, 10*(3), 265-276.

Moglo, K., & Shirazi-Adl, A. (2003). On the coupling between anterior and posterior cruciate ligaments, and knee joint response under anterior femoral drawer in flexion: a finite element study. *Clinical Biomechanics, 18*(8), 751-759.

Moglo, K., & Shirazi-Adl, A. (2005). Cruciate coupling and screw-home mechanism in passive knee joint during extension–flexion. *Journal of biomechanics, 38*(5), 1075-1083.

Moller, J. T., Weeth, R. E., & Keller, J. O. (1985). Unicompartmental arthroplasty of the knee: cadaver study of tibial component placement. *Acta Orthopaedica, 56*(2), 115-119.

Mononen, M. E., Jurvelin, J. S., & Korhonen, R. K. (2013). Effects of radial tears and partial meniscectomy of lateral meniscus on the knee joint mechanics during the stance phase of the gait cycle—a 3D finite element study. *Journal of Orthopaedic Research, 31*(8), 1208-1217.

Mononen, M. E., Jurvelin, J. S., & Korhonen, R. K. (2015). Implementation of a gait cycle loading into healthy and meniscectomised knee joint models with fibril-reinforced articular cartilage. *Computer methods in biomechanics and biomedical engineering, 18*(2), 141-152.

Moore, T. M., & HARVEYJR, J. P. (1974). Roentgenographic measurement of tibial-plateau depression due to fracture. *The Journal of Bone and Joint Surgery (American), 56*(1), 155-160.

Mow, V. C., & Guo, X. E. (2002). Mechano-electrochemical properties of articular cartilage: their inhomogeneities and anisotropies. *Annual Review of Biomedical Engineering, 4*(1), 175-209.

Mow, V. C., Holmes, M. H., & Michael Lai, W. (1984). Fluid transport and mechanical properties of articular cartilage: a review. *Journal of biomechanics, 17*(5), 377-394.

Mulvey, M. R., Macfarlane, G. J., Beasley, M., Symmons, D. P., Lovell, K., Keeley, P., . . . McBeth, J. (2013). Modest Association of Joint Hypermobility With Disabling and Limiting Musculoskeletal Pain: Results From a Large-Scale General Population–Based Survey. *Arthritis Care & Research, 65*(8), 1325-1333.

Muybridge, E. (1883). The attitudes of animals in motion. *Journal of the Franklin Institute, 115*(4), 260-274.

Nelitz, M., Seitz, A. M., Bauer, J., Reichel, H., Ignatius, A., & Dürselen, L. (2013). Increasing posterior tibial slope does not raise anterior cruciate ligament strain but decreases tibial rotation ability. *Clinical Biomechanics*.

Neptune, R., Zajac, F., & Kautz, S. (2004). Muscle force redistributes segmental power for body progression during walking. *Gait & posture, 19*(2), 194-205.

Nielsen, S., Rasmussen, O., Ovesen, J., & Andersen, K. (1984). Rotatory instability of cadaver knees after transection of collateral ligaments and capsule. *Archives of Orthopaedic and Trauma Surgery, 103*(3), 165-169.

Paci, J. M., Scuderi, M. G., Werner, F. W., Sutton, L. G., Rosenbaum, P. F., & Cannizzaro, J. P. (2009). Knee medial compartment contact pressure increases with release of the type I anterior intermeniscal ligament. *The American Journal of Sports Medicine, 37*(7), 1412-1416.

Paletta, G. A., Manning, T., Snell, E., Parker, R., & Bergfeld, J. (1997). The effect of allograft meniscal replacement on intraarticular contact area and pressures in the human knee a biomechanical study. *The American Journal of Sports Medicine, 25*(5), 692-698.

Pandy, M. G., & Andriacchi, T. P. (2010). Muscle and joint function in human locomotion. *Annual review of biomedical engineering, 12*, 401-433.

Pena, E., Calvo, B., Martinez, M., & Doblare, M. (2006). A three-dimensional finite element analysis of the combined behavior of ligaments and menisci in the healthy human knee joint. *Journal of biomechanics, 39*(9), 1686-1701.

Perron, M., Malouin, F., Moffet, H., & McFadyen, B. J. (2000). Three-dimensional gait analysis in women with a total hip arthroplasty. *Clinical Biomechanics, 15*(7), 504-515.

Perry, J., & Davids, J. R. (1992). Gait analysis: normal and pathological function. *Journal of Pediatric Orthopaedics, 12*(6), 815.

Pierce, J. E., & Li, G. (2005). Muscle forces predicted using optimization methods are coordinate system dependent. *Journal of biomechanics, 38*(4), 695-702.

Plas, F., Viel, É., & Blanc, Y. (1989). *La marche humaine: kinésiologie dynamique, biomécanique et pathomécanique*: Masson.

Poh, S. Y., Yew, K. S. A., Wong, P. L. K., Koh, S. B. J., Chia, S. L., Fook-Chong, S., & Howe, T. S. (2011). Role of the anterior intermeniscal ligament in tibiofemoral contact mechanics during axial joint loading. *The Knee*.

Radin, E. L., de Lamotte, F., & Maquet, P. (1984). Role of the Menisci in the Distribution of Stress in the Knee. *Clinical orthopaedics and related research, 185*, 290-294.

Ramakrishnan, H., & Kadaba, M. (1991). On the estimation of joint kinematics during gait. *Journal of Biomechanics, 24*(10), 969-977.

Ratcliffe, A., Fryer, P. R., & Hardingham, T. E. (1984). The distribution of aggregating proteoglycans in articular cartilage: comparison of quantitative immunoelectron microscopy with radioimmunoassay and biochemical analysis. *Journal of Histochemistry & Cytochemistry, 32*(2), 193.

Renstrom, P., Ljungqvist, A., Arendt, E., Beynnon, B., Fukubayashi, T., Garrett, W., . . . Krosshaug, T. (2008). Non-contact ACL injuries in female athletes: an International Olympic Committee current concepts statement. *British Journal of Sports Medicine, 42*(6), 394-412.

Riley, P. O., Paolini, G., Della Croce, U., Paylo, K. W., & Kerrigan, D. C. (2007). A kinematic and kinetic comparison of overground and treadmill walking in healthy subjects. *Gait & posture, 26*(1), 17-24.

Sakane, M., Fox, R. J., Glen, S. L. Y. W., Livesay, A., Li, G., & Fu, F. H. (1997). In situ forces in the anterior cruciate ligament and its bundles in response to anterior tibial loads. *Journal of Orthopaedic Research, 15*(2), 285-293.

Sandholm, A., Schwartz, C., Pronost, N., de Zee, M., Voigt, M., & Thalmann, D. (2011). Evaluation of a geometry-based knee joint compared to a planar knee joint. *The Visual Computer, 27*(2), 161-171.

Sasaki, K., & Neptune, R. R. (2010). Individual muscle contributions to the axial knee joint contact force during normal walking. *Journal of biomechanics, 43*(14), 2780-2784.

Seedhom, B. (1979). Transmission of the load in the knee joint with special reference to the role of the menisci part I: anatomy, analysis and apparatus. *Engineering in medicine, 8*(4), 207-219.

Seitz, A. M., Lubomierski, A., Friemert, B., Ignatius, A., & Dürselen, L. (2012). Effect of partial meniscectomy at the medial posterior horn on tibiofemoral contact mechanics and meniscal hoop strains in human knees. *Journal of Orthopaedic Research, 30*(6), 934-942.

Sekaran, S. V., Hull, M. L., & Howell, S. M. (2002). Nonanatomic location of the posterior horn of a medial meniscal autograft implanted in a cadaveric knee adversely affects the pressure distribution on the tibial plateau. *The American Journal of Sports Medicine, 30*(1), 74-82.

Shakoor, N., & Block, J. A. (2006). Walking barefoot decreases loading on the lower extremity joints in knee osteoarthritis. *Arthritis & Rheumatism, 54*(9), 2923-2927.

Shao, Q., MacLeod, T. D., Manal, K., & Buchanan, T. S. (2011). Estimation of ligament loading and anterior tibial translation in healthy and ACL-deficient knees during gait and the influence of increasing tibial slope using EMG-driven approach. *Annals of biomedical engineering, 39*(1), 110-121.

Shelburne, K., & Pandy, M. (1998). Determinants of cruciate-ligament loading during rehabilitation exercise. *Clinical Biomechanics, 13*(6), 403-413.

Shelburne, K., Torry, M., & Pandy, M. (2005). Muscle, ligament, and joint-contact forces at the knee during walking. *Medicine and Science in Sports and Exercise, 37*(11), 1984-1956.

Shelburne, K. B., Kim, H. J., Sterett, W. I., & Pandy, M. G. (2011). Effect of posterior tibial slope on knee biomechanics during functional activity. *Journal of Orthopaedic Research, 29*(2), 223-231.

Shelburne, K. B., & Pandy, M. G. (1997). A musculoskeletal model of the knee for evaluating ligament forces during isometric contractions. *Journal of biomechanics, 30*(2), 163-176.

Shelburne, K. B., & Pandy, M. G. (2002). A dynamic model of the knee and lower limb for simulating rising movements. *Computer Methods in Biomechanics & Biomedical Engineering, 5*(2), 149-159.

Shelburne, K. B., Pandy, M. G., Anderson, F. C., & Torry, M. R. (2004). Pattern of anterior cruciate ligament force in normal walking. *Journal of biomechanics, 37*(6), 797-805.

Shelburne, K. B., Torry, M. R., & Pandy, M. G. (2006). Contributions of muscles, ligaments, and the ground-reaction force to tibiofemoral joint loading during normal gait. *Journal of Orthopaedic Research, 24*(10), 1983-1990.

Shepherd, D., & Seedhom, B. (1999). Thickness of human articular cartilage in joints of the lower limb. *Annals of the rheumatic diseases, 58*(1), 27-34.

Shim, V. B., Besier, T. F., Lloyd, D. G., Mithraratne, K., & Fernandez, J. F. (2016). The influence and biomechanical role of cartilage split line pattern on tibiofemoral cartilage stress distribution during the stance phase of gait. *Biomechanics and modeling in mechanobiology, 15*(1), 195-204.

Shirazi, R., & Shirazi-Adl, A. (2005). Analysis of articular cartilage as a composite using nonlinear membrane elements for collagen fibrils. *Medical Engineering & Physics, 27*(10), 827-835.

Shirazi, R., & Shirazi-Adl, A. (2009). Analysis of partial meniscectomy and ACL reconstruction in knee joint biomechanics under a combined loading. *Clinical Biomechanics, 24*(9), 755-761.

Shirazi, R., Shirazi-Adl, A., & Hurtig, M. (2008). Role of cartilage collagen fibrils networks in knee joint biomechanics under compression. *Journal of biomechanics, 41*(16), 3340-3348.

Shumway-Cook, A., & Woollacott, M. H. (2007). *Motor control: translating research into clinical practice*: Lippincott Williams & Wilkins.

Simon, R., Everhart, J., Nagaraja, H., & Chaudhari, A. (2010). A case-control study of anterior cruciate ligament volume, tibial plateau slopes and intercondylar notch dimensions in ACL-injured knees. *Journal of biomechanics, 43*(9), 1702-1707.

Sonnery-Cottet, B., Archbold, P., Cucurulo, T., Fayard, J.-M., Bortolletto, J., Thaunat, M., . . . Chambat, P. (2011). The influence of the tibial slope and the size of the intercondylar notch on rupture of the anterior cruciate ligament. *Journal of Bone & Joint Surgery, British Volume, 93*(11), 1475-1478.

Spyropoulos, P., Pisciotta, J. C., Pavlou, K. N., Cairns, M., & Simon, S. R. (1991). Biomechanical gait analysis in obese men. *Archives of physical medicine and rehabilitation, 72*(13), 1065-1070.

Steele, K. M., DeMers, M. S., Schwartz, M. H., & Delp, S. L. (2012). Compressive tibiofemoral force during crouch gait. *Gait & posture, 35*(4), 556-560.

Stijak, L., Herzog, R. F., & Schai, P. (2008). Is there an influence of the tibial slope of the lateral condyle on the ACL lesion? *Knee Surgery, Sports Traumatology, Arthroscopy, 16*(2), 112-117.

Sutherland, D. H. (2001). The evolution of clinical gait analysis: Part II Kinematics. *Gait & posture, 16*(2), 159-179.

Taylor, W. R., Heller, M. O., Bergmann, G., & Duda, G. N. (2004). Tibio-femoral loading during human gait and stair climbing. *Journal of Orthopaedic Research, 22*(3), 625-632.

Tetsworth, K., & Paley, D. (1994). Malalignment and degenerative arthropathy. *Orthopedic Clinics of North America, 25*(3), 367-378.

Thelen, D. G., Anderson, F. C., & Delp, S. L. (2003). Generating dynamic simulations of movement using computed muscle control. *Journal of biomechanics, 36*(3), 321-328.

Titianova, E. B., Mateev, P. S., & Tarkka, I. M. (2004). Footprint analysis of gait using a pressure sensor system. *Journal of Electromyography and Kinesiology, 14*(2), 275-281.

Todd, M. S., Lalliss, S., Garcia, E. S., DeBerardino, T. M., & Cameron, K. L. (2010). The relationship between posterior tibial slope and anterior cruciate ligament injuries. *The American Journal of Sports Medicine, 38*(1), 63-67.

Valente, G., Pitto, L., Stagni, R., & Taddei, F. (2015). Effect of lower-limb joint models on subject-specific musculoskeletal models and simulations of daily motor activities. *Journal of biomechanics, 48*(16), 4198-4205.

Viel, E. (2000). *La marche humaine, la course et le saut: biomécanique, explorations, normes et dysfonctionnements* (Vol. 9): Elsevier Masson.

Wahl, C. J., Westermann, R. W., Blaisdell, G. Y., & Cizik, A. M. (2012). An association of lateral knee sagittal anatomic factors with non-contact ACL injury: sex or geometry? *The Journal of Bone & Joint Surgery, 94*(3), 217-226.

Walker, P., & Hajek, J. (1972). The load-bearing area in the knee joint. *Journal of biomechanics, 5*(6), 581-589.

Walker, P. S., & Erkman, M. J. (1975). The role of the menisci in force transmission across the knee. *Clinical orthopaedics and related research, 109*, 184.

Wall, S. J., Rose, D. M., Sutter, E. G., Belkoff, S. M., & Boden, B. P. (2012). The Role of Axial Compressive and Quadriceps Forces in Noncontact Anterior Cruciate Ligament Injury A Cadaveric Study. *The American Journal of Sports Medicine, 40*(3), 568-573.

Walter, J. P., D'Lima, D. D., Colwell, C. W., & Fregly, B. J. (2010). Decreased knee adduction moment does not guarantee decreased medial contact force during gait. *Journal of Orthopaedic Research, 28*(10), 1348-1354.

Wang, H., Chen, T., Koff, M. F., Hutchinson, I. D., Gilbert, S., Choi, D., . . . Maher, S. A. (2014). Image based weighted center of proximity versus directly measured knee contact location during simulated gait. *Journal of biomechanics, 47*(10), 2483-2489.

Weber, W., & Weber, E. F. (1836). *Mechanik der menschlichen Gehwerkzeuge: eine anatomisch-physiologische Untersuchung* (Vol. 1): Dietrich.

Weinberg, D. S., Williamson, D. F., Gebhart, J. J., Knapik, D. M., & Voos, J. E. (2017). Differences in Medial and Lateral Posterior Tibial Slope: An Osteological Review of 1090 Tibiae Comparing Age, Sex, and Race. *The American Journal of Sports Medicine, 45*(1), 106-113.

White, R., Agouris, I., Selbie, R., & Kirkpatrick, M. (1999). The variability of force platform data in normal and cerebral palsy gait. *Clinical Biomechanics, 14*(3), 185-192.

Whittle, M. W. (1996). Clinical gait analysis: A review. *Human Movement Science, 15*(3), 369-387.

Wilson, W., Huyghe, J., & Van Donkelaar, C. (2007). Depth-dependent compressive equilibrium properties of articular cartilage explained by its composition. *Biomechanics and modeling in mechanobiology, 6*(1-2), 43-53.

Winby, C., Gerus, P., Kirk, T., & Lloyd, D. (2013). Correlation between EMG-based co-activation measures and medial and lateral compartment loads of the knee during gait. *Clinical Biomechanics, 28*(9), 1014-1019.

Winby, C. R., Lloyd, D. G., Besier, T. F., & Kirk, T. B. (2009). Muscle and external load contribution to knee joint contact loads during normal gait. *Journal of biomechanics, 42*(14), 2294-2300.

Wong, J., Steklov, N., Patil, S., Flores-Hernandez, C., Kester, M., Colwell, C. W., & D'Lima, D. D. (2011). Predicting the effect of tray malalignment on risk for bone damage and implant subsidence after total knee arthroplasty. *Journal of Orthopaedic Research, 29*(3), 347-353.

Woo, S. L., Fox, R. J., Sakane, M., Livesay, G. A., Rudy, T. W., & Fu, F. H. (1998). Biomechanics of the ACL: measurements of in situ force in the ACL and knee kinematics. *The Knee, 5*(4), 267-288.

Xiao, M., & Higginson, J. S. (2008). Muscle function may depend on model selection in forward simulation of normal walking. *Journal of biomechanics, 41*(15), 3236-3242.

Yang, N., Canavan, P., Nayeb-Hashemi, H., Najafi, B., & Vaziri, A. (2010a). Protocol for constructing subject-specific biomechanical models of knee joint. *Computer methods in biomechanics and biomedical engineering, 13*(5), 589-603.

Yang, N. H., Nayeb-Hashemi, H., Canavan, P. K., & Vaziri, A. (2010b). Effect of frontal plane tibiofemoral angle on the stress and strain at the knee cartilage during the stance phase of gait. *Journal of Orthopaedic Research, 28*(12), 1539-1547.

Yeow, C. H., Cheong, C. H., Ng, K. S., Lee, P. V. S., & Goh, J. C. H. (2008). Anterior Cruciate Ligament Failure and Cartilage Damage During Knee Joint Compression A Preliminary Study Based on the Porcine Model. *The American Journal of Sports Medicine, 36*(5), 934-942.

Zajac, F. E., Neptune, R. R., & Kautz, S. A. (2002). Biomechanics and muscle coordination of human walking: Part I: Introduction to concepts, power transfer, dynamics and simulations. *Gait & posture, 16*(3), 215-232.

Zajac, F. E., Neptune, R. R., & Kautz, S. A. (2003). Biomechanics and muscle coordination of human walking: part II: lessons from dynamical simulations and clinical implications. *Gait & posture, 17*(1), 1-17.

Zatsiorky, V., Werner, S., & Kaimin, M. (1994). Basic kinematics of walking: step length and step frequency: a review. *Journal of sports medicine and physical fitness, 34*(2), 109-134.

Zhang, L.-Q., Shiavi, R. G., Limbird, T. J., & Minorik, J. M. (2003). Six degrees-of-freedom kinematics of ACL deficient knees during locomotion—compensatory mechanism. *Gait & posture, 17*(1), 34-42.

Zhao, D., Banks, S. A., D'Lima, D. D., Colwell, C. W., & Fregly, B. J. (2007a). In vivo medial and lateral tibial loads during dynamic and high flexion activities. *Journal of Orthopaedic Research, 25*(5), 593-602.

Zhao, D., Banks, S. A., Mitchell, K. H., D'Lima, D. D., Colwell, C. W., & Fregly, B. J. (2007b). Correlation between the knee adduction torque and medial contact force for a variety of gait patterns. *Journal of Orthopaedic Research, 25*(6), 789-797.